

Phosphorylation mediated regulation of MRTF-A

Richard Panayiotou

University College London

and

Cancer Research UK London Research Institute

PhD Supervisor: Dr Richard Treisman

A thesis submitted for the degree of

Doctor of Philosophy

University College London

September 2014

Declaration

I, Richard Panayiotou confirm that the work presented in this thesis is my own. Where information has been derived from other sources, I confirm that this has been indicated in the thesis.

Abstract

The transcription factor SRF (Serum Response Factor) regulates expression of target genes in response to changes in actin dynamics, by virtue of association with the Myocardin Related Transcription Factor (MRTF) family of transcription cofactors. MRTF-A senses changes in actin dynamics via direct G-actin binding to its RPEL domain. While bound to actin MRTF-A continuously shuttles between the nucleus and cytoplasm, but localises to the cytoplasm due to a high export rate. Because MRTF-A is exported by Crm1 in an actin dependent manner, dissociation from actin leads to nuclear accumulation and SRF activation. Concomitantly, MRTF-A is phosphorylated on multiple residues. The aim of this thesis was to determine the role of phosphorylation in MRTF-A function.

An MRTF-A derivative lacking all 26 identified phosphorylation sites was generated. Evidence is presented that phosphorylation of MRTF-A is required for its full capacity to activate SRF. One phosphorylation site, S98, is located within the RPEL domain. Phosphorylation of S98 attenuates actin binding to the RPEL domain and promotes nuclear accumulation of MRTF-A. I found that S98 is phosphorylated by ERK, which relies on an ERK binding motif just N-terminal of S98. Thus S98 represents a means by which MAP kinase signalling can impinge on MRTF-A regulation. In contrast, S33 phosphorylation promotes export of MRTF-A conferred by a Crm1 NES that was identified within its N-terminus. I have shown that this NES can act as an autonomous NES, but cooperates with the RPEL domain to confer actin dependent Crm1 mediated export. MRTF-A phosphorylation, can therefore fine-tune MRTF-A regulation by affecting both localisation and activity.

Acknowledgement

I would like to thank my supervisor Richard Treisman for giving me the opportunity to work in his lab, for his supervision, support and advice.

I thank my thesis committee, Michael Way and Peter Parker for their input and support along the way.

The work presented here would not have been possible without the help and advice from everyone in the lab. I would like to thank Mathew, Anastasia Magdalena, Laura, Charlie, Francesco, Diane, Cyril and Cynthia for fruitful and interesting discussions. I especially would like to thank Patrick for always being supportive and for making sure I have my five a day! Also Jessica for constructive criticism, technical help and encouragement. Many thanks also to Lucy for helping with all the admin issues.

Thanks to Nicola O'Reilly and the peptide synthesis lab for helping with antibody generation and always being friendly and accommodating. I thank Graham and everyone in the Equipment Park, for all the sequencing. Thanks also to Sally and the graduate team.

Most importantly I would like to thank my family and friends, especially Kyriakos for being supportive until the end, and my partner Constantia, for being incredibly patient and supportive throughout this whole experience.

Table of Contents

Abstract	3
Acknowledgement	4
Table of Contents	5
Table of figures	8
List of tables	10
Abbreviations	11
Chapter 1. Introduction	14
1.1 Signal transduction	14
1.1.1 Post translational modification	14
1.1.2 Phosphorylation	15
1.1.3 Mitogen-activated protein kinases (MAPKs)	16
1.1.4 Regulation of transcription factors by phosphorylation	24
1.2 Nucleocytoplasmic shuttling	27
1.2.1 The nuclear pore complex	28
1.2.2 The NPC selectivity barrier	30
1.2.3 Nuclear transport receptors: The karyopherin family	33
1.2.4 Ran and the Ran GTPase system	33
1.2.5 Nuclear import	36
1.2.6 Nuclear export	37
1.2.7 Crm1	38
1.2.8 Measuring nucleocytoplasmic transport	43
1.2.9 Regulation of transcription factor activity through controlled localisation ..	46
1.3 Actin	47
1.3.1 Monomeric actin	47
1.3.2 Filamentous actin	51
1.3.3 Dynamics of actin polymerisation	52
1.3.4 Control of actin cytoskeleton by Rho GTPases	55
1.3.5 RPEL motif containing proteins	58
1.3.6 Actin binding drugs	59
1.3.7 Role of nuclear actin	61
1.4 MRTFs	63
1.4.1 Domain organization of MRTFs	64
1.4.2 Regulation of MRTF-A by actin	70
1.4.3 Regulation of MRTF-A by post-translational modifications	73
Chapter 2. Materials & Methods	74
2.1 Chemicals and reagents	74
2.2 Buffers and solutions	75
2.3 Molecular cloning	77
2.3.1 Bacterial strains	77
2.3.2 Transformation	77
2.3.3 Expression vectors	77
2.3.4 Purification of plasmid DNA	80
2.3.5 Agarose gel electrophoresis	80
2.3.6 Recombinant DNA techniques	80
2.3.7 Cloning using the In-Fusion HD Cloning Kit (Clontech Laboratories, Inc) 97	

2.3.8 Sequencing.....	100
2.4 Oligonucleotides.....	100
2.5 Peptides.....	104
2.6 Mammalian cell culture.....	104
2.7 siRNA transfection.....	105
2.8 Luciferase reporter assays.....	106
2.9 Quantitative real-time PCR.....	107
2.10 Immunofluorescence microscopy.....	110
2.10.1 Rev NES detection assay.....	111
2.11 Protein Expression and Purification.....	112
2.11.1 Expression and purification of recombinant MRTF-A fragments.....	112
2.11.2 Purification of Crm1.....	113
2.11.3 Purification of Ran Q69L.....	116
2.11.4 Purification of rabbit skeletal muscle actin.....	117
2.12 Protein analysis.....	119
2.12.1 GST affinity pull-down assays.....	119
2.12.2 RhoGTP pull-down assay.....	120
2.12.3 SDS-PAGE.....	120
2.12.4 Protein detection.....	121
2.13 Fluorescence polarisation assay.....	123
2.14 Analytical gel filtration.....	124
2.15 IP/Kinase assay.....	124
2.16 λ-phosphatase assay.....	126
Chapter 3. Characterisation of MRTF-A phosphorylation.....	128
3.1 Aims.....	128
3.2 MRTF-A phosphorylation correlates with the onset of activity.....	128
3.3 Actin dissociation and ERK activation lead to MRTF-A phosphorylation.....	130
3.4 Nuclear localisation is required but not sufficient for full MRTF-A phosphorylation.....	133
3.5 MRTF-A dimerisation and binding to SRF are dispensable for phosphorylation.....	136
3.6 Phosphorylation is required for full activity.....	141
3.7 Kinase siRNA screen.....	148
3.8 Are DYRK kinases involved in MRTF-A regulation?.....	152
3.9 Are cyclin dependent kinases involved in MRTF-A regulation?.....	163
3.10 Summary.....	167
Chapter 4. Regulation of MRTF-A by the MAPK pathway.....	168
4.1 Aims.....	168
4.2 ERK signalling activates MRTF-A.....	168
4.3 ERK directly binds MRTF-A and phosphorylates S98.....	173
4.4 S98 phosphorylation affects actin binding by the RPEL domain.....	176
4.5 ERK promotes MRTF-A nuclear accumulation through S98 phosphorylation.....	184
4.6 Ser33 is basally phosphorylated.....	189
4.7 S33 phosphorylation prevents nuclear accumulation.....	194
Chapter 5. Identification of a Crm1 NES in the N-terminus of MRTF-A ...	199
5.1 Aims.....	199
5.2 Multiple export signals in MRTF-A.....	199

5.3	The MRTF-A and Phactr1 RPEL domains are not interchangeable	202
5.4	The MRTF-A N-terminus contains a Crm1 dependent export signal	211
5.5	RPEL domain sequences cooperate with the N-terminus for export activity	214
5.6	Mapping the N-terminal NES	217
5.7	Actin binding to RPEL1 may facilitate export	222
5.8	Leucine rich NES in the N-terminus directly binds Crm1	224
5.9	Probing Spacer1 for an export signal	229
5.10	Probing Spacer 2 for an export signal	231
5.11	The role of S33 and S98 in regulation of export	233
Chapter 6.	Discussion	237
6.1	Outline	237
6.2	Rho and MEK-ERK signalling converge on MRTF-A	238
6.3	Actin controls phosphorylation	238
6.4	What are the kinases that phosphorylate MRTF-A?	239
6.5	The role of phosphorylation in MRTF transcriptional activity	241
6.6	Regulation of MRTF-A nuclear accumulation by ERK	245
6.7	S98 phosphorylation affects actin binding to RPEL1	246
6.8	MRTF-A export	249
6.9	The MRTF-A RPEL domain is not sufficient for Crm1-mediated export.	250
6.10	A nuclear export signal in the N-terminus	251
6.11	The N-terminus and RPEL domain cooperate to confer actin regulated shuttling	252
6.12	The role of phosphorylation in the N-terminal region of MRTF-A	255
6.13	Conclusions	259
	Reference List	260

Table of figures

Figure 1.1 Overview of the mitogen-activated protein kinase (MAPK) signalling pathways.	18
Figure 1.2 Regulation of transcription factors by phosphorylation.	26
Figure 1.3 Schematic representation of the nuclear pore complex.....	29
Figure 1.4 Models that describe passage through the NPC.....	32
Figure 1.5 Overview of nucleocytoplasmic transport.....	35
Figure 1.6 Structure of Crm1.....	41
Figure 1.7 Structure of monomeric actin.	49
Figure 1.8 Regulation of actin filament dynamics by actin binding proteins.....	54
Figure 1.9 Rho GTPases orchestrate the functions of ABPs to regulate actin dynamics.	57
Figure 1.10 Domain organisation of MRTF family members.....	66
Figure 1.11 Crystallography structures of MRTF-A RPEL domain and actin	70
Figure 1.12 MRTF-A nucleocytoplasmic shuttling.....	72
Figure 2.1 Plasmids used in this thesis.	79
Figure 3.1 MRTF-A phosphorylation correlates with the onset of transcriptional activity	130
Figure 3.2 Serum induced MRTF-A phosphorylation depends on an intact RhoA and MAPK pathway.....	133
Figure 3.3 Nuclear localisation is not sufficient for MRTF-A phosphorylation	136
Figure 3.4 Activation potential of dimerisation defective and SRF binding defective MRTF-A.....	139
Figure 3.5 Ternary complex formation and dimerisation are dispensable for MRTF-A phosphorylation.....	141
Figure 3.6 Generation of a non phosphorylatable MRTF-A derivative	145
Figure 3.7 MRTF-A phosphorylation is required for full activity.....	147
Figure 3.8 The defect in ST/A activity is actin binding independent.....	147
Figure 3.9 Strategy for identification of kinases that phosphorylate MRTF-A	149
Figure 3.10 Kinase siRNA screen	151
Figure 3.11 MRTF-A phosphorylation after kinase knockdown.....	151
Figure 3.12 Effect of DYRK knockdown on MRTF-A target genes.....	154

Figure 3.13 Combination knockdowns of DYRK family members	157
Figure 3.14 DYRK inhibitor Harmine attenuates MRTF-A target gene induction .	157
Figure 3.15 Effect of DYRK overexpression on MRTF-A target gene expression	159
Figure 3.16 Expressed DYRK1A and DYRK1B are functional kinases.....	161
Figure 3.17 DYRK and MRTF-A kinase assay.....	163
Figure 3.18 CDK knockdown does not impair MRTF-A reporter activation.....	165
Figure 3.19 Flavopiridol blocks MRTF-A reporter activation	166
Figure 4.1 TPA induces MRTF-A target gene activation	171
Figure 4.2 TPA treatment downregulates Rho activity in 3T3 cells	172
Figure 4.3 TPA leads to MRTF-A phosphorylation.....	173
Figure 4.4 ERK directly binds MRTF-A and phosphorylates Ser98	176
Figure 4.5 S98 phosphorylation does not affect actin binding in the context of the RPEL1 peptide alone	180
Figure 4.6 S98 phosphorylation does not affect actin binding to Spacer1	182
Figure 4.7 S98 phosphorylation blocks actin binding to RPEL1 in the context of the RPEL domain	184
Figure 4.8 TPA leads to MRTF-A nuclear localisation	187
Figure 4.9 Activation of the MAPK pathway promotes S98 phosphorylation and nuclear accumulation	189
Figure 4.10 Generation of a pSer33 specific antibody	192
Figure 4.11 S33 phosphorylation	193
Figure 4.12 MAPK activation leads to MRTF-A nuclear accumulation through S98 phosphorylation	196
Figure 4.13 Alanine substitution of STS544/545/549 does not block export.....	198
Figure 5.1 MRTF-A possesses multiple putative classical export sequences.....	201
Figure 5.2 Alignment of MRTF-A and Phactr1 RPEL domains	206
Figure 5.3 The RPEL domains of MRTF-A and Phactr1 are not functionally interchangeable.....	208
Figure 5.4 Cellular localisation of the chimera is determined by actin dependent export	210
Figure 5.5 The MRTF-A N-terminus confers Crm1 mediated export.....	214

Figure 5.6 The N-terminus and RPEL domain together provide Crm1 dependent and actin regulated export.....	217
Figure 5.7 The RPEL domain potentiates the export activity of the N-terminus...	220
Figure 5.8 A short sequence containing the N-terminal NES is sufficient for export	221
Figure 5.9 Presence of RPEL1-Spacer1 potentiates NES activity of the N-terminus	224
Figure 5.10 Classical NES element in the N-terminus of MRTF-A.....	226
Figure 5.11 Crm1 directly interacts with the MRTF-A N-terminus	227
Figure 5.12 RPEL domain enhances N-terminal NES activity.....	228
Figure 5.13 Probing Spacer1 for an export signal.....	230
Figure 5.14 Probing Spacer 2 for an export signal.....	233
Figure 5.15 The role of S33 and S98 in MRTF-A export.....	236
Figure 6.1 MAPK signalling promotes full phosphorylation and activation of MRTF-A	244
Figure 6.2 Potential mechanism by which S98 phosphorylation blocks actin binding to RPEL1	249
Figure 6.3 Binding of Crm1 to the N-terminal NES is facilitated by RPEL1-Spacer1	254
Figure 6.4 Effect of S98 phosphorylation on regulation of MRTF-A localisation ..	257
Figure 6.5 Effect of cell density on MRTF-A (2-204) PK localisation	258

List of tables

Table 1: Actin binding proteins and their function	50
--	----

Abbreviations

aa: aminoacid

ABPs: actin-binding protein

ActD: Actinomycin D

Amp: Ampicillin

ARM: armadillo

ATP: Adenosine Triphosphate

BDNF: Brain derived neurotrophic factor

BSA: Bovine serum albumin

CB: Cytochalasin B

Cc: critical concentration

CD: Cytochalasin D

Cdks: cyclin dependent kinase

cDNA: complementary DNA

CKII: casein kinase II

CRM1: Chromosome region maintenance 1

DAPI: 4',6'-diamidino-2-phenylindole

Dia1: diaphanous related formin 1

dNTP: deoxynucleotide triphosphate

DTT: Dithiothreitol

DYRK: dual-specificity tyrosine-phosphorylated and regulated kinase

EGF: epidermal growth factor

ERK: Extracellular signal-regulated kinase

F-actin: filamentous actin

FCS: Fetal calf serum

FLIP: fluorescence loss in photobleaching

FP: Fluorescence polarisation

FRAP: Fluorescence recovery after photobleaching

FRET: Forster resonance energy transfer

G-actin: globular actin

GEF: guanine exchange factors

GFP: green fluorescence protein

GPCR: G-protein coupled receptor
GTP: guanosine triphosphate
His: histidine
HMM: hidden Markov model
IPTG: Isopropyl- β -D-thiogalactopyranoside
I κ B: inhibitor of NF- κ B
JNK: c-Jun N-terminal kinase
Kan: Kanamycin
KSR: kinase suppressor of Ras
LIMK1: LIM domain kinase 1
LMB: Leptomycin B
LPA: lysophosphatidic acid
LZ: leucine zipper
MAPK: Mitogen-activated protein kinase
MAPKK: MAP kinase kinase
MAPKKK: MAP kinase kinase kinase
Med23: Mediator complex subunit 23
MEK: MAPK/ERK kinase
MICAL2: molecule interacting with CasL
MKPs: MAPK phosphatases
MP-1: MEK partner 1
MRTF: Myocardin related transcription factor
NES: nuclear export sequence
NF- κ B: Nuclear factor κ B
NF-AT: Nuclear factor of activated T cells
NGF: neuronal growth factor
NLS: nuclear localisation signal
NN: Neural network
NPC: nuclear pore complex
NTF2: Nuclear transport factor 2
NTR: nuclear transport receptor
Nup: nucleoporin
PAK: p21-activated kinase
PCR: Polymerase chain reaction

PDGF: platelet derived growth factor
Phactr: phosphatase and actin regulator
PKA: protein kinase A
PKC: protein kinase C
PMSF: Phenylmethyl-sulphonyl fluoride
PP1: protein phosphatase 1
Pro: proline
PTHrP: Parathyroid hormone related protein
PTM: post-translational modification
RanBD: Ran binding domain
RBD: Ras binding domain
RCC1: regulator of chromosome condensation 1
Rsk: ribosomal S6 kinase
SAP: SAF-A /B, Acinous and PIAS
SDS-PAGE: sodium dodecyl sulfate polyacrylamide electrophoresis
Ser: serine
SREBP-2: sterol regulatory element binding protein 2
SRF: serum response factor
TCF: ternary complex factor
TE: Tris-EDTA
Thr: threonine
TPA: tetradecanoyl phorbol acetate
Tyr: tyrosine
WT1: Wilms' tumour 1

Chapter 1. Introduction

1.1 Signal transduction

All aspects of cell behaviour, including growth, proliferation, survival or death, are dynamically regulated in response to internal and external cues. Cells continuously receive information regarding their surrounding environment, using receptors to sense concentrations of hormones, growth factors or extracellular matrix composition. Cells also sense changes in the intracellular milieu, such as changes in concentration of metabolites, structure proteins such as actin, or stresses such as DNA damage or unfolded proteins. Information regarding all these parameters must be transformed or transduced into signals that are capable of eliciting a set of molecular responses that together develop an appropriate cellular response. These signals are often in the form of post-translational modifications (PTMs) of proteins, orchestrated by groups of proteins that constitute signalling pathways. A major target for such pathways is gene expression machinery, which forms the focus of this introduction.

1.1.1 Post translational modification

Post translational modification (PTM) is any process that changes a protein, after it has been translated, leading to changes in its structure and/or function. Modification can be permanent, as is the case with cleavage and removal of part of the protein, or reversible as in the case of covalent attachment of chemical moieties. Enzymes that introduce or remove PTMs are major targets for signal transduction pathways.

Since PTMs are biochemical reactions catalysed by enzymes, a single enzyme can modify multiple targets leading to signal amplification. Antagonising enzymes, which reverse the modification, allow cells to dynamically regulate the

target protein ensuring fast and controlled execution of cellular processes. A single protein can be the recipient of multiple and different PTMs allowing integration of signals at a single target. Signals from parallel signalling pathways can be integrated by converging onto a common component protein whose function will be defined by the combination of PTMs it has received. For example the transcriptional activity, cellular localisation and stability of p53 can be independently regulated by different forms of PTM (Lavin and Gueven, 2006; Kruse and Gu, 2008).

There are several different types of PTM including phosphorylation, ubiquitination, SUMOylation, oxidation, neddylation, acetylation and methylation. Some are historically associated with specific processes, for example poly-ubiquitination was initially best known as a degradation signal and phosphorylation was thought of as distinctive of glycogen metabolism (Johnson, 2009). As the field of signalling advanced it became evident that the different PTMs were widespread phenomena, not confined to specific cellular processes. In most cases, reversible PTMs are in essence a means to create or impair an interaction surface, either directly or allosterically. The new conformational state has context specific functional consequences; for example, in some cases PTMs can alter the enzymatic activity of a protein. In the next section I will focus on phosphorylation, one of the most common and well-studied PTMs.

1.1.2 Phosphorylation

Phosphorylation is the transfer of the terminal or γ -phosphate of ATP to a functional group of a target substrate. Substrates can be lipids, such as the membrane resident phosphoinositides, or proteins. In higher eukaryotes protein phosphorylation occurs on three residues; serine (Ser), threonine (Thr) and tyrosine (Tyr). Global phosphoproteomics studies showed that in resting cells, the relative abundance of phospho-serine, -threonine or -tyrosine was 86.4%, 4.8% and 1.8% respectively (Olsen et al., 2006). Histidine (His) phosphorylation has also been reported but is a rare event (Wagner and Vu, 1995; Attwood, 2013).

Phosphorylation can have strong effects on the conformation and hence function of a protein. Serine, threonine and tyrosine residues have a hydroxyl group

on their side chains, to which the relatively bulky phosphate group is covalently attached. At physiological pH the phosphate group exists as a dianion, adding a double negative charge to the previously neutral location (Johnson and Lewis, 2001). The phosphorylated side chain can now form new intra- or inter-molecular interactions through hydrogen bonds or salt bridges. The resulting conformational changes can affect enzymatic activity of an active site or interactions with binding partners that can potentially affect any aspect of the proteins' function (activity, localisation, half-life etc).

Each phosphorylatable residue can be attached to only one phosphate providing a form of binary code that might appear inflexible. However, a single protein can possess multiple phosphorylation sites, which can affect each other's function and allow tunable thresholds and diverse functional outcomes (Kõivomägi et al., 2013). For Src kinases, C-terminal phosphorylation maintains the protein in a latent state, while phosphorylation of the activation loop is required for activation (Boggon and Eck, 2004).

Phosphorylation is catalysed by protein kinases. Over 500 kinases have been identified making up a 1.7% of the total number of human genes. Several kinases can sequentially phosphorylate each other, forming a signalling cascade. One of the most intensively studied signalling cascades is the Raf-MEK-ERK mitogen-activated protein kinase cascade.

1.1.3 Mitogen-activated protein kinases (MAPKs)

1.1.3.1 MAPK signalling cascade

The mitogen-activated protein kinase pathway is highly conserved in eukaryotes and it responds to a multitude of intra- and extracellular signals to regulate a wide range of cell processes including proliferation, survival and differentiation, reviewed in (Yang et al., 2003; Kyriakis and Avruch, 2012). The pathway features a three-tiered architecture (Figure 1.1), at the end of which three families/groups of MAPKs are found: the extracellular signal-regulated kinase (ERK) family, the p38 family and the c-Jun N-terminal kinase (JNK) family. Stress or ligand activated cell surface receptors lead to the activation of the first tier, the

MAP kinase kinase kinase (MAPKKK), MAPKKKs in turn activate the tier 2 kinases, the MAPKKs, through phosphorylation. MAPKKs in turn phosphorylate and activate the third tier, the MAPKs, downstream of which are a multitude of substrates; including further kinases such as the ribosomal S6 kinases (Rsk) (Raman et al., 2007). Often substrates are transcription factors, whose DNA binding or activity is affected. One extensively studied case is that of Elk1/serum response factor (SRF). ERK phosphorylates the transcription activation domain of Elk1 at multiple positions, causing transcriptional activation, by facilitating recruitment of the Mediator complex through Med23 (Cruzalegui et al., 1999; G. Wang et al., 2005).

1.1.3.2 *The ERK1/2 module*

Extracellular regulated kinase-1 (ERK1) and ERK2 were first noticed as two proteins which became tyrosine phosphorylated after growth factor stimulation (Cooper et al., 1982). A decade later their complementary DNAs (cDNAs) were cloned and were found to be highly related, sharing 83% sequence identity (Johnson, 2009; Boulton et al., 1990; 1991). Both are ubiquitously expressed, are activated in response to a variety of stimuli (Olsen et al., 2006; Boulton et al., 1990; Cooper et al., 1982) and share many but not all functions (Wagner and Vu, 1995; Lloyd, 2006).

Despite being co-expressed in the majority of tissues, the relative amounts of each isoform can be different between tissues (Johnson and Lewis, 2001; Boulton et al., 1991). The phenotypes of knockout mice are also different. ERK2 $-/-$ mice die during development (Kõivomägi et al., 2013; Hatano et al., 2003; Yao et al., 2003), while ERK1 $-/-$ mice are born but have a defect in thymocyte maturation (Raman et al., 2007; Pagès et al., 1999). From these studies it was not clear whether there was a gene dosage effect. Lefloch et al. ablated ERK1 or ERK2 in cell based assays and investigated their relative contribution to immediate early gene expression and proliferation (Lefloch et al., 2008). The authors showed that a depletion of either ERK1 or ERK2 lowered immediate early gene expression but only ERK2 depletion would block proliferation. They next demonstrated that very low levels of ERK activity are sufficient for proliferation and the contribution of ERK1 was only uncovered upon sufficient depletion of ERK2. The authors

proposed that differences in ERK1 and ERK2 expression are responsible for the apparent differences seen between ERK1 and ERK2 knockout mice.

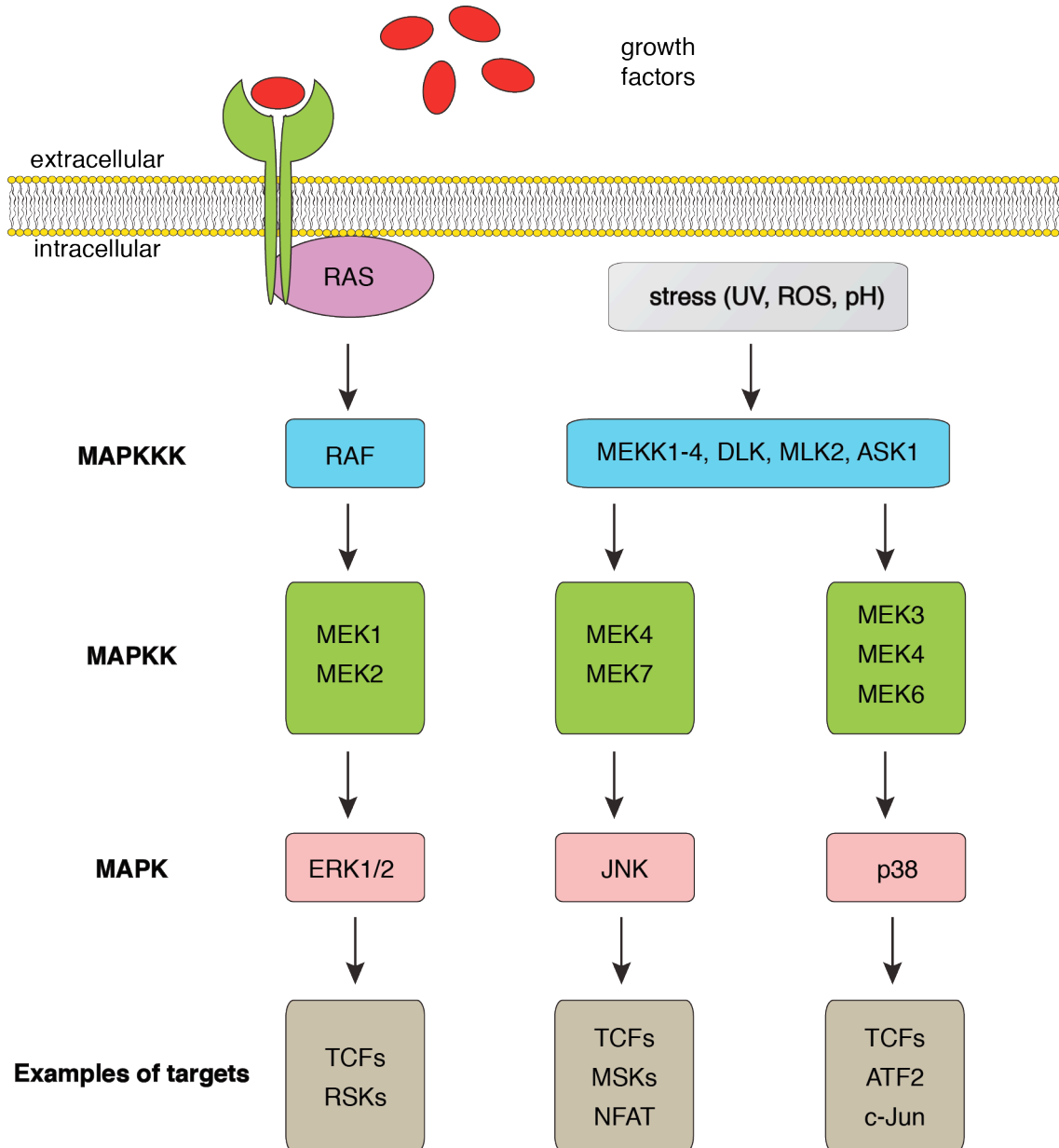


Figure 1.1 Overview of the mitogen-activated protein kinase (MAPK) signalling pathways.

MAPKs can be divided into three categories: ERK, JNK and p38, and each category is comprised of a 3-tier architecture: MAPKKKs phosphorylate MAPKKs, which in turn phosphorylate and activate MAPKs. Some examples of transcription factors and kinases targeted by MAPKs are indicated.

1.1.3.3 Activation

In mammalian cells ERK1/2 are activated in response to stimulation with growth factors such as epidermal growth factor (EGF), platelet derived growth factor (PDGF) and insulin, which activate receptor tyrosine kinases. Ligand binding induces dimerisation and activation of the receptors, seeding the assembly of signalling complexes that activate the membrane localised small GTPase Ras (Cooper et al., 1982; Lemmon and Schlessinger, 2010). Ras is also activated by lysophosphatidic acid (LPA), thrombin and other agonists of G-protein coupled receptors (GPCRs), although the mechanisms involved are less clear (Downward, 2003; van Corven et al., 1993). Active Ras, RasGTP, in turn activates Raf, the apical kinase or MAPKKK of the ERK1/2 signalling cascade.

Raf is a family of three proteins (A-Raf, B-Raf and C-Raf or Raf1) of which Raf1 is ubiquitously expressed and most intensively studied (Storm et al., 1990). Raf1 activation is a complex set of molecular events that involves membrane recruitment, protein-protein interactions, dimerisation and phosphorylation. Raf1 is recruited to the membrane by binding to RasGTP via its Ras binding domain (RBD) (Wittinghofer and Nassar, 1996). This recruitment step is not sufficient for activation and is itself subject to multiple modes of regulation. Binding of 14-3-3 to the C-terminus of Raf1 then stimulates the phosphorylation of multiple residues essential for activation, reviewed in (Wellbrock et al., 2004). Multiple kinases and the respective signalling pathways have been suggested to feed into Raf signalling through these phosphorylation sites, either positively or negatively affecting Raf1 activation. Examples include protein kinase A (PKA), p21-activated kinase (PAK) and protein kinase C (PKC) (Dumaz et al., 2002; Kolch et al., 1993; Schönwasser et al., 1998; Chaudhary et al., 2000). Direct activation of Raf1 by PKCs, can be induced using tetradecanoyl phorbol acetate (TPA). TPA is an analog of diacyl glycerol, which binds and activates PKC and is frequently used experimentally to activate the MAPK pathway (Marquardt et al., 1994; Schönwasser et al., 1998).

The only widely accepted substrates of Raf1 are MAPK/ERK kinases 1/2 (MEK1/2), the second tier kinases of the ERK1/2 cascade. MEK1/2 are activated after a double serine phosphorylation within their activation domain (S217 and S221 for MEK1) by Raf1 (Zheng and Guan, 1994). Substitution of these two residues to acidic residues and deletion of a small N-terminal sequence (aa32-51)

results in a constitutively active kinase (Mansour et al., 1994). Amounts of cellular MEK in most cell types tested are higher than those of Raf, allowing for signal amplification (Fujioka et al., 2006). Activated MEK1/2, being dual specificity kinases, phosphorylate the regulatory Thr and Tyr residues in the activation loop of ERK1/2 (Ahn et al., 1992).

A small molecule commonly used to inhibit ERK activation by MEK1/2, is U0126. U0126 is not an ATP competitor, instead it allosterically affects the activity of MEK, meaning that it binds MEK in a unique site (or at least less conserved than the ATP pocket) and is also able to inhibit constitutively active MEK mutants (Duncia et al., 1998). Evidence that U0126 inhibits MEK activation rather than MEK activity were later explained by the lower affinity of U0126 for activated rather than inactive MEK (Sheth et al., 2011; Davies et al., 2000)

Signal propagation down the cascade is organised by scaffold proteins, ensuring efficiency, spatial regulation and specificity. Several scaffolds have been identified in mammals, including kinase suppressor of Ras (KSR), MEK partner 1 (MP-1) and β -arrestin (Therrien et al., 1996; Luttrell et al., 2001). KSR coordinates membrane assembly of Raf-MEK-ERK. Upon activation of Ras, KSR translocates to the membrane, bringing the pathway components in close proximity and greatly enhancing activation efficiency (Brennan et al., 2011). Upon angiotensin stimulation, β -arrestin-2 facilitates assembly of the Raf-MEK-ERK complex in endosomal vesicles and enhances Raf-MEK dependent activation of ERK (Luttrell et al., 2001).

Scaffolds can also have an impact on the kinetics of ERK signalling. Depletion of p14, an adaptor protein for the scaffold MP-1, results in its mislocalisation and a consequent shortening in the duration of ERK signalling (Teis et al., 2002).

1.1.3.4 Docking of ERK to substrates

ERK is a proline (Pro) directed Ser/Thr kinase, which means that it phosphorylates Ser/Thr residues followed by a proline. The optimal primary sequence is Pro-X-Ser/Thr-Pro but Ser/Thr-Pro is sufficient and represents the minimal consensus (Gonzalez et al., 1991; Clark-Lewis et al., 1991). There is therefore a specificity overlap with other proline directed kinases such as the cyclin-

dependent kinases (CDKs) (Northwood et al., 1991; Hall and Vulliet, 1991). The presence of this minimal consensus in a protein does not necessarily make it an *in vivo* target. An important determinant of ERK substrate specificity is the presence of docking sites through which they can recruit ERK and in some cases other MAPKs as well. The docking sites can increase local concentration of the kinase and promote substrate phosphorylation.

The best characterised ERK binding motif is the D-domain, which is composed of a cluster of basic residues followed shortly by Leu-X-Leu (Yang et al., 1998; Sharrocks et al., 2000). The D-domain can be recognised by all MAPKs but subtle differences in the sequence can discriminate between them (Garai et al., 2012). The location of the D-domain can be either N- or C-terminal to the target site and is recognised by the common docking (CD) domain of ERK (Tanoue and Nishida, 2003). The D-domain is present in the ternary complex factor (TCF) family of SRF cofactors, and I will demonstrate a similar motif in myocardin related transcription factor A (MRTF-A) (see chapter 4).

Another ERK docking motif is the DEF domain or FxFP motif. This domain is recognised only by ERK and p38 α and is most often found downstream of the phospho-acceptor site (Tanoue and Nishida, 2003; Whitmarsh, 2007). However, ERK binding cannot be predicted based on the presence of the aforementioned docking sequences, as ERK docking sites that do not bear any resemblance to either motif have also been reported (Molina et al., 2005).

1.1.3.5 Subcellular localisation of ERK

ERK phosphorylates many nuclear proteins, and to do so it must translocate to the nucleus. In fact inactivation of Crm1 mediated export using Leptomycin B (LMB), results in ERK nuclear accumulation, indicating that ERK continuously shuttles via the nucleus (Volmat et al., 2001). In resting 3T3 cells ERK is inactive and predominantly cytoplasmic, although recent studies have demonstrated periodical nuclear activity. In HeLa cells it is evenly distributed. In both cases, activation leads to rapid and sustained nuclear accumulation, which is the net effect of an unequal acceleration in import and export rates (Volmat et al., 2001; Chen et al., 1992; Ando et al., 2004).

Cytoplasmic retention of ERK in resting cells is brought about by association with various anchor proteins, including MEK and the tubulin cytoskeleton (Chuderland and Seger, 2005; Reszka et al., 1995). Stimulation leads to an activation loop conformational change and detachment of ERK from cytoplasmic anchors (Wolf et al., 2001). In the latter studies it was shown that GFP-ERK lacking the regulatory phosphorylation sites (183-TEY-185) was unable to accumulate in the nucleus under non-saturating conditions (of MEK). This was in agreement with the observation that inhibition of MEK activity greatly reduced ERK nuclear accumulation (Lenormand et al., 1998). Wolf et al. show that residues 176-DHT-178 are important for dissociation from MEK and propose that they serve as a lever that causes dissociation (Wolf et al., 2001). Inactive ERK derivatives have been reported to be nuclear in other studies, however, they involved microinjection or overexpression which can saturate cytoplasmic anchors (Khokhlatchev et al., 1998; Fukuda et al., 1997; Rubinfeld et al., 1999). Volmat et al. have reported continued nuclear accumulation of endogenous ERK 3h after stimulation (Volmat et al., 2001), by which time ERK is inactive. It is possible that the initial phosphorylation is only required for initial detachment from anchor proteins and not for nuclear translocation.

Translocation of ERK has been shown to occur both passively (by diffusion) and actively (Zehorai et al., 2010). It was recently discovered that a three-residue motif, 244-Ser-Pro-Ser-246, is responsible for signal induced nuclear accumulation of ERK as well as passive translocation (Chuderland et al., 2008). The motif appears to be a general nuclear translocation signal. Fusion of a 19-residue sequence containing the SPS motif led to nuclear translocation of non-diffusible proteins.

Phosphorylation of the SPS motif in ERK was shown to be required for both passive and active nuclear translocation, warranting a search for the responsible kinase or kinases. Plotnikov et al. showed that inhibition or depletion of casein kinase II (CKII) blocked phosphorylation of the SPS motif and prevented ERK nuclear translocation. In addition, they were able to phosphorylate the motif *in vitro* using recombinant CKII and were able to co-immunoprecipitate the complex from cell lysates. They also demonstrated that phosphorylation of the SPS motif is a distinct step that follows release from anchor proteins that prevent its phosphorylation (Plotnikov et al., 2011).

1.1.3.6 Inactivation by phosphatases

The amplitude and duration of the ERK signal is also regulated by phosphatases that dephosphorylate and inactivate ERK (Owens and Keyse, 2007). Removal of either of the phosphates from the TEY motif in the ERK activation loop renders it inactive (Anderson et al., 1990). MAPK phosphatases (MKPs) are divided into three categories according to their specificity. These are the Ser/Thr phosphatases, the Tyrosine phosphatases and the dual specificity phosphatases (Keyse, 2000; Farooq and Zhou, 2004). There are ten dual specificity MKPs expressed in human, and they can be divided into Class I, II and III. Class I phosphatases are inducible. ERK activity promotes their de-novo synthesis after which they translocate to the nucleus to provide negative feedback. Class II is composed of cytoplasmic phosphatases. Class III phosphatases are found in either cellular compartment and preferentially target JNK and p38. Between them, the different classes of phosphatases form a complex network enabling negative regulation of ERK signalling (Roskoski, 2012; Owens and Keyse, 2007).

1.1.3.7 Variations in ERK signalling dynamics produce different responses

Signalling dynamics of ERK can be defined as the shape of the curve that describes the concentration, localisation and activity of ERK over time. As described above these parameters are affected by the stimulating extracellular ligand, the scaffolds and the phosphatases, which will all impinge on the efficiency and duration of ERK phosphorylation and activation in a given location.

Quantitative differences in the signalling dynamics of a signalling pathway can produce qualitatively different responses. An early report of such a case involved stimulation of PC12 neuronal precursor cells with two different growth factors, neuronal growth factor (NGF) and EGF. NGF led to differentiation and EGF led to proliferation. It was shown that the difference in cell fate was not due to activation of different signalling pathways, but instead that the two ligands produced distinctly different ERK activation profiles. EGF produced transient ERK activation, while NGF produced sustained ERK activation, which could presumably be sensed by downstream effectors such as transcription factors (Marshall, 1995).

In further work, Grammer and Blenis showed it was possible to alter the ERK signal elicited by EGF and NGF, thereby swapping the expected outcomes. Using TPA, the normally transient ERK activation elicited by EGF, was converted to a sustained response, leading to differentiation. Conversely the PKC inhibitor Gö7874, made the NGF induced ERK activation a transient one, leading to proliferation (Grammer and Blenis, 1997).

At least one mechanism by which the different ERK signalling profiles were decoded is demonstrated with the example of the c-Fos protein. In Swiss 3T3 fibroblasts, the transient ERK activity achieved by EGF stimulation led to a small induction of the immediate early gene *Fos*. PDGF produced sustained ERK activity, significant *Fos* induction and cell proliferation (Murphy et al., 2002). The c-Fos protein is unstable and rapidly degraded, unless phosphorylated by ERK. Upon sustained ERK activity c-Fos is synthesised, phosphorylated, stabilised and able to promote proliferation (Murphy et al., 2002).

The recent development of sensitive FRET biosensors for ERK activation has enabled live monitoring of ERK activity, on a single cell basis, in asynchronous cell populations (Aoki et al., 2012). It was shown that cell density affected the frequency of stochastic ERK activity pulses and that their frequency, but not the amplitude, correlated with cell proliferation. In addition, using a light activatable Raf protein the authors were able to control ERK activity frequency to accelerate cell proliferation. RNA sequencing analysis suggested the involvement of SRF in the expression of genes which responded to pulsatile rather than sustained ERK activity (Aoki et al., 2013).

1.1.4 Regulation of transcription factors by phosphorylation

Phosphorylation is a common mechanism employed to regulate transcription factor activity, allowing control over transcription of proteins necessary for appropriate cellular responses to stimuli. Phosphorylation or dephosphorylation can directly affect transcription factor behaviour including localisation, stability, interactions with other proteins and DNA binding. Examples are shown in Figure 1.2. In essence, what is important is the concentration of the transcription factor at

the target gene location and the potency with which it can promote transcription of the target.

Wilms' tumour 1 (WT1) is a transcription factor that differentially affects genes; it can either activate or suppress their transcription. WT1 binds DNA target sequences using its positively charged zinc finger domain. Phosphorylation of two serine residues within the zinc finger domain inhibits DNA binding (Fig 1.2 A) (Toska and Roberts, 2014; Sakamoto et al., 1997).

Nuclear factor of activated T cells (NF-AT) localisation is phosphorylation dependent. An increase in calcium levels activates the phosphatase calcineurin, which dephosphorylates NF-AT. A subsequent conformational change leads to exposure of at least one nuclear localisation signal allowing nuclear accumulation and access to DNA target sequences (Fig 1.2 B)(Rao et al., 1997).

The transcription cofactor Elk1, a member of the TCF family, associates with DNA via the serum response factor (SRF). Upon ERK activation, phosphorylation of the Elk1 C-terminal transactivation domain leads to robust activation of the *Fos* gene. Multiple phosphorylations within the transactivation domain lead to recruitment of the Mediator complex and transcriptional activation (Fig 1.2 C) (Cruzalegui et al., 1999; Marais:1993uf Galbraith et al., 2013; G. Wang et al., 2005).

In unstressed cells the transcription factor p53 is bound by Mdm2. This interaction leads to the continuous ubiquitination and degradation of p53. DNA damage activates ATM/ATR signalling, which leads to p53 phosphorylation, interruption of the Mdm2 association and stabilisation of p53 levels, and transcriptional activity (Fig 1.2 D) (Prives, 1998; Moll and Petrenko, 2003; Lavin and Gueven, 2006).

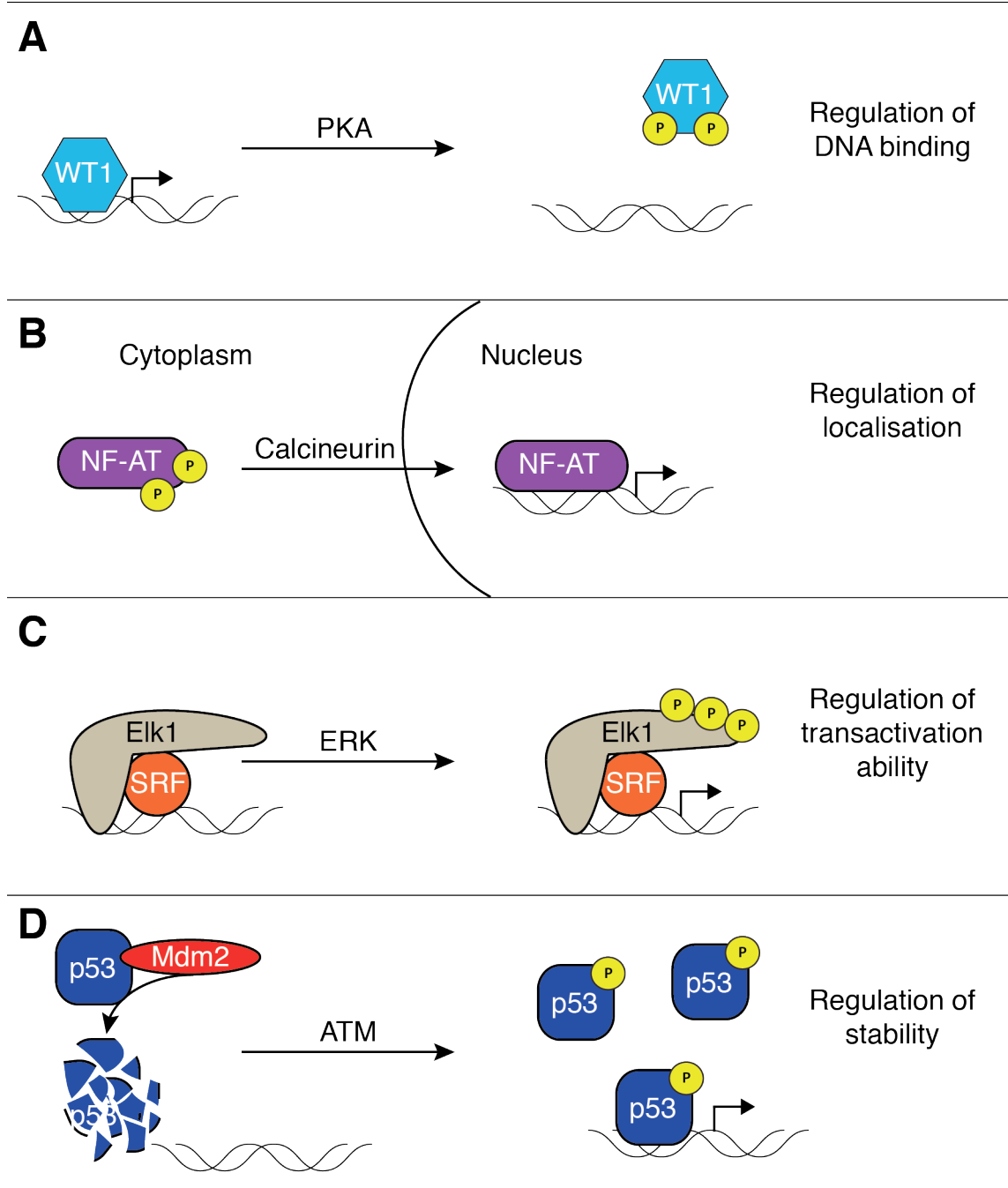


Figure 1.2 Regulation of transcription factors by phosphorylation.

Protein phosphorylation has context specific consequences. **A.** Phosphorylation of Wilms' tumour 1 (WT1) by PKA and PKC on S365 and S393 respectively blocks its ability to bind DNA. **B.** In the phosphorylated form, NF-AT adopts a conformation in which the NLS is masked. Dephosphorylation allows nuclear translocation and activation of target genes. **C.** Activation of MAPK signalling leads to

phosphorylation of Elk1 on multiple sites within its C-terminal transactivation domain. Once phosphorylated Elk1 facilitates transcriptional activation by recruiting the Mediator complex through direct interaction with Med23. **D.** p53 is continuously poly-ubiquitinated by Mdm2 and sent for proteasomal degradation. Stress activated protein kinases such as ATM, ATR and p38 phosphorylate and stabilise p53 by inhibiting the interaction with Mdm2.

1.2 Nucleocytoplasmic shuttling

The nucleus and cytoplasm are hosts to very different processes vital for cell function. The two compartments therefore contain very different sets of proteins. Some proteins are found exclusively in one compartment, however, in the case of nuclear proteins, they must first be synthesised and then sent to the nucleus. Conversely, the mRNA required for protein synthesis in the first place, originates from the nucleus. The two compartments must therefore cooperate and exchange both information and protein components.

Many proteins possess signal peptides, which define the location of the protein once it is translated. Histones, which are required for chromatin assembly, are synthesised in the cytoplasm and subsequently imported into the nucleus where they can carry out their function. This implies that once translated a histone must either make its way to the nucleus by diffusion, or that it is recognised and actively imported into the nucleus. In addition it must “qualify” for nuclear localisation since not all proteins can be found in the nucleus.

The first evidence suggesting selective nuclear entry came from microinjection experiments by Bonner in 1975. By microinjecting radiolabelled proteins into the cytoplasm of oocytes they showed that small proteins were able to equilibrate between the nucleus and cytoplasm, whereas larger proteins were excluded from the nucleus. Interestingly, if the large protein was destined for the nucleus it would be granted nuclear access. In the case of histones nuclear accumulation would occur at equal or faster rates than other smaller proteins suggesting the presence of active import (Bonner, 1975a; 1975b).

Not all proteins have a static subcellular localisation like histones. As described in section 1.1.3.5 some proteins like ERK, accumulate in the nucleus in a signal dependent manner. The case of ERK is a complicated one, but it demonstrates a variety of ways by which nuclear accumulation can be achieved. In resting cells ERK appears cytoplasmic despite its slow rate of shuttling through the nucleus. This can be achieved either by cytoplasmic anchoring, or a nuclear export rate which is faster than the import rate. Upon stimulation ERK accumulates in the nucleus by addressing both mechanisms that render it cytoplasmic. Phosphorylation leads to detachment from cytoplasmic anchors, and an increase in the rate of import. ERK localisation is therefore defined by the net effect of import, export and the stoichiometric capacity of anchors.

1.2.1 The nuclear pore complex

For a protein to enter or exit the nucleus, it must translocate via a nuclear pore, a large protein complex spanning the nuclear envelope. The nuclear pore complex (NPC) is a ~50MDa complex comprised of multiple copies of approximately 30 different nucleoporins (Nups) (Hetzer, 2010). Nups can be grouped into three categories (See Figure 1.3): (i) The transmembrane Nups, which line the “wall” of the hole in the nuclear envelope, form the interface with membrane lipids and anchor the NPC. (ii) FG-Nups contain phenylalanine-glycine (FG) repeats and constitute 30% of all Nups that make up the pore. (iii) Structural Nups (50% of all Nups) form a scaffold or framework that interacts both with the FG and transmembrane Nups (Wälde and Kehlenbach, 2010).

The framework stabilises the sharply bent nuclear envelope and forms the central channel through which transport of macromolecules occurs (Devos et al., 2004). Transport of these macromolecules is regulated by the FG-Nup filaments that fill the central channel and also extend from the NPC into the cytoplasm and nucleoplasm (Strambio-De-Castillia et al., 2010). On the nucleoplasmic side the filaments are attached to a distal ring, forming the nuclear basket (Alber et al., 2007). Simply put, one can imagine the NPC as a stent holding open a channel in the nuclear envelope, and this channel is filled with a meshwork of flexible

filaments that obstruct the passage of molecules larger than ~40 kDa (Terry and Wentz, 2009; N. P. C. Allen et al., 2002; Bayliss et al., 2000; Denning et al., 2002).

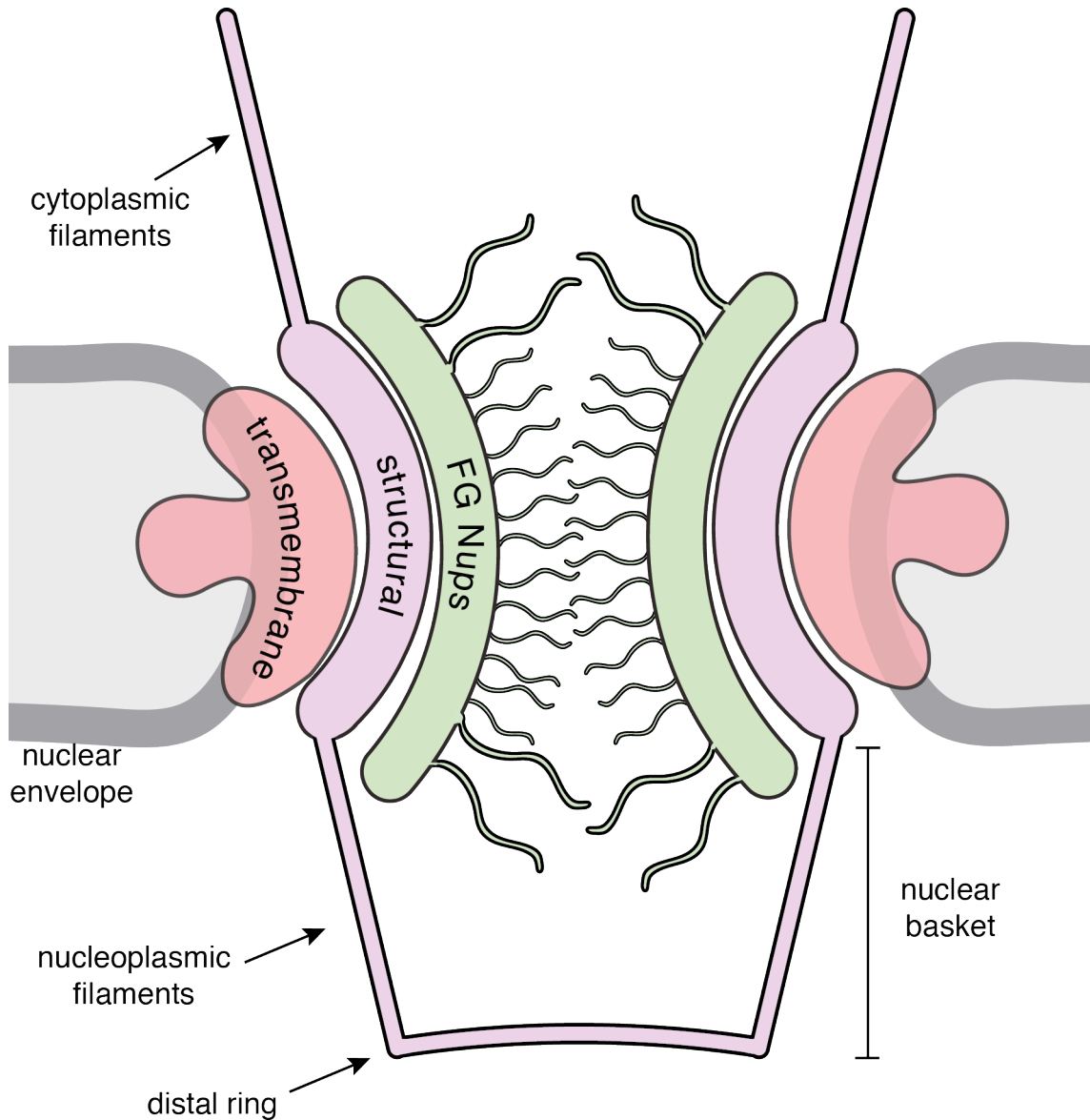


Figure 1.3 Schematic representation of the nuclear pore complex

The nuclear pore complex (NPC) is an assembly of multiple copies of 30 different proteins known as nucleoporins (Nups), which can be split into three categories: (i) The transmembrane Nups shown in pink anchor the NPC in the nuclear membrane, (ii) Structural Nups shown in purple form the scaffold and (iii) FG Nups shown in green form the hydrophobic environment of the nuclear pore.

1.2.2 The NPC selectivity barrier

NPCs are semi permeable pores; small proteins, metabolites or ions can freely diffuse between the nucleus and cytoplasm, but macromolecule translocation is regulated. Since the NPC is not a motor and possesses no enzymatic activity, its ability to behave as a selective barrier is brought about by its components and their specific architecture (Wente and Rout, 2010).

In the case of passively diffusing small particles, their size strongly correlates with their translocation rate. It is thought that a 9nm diameter is available for passive diffusion through the NPC (Paine et al., 1975; Alber et al., 2007). With increasing size, translocation becomes increasingly inefficient. Diffusion of ovalbumin, which has a 6nm diameter and 46kDa mass, is negligible (Görllich and Kutay, 1999).

Despite the physical restrictions of the nuclear pore, molecules much larger than 9nm or 40 kDa can traverse the NPC, at high efficiencies, often against a concentration gradient, in an energy dependent manner (Breeuwer and Goldfarb, 1990). Active transport across the NPC requires the binding of soluble nuclear transport receptors (NTRs) to a protein via a specific transport sequence. NTRs then guide their cargo through the FG-Nup mesh of the NPC (Dingwall et al., 1982; Wälde and Kehlenbach, 2010). The mechanism by which transport complexes traverse the NPC is not entirely understood, although several models have been proposed (Wälde and Kehlenbach, 2010).

According to the hydrogel model (Figure 1.4 A) (Frey and Görllich, 2007; Frey et al., 2006) the FG-Nups form a sieve that allows small molecules through, but not large ones. The sieve is formed through interaction between the FG-repeats within and between the filament-shaped FG-Nups. The resulting meshwork and entrapped cytoplasm form a hydrogel. Such a hydrogel was reconstituted successfully *in-vitro* using FG-Nups, and this hydrogel demonstrated some of the selective properties of the NPC. For example movement through the hydrogel was restricted for inert molecules, whereas facilitated diffusion was observed for NTRs (Frey and Görllich, 2009). NTRs are able to interact with FG repeats and in doing so disrupt the mesh as they pass through carrying their cargo with them. More recently direct evidence for this model was provided in a physiological context,

using NPCs reconstituted from frog *Xenopus laevis* extracts (Hülsmann et al., 2012).

The polymer brush model (Rout et al., 2003) (Figure 1.4 B), is based on thermodynamic factors. Movement of a molecule into the restricted volume of an NPC would lead to a loss of entropy, which is energetically unfavourable. This effect is exacerbated by the presence of a barrier formed by the FG-Nups. In this model the FG-Nups do not form an adhesive meshwork, but rather wave back and forth in the channel space. Inert molecules are therefore excluded. Because of their ability to bind FG-Nups, NTRs release binding energy, which compensates for the loss of entropy and drives translocation through the pore.

The forest model is based on evidence that not all FG-domains are cohesive (Patel et al., 2007), meaning that FG-Nups can adopt a globular collapsed coil conformation, or a more extended coil conformation; by analogy the “shrubs” and “trees” of a forest (Figure 1.4 C). While the shrubs line the area close to the structural Nups of the pore wall, the trees point towards the center forming a tunnel. Together they form a meshwork much like in the hydrogel model, but with a tunnel running down the core. Cargo is then channelled down the tunnel, which is flexible to dilate if the cargo is bulky. It is further postulated that an alternative, more peripheral route is available for smaller cargo. Smaller cargo could translocate via the zone where the extended coils, or tree stalks are. This fits with observations of cargo found traversing via a more peripheral route (Yamada et al., 2010).

The reduction in dimensionality model (Figure 1.4 D) was hypothesised in part due to observations of a high number of apparently immobile NTRs, saturating the FG-domains in NPCs (Paradise et al., 2007; Peters, 2005; 2009). In this case a channel lined with NTRs is formed, through which small particles can traverse, whereas larger ones cannot due to size. NTR-cargo complexes however can interact with FG-Nups at the entrance of the pore and randomly move in either of the two available directions along the central channel wall. The NTR-cargo complex displaces the cargo-free NTRs it encounters by competing for FG-domain binding.

At present, there is evidence supporting each of the models and each model is able to explain some but not all observations. Further studies into the biophysical properties of FG-Nups and their interactions with NTRs, in conditions which are as physiological as possible, are required.

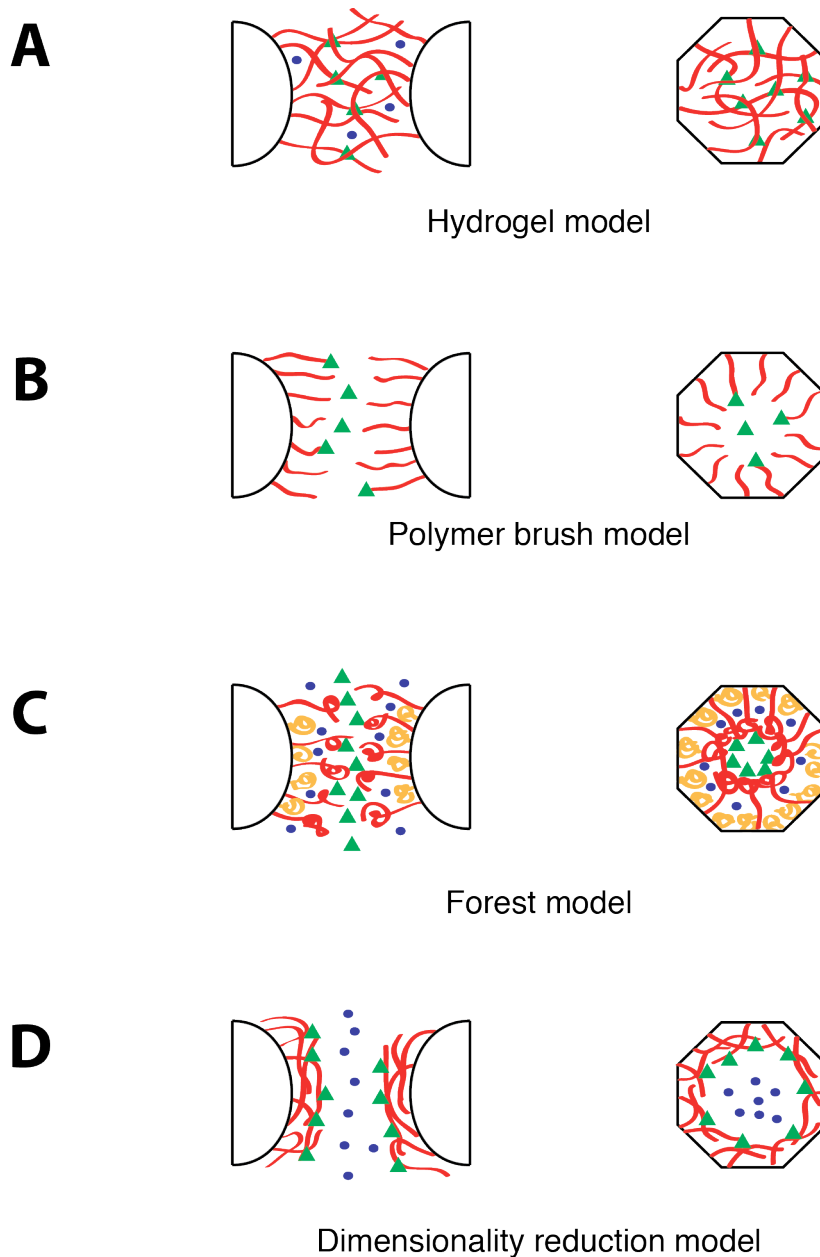


Figure 1.4 Models that describe passage through the NPC

Several models have been proposed to describe the mechanisms that define passage through the NPC. Small molecules that can passively diffuse through the pore are shown as blue circles. Large molecules that traverse the pore by active transport are shown as green triangles. **A**. The hydrogel model **B**. The polymer brush model **C**. The forest model **D**. Reduction in dimensionality model. Detailed descriptions in text. Adapted from (Wälde and Kehlenbach, 2010).

1.2.3 Nuclear transport receptors: The karyopherin family

The majority of macromolecules that translocate between the nucleus and cytoplasm require soluble NTRs to escort them across the NPC. Most NTRs belong to the β karyopherin family of proteins (or importin β -like proteins) which includes 14 and 20 members in yeast and humans respectively (Mosammaparast and Pemberton, 2004). Even though sequence similarity between them is low (~20%), they are all predicted to be composed of multiple tandem HEAT repeats (Mosammaparast and Pemberton, 2004). The HEAT motif consensus is a degenerate ~40 residue sequence that forms a helix loop helix structure. Multiple HEAT motifs in sequence, stack up in parallel and give rise to a superhelical arch structure which is flexible and able to bind a variety of cargoes (Conti et al., 2006; Andrade et al., 2001).

Karyopherins can function to move cargo into or out of the nucleus and accordingly they are classified as importins or exportins. Their function is determined by their ability to recognise either nuclear import sequences (NLSs) or nuclear export sequences (NESs) present on the cargo. Some karyopherins bind to their cargo after it has been recognised by an adaptor protein (Macara, 2001; Mosammaparast and Pemberton, 2004). In some cases a karyopherin can carry out both import and export. For example, Exportin 4, known to be responsible for the export of SMAD3, has been shown to facilitate import of the transcription factors Sox-2 and SRY (Gontan et al., 2009).

Since karyopherins themselves translocate in and out the nucleus with their cargoes, a mechanism is required to define cargo binding, cargo release and their timely recycling so that they can repeat the cycle.

1.2.4 Ran and the Ran GTPase system

Ran is a member of the Ras superfamily of small GTPases. As such, it can be found in the GTP or GDP bound state. Nucleotide binding occurs through the G-domain, in which the switch I and switch II loops are present (Milburn et al., 1990).

Depending on the nucleotide bound the switch regions adopt distinctly different conformations (Vetter and Wittinghofer, 2001).

RanGTP is present at high concentrations in the nucleus, where it triggers release of newly imported cargo from importins and promotes formation of export complexes (Weis, 2003). GTP hydrolysis and the resulting conformational switch in Ran drive dissociation from Imp β and Crm1 release of cargo in the cytoplasm. Therefore the processes of active import and export create a flux of RanGTP out of the nucleus, followed by GTP hydrolysis and an accumulation of RanGDP in the cytoplasm. In the absence of a replenishing system, nuclear RanGTP depletion would bring shuttling to a halt.

In order to replete the nuclear RanGTP pool RanGDP is transported back to the nucleus and the GDP nucleotide is exchanged for a GTP. Nuclear transport factor 2 (NTF2), a transport factor with no similarity to the karyopherins, specifically recognises and binds RanGDP. NTF2 transports RanGDP to the nucleus by virtue of its ability to bind FG-Nups and traverse the NPC (Moore and Blobel, 1994). Once in the nucleus the nucleotide is exchanged.

Ran binds guanine nucleotides with high affinity. After hydrolysis of GTP to GDP, in order to re-load Ran with GTP, guanine exchange factors (GEFs) are required (Vetter and Wittinghofer, 2001). The GEF for Ran is regulator of chromosome condensation 1 (RCC1) (Bischoff and Ponstingl, 1991a; 1991b). RCC1 is anchored in the nucleus by association with chromatin via the histones H2A and H2B (Nemergut et al., 2001). RCC1 binds Ran and forces the switch II region to adopt a conformation that displaces the so-called P-loop of Ran. P-loops are G-protein regions that are critical for nucleotide binding (Vetter and Wittinghofer, 2001). Thus the Ran/GDP interaction is destabilised allowing for nucleotide exchange and the replenishment of nuclear RanGTP.

Ran and the Ran GTPase system therefore orchestrate nucleocytoplasmic transport by providing the energy and directionality for nuclear import and export cycles (summarised in Figure 1.5).

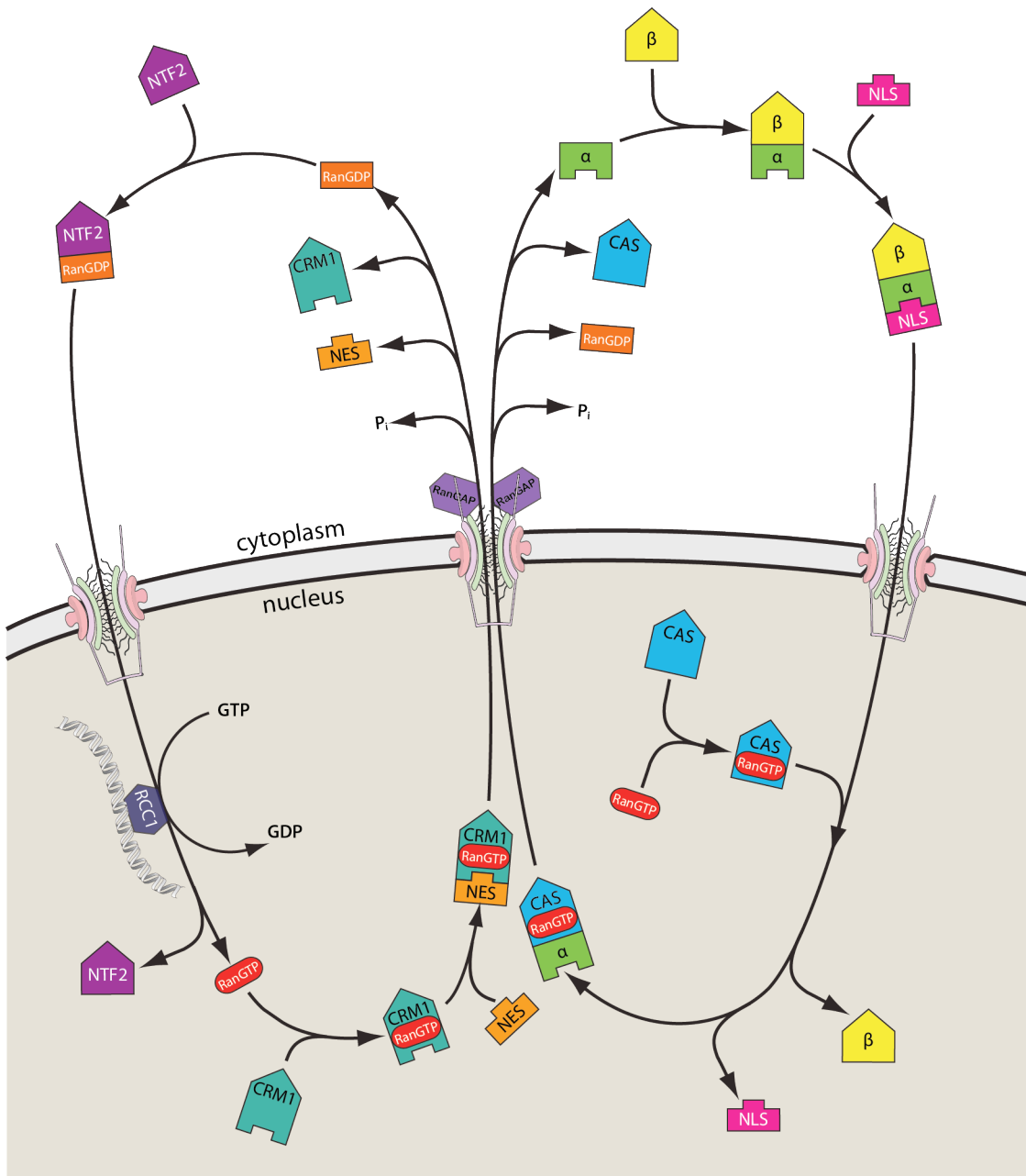


Figure 1.5 Overview of nucleocytoplasmic transport.

An overview showing the Impα/β import (right) and Crm1 export (left) cycles and the Ran/RanGTPase system that maintains and drives them.

1.2.5 Nuclear import

Proteins with an exposed or physically accessible NLS are recognised in the cytoplasm by importins, which enable translocation through the NPC. An NLS and the appropriate importin are the minimum requirements for facilitated translocation (Palacios et al., 1997). This can be demonstrated by the fusion of an NLS to a non nuclear protein, which consequently accumulates in the nucleus (Goldfarb et al., 1986).

The classical NLS sequence is a simple stretch of five basic amino acids KKKRK (Goldfarb et al., 1986). Alternatively, some proteins possess a bipartite NLS, which is comprised of two basic clusters separated by a spacer usually 10 residues long (Dingwall and Laskey, 1998). Other sequences also exist, such as the SPS motif of ERK, which is recognised by importin 7 (Chuderland et al., 2008). In the case of the classical monopartite and bipartite NLSs, the importin responsible for their recognition is importin β (Imp β). Imp β was initially identified because of its ability to bind these basic sequences. Binding however, is not direct, but rather occurs through the adaptor importin α (Imp α) (Görlich et al., 1995; Chi et al., 1995). Imp α directly recognises NLSs through an NLS-binding domain adjacent to its Imp β binding domain (Görlich et al., 1995). The NLS binding domain consists of 10 armadillo (ARM) repeats which much like the HEAT repeats of Imp β , form a flexible superhelical structure, with a concave surface through which it can accommodate different cargoes (Andrade et al., 2001). An array of binding pockets available within the ARM repeats is differentially used to bind different NLSs. Monopartite and bipartite NLSs bind to a different number of pockets and even within common pockets form different interactions. Therefore it does not necessarily mean a bipartite NLS is bound with higher affinity (Conti and Kuriyan, 2000; Kosugi et al., 2009).

Imp β , like most karyopherins do, can also directly recognise cargo using its 19 HEAT repeats in distinctly different ways. Parathyroid hormone related protein (PTHrP) is bound directly, using the N-terminal HEAT repeats, as opposed to the C-terminal repeats used to bind Imp α (Cingolani et al., 2002). In contrast, to bind sterol regulatory element binding protein 2 (SREBP-2), Imp β adopts a relatively more open conformation forming a greater number of interactions compared to PTHrP and Imp α (Lee et al., 2003).

Because importins are able to directly interact with the FG-Nups, importin/cargo complexes dock onto the NPC. As explained in section 1.2.2, translocation occurs through sequential interactions between importins and the FG-Nups occupying the NPC channel. Once the importin/cargo complex arrives on the nucleoplasmic face of the NPC, the cargo is released, which is triggered by binding of RanGTP.

The structure of the Imp β /RanGTP complex shows that Ran forms extensive interactions with the concave surface of the HEAT repeat arch (Vetter, Arndt, et al., 1999). Out of the 19 HEAT repeats of Imp β , the G-domain of Ran binds the first three N-terminal HEAT repeats, as well as HEAT repeat 8 and HEAT repeats 12-14. Thus, RanGTP binding is mutually exclusive with that of known cargo because of an overlap in binding sites. Moreover Ran binding induces a more extended conformation of the Imp β arch which may be less compatible with cargo binding (Cook et al., 2007).

In the situations where cargo is bound via Imp α , it is proposed that RanGTP induced dissociation of Imp β leads to a destabilisation of the Imp α /cargo interaction. This occurs because in the absence of Imp β , the Imp β binding sequence binds the NLS binding domain of Imp α thereby displacing and releasing the cargo (Goldfarb et al., 2004; Kobe, 1999; Harreman et al., 2003). Interactions between Imp α and nucleoporins that promote cargo release have also been shown to play a role (Gilchrist et al., 2002; Matsuura and Stewart, 2005). Finally, it has been proposed that Cse1/CAS, the exportin for Imp α also promotes cargo release from Imp α (Gilchrist et al., 2002). It is possible that all three mechanisms may contribute to cargo release.

1.2.6 Nuclear export

Upon RanGTP binding and consequent cargo release, importins directly translocate back to the cytoplasm in an energy and Ran independent manner (Kose et al., 1999; Görlich and Kutay, 1999). The adaptor Imp α however, is exported by the exportin CAS (cellular apoptosis susceptibility, or Cse in yeast), yet another protein composed of multiple tandem HEAT repeats (Solsbacher et al., 1998). The only export cargo known for CAS is Imp α , to which it binds with high

affinity. CAS, Imp α and RanGTP form a ternary complex, in which Imp α is seen in the autoinhibited state, suggesting it can only be bound and exported after cargo release (Kobe, 1999).

One of the most intensely studied and versatile exportins is chromosome maintenance 1 (Crm1 or Xpo1) (Güttler et al., 2010). Crm1 shuttles between the nucleus and the cytoplasm mediating export of a broad range of structurally and functionally unrelated proteins (Ho et al., 2000; Fornerod et al., 1997; Xu et al., 2012; Fu et al., 2013). Like CAS, Crm1 forms a ternary complex with RanGTP and its cargo. Crm1 binds either cargo or RanGTP weakly, but binds both cooperatively, to form a ternary complex (Paraskeva et al., 1999; Petosa et al., 2004). The ternary complex translocates to the cytoplasm and after hydrolysis of the Ran bound GTP the cargo is released from Crm1 (Kutay et al., 1997; Fornerod et al., 1997).

1.2.7 Crm1

Crm1 is a 120 kDa protein made up of 21 HEAT repeats, which are thought to adopt a horseshoe-like conformation (Figure 1.6 A) (Monecke et al., 2009). When Crm1 is not bound by Ran, the NES-binding hydrophobic cleft, which is formed by HEAT repeats 11 and 12, is inaccessible (Güttler et al., 2010; Dong et al., 2009). Interestingly, unlike the other karyopherins mentioned, cargo is not bound via the inner arched surface, but on the outer, which is where the NES binding cleft is located.

In addition to a closed cleft two additional structural features characterise the inactive conformation of Crm1 (Figure 1.6 B). The highly conserved loop connecting the helices of HEAT repeat 9 (H9 loop) interacts with the back of the NES binding cleft promoting a closed conformation (Saito and Matsuura, 2013; Monecke et al., 2013). Finally, the second helix of HEAT repeat 21 (H21B), instead of being packed against adjacent helices, crosses the horseshoe shape and interacts with HEAT repeat 9 and 10 on the inner concave surface. In doing so the H9 loop inhibitory conformation is stabilised (Dong et al., 2009; Saito and Matsuura, 2013; Fox et al., 2011).

For Crm1 to adopt the active state helix H21B must pack in the same plane as the rest of the helices forming the horseshoe, and the H9 loop must be

displaced from behind the NES binding cleft (Fox et al., 2011; Saito and Matsuura, 2013). These conformational changes have been employed in both proposed models attempting to explain binding cooperativity in ternary complex formation (Crm1/RanGTP/cargo).

Saito and Matsuura proposed that first, RanGTP binds to the inner concave surface and displaces helix H21B. This rearrangement would facilitate closure of the horseshoe, which in turn would displace the H9 loop and allow opening of the NES cleft. The conformation can then be stabilised by NES binding, explaining positive cooperativity (Saito and Matsuura, 2013).

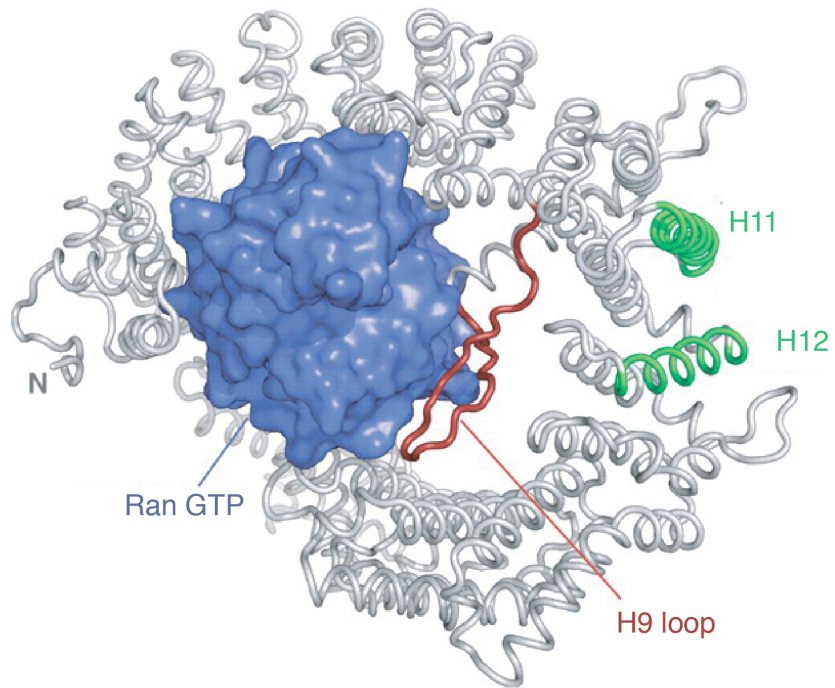
Monecke et al. propose that unliganded Crm1 exists in equilibrium between closed and open conformations, defined by the states of the H9 loop and H21B helix. Interaction with either RanGTP or cargo stabilises the compact horseshoe state, which corresponds to an open NES cleft. This initial event makes binding of the second component energetically more favourable (Monecke et al., 2013).

One model is based on induced fit mechanism while the other on a conformational selection, but both models rely on the same key features: rearrangement of the H21B helix, displacement of the H9 loop and opening of the NES groove driven by a compaction of the horseshoe shape resulting in an open NES binding cleft.

1.2.7.1 *Leptomycin B*

Leptomycin B (LMB) is a frequently used small molecule inhibitor of Crm1. It is a 540Da polyketide, which is able to covalently modify Cys528 within the NES binding cleft of Crm1 (Kudo et al., 1999). It has recently been shown that after LMB forms a covalent bond to the reactive cysteine Cys528, a subsequent reaction driven by the NES binding site itself, leads to hydrolysis of the LMB molecule (Q. Sun et al., 2013). Although LMB binding is sufficient to inhibit recognition of NES targets, based on a Crm1/LMB crystal structure, the authors suggest the hydrolysis reaction optimises the LMB-Crm1 interaction, forming a basis for the potency and longevity of the inhibition.

A



B

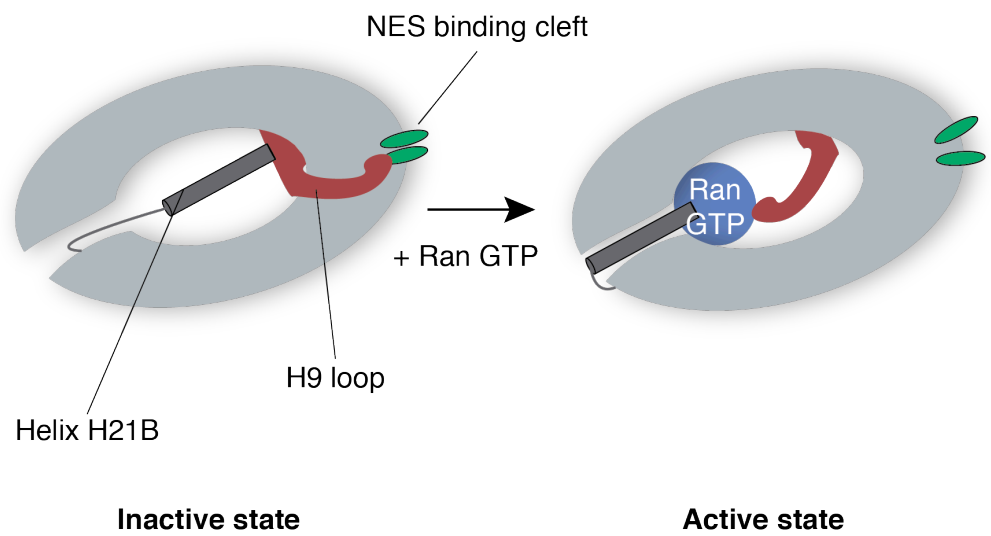


Figure 1.6 Structure of Crm1.

A. Crm1 (grey) bound by RanGTP (blue). When bound by RanGTP Crm1 adopts the active state. In this state, the NES binding cleft, which is formed by helices of HEAT repeats 11 and 12 (green), is open and can bind an NES. The H9 loop is shown in red. From Monecke et al. Crystal Structure of the Nuclear Export Receptor CRM1 in Complex with Snurportin1 and RanGTP (2009) *Science* 324(5930): 1087-1091. Reprinted with permission from AAAS **B.** Schematic representation of the inactive and active states of Crm1. Left: In the inactive state, when Crm1 is not bound by RanGTP, the NES binding cleft is closed and inaccessible to NESs. The closed conformation is stabilised by interactions with the H9 loop, which itself is stabilised in the inhibitory conformation by helix H21B. Right: Upon Ran binding helix H21B and the H9 loop are displaced, allowing opening of the NES binding cleft.

1.2.7.2 Cargo recognition by Crm1

Multiple mutagenesis and computational studies have led to the determination of the following leucine rich NES consensus sequence recognised by Crm1: $\Phi^1-X(2-3)-\Phi^2-X(2-3)-\Phi^3-X-\Phi^4$ (in which Φ is any hydrophobic residue, x is any amino acid). However the consensus is so broad that it frequently appears in proteins without necessarily acting as a functional NES (Henderson and Eleftheriou, 2000; la Cour et al., 2004; Kutay and Güttinger, 2005; Engelsma et al., 2004).

More recent structural studies have revealed how Crm1 is able to recognise such a broad set of NESs. Guttler et al. showed that the NES binding cleft does not adapt to accommodate for the varying positions of the hydrophobic residues. Instead different NES ligands bind to the same set of hydrophobic residues in the rigid NES binding cleft, docking to the NES cleft with strikingly different conformations. For example, the spinophilin NES binds the cleft as a helix, while the Rev NES binds in an extended conformation (Güttler et al., 2010). In fact the authors propose that there is a Rev-like NES consensus: $\Phi^0\Phi^{1Pro}-X(2-3)-\Phi^2-X(2-3)-\Phi^3-X-\Phi^4$.

The affinity of leucine rich NESs for Crm1 is relatively weak. Other exportins, including CAS, bind their cargo in the low-nanomolar range, whereas in most cases Crm1 substrates exhibit a 100-500 fold lower affinity for Crm1 binding (Kutay et al., 1997; Askjaer et al., 1999; Paraskeva et al., 1999; Kutay et al., 1998). The low affinity appears to be required for normal function of the export cycle, since synthetic high affinity NESs, which bind Crm1 with high affinity, lead to entrapment of the ternary complex at the NPC. This suggests that weak NES-Crm1 affinity has been selected to allow for efficient release of cargo and NPC dissociation (Engelsma et al., 2004).

1.2.7.3 Crm1 cargo release

Dissociation of export ternary complexes is triggered by hydrolysis of the Ran bound GTP to GDP. The same hydrolysis reaction is what dissociates importin/Ran complexes that are recycled back to the cytoplasm. As mentioned above, the switch regions of Ran adopt different conformations depending on

whether GTP or GDP is bound. In addition, a second major conformational change is the rearrangement of the C-terminal extension. In the GDP form the C-terminal extension packs against the G-domain and sterically hinders interaction with karyopherins (Vetter, Nowak, et al., 1999). The C-terminus rearrangement is perhaps the most important change, as a truncated mutant is able to bind Crm1 while bound to GDP (Nilsson et al., 2002). Hydrolysis of GTP and the consequent conformational changes, change the affinity of Ran to bind karyopherins from subnanomolar for the GTP-bound state, to 10 μ M for the GDP bound state (Vetter, Arndt, et al., 1999; Görlich et al., 1996).

Ran itself, like all GTPases, features low intrinsic activity that can be enhanced several-fold by regulatory proteins (Klebe et al., 1995). The timing of GTP hydrolysis is controlled by cytoplasmic proteins. When RanGTP arrives to the cytoplasm as part of the export complex, Ran binding protein 1 (RanBP1) and RanBP2 can bind it (Bischoff and Görlich, 1997; Bischoff et al., 1995). RanBP1 is a 23kDa soluble protein that can bind to RanGTP via its Ran binding domain (RanBD) (Coutavas et al., 1993). RanBP2 is a nucleoporin component of the NPC fibrils that extend into the cytoplasm and possesses four RanBDs (Delphin et al., 1997). Both RanBPs promote dissociation of RanGTP and stimulate Ran GTPase activating protein (RanGAP) mediated hydrolysis (Bischoff et al., 1995; Bischoff and Görlich, 1997).

RanGAP features a conserved N-terminal GAP domain and a C-terminus with which it binds to RanBP2 at the cytoplasmic face of the NPC (Mahajan et al., 1997; Matunis et al., 1996; Haberland and Gerke, 1995). RanGAP forms extensive interactions with RanGTP, thereby correctly orienting and stabilising the catalytically active conformation of Ran that enables GTP hydrolysis (Seewald et al., 2002).

1.2.8 Measuring nucleocytoplasmic transport

Being able to measure protein mobility is crucial for understanding protein regulation (Haché et al., 1999; Meyer et al., 2002; Johnson et al., 1999). Signal induced nuclear accumulation of a transcription factor or the shuttling of proteins

involved in mRNA transport can be highly dynamic and therefore methods are needed to assess kinetics.

Immunostaining involves fixation of samples and this only reveals bulk protein concentrations but does not address the dynamics of shuttling. For example, for a protein continuously shuttling between the nucleus and cytoplasm, if the export rate is significantly faster than the import rate the majority of the protein will be localised at the cytoplasm at steady state. Immunostaining will show the cytoplasmic location of the protein, but will not reveal the fact that the protein is continuously shuttling, unless the kinetics of movement can be manipulated. In this regard inhibition of Crm1 by LMB has proved useful in many cases, to demonstrate shuttling of apparently cytoplasmic proteins, including MRTFs (Vartiainen et al., 2007).

The classical heterokaryon assay is one way to assess shuttling properties of predominantly nuclear proteins (Flach et al., 1994). It involves the use of two nuclei from different species. Co-incubation of the nuclei allows a shuttling protein to exchange between the two nuclei, which can then be detected using species-specific antibodies in immunofluorescence.

Fluorescence recovery after photobleaching (FRAP) and fluorescence loss in photobleaching (FLIP) are two techniques which enable direct measurement of protein movement. They allow direct measurement of import and export rates of a protein. Both techniques were made possible by the discovery of green fluorescent protein (GFP) (Tsien, 1998). Expression of GFP tagged proteins enabled live cell imaging. Further discovery of GFP-like proteins allowed simultaneous observation of multiple events (Miyawaki, 2005; Day and Davidson, 2009). Further development led to more stable versions of these fluorophores, as well as photoactivatable GFP (Patterson and Lippincott-Schwartz, 2002). These developments paved the way to major advances in our ability to measure protein movement.

In FRAP, a region where the GFP-protein of interest is present is bleached using a high-intensity laser, and recovery of the signal by unbleached protein is measured. For example the whole nucleus can be bleached and the kinetics of movement of the non-bleached GFP-protein from the cytoplasm to the nucleus can be accurately measured (Snapp et al., 2003).

In FLIP the high-intensity laser is used repeatedly to constantly bleach a certain area and the effect on fluorescence in non bleached regions is monitored.

For example, if a protein appears to be equally distributed between the nucleus and cytoplasm, the high-intensity laser can be used to repeatedly bleach a specific spot in the cytoplasm. By measuring fluorescence intensity of the nucleus one can determine the speed at which the protein shuttles between the two compartments. If the protein does not shuttle, nuclear fluorescence should remain constant as the cytoplasm gradually bleaches. If however the protein does shuttle, as the nuclear and cytoplasmic compartments equilibrate nuclear fluorescence will decrease as well (Köster et al., 2005; Snapp et al., 2003).

There are many applications to these techniques but they fall beyond the scope of this thesis (reviewed in (Miyawaki, 2011; Köster et al., 2005; J. N. Henderson, 2006; Belaya, 2006)). Whether they are used in combination with pharmacological inhibitors, stimulus induced changes in steady state or even heterokaryon assays, FRAP and FLIP enable direct measurements of the kinetics of protein movement, and allow accurate investigation of protein regulation.

Shuttling is a function of import, export and possible interactions of a protein that may anchor it in a particular compartment. Since import and export are conferred by NLS and NES sequences respectively, then identification of these elements is crucial to characterising the shuttling behaviour of a protein. Although there are exceptions, a sequence suspected to be an export signal could be fused onto another protein and tested for its ability to confer export. This is the basis of the Rev export assay.

The Rev assay uses the HIV-1 Rev protein as a reporter for export activity. Rev is an RNA binding protein, which localises to nucleoli. Rev continuously shuttles between the nucleus and cytoplasm by virtue of identified and characterised NLS and NES sequences. Inactivation of the NES renders the protein localised to nucleoli. Shuttling can be restored upon fusion to its own NES sequence or any other functional NES sequence. Henderson and Eleftheriou employed this strategy to identify NESs and compare their relative strengths (Henderson and Eleftheriou, 2000). It should be noted that the assay relies on the ability of the NES to relocalise the Rev GFP fusion to the cytoplasm and so a NES must be sufficiently effective to compete with the Rev NLS, complicating the interpretation. There are cases where a known NES was too weak to score in the assay (B. R. Henderson and Eleftheriou, 2000).

1.2.9 Regulation of transcription factor activity through controlled localisation

Many signalling pathways culminate in the activation of transcription factors. Often transcription factors have restricted access to their targets due to cytoplasmic retention. Once activated, through masking or unmasking of NES or NLS elements, they can accumulate in the nucleus and activate their target genes. In most cases multiple levels of control exist and localisation is one step of the activation process (Whitmarsh and Davis, 2000; Ziegler and Ghosh, 2005).

The transcription factor NF-AT is cytoplasmic in resting cells (Rao et al., 1997; Crabtree, 1999). A rise in intracellular calcium concentration activates the phosphatase calcineurin, which dephosphorylates multiple residues on NF-AT. An intramolecular rearrangement unmasks at least one NLS which drives nuclear translocation (J. Zhu et al., 1998).

Nuclear factor κ B (NF- κ B) is also cytoplasmic in the absence of stimulation. Binding to inhibitor of NF- κ B (I κ B) retains NF- κ B in the cytoplasm by two mechanisms. First, association with I κ B masks the NLS of NF- κ B, and secondly I κ B contains an NES, which ensures cytoplasmic localisation (Ghosh et al., 1998; Ghosh and Karin, 2002; Hayden and Ghosh, 2004). Contrary to what was assumed for a long time, NF- κ B in fact continuously shuttles through the nucleus. LMB treatment is sufficient to cause nuclear accumulation, indicating that it is continuously imported and then also exported (Ghosh and Karin, 2002). In response to signals, I κ B is phosphorylated and marked for proteasomal degradation. I κ B is therefore rapidly degraded. As a consequence the NLS of NF- κ B is exposed allowing for nuclear accumulation (Ghosh et al., 1998).

The Forkhead transcription factor FKHR1 localisation is controlled by the kinase Akt (Brunet et al., 1999; Biggs et al., 1999). Phosphorylation by Akt results in association with 14-3-3 proteins, which possess an NES which drives nuclear export (Brunet et al., 1999; Rittinger et al., 1999).

Protein subcellular localisation can occur because of a simple change, for example detachment from anchorage and exposure of a localisation signal. In other cases multiple parameters can change, some for different durations. The net effect may be brought about by an imbalance of import/export rates, de-novo synthesis of

anchors and signalling kinetics. Tools such as photoactivatable and even switchable fluorophores and techniques such as FRAP and FLIP are powerful tools in the investigation of such mechanisms.

1.3 Actin

Actin is a highly conserved, abundant protein in eukaryotic cells. It is found primarily in two forms, the monomeric or globular form (G-actin) and the polymerised or filamentous form (F-actin). Interconversion between the two forms is a highly dynamic process, important for a vast range of cell functions including cell shape, motility, adhesion and division (Remedios et al., 2003). In order to be involved in such a variety of processes, actin is regulated by a multitude of proteins that can bind and control its polymerisation on a pan-cellular or very localised subcellular level (Remedios et al., 2003). Actin is also a target of post translational modifications such as methylation and oxidation (Raghavan et al., 1989).

Mammals possess six actin genes. The γ_{smooth} -actin and three α -actin proteins are expressed mainly in skeletal, cardiac and smooth muscle, whereas β -actin and γ_{cyto} -actin are expressed ubiquitously. All actins share at least 93% and up to 99% sequence similarity with one another and most variations are found in the N-terminus (Perrin and Ervasti, 2010; Herman, 1993). There is some evidence supporting isoform specific functions, reviewed in (Perrin and Ervasti, 2010). This thesis concerns a novel family of G-actin binding proteins, the MRTFs, whose activity is controlled by signal-induced fluctuations in G-actin concentration.

1.3.1 Monomeric actin

Monomeric actin (G-actin) is a 375 amino acid polypeptide chain that folds into two major domains, the α and β major domains. Each of these major domains is composed of two subdomains (see Figure 1.7). The α and β domains share relatively few contacts and are separated by a flexible hinge region, resulting in the formation of two clefts that can move relative to each other. The upper cleft, between subdomains 2 and 4, binds ATP and an associated Mg^{2+} , which bridge

and stabilise the α and β domains (Kabsch et al., 1990; Dominguez and Holmes, 2011). The bottom cleft, between subdomains 1 and 3, is lined predominantly by hydrophobic residues (Oda et al., 2009). This cleft forms important contacts between actin units within a filament, and is the major binding site for the majority of G-actin-binding proteins (ABPs) (Dominguez, 2004). Nucleotide binding in the upper cleft causes conformational changes in the lower cleft. This provides the basis of how nucleotide binding affects interactions between actin molecules in filaments or with ABPs (Kudryashov et al., 2010; Pfaendtner et al., 2009). Due to its structural flexibility and different nucleotide states actin can interact with many different proteins. This enables actin to be involved in many different processes and also for many proteins to regulate actin polymerisation (see table 1.1).

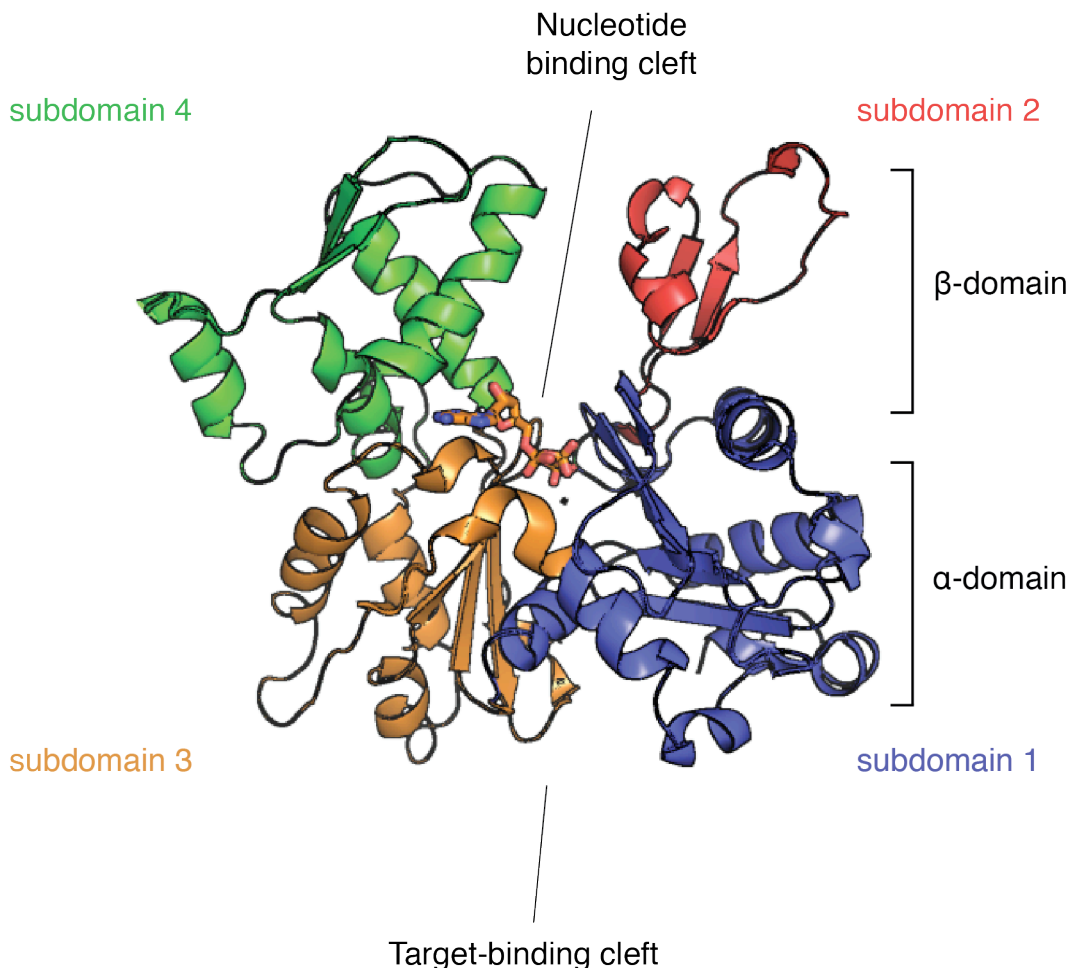


Figure 1.7 Structure of monomeric actin.

Ribbon representation of G-actin structure indicating the four subdomains in different colours. Subdomain 1 (residues 1-32, 70-144 and 338-372) is blue; subdomain 2 (residues 33-69) is red; subdomain 3 (residues 145-180 and 270-337) is orange; subdomain 4 (residues 181-269) is green. PDB2v52, rabbit Acta1, P68135.

Table 1: Actin binding proteins and their function

Protein	Function
Dia	Promotes nucleation and elongation of filaments. Associates with barbed ends. Recruits Profilin/actin complexes. Highly processive
Arp2/3 complex	Promotes branching. Binds to existing filaments and nucleates a branch that grows out at a 70° angle.
Profilin	Promotes polymerisation. Binds G-actin and prevents spontaneous nucleation. Also promotes nucleotide release, promoting actin-ATP availability. Recruited with actin to the + end of filaments and then dissociates.
ADF/Cofilin	Promotes actin filament disassembly. Binds actin filaments at minus end and promotes actin-GDP dissociation. Promotes G-actin recycling, as liberated monomers become available for plus end incorporation.
Gelsolin	Caps and severs actin filaments. Binds and caps plus end of filament. Capped filaments are readily disassembled by the action of cofilin, but Gelsolin itself possesses weak severing activity.
Tropomodulin	Capping. Binds and caps minus ends of filaments.
CapG	Capping. Binds and caps + ends and inhibits elongation.
Fascin	Bundles actin filaments. Binds and crosslinks filaments together.
WAVE	Nucleation promoting factor. Activates Arp2/3 complex in response to Rac signaling.
WASP	Nucleation promoting factor. Activates Arp2/3 complex in response to Cdc42 signaling.
IRSp53	Coordinates plasma membrane curvature to actin dynamics. Directly interacts with WASP and membrane.
MRTF	Links actin dynamics to transcription. Directly binds G-actin via its RPEL domain. Regulates transcription of multiple ABPs, actin regulators and actin itself.
Phactr1	Nucleocytoplasmic shuttling and interaction with protein phosphatase 1 (PP1) are regulated by actin. Actin competes with PP1 and Impα/β for binding.
RhoGAP12	Contains a single RPEL motif, through which actin regulates its ability to inactivate Rac.

1.3.2 Filamentous actin

G-actin possesses weak ATPase activity and since it preferentially binds ATP, ATP most often occupies the upper cleft. The conformational differences between ATP or ADP actin primarily involve two loops: the Ser14-loop and the sensor loop. These two loops embrace the phosphates of ATP, with Ser14 hydrogen bonding to the γ -phosphate. After hydrolysis and γ -phosphate release, Ser14 loses contact with the γ -phosphate and contacts the β -phosphate instead. In doing so the Ser14 loop moves the sensor loop into the space vacated by the γ -phosphate, thereby sensing nucleotide status. These conformational changes appear to be transmitted to subdomain 2 (Graceffa and Dominguez, 2003). The changes in subdomain 2 involve the D-loop which forms critical interactions with the next actin in a filament (Wawro et al., 2005). Since ATP stabilises the α and β major domains, γ -phosphate release also compromises the rigidity of the structure and allows the domains to move relative to each other (Galkin et al., 2002; Oda et al., 2009; Tirion et al., 1995).

Assembly of G-actin into filaments, is accompanied by an increase in ATPase activity, yielding ADP + Pi. Actin-ATP and actin-ADP-Pi are functionally indistinguishable, probably because the presence of Pi prevents the rearrangement of Ser14 and sensor loops. Release of Pi yields actin-ADP, which leads to increased dissociation of the actin molecule from the filament and depolymerisation.

F-actin is a helical arrangement of two strands where interaction between actins within the same strand are stronger than those between strands (Hanson and Lowy, 1963; Holmes et al., 1990). Actin-ATP which has been incorporated into a filament is conformationally different to non-polymerised actin, consistent with the fact that once polymerised ATPase activity is enhanced (Tirion et al., 1995; Lorenz et al., 1993; Oda et al., 2009). The change has been described as a “flattening” of the molecule.

As seen for many biological polymers, F-actin does not form crystals suitable for analysis by X-ray crystallography (Tirion et al., 1995). Hence several models exist to describe F-actin, assembled from the available G-actin structures (Holmes et al., 1990; Lorenz et al., 1993; Tirion et al., 1995). No single model is able to describe F-actin, as differences in the twist of the helix and the tilt between units within the same filament can be seen (Egelman et al., 1982; Galkin et al.,

2002; Schmid et al., 2004). F-actin is therefore structurally polymorphic and should probably be viewed as a collection of different states (Galkin et al., 2010).

1.3.3 Dynamics of actin polymerisation

Actin polymerisation can be simulated *in vitro* using purified actin. In low salt conditions actin maintains its monomeric form. Increasing salt concentration (particularly Mg^{2+}), leads to the rapid formation of F-actin (Carlier, 1991a; 1991b; Korn, 1982). The filaments possess a barbed end (plus end) and a pointed end (minus end). At the plus end, actin monomers assemble at a faster rate than at the minus end (Pollard, 1986).

When polymerisation is initiated *in vitro* G-actin is depleted as the filaments are formed. Eventually a balance between G-actin and F-actin is achieved, at which point filament length remains constant, but is a result of constant association and dissociation of G-actin; an effect known as treadmilling. The concentration of actin required to maintain this steady state, the critical concentration (C_c), is a function of the rate of association and dissociation of G-actin. In addition the C_c is different for each end of the filament, $0.1\mu M$ for the plus end and $0.7\mu M$ for the minus end (Pollard and Borisy, 2003). This difference essentially means that as G-actin concentration drops during a polymerisation reaction, the minus end stops growing while the plus end continues. Moreover as ATP is hydrolysed by incorporated actin, actin-ADP is formed. When addition of actin-ATP to the minus end slows down enough, the minus end is occupied by actin-ADP and has a higher dissociation rate. The minus end therefore begins to depolymerise. Actin monomers are hence continuously fluxed through the filament, added as actin-ATP to the continuously growing plus end, converting to actin-ADP and dissociating once reaching the receding minus end “front” (Pollard and Borisy, 2003).

Cellular concentrations of actin can be up to 400 fold higher than its critical concentration ($65\text{-}300\mu M$), yet a G-actin pool is able to be maintained and F-actin formation is controlled, dynamic and can occur at incredibly fast rates (Remedios et al., 2003). This is achievable through the actions of a multitude (over 160) of actin binding proteins, each acting in a way that promotes or inhibits F-actin formation (Remedios et al., 2003) (See table 1.1). Some ABPs can nucleate, stabilise or

sever filaments. In addition some ABPs sequester G-actin or promote nucleotide exchange and replenish G-actin-ATP. Together these regulators of actin polymerisation cooperate to bring about events such as the classical example of protrusion of the leading edge of a motile cell (Pollard and Borisy, 2003) (See Figure 1.8).

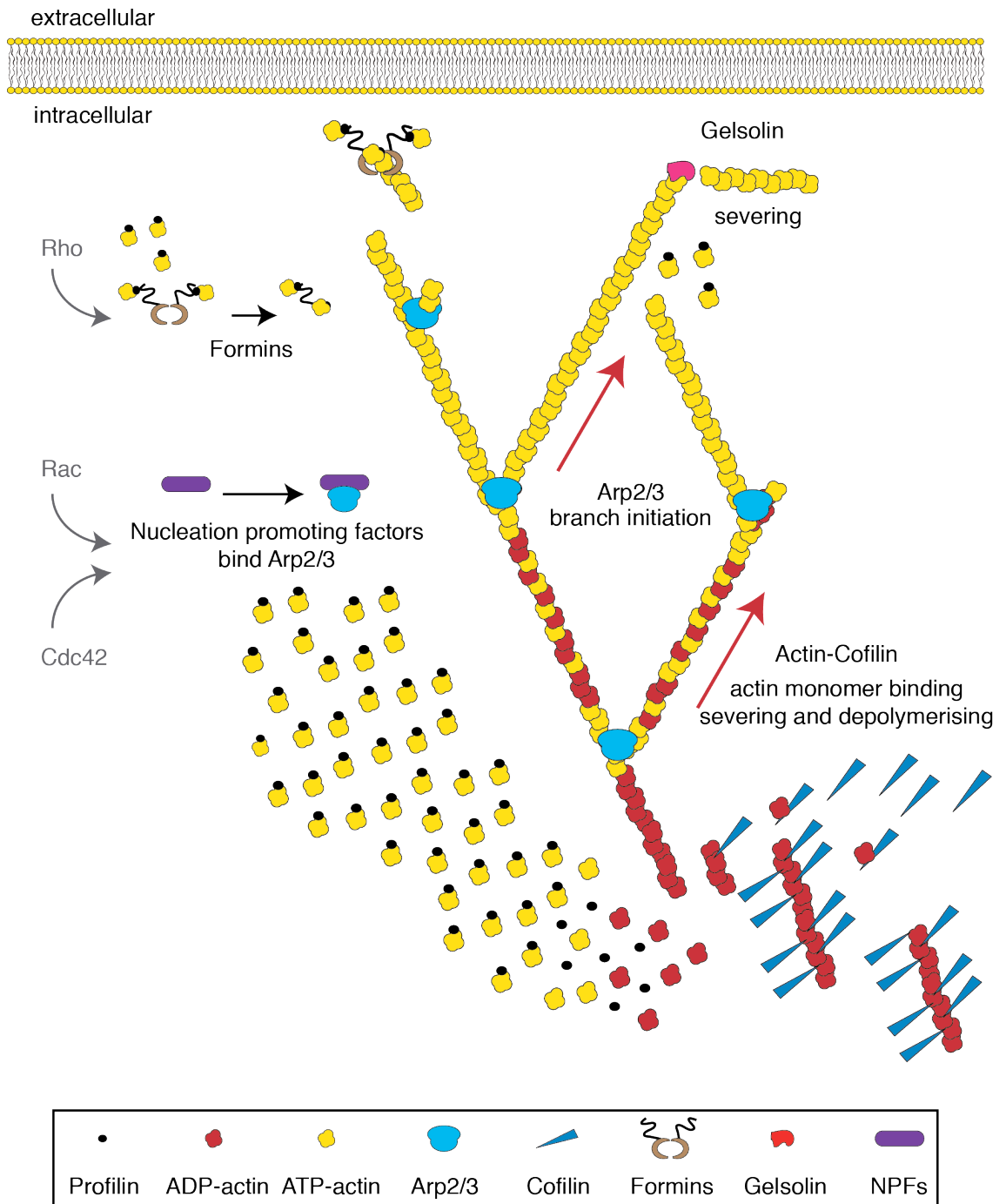


Figure 1.8 Regulation of actin filament dynamics by actin binding proteins.

A variety of actin binding proteins with different functions, cooperate to regulate assembly and disassembly of F-actin filaments. Formins catalyse *de novo* filament nucleation and elongation; Gelsolin caps and severs filaments; Nucleation promoting factors such as WAVE and WASP activate arp2/3 causing branching of filaments; Profilin and Cofilin promote polymerisation and depolymerisation respectively. Adapted from (Pollard and John A Cooper, 2009).

1.3.4 Control of actin cytoskeleton by Rho GTPases

Actin dynamics are directly controlled by the above mentioned regulators. The regulators themselves are subject to incoming signalling, which affects their own function, enabling control over F-actin formation.

The Rho family of GTPases plays a central role in spatial and temporal control of actin dynamics. This family consists of 20 members, of which RhoA, Rac and Cdc42 are the best studied (Heasman and Ridley, 2008). Like other members of the Ras superfamily, Rho GTPases are GTP binding proteins that have weak intrinsic GTPase activity. Signal induced association with GAPs and GEFs, regulates their GTPase activity or nucleotide loading, defining whether they are in the GTP bound active state, or the GDP bound inactive state. Nucleotide binding defines conformational state and therefore binding to proteins which they can activate.

Cdc42 is important for cell polarity and filopodia formation. Filopodia are finger-like projections thought to be important for a cell to sense its environment (Gupton and Gertler, 2007). Filopodia contain F-actin bundles, which are formed due to the combined activities of multiple ABPs orchestrated by Cdc42 (Fig 1.9) (Ridley, 2011).

Out of the three Rac isoforms (Rac1, Rac2 and Rac3) Rac1 is the best studied and unlike the other isoforms, it is ubiquitously expressed (Didsbury et al., 1989). Rac proteins affect activity of multiple ABPs, to stimulate formation of lamellipodia and membrane ruffles (Wittmann and Waterman-Storer, 2001). These structures are thin cytoplasmic sheets formed at the front of a migrating cell. The force required for the protrusions is generated by branched actin polymerisation, accomplished by ABP activity organised by activated Rac (Fig1.9) (Lauffenburger and Horwitz, 1996; Ridley, 2011; Ballestrem et al., 2000).

RhoA, RhoB and RhoC, share high homology and when overexpressed in fibroblasts they all induce stress fibre formation (Wheeler and Ridley, 2004). RhoA is the prototypical member of the Rho family. Because it can associate with many different proteins RhoA is involved in multiple signalling pathways. Two of the main effectors of RhoA are the Rho associated coiled coil forming kinase (ROCK) and diaphanous related formin 1 (Dia1) (Campellone and Welch, 2010). Activated

ROCK phosphorylates the kinase LIMK1. LIMK1 in turn phosphorylates and inactivates cofilin, thereby stabilising actin filaments. Dia1 nucleates and assembles actin filaments using its FH2 domain (Campellone and Welch, 2010; Wallar et al., 2006). Thus ROCK and Dia1 cooperate to promote actin polymerisation and stress fibre formation (Figure 1.9).

The clostridial enzyme C3-transferase has been widely used in the investigation of Rho function. C3 transferase is able to irreversibly ADP ribosylate and inactivate RhoA, Rho B and RhoC (Wilde and Aktories, 2001).

Rho GTPases are also targets of regulatory phosphorylation and ubiquitin mediated proteasomal degradation (P Lang, 1996; H.-R. Wang et al., 2003). An additional layer of regulation is post translational modification and scaffold mediated recruitment of the regulatory GAPs and GEFs that affect RhoGTPase activity (Marinissen and Gutkind, 2005).

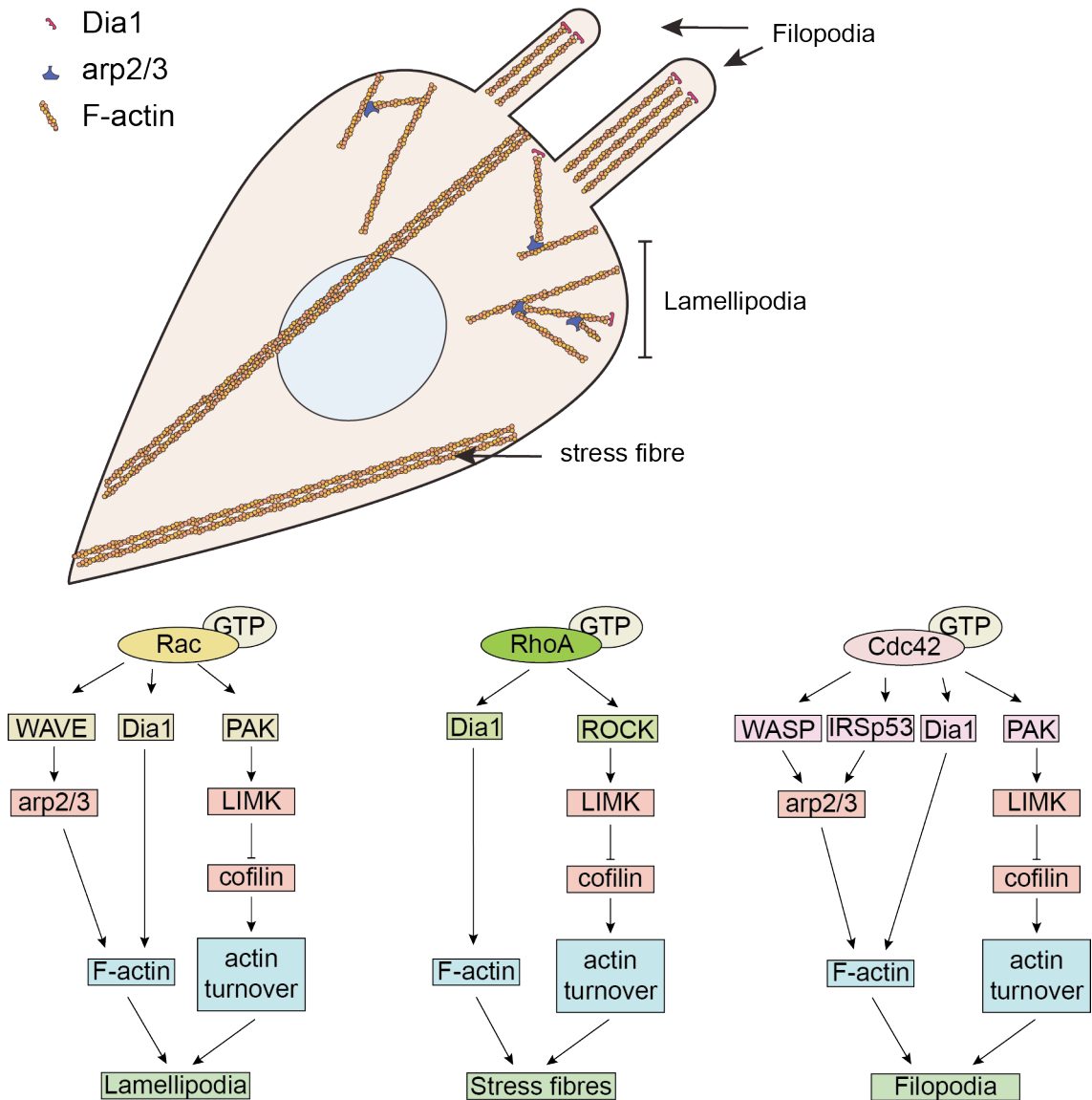


Figure 1.9 Rho GTPases orchestrate the functions of ABPs to regulate actin dynamics.

The Rho GTPases Rac, RhoA and Cdc42 utilise different sets of actin binding proteins to regulate F-actin assembly. Rac stimulates lamellipodia formation in migrating cells. RhoA stimulates formation of stress fibres facilitating cell motility and contractility. Cdc42 stimulates formation of filopodia, which play a role in sensing the extracellular environment.

1.3.5 RPEL motif containing proteins

The RPEL motif is a G-actin-binding element (Guettler et al., 2008) present in some proteins which have been shown to be regulated by actin. Three families of RPEL proteins have been described.

Two RhoGAP subfamilies have been shown to possess single RPEL motifs, of which the Rac-specific GAP RhoGAP12 is currently under investigation in the laboratory (Dr J. Diring, unpublished data). Actin inhibits RhoGAP12 activity by competing with Rac binding.

The transcription cofactor MRTF-A senses G-actin concentrations by direct binding through its RPEL domain. The RPEL domain, contains three RPEL repeats that cooperatively bind actin to regulate MRTF-A nucleocytoplasmic shuttling and activity (Vartiainen et al., 2007; Miralles et al., 2003). MRTF-A will be described in more detail in the next section.

The phosphatase and actin regulator (Phactr) family of proteins is also regulated by actin by virtue of RPEL motifs. The family contains four members, Phactr1, Phactr2, Phactr3 and Phactr4. The founding member, Phactr1, was first identified in a yeast-two-hybrid screen designed for the detection of protein phosphatase 1 (PP1) interacting proteins (P. B. Allen et al., 2004). It was found to interact with PP1, but also with G-actin via sequences containing RPEL motifs, which are highly conserved between family members.

Using the GST fused RPEL motifs of Phactr3, Sagara and colleagues showed that actin binding was direct and was important for the full length protein to regulate PP1 activity and cell motility (Sagara et al., 2009). Phactrs possess four RPEL motifs. One N-terminal and three clustered in the C-terminus, adjacent and partly overlapping with the extreme terminal PP1 binding site (Wiezlak et al., 2012). The C-terminal RPELs are separated by short spacers and are referred to as the Phactr RPEL domain. It has been shown that PP1 and actin competed for binding to the RPEL domain of Phactr1 (Wiezlak et al., 2012; Huet et al., 2013). Structural analysis revealed that each RPEL motif, including the N-terminal RPEL interacts with one actin molecule (Mouilleron et al., 2012).

In their analysis, Huet and colleagues showed that in NIH-3T3 cells, all Phactr family members exhibit pancellular localisation at steady state. Using FRAP, they demonstrated that Phactr4 is continuously imported. Upon bleaching of the

nucleus, the authors observed recovery of fluorescence, meaning that unbleached Phactr4-GFP was imported from the cytoplasm. This observation suggests Phactr4 may shuttle between the nucleus and cytoplasm (Huet et al., 2013).

A separate analysis of Phactr localisation in NIH-3T3 cells showed that Phactr1 and 2 were predominantly cytoplasmic while Phactr 3 and 4 were pan-cellular (Wiezlak et al., 2012). Serum induced depletion of the G-actin pool led to nuclear accumulation of Phactr1, but not the other family members. Detailed molecular analysis showed that actin competes with importins for binding to nuclear localisation signals associated with the RPEL elements and the integrity of the RPEL motifs is required for cytoplasmic localisation.

LMB treatment did not lead to Phactr1 nuclear accumulation suggesting that Phactr1 is anchored in the cytoplasm and blockage of export alone is not sufficient for nuclear accumulation (Wiezlak et al., 2012). Alternatively Phactr1 is exported by a factor other than Crm1. This notion is supported by the observation that LMB does not potentiate the duration of serum induced Phactr1 nuclear accumulation (Magdalena Kratochvílova, unpublished).

RhoGAP12, MRTFs and Phactrs demonstrate how the status of actin in cells can be directly sensed by RPEL domain containing proteins, which coordinate actin dynamics to their respective function; Rac GAP activity in the case of RhoGAP12, transcription in the case of MRTF and PP1 regulation in the case of Phactr. Investigations of RhoGAP, MRTF and Phactr regulation required manipulation of actin binding and polymerisation properties. For this reason actin binding toxins played a crucial role and were extensively used.

1.3.6 Actin binding drugs

Actin conformation is crucial for defining the interactions it can make and therefore its function. Toxins that are able to bind actin can directly or indirectly obscure actin interaction surfaces. Small molecules that directly bind actin can be divided into two main categories, those that disrupt filament assembly and those that promote it (reviewed in (Fenteany and S. Zhu, 2003)).

1.3.6.1 *Cytochalasins*

Cytochalasins are a group of membrane permeant fungal metabolites best known for their ability to destabilise actin filaments. The mode of action is possibly the sum of different effects on actin function. Cytochalasins have been reported to bind the barbed end (plus end) of filaments and inhibit both association and dissociation of monomers. They have also been shown to promote ATP hydrolysis by stabilising dimer formation leading to increased actin-ADP concentration. Cytochalasin B (CB) and cytochalasin D (CD) are the most frequently used, with preference for CD as it is more selective. CB was shown to also inhibit monosaccharide transport (Cooper, 1987; Peterson and Mitchison, 2002).

1.3.6.2 *Latrunculins*

Latrunculins are generally more potent than cytochalasins at inhibiting actin polymerisation. Latrunculin A, the most potent family member binds actin in a 1:1 stoichiometry and in addition prevents nucleotide exchange (Coué et al., 1987). Insights from a high resolution structure suggest binding of Latrunculin A to actin causes conformational changes that lock the nucleotide in place and disfavour polymerisation. Latrunculin B binds actin in a very similar way but is less potent (Morton et al., 2000). Both drugs bind G-actin reversibly (Spector et al., 1983).

1.3.6.3 *Phalloidin*

Phalloidin is a heptapeptide that binds and stabilises F-actin. On doing so phalloidin lowers the critical concentration ten-fold and promotes filament polymerisation (J A Cooper, 1987). Since Phalloidin is not membrane permeant it is mostly used in a fluorophore conjugated form, to label F-actin in permeabilised fixed cells (Wulf et al., 1979).

1.3.7 Role of nuclear actin

Evidence suggesting the presence of actin in the nucleus was first obtained 40 years ago (Lane, 1969). Given its size, 42kDa, actin is at the limit of being capable of passive diffusion through the nuclear pore complex and it is possible it could freely move between the nucleus and cytoplasm (Bohnsack et al., 2006). G-actin rapidly shuttles between the nucleus and cytoplasm. Nuclear import is mediated by importin 9 and export by exportin 6 (Dopie et al., 2012; Stüven et al., 2003).

Using FRAP and FLIP Dopie and colleagues, showed that actin exchange between the two compartments occurs rapidly suggesting equilibration between the two can be fast (Dopie et al., 2012). In cells expressing actin-GFP, nuclear fluorescence recovered in 3 phases after bleaching. Fast recovery is probably by rapid import of G-actin in the nucleus. The second phase is likely to be due to actin exchange with the bleached short actin filaments, and the short phase is probably the exchange of actin with stable actin-containing complexes. Importantly, fluorescence recovery of cells expressing the non-polymerising derivative actin R62D GFP occurred in two phases, supporting the idea that the second recovery phase is filament associated.

Analogous to the example with transient or sustained ERK signalling, the same concept can apply with nuclear actin. A transient change in the G- to F-actin ratio in the nucleus would differentially affect nuclear actin binding proteins according to the stability of their association with actin.

G-actin has long been shown to have a role in the nucleus, namely, in gene expression. It has been shown to regulate activity of the transcription co-factor MRTF, as well as play a role in promoting transcription by all three polymerases (Vartiainen, 2008; Percipalle, 2013). It has also been shown to be a component of chromatin remodelling complexes, such as INO80 and the histone acetyltransferase NuA4 (Shen et al., 2000; Galarnau et al., 2000). The existence of actin filaments in the nucleus, however, has been elusive and controversial.

Nuclear actin concentration is generally low and detection of nuclear filaments proved difficult, while G-actin or oligomers are readily detectable (Schoenenberger et al., 2005; Jockusch et al., 2006). A significant amount of evidence indirectly pointed towards the possibility of nuclear actin filaments,

including the nuclear localisation of F-actin assembly proteins such as arp2/3 and WASP (Wu et al., 2006; Yoo et al., 2007).

Recently, Baarlink and colleagues showed that serum stimulation of fibroblasts leads to nuclear actin filament formation (Baarlink et al., 2013). Visualisation of the filaments was accomplished using “Lifeact”, a 17 amino acid peptide able to bind actin monomers and filaments (Riedl et al., 2008). Lifeact was fused to an NLS, yielding the nuclear restricted Lifeact-NLS-GFP. Upon serum stimulation rapid and transient formation of actin filaments was observed, and this was dependent on the presence of Dia1. In addition, by using a photoactivatable tool, nuclear Dia1 was specifically activated, showing that nuclear actin polymerisation could be signal-inducible. Importantly this was accomplished without overexpressing actin, which was a common caveat of previous studies.

With the presence of actin filaments in the nucleus confirmed, many questions arise. Does the signal get from the cell membrane to nuclear actin regulators directly or do they translocate to the nucleus? Also, with respect to depletion of nuclear G-actin it is important to know the speed of equilibration between the two compartments. The functional significance of nuclear Dia activity and F-actin formation was demonstrated by assessing activity of the G-actin binding protein MRTF-A. At low G-actin concentrations MRTF-A dissociates from actin and activates target genes. Specific inhibition of nuclear Dia activity inhibited serum induced MRTF-A activation despite normal F-actin formation in the cytoplasm, suggesting that MRTF-A activity can be regulated by changes in nuclear actin dynamics.

A recent report on MICAL2 (molecule interacting with CasL) demonstrates another mode of G-/F-actin regulation in the nucleus (Lundquist et al., 2014). MICAL2 is a nuclear, mono-oxygenase-domain containing protein. MICAL1 has been shown to directly bind F-actin and oxidise methionine 44 leading to filament disassembly (Hung et al., 2011). Lundquist and colleagues show that nuclear MICAL2 catalyses nuclear F-actin disassembly (Lundquist et al., 2014). Interestingly instead of increasing nuclear G-actin concentration, the action of MICAL2 decreased G-actin, which in turn allowed MRTF-A activation. Actin derivatives mimicking the non-oxidisable (M44L) and oxidised (M44Q) forms, were more and less nuclear relative to wild type actin GFP, respectively (Lundquist et al., 2014).

1.4 MRTFs

The Myocardin related transcription factors are a family of 3 members: Myocardin, MRTF-A and MRTF-B. The MRTFs are transcription co-activators, first identified as co-factors of the transcription factor SRF (serum response factor) (D.-Z. Wang et al., 2002).

Along with the discovery of immediate early genes (Cochran et al., 1984; Greenberg and Ziff, 1984), SRF for years served as the paradigm for converting extracellular signals to changes in gene expression (Hill and Treisman, 1995; Treisman, 1996; Posern and Treisman, 2006). By associating with TCFs, a subfamily of Ets domain proteins, SRF allows regulation of *c-fos* by the MAP kinases (Shaw et al., 1989; Treisman, 1995). It was later discovered that SRF could respond to serum induced signals independently of TCFs, suggesting that other co-factors could associate with SRF (Hill et al., 1994). Soon after it was shown that the TCF-independent pathway required Rho activity (Hill et al., 1995). Sotiropoulos and colleagues showed that it was in fact changes in actin dynamics that activated SRF. Using actin-binding drugs and other cytoskeletal manipulations, they demonstrated that G-actin levels control SRF activity (Sotiropoulos et al., 1999; Posern et al., 2002).

The discovery of Myocardin, the founding member of the MRTF family, provided the first evidence that other co-factors could bind SRF. Being expressed only in cardiac and smooth muscle, Myocardin could not be the transducer of the effects of G-actin levels on SRF (D. Wang et al., 2001). MRTF-A functional and biochemical properties indicated that MRTF-A and probably MRTF-B were the elusive link between Rho signalling, actin dynamics and SRF activation (Ma et al., 2001; Mercher et al., 2001; D.-Z. Wang et al., 2002). MRTF-A was shown to associate with G-actin via its N-terminal RPEL domain, which was required for its subcellular localisation and ability to activate SRF in response to Rho-actin signalling (Miralles et al., 2003).

A recent report has shown that in fibroblasts MRTF controls genes important for cell growth, cytoskeletal dynamics, cell adhesion, mechanosensing and circadian rhythm (Esnault et al., 2014). Indeed MRTF depletion has been shown to

reduce adhesion, spreading and motility of the metastatic cell lines B16F2 and MDA-MB-231, and to be required for experimental metastasis (Medjkane et al., 2009). Also, Gerber et al. have shown that circadian signals cause rhythmic activation of MRTF, but also that the core circadian clock component Per2 is itself regulated by MRTF (Gerber et al., 2013).

While MRTF-A knockout mice are viable, females are unable to nurse their offspring (S. Li et al., 2006; Y. Sun et al., 2006). The defect is caused by dedifferentiation and apoptosis of mammary gland myoepithelial cells required for milk ejection. The surprisingly restricted defect, despite ubiquitous MRTF-A expression, suggests redundancy amongst MRTF-A family members. The mammary gland phenotype may arise due to non-redundant functions between MRTFs or due to a dose dependent defect (Y. Sun et al., 2006; S. Li et al., 2006).

MRTF-B inactivation leads to embryonic lethality (between E13.5 and E14.5) (Oh et al., 2005) or between E17.5 and postnatal day 1 (J. Li et al., 2005). The mice die from a spectrum of cardiovascular abnormalities and failure of smooth muscle cell differentiation in brachial arch arteries.

1.4.1 Domain organization of MRTFs

MRTF family members share a common organisation of functional domains, which have a high sequence similarity (see Figure 1.10) (D.-Z. Wang et al., 2002).

1.4.1.1 B1 and Q regions

MRTFs share over 80% homology in the B1 region, which is rich in basic residues (Wang et al., 2002), and over 60% in the glutamine rich (Q) region. B1 and Q regions are important for SRF binding. Deletion of B1 abolished MRTF-SRF complex formation and deletion of Q reduced it (Miralles et al., 2003).

The B1 region was shown to be important for efficient nuclear import of MRTF-A after serum stimulation (Miralles et al., 2003). Being a stretch of basic residues, B1 could constitute a classical NLS. However, since B1 also mediates SRF binding, it was hypothesised that SRF binding could provide nuclear

anchorage and contribute to nuclear accumulation by retention. Alternatively SRF binding could cause occlusion of an export sequence. These possibilities were excluded by alanine substitutions of key basic residues which completely blocked complex formation and had no effect on localisation (Zaromytidou, 2007).

Within the Q-region (QQQQLFLQLQLLNQQQQQQQQQQ) the leucine residues have been shown to function as an export signal (Muehlich et al., 2008), explaining why deletion of the Q-region promotes nuclear localization (Miralles et al., 2003). Mutational analysis showed that there was no correlation between SRF binding and nuclear retention, in agreement with the observations for B1 (Zaromytidou, 2007).

1.4.1.2 The SAP domain

The SAF-A /B, Acinous and PIAS (SAP) domain, which is found in many different nuclear proteins involved in chromatin remodelling, is predicted to form two amphipathic helices competent of DNA binding (Aravind and Koonin, 2000). NMR determination of the yeast SAP domain of SUMO E3 ligases, revealed they are four-helix bundles, capable of binding A/T rich DNA (Suzuki et al., 2009).

SAP domain deletion in Myocardin resulted in impaired activation of a subset of target genes (Wang et al., 2001). Deletion in the context of MRTF-A had no significant effect on localisation or *in-vitro* SRF binding (Miralles et al., 2003).

1.4.1.3 The Leucine Zipper and transactivation domains

MRTFs feature a leucine zipper domain (LZ) that enables formation of homo- and heterodimers between MRTF-A and B. Deletion of the LZ resulted in a reduction of ternary complex (MRTF, SRF, DNA) formation in bandshift assays, suggesting MRTF-A preferentially binds SRF as a dimer. Myocardin appears to bind SRF as a monomer (Miralles et al., 2003).

Fusion of the C-terminus of MRTFs to the LexA DNA binding domain shows they can act as autonomous transcription units in a LexA reporter system. Inclusion of the LZ in the LexA fusion doubled the activation efficiency. Stimulation did not affect activity of this moiety with or without the LZ present (Miralles et al., 2003).

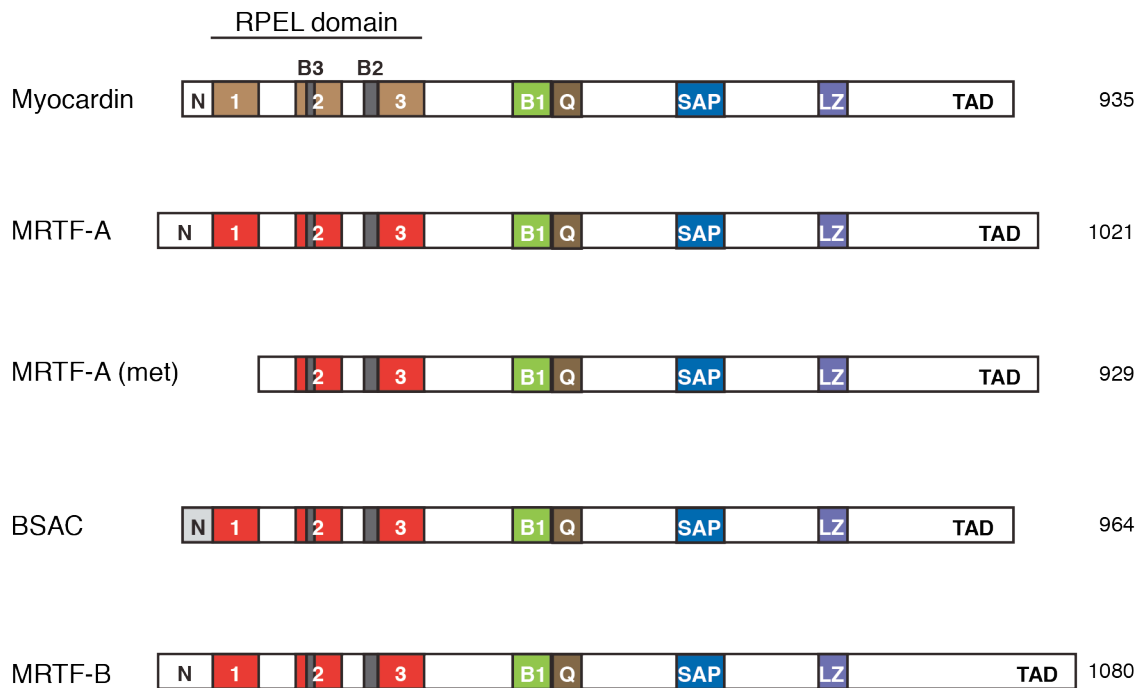


Figure 1.10 Domain organisation of MRTF family members.

MRTF family members share a common organisation of homologous functional domains. The RPEL domain mediates direct actin binding. In the case of Myocardin actin is only weakly bound; the B1 and Q regions mediate SRF binding; family members also possess a SAP domain, which is involved in chromatin remodelling; the leucine zipper mediates homo- and hetero dimerisation, except in the case of Myocardin which binds SRF as a monomer. All family members contain a transactivation domain within their C-terminus, through which SRF activity is stimulated. A detailed description of the domains can be found in the text.

1.4.1.4 The RPEL domain

The RPEL domain is located at the N-terminus of the MRTF proteins (Figure 1.10). It contains three RPEL motifs (PFAM 02755), separated by two spacer regions. The name of the motif is derived from the near invariant RPxxxEL core. The RPEL domain enables MRTFs to sense cellular levels of G-actin, and is required for responsiveness to Rho-actin signalling (Miralles et al., 2003; Posern et al., 2004). Using their RPEL domains, MRTF-A and MRTF-B but not Myocardin, directly bind and are subjected to regulation by G-actin (Guettler et al., 2008; Posern et al., 2004).

Each RPEL motif constitutes an actin binding element, able to bind actin at a 1:1 stoichiometry (Guettler et al., 2008). Actin binding by the intact domain however occurs cooperatively, as the apparent affinity is higher than that of any of the RPEL motifs alone (Mouilleron et al., 2008; 2012). When bound to actin single RPEL motifs adopt an L-shaped conformation comprised of two helices, the $\alpha 1$ and $\alpha 2$ helices connected by the R-loop. Helix $\alpha 1$ binds actin in the hydrophobic cleft formed between subdomains 1 and 3, explaining the ability of the RPEL domain to inhibit actin polymerisation (Posern et al., 2004; Mouilleron et al., 2008). Helix $\alpha 2$ interacts with a hydrophobic ledge on subdomain 3. Cooperativity arises from the ability of actin bound RPEL motifs to form secondary contacts with subsequent actins bound in the RPEL domain, thereby contributing to the strength of the interaction (Mouilleron et al., 2011; 2012).

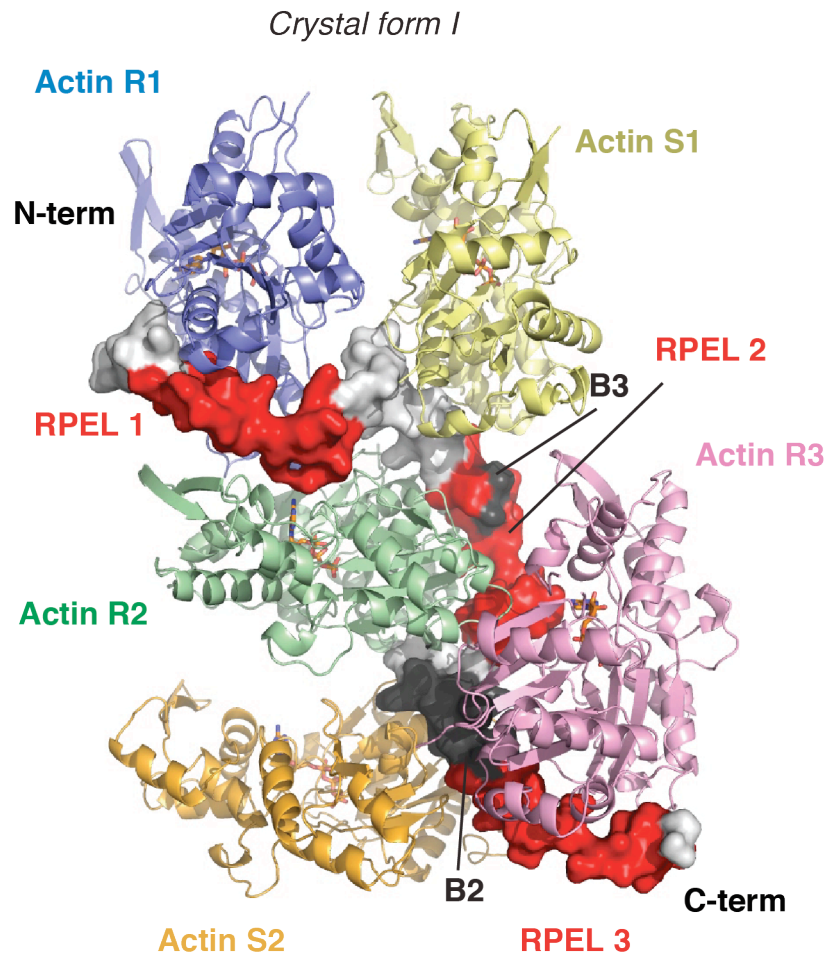
Solution of the structure of the RPEL domain with actin, revealed that the RPEL motifs are not the only actin binding elements within the RPEL domain (Mouilleron et al., 2011). The RPEL domain formed a pentavalent complex with actin, by binding actin to each of the RPEL motifs, but also one actin on each spacer, referred to as spacer 1 (S1) and spacer 2 (S2) (Figure 1.11 A).

The same study also identified a trivalent G-actin complex. In this complex, RPEL motif 1 (RPEL1), spacer1 and RPEL2 bound actin, whereas spacer2 and RPEL3 did not (Figure 1.11 B) (Mouilleron et al., 2011). Analysis by size exclusion chromatography (SEC) revealed that both the pentameric and the trimeric complexes can exist in solution, but the trimeric complex is more stable. SEC analysis of actin incubated with an excess of RPEL domain leads to the detection of the trimeric complex, demonstrating the cooperative manner in which the RPEL

domain binds actin. Inclusion of actin in the running buffer during separation, allowed detection of the pentameric complex, which was dependent on the integrity of key residues required for spacer 2 and RPEL3 to bind actin. The results indicate that a stable trimeric complex is readily formed via RPEL1-spacer1-RPEL2 and that the spacer2-RPEL3 actins associate relatively weakly. In addition, binding of actin by spacer2 was dependent on actin binding by RPEL3 (Mouilleron et al., 2011).

Formation of the pentameric complex provided an explanation as to why high G-actin concentrations block MRTF-A nuclear accumulation (Vartiainen et al., 2007; Mouilleron et al., 2011). Embedded within the RPEL domain is a bipartite NLS comprised of two basic elements B2 and B3. B2 is embedded in spacer 2 and B3 in RPEL2 (see Figure 1.11). This bipartite NLS is recognised by the Imp α/β heterodimer which competes with actin for binding (Pawłowski et al., 2010).

A



B

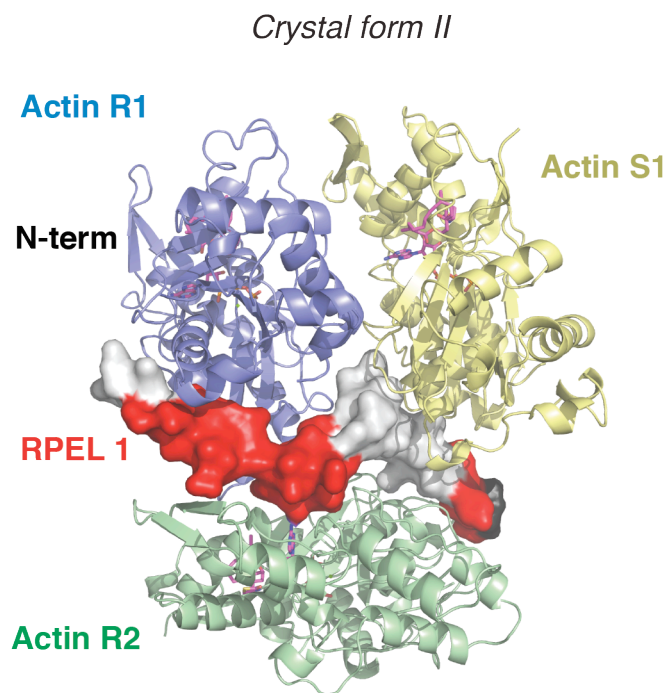


Figure 1.11 Crystallography structures of MRTF-A RPEL domain and actin

Crystallisation of the RPEL domain of MRTF-A (67-199) led to the solution of two distinct crystal forms. RPEL motifs are shown in red; spacers are in grey; the B2 and B3 elements are dark grey. **A.** In the pentameric actin/RPEL complex each RPEL motif and spacer element binds actin via primary contacts. Each RPEL/actin unit also forms secondary contacts with the next actin in the complex. In this complex the B2 and B3 elements that form the bipartite NLS are masked. **B.** In the trimeric RPEL/actin complex actin is bound by RPEL1, Spacer1 and RPEL2. From Mouilleron et al. Structure of a Pentavalent G-Actin•MRTF-A Complex Reveals How G-Actin Controls Nucleocytoplasmic Shuttling of a Transcriptional Coactivator (2011) *Sci. Signal.*, 4(177): ra40. Reprinted with permission from AAAS.

1.4.2 Regulation of MRTF-A by actin

G-actin regulates MRTF-A nuclear transport and activity (Figure 1.12) (Miralles et al., 2003; Vartiainen et al., 2007). In NIH-3T3 cells, MRTF-A continuously shuttles between the nucleus and cytoplasm. In most resting cells MRTF-A is predominantly cytoplasmic because the rate of export is higher than the rate of import. Export is mediated by Crm1 and is actin dependent. Serum induced Rho activation and consequent G-actin depletion leads to a reduction in export and concomitant MRTF-A nuclear accumulation. Reduction in G-actin binding to MRTF-A was confirmed by a decrease in Forster resonance energy transfer (FRET) efficiency between mCherry-actin and MRTF-A-GFP. CD, which binds to actin competitively with the RPEL domain, almost completely eliminated FRET efficiency and blocked export (Vartiainen et al., 2007).

LMB treatment traps MRTF-A in the nucleus without disrupting the interaction between MRTF-A and actin. Comparison of LMB and serum induced nuclear accumulation revealed that import rate was almost identical, showing that nuclear accumulation was regulated at the level of export (Vartiainen et al., 2007). Artificially increasing G-actin levels, for example by LatB treatment or C3-transferase transfection, led to import inhibition (Vartiainen et al., 2007).

Regulation of MRTF-A by actin is conferred by the RPEL domain. Removal of the RPEL domain or mutation of the RPEL motifs relieves MRTF-A from

regulation by G-actin (Miralles et al., 2003). In fact, the N-terminus and RPEL domain are sufficient to confer actin regulated MRTF-A-like shuttling characteristics. A reciprocal swap between the MRTF-A RPEL domain and that of Myocardin, which binds actin very weakly, renders MRTF-A constitutively nuclear and independent of actin regulation. Conversely, Myocardin becomes regulated by actin (Guettler et al., 2008). In addition, fusion of the MRTF-A RPEL domain to the normally cytoplasmic pyruvate kinase confers MRTF-A like shuttling characteristics (Guettler et al., 2008).

Mutation of each actin-binding element in the RPEL domain (RPEL1, spacer1, RPEL2, spacer2, RPEL3) revealed that integrity of the whole RPEL domain is required for correct MRTF-A regulation by actin (Mouilleron et al., 2008; 2011). Mutation of RPEL3 results in strong MRTF-A deregulation despite the fact that it is a weak actin binder and does not appear involved in the stable trimeric complex seen *in-vitro*. This observation shows RPEL3 can bind actin in cells and contributes to MRTF-A regulation. However, the functional significance of RPEL3 is determined by the engagement of actin with the preceding actin binding elements (Guettler et al., 2008). It is possible the trimeric complex readily forms *in-vivo* and is refractory to small changes in G-actin levels, but enables spacer2-RPEL3 to sense more subtle fluctuations.

In addition to regulating MRTF-A localisation, actin independently regulates MRTF-A activity. This was demonstrated either by fusion of an SV40 NLS sequence to MRTF-A, or by LMB treatment, both of which lead to MRTF-A nuclear entrapment while preserving actin binding. In both cases, actin dissociation was required for activation of target gene transcription (Vartiainen et al., 2007).

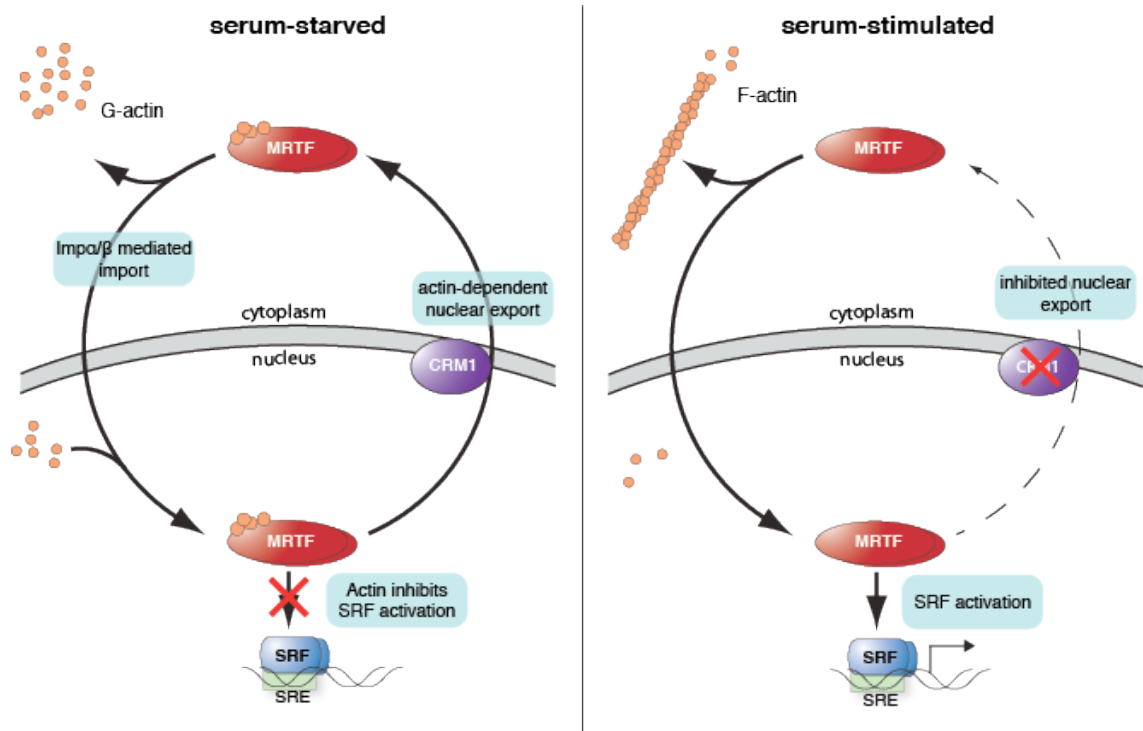


Figure 1.12 MRTF-A nucleocytoplasmic shuttling.

Actin regulates nucleocytoplasmic shuttling of MRTF-A. In the absence of growth factors MRTF-A continuously shuttles between the nucleus and cytoplasm. Under these conditions MRTF-A is predominantly cytoplasmic due to a high rate of export, which is mediated by Crm1. Serum stimulation activates Rho, which leads to actin polymerisation, G-actin depletion and dissociation from MRTF-A. Because Crm1 mediated export of MRTF-A is actin dependent, MRTF-A accumulates in the nucleus and activates SRF target genes.

1.4.3 Regulation of MRTF-A by post-translational modifications

MRTF-A has previously been shown to be regulated by PTM. Nagakawa and Kuzumaki showed that serum stimulation or active Rho expression, promote MRTF-A SUMOylation on three lysine residues close to the leucine zipper domain. Using GAL4-SUMO-1-MRTF fusions they show that SUMOylation represses MRTF-A activity without affecting localisation or SRF binding (Nakagawa and Kuzumaki, 2005).

Serum stimulation leads to MRTF-A phosphorylation on multiple sites, which can be seen as a reduction in electrophoretic mobility in SDS-PAGE (Miralles et al., 2003; Olsen et al., 2006; Gnad et al., 2011). Inhibition of MEK1/2 using U0126 or inhibition of Rho using C3-transferase reduced phosphorylation of MRTF-A, while inhibition of both Rho and MEK-ERK signalling completely blocked it (Miralles et al., 2003). Serum induced phosphorylation of MRTF-A is therefore dependent on Rho and MEK-ERK signalling.

In neurons MRTF-A has been reported to be constitutively nuclear but still regulated. Brain derived neurotrophic factor (BDNF) treatment resulted in MRTF-A activation and phosphorylation, both of which were sensitive to inhibition of MEK-ERK signalling (Kalita et al., 2006). At least in this system phosphorylation is not a prerequisite for nuclear accumulation and appears to correlate with transcriptional activation.

In contrast, another study reported a negative role for MAPK signalling on MRTF-A. Muehlich and colleagues reported that ERK mediated phosphorylation of residues Ser449, Thr450 and Ser454 in human MRTF-A (Ser540, T541 and S545 in mouse) promotes actin association resulting in nuclear export (Muehlich et al., 2008).

The aim of this thesis is to investigate the role of MRTF-A phosphorylation and how MAPK signalling is involved in MRTF-A regulation.

Chapter 2. Materials & Methods

2.1 Chemicals and reagents

Chemical	Supplier
3MM paper	Whatman plc
4',6'-diamidino-2-phenylindole (DAPI)	Molecular Probes
Agarose	Life technologies
Ampicillin	Sigma-Aldrich
Anti-Flag M2 agarose beads	Sigma-Aldrich
ATP (disodium salt)	Sigma-Aldrich
ATP, [γ - ^{32}P] 10mCi/mL	Perkin Elmer
Benzamidine	Sigma-Aldrich
Bromophenol Blue	BioRad
Bovine serum albumin (BSA)	Sigma-Aldrich
Chloramphenicol	Boehringer Mannheim
Complete protease inhibitor cocktail tablets	Roche
Coomassie Brilliant Blue	BioRad
Cytochalasin D	Calbiochem
Dimethyl sulfoxide (DMSO)	Fisher Scientific
Dithiothreitol (DTT)	Calbiochem
DMEM	Life technologies
Ethidium Bromide	Boehringer Mannheim
Fetal calf serum (FCS)	Life technologies
Glutathione sepharose 4B	GE Healthcare
Import Ligand, fluorescent	Sigma-Aldrich

Isopropyl- β -D-thiogalactopyranoside (IPTG)	MP Biomedicals
Kanamycin	Sigma-Aldrich
Latrunculin B	Calbiochem
Lipofectamine2000	Life technologies
Optimem	Life technologies
Orange G	Sigma-Aldrich
P-81 phosphocellulose squares	Merck Millipore
Phenylmethyl-sulphonyl fluoride (PMSF)	Sigma-Aldrich
Protease inhibitors	Roche
PROTRAN transfer membranes	Whatman plc
Slide-A-Lyzer dialysis cassettes	Pierce Biotechnology Inc
Tetracyclin	Sigma-Aldrich
Triton X-100	Sigma-Aldrich
Tween 20	Sigma-Aldrich

2.2 Buffers and solutions

Deionised Milli-Q water (Millipore purification systems) was used to prepare the buffers. The most commonly used buffers and solutions are listed below:

Phosphate Buffered Saline (PBS)	137 mM NaCl
	2.7 mM KCl
	10 mM Na ₂ HPO ₄
	1.8 mM KH ₂ PO ₄ pH 7.4
Tris-Buffered Saline (TBS)	50 mM Tris-HCl pH 7.5
	150 mM NaCl

Tris/Borate/EDTA (1x TBE)	80 mM Tris base	
	89 mM Boric acid	
	2 mM EDTA	
Luria broth (LB) medium	1% w/v Bacto-tryptone	
	0.5% w/v Bacto-yeast extract	
	1% w/v NaCl	
SOC medium	2% w/v Bacto-tryptone	
	0.5% w/v Bacto-yeast extract	
	10 mM NaCl	
	2.5 mM KCl	
	10 mM MgCl ₂	
	20 mM glucose	
Mowiol	6 ml glycerol	mixed at 50°C and filtered (0.45 µm)
	2.4 g Mowiol 4-88 (Calbiochem)	
	12 ml Tris-HCl pH 8.5	
	6 ml water	
	2.5% w/v 1,2-diazabicyclo-[2.2.2]octane (Dabco, Sigma-Aldrich)	
Tris-EDTA (TE)	10mM Tris-HCl pH 8.0	
	1mM EDTA pH 8.0	

2.3 Molecular cloning

2.3.1 Bacterial strains

One Shot® TOP10 Chemically Competent *E. coli* (Life Technologies) were used for cloning and plasmid propagation. Genotype: F- *mcrA* Δ (*mrr-hsdRMS-mcrBC*) Φ 80*lacZ* Δ M15 Δ *lacX74* *recA1* *araD139* Δ (*araleu*)7697 *galU* *galK* *rpsL* (StrR) *endA1* *nupG*

2.3.2 Transformation

One vial (50 μ L) of chemically competent Top10 bacteria were thawed on ice and incubated with DNA for 30 minutes. The bacteria were then heat-shocked for 40 seconds at 42°C on a thermoblock and immediately returned to ice for 2 minutes. Pre-warmed SOC medium was next added and the vial was incubated for 1 hour at 37°C on a shaker. The bacteria were plated on LB agar containing the appropriate antibiotic (30 μ g/mL kanamycin or 100 μ g/mL ampicillin) and incubated at 37°C for approximately 15 hours.

2.3.3 Expression vectors

All MRTF-A constructs used in this study were derivatives of pEF-Flag-MRTF-A (Figure 2.1) (Miralles et al., 2003). The MRTF-A cDNA sequence was inserted between BamHI and XbaI sites. The pEF-Flag-MRTF-A plasmid used in this study was generated by Dr F. Miralles. The nucleotide sequence was modified from 5'-⁵²¹AGCTGGTGGAGA⁵³²-3' to 5'-⁵²¹AACTAGTAGAAA⁵³²-3' to make the plasmid resistant to the siRNA used in the lab; the amino acid sequence remained unchanged. The non-phosphorylatable derivative, E3, was generated by Dr F. Miralles.

pEF-HA-DYRK1A-WT, pEF-HA-DYRK1A-K188R, pEF-HA-DYRK1B WT and pEF-HA-DYRK1B K140R were generated by Dr F. Miralles. cDNAs were inserted into the pEF-HA vector using the BamHI and XbaI restriction sites. Products are N-terminally HA tagged.

pEF-Flag-Pyruvate kinase was obtained from Dr F. Miralles and encodes the first 1270 nucleotides corresponding to chicken pyruvate kinase, cloned into the pEF-Flag vector (Hill and Treisman, 1995), using the BamHI and EcoRI restriction sites. MRTF-A 2-204 was inserted between the Flag and pyruvate kinase coding sequences using the BamHI site (Figure 2.1), as previously described (Guettler et al., 2008).

pRev(1.4)-GFP and pRev(1.4)-NES-GFP were obtained from Dr B.R. Henderson (B. R. Henderson and Eleftheriou, 2000). Sequences were inserted between the Rev and GFP coding sequences using the BamHI and AgeI restriction sites (Figure 2.1).

The plasmid encoding the constitutively active form of mDia1 is described in (Copeland and Treisman, 2002). This plasmid encodes for the FH1 and FH2 domains (amino acids 567-1181) of mDia, which are constitutively active in the absence of the regulatory region of the protein.

2.3.3.1 Bacterial Expression vectors

pET-41a-3C Δ is a modified form of pET-41a (Novagen, Inc). The enterokinase site was replaced with a 3C-protease site and all restriction sites 5' of the BamHI site were deleted (Figure 2.1).

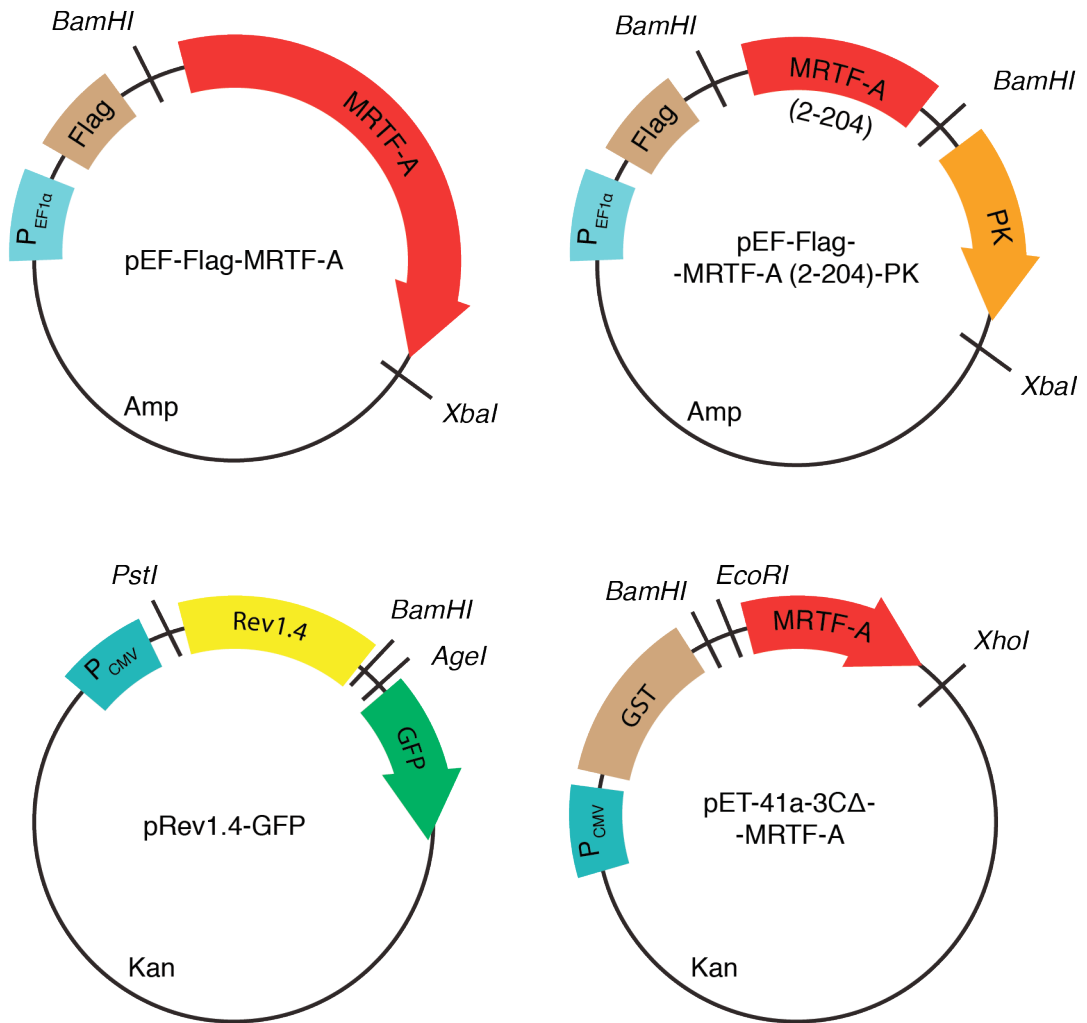


Figure 2.1 Plasmids used in this thesis.

Shown are the pEF-Flag-MRTF-A, pEF-Flag-MRTF-A (2-204)-PK, pRev1.4-GFP and pET-41a-3CΔ-MRTF-A plasmids with their corresponding antibiotic resistance indicated; Kanamycin (Kan) or Ampicillin (Amp). Promoters are shown in blue ($P_{EF1\alpha}$ corresponds to the promoter/enhancer region of elongation factor 1 α and P_{CMV} corresponds to the Cytomegalovirus promoter). Coding sequences are shown in colour. Restriction endonuclease sites that were frequently used are also indicated.

2.3.4 Purification of plasmid DNA

A single bacterial colony was used to inoculate LB medium (5mL for minipreps and 100mL for maxipreps) supplemented with the appropriate antibiotic. Cultures were incubated overnight at 37°C, 200rpm. For minipreps the bacteria were pelleted and submitted to the CRUK Equipment park miniprep service. For Maxipreps DNA was isolated using the QIAGEN plasmid maxi kit, according to the manufacturer's instructions. Isolated DNA was stored in TE buffer at 0.5µg/µL.

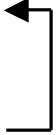
2.3.5 Agarose gel electrophoresis

Depending on the size of DNA fragments to be analysed, 0.5-1.5% w/v agarose gels were prepared using 1x TBE pH 8 and with a final concentration of 0.5µg/mL ethidium bromide. Samples were mixed with 5x DNA loading buffer (0.01% w/v Orange G, 80% Glycerol, 50mM EDTA). Electrophoresis was performed in 1x TBE buffer at 100V. NEB 2-log ladder (New England Biolabs (NEB)) was used for estimation of fragment size.

2.3.6 Recombinant DNA techniques

2.3.6.1 Polymerase Chain Reaction

Polymerase chain reaction (PCR) was used for amplification of DNA for subcloning and site directed mutagenesis. Pfu Turbo DNA polymerase (Stratagene) was used because of its proofreading ability. PCR reactions were set up as follows:

PCR set-up (50μL)		
20ng DNA template		
1.5 μ L (10 μ M) Forward primer		
1.5 μ L (10 μ M) Reverse primer		
5 μ L (100mM) dNTP mix (25mM each)		
5 μ L 10x PCR buffer		
1 μ L (2.5U/ μ L) Pfu Turbo		
Up to 50 μ L with water		
Thermal cycling		
95°C	2 min	 20-30 cycles
95°C	30 sec	
50-60°C	1 min	
68°C	2 min/Kb	
72°C	2 min/Kb +2 min	
4°C	hold	

2.3.6.2 Restriction Endonuclease digestion

All restriction enzymes and buffers were from NEB and reactions were set up according to NEB recommendations. Generally 10 units of restriction enzyme were used for up to 5 μ g of plasmid DNA, for a 1-2 hour digestion.

2.3.6.3 Dephosphorylation of 5' phosphates of DNA ends

To prevent vector re-circularisation without insert, 5' phosphates were removed from digested vectors using Antarctic Phosphatase. 5.5 μ L of AP-reaction buffer and 1 μ L (5 units) of Antarctic phosphatase were added directly to the restriction enzyme reaction. The mixture was incubated for 15 min and enzymes were heat inactivated at 70°C for 5 min.

2.3.6.4 Purification of DNA fragments

DNA fragments generated by PCR or after restriction digests were purified using the QIAquick PCR purification kit (Qiagen). When multiple fragments were generated, the reaction was resolved by agarose gel electrophoresis. The desired DNA fragment(s) was cut out of the gel and DNA was recovered using the QIAquick gel extraction kit (Qiagen), according to the manufacturer's instructions.

2.3.6.5 DNA ligation

Concentrations of vector and insert were quantified by measuring absorption at 260nm using the NanoDrop ND-1000 spectrophotometer (Thermo Fisher Scientific). 150ng of digested and 5' dephosphorylated vector and a 3-fold molar excess of digested insert were mixed with 1µL 10x T4 DNA ligase buffer and water up to 9µL. After a 5 min incubation at 50°C the mixture was placed on ice for 10 minutes. 1µL (400 units) of T4 DNA ligase was mixed into the reaction. The ligation was carried out for 15 minutes at room temperature, or overnight at 16°C. 2-6µL of the reaction were next used for transformation of TOP10 bacteria (see section 2.3.2).

2.3.6.6 Site directed mutagenesis: Amino acid substitutions using QuikChange

Amino acid substitutions were carried out using the QuikChange Site Directed Mutagenesis kit (Stratagene) according to the manufacturer's guidelines. A pair of complementary primers, 33-45 nucleotides in length, was designed with up to 3 codon changes in the centre of each primer. A PCR reaction was set up as described in section 2.3.6.1, but the number of cycles was restricted to 18. The entire template vector was amplified and then digested for 1.5 hours with *DpnI*. The remaining DNA was precipitated by the addition of 5.5 µL NaOAc (3M pH 5.2) and 160µL 96% ethanol. Precipitated DNA was pelleted, washed three times in 70% ethanol and air dried. The DNA was resuspended in 10µL of water, half or all of which was used to transform TOP10 bacteria.

Constructs generated and primers used are shown in the table below.

Primers used for amino acid substitutions with the QuikChange method	
Plasmid	Description. Primers (5' to 3')
pEF-MRTF-A E3a	Template: pEF-MRTF-A E3 Change: AAA204/205/206SSS Forward Primer: ccaaaggtagcagacAGtTccTccttcgacgaggacgccg Reverse Primer: cggcgtcctcgtcgaaggAggAaCTgtctgctacctttgg
pEF-MRTF-A E3b	Template: pEF-MRTF-A E3a Change: AA211/212SS Forward Primer: tccttcgacgaggacAGcAGcgatgccctggctcct Reverse Primer: aggagccagggcatcgCTgCTgtcctcgtcgaagga
pEF-MRTF-A E3c	Template: pEF-MRTF-A E3b Change: S33A Forward Primer: tctgtctgcggcccccGccccagagcgaagctgt Reverse Primer: acagcttcgctctgggggGCgggggcccgcagacaga
pEF-MRTF-A E3d	Template: pEF-MRTF-A E3c Change: A402T Forward Primer: tggaaagcagtgccctAccccatcacgcagcctctcca Reverse Primer: tggagaggctgcgtgatggggTaggggcactgcttcca
pEF-MRTF-A E3f	Template: pEF-MRTF-A E3d Change: T545A Forward Primer: ggcagcacaggctccGcccccccgctggctccca Reverse Primer: tgggagccacggggggtgCggagcctgtgctgcc
pEF-MRTF-A E3g	Template: pEF-MRTF-A E3f Change: T551A Forward Primer: cccccgctggctcccGcccccttcagagcgctca Reverse Primer: tgagcgctctgaaggggCgggagccacggggg
pEF-MRTF-A E3h	Template: pEF-MRTF-A E3g Change: S587A Forward Primer: agctcacctgcaggccGccccactgcagatagtg Reverse Primer: cactatctgcagtggggCggcctgcagggtgagct
pEF-MRTF-A E3i	Template: pEF-MRTF-A E3h Change: S601A Forward Primer: ggtgcccgctgctgcgGcctgctgtctagccct

	Reverse Primer: aggggctagacagcaggCcgagcagcgggcacc
pEF-MRTF-A E3j or 26ST/A	Template: pEF-MRTF-A E3i Change: S775A Forward Primer: ggcttgctgcagggGCCccccagcagcccttg Reverse Primer: caagggctgctgggggGCCcctgcaggcaagcc
pEF-MRTF-A LL74/76AA	Template: pEF-MRTF-A Forward Primer: gagcggagaagaatgtgGCgcagGCgaagctccagcagcgg Reverse Primer: ccgctgctggagcttcGCctgcGCcacattcttccgctc
pEF-MRTF-A $\alpha 1^{AA}$	Template: pEF-MRTF-A Change: LL74/78AA Forward Primer: gagcggagaagaatgtgGCgcagttgaagGCCcagcagcggcggacc Reverse Primer: ggtccgcccgtgctggGCcttcaactgcGCcacattcttccgctc
pEF-26ST/A x23	Template: pEF-26ST/A Change: R81A Forward Primer: ttgaagctccagcagGCgcggaccggaggaa Reverse Primer: ttctcccgggtccgcGCctgctggagcttcaa
pEF-26ST/A xx3	Template: pEF-26ST/A x23 Change: R125A Forward Primer: cggaagatccgttccGCgcccagagagcagagc Reverse Primer: gctctgctctctcgggcGCggaacggatcttccg
pEF-26ST/A xxx	Template: pEF-26ST/A xx3 Change: R169A Forward Primer: gaaaagattgcacagGCgcctggcccatggaa Reverse Primer: ttccatggggccaggCGCctgtgcaatcttttc
pEF-E3 x23	Template: pEF-E3 Change: R81A Forward Primer: ttgaagctccagcagGCgcggaccggaggaa Reverse Primer: ttctcccgggtccgcGCctgctggagcttcaa
pEF-E3 xx3	Template: pEF-E3 x23 Change: R125A Forward Primer: cggaagatccgttccGCgcccagagagcagagc Reverse Primer: gctctgctctctcgggcGCggaacggatcttccg
pEF-E3 xxx	Template: pEF-E3 xx3

	<p>Change: R169A</p> <p>Forward Primer: gaaaagattgcacagGCgcttgccccatggaa</p> <p>Reverse Primer: ttccatggggccaggCGCctgtgcaatcttttc</p>
pEF-MRTF-A Y330A	<p>Template: pEF-MRTF-A</p> <p>Change: Y330A</p> <p>Forward Primer: gtgaagaagctcaagGCccaccagtacatcccc</p> <p>Reverse Primer: ggggatgtactggtgcGCcttgagcttcttcac</p>
pEF-MRTF-A Y330A ΔLZ	<p>Template: pEF-MRTF-A ΔLZ</p> <p>Change: Y330A</p> <p>Forward Primer: gtgaagaagctcaagGCccaccagtacatcccc</p> <p>Reverse Primer: ggggatgtactggtgcGCcttgagcttcttcac</p>
pEF-MRTF-A RK70/71AA	<p>Template: pEF-MRTF-A</p> <p>Change: RK70/71AA</p> <p>Forward Primer: cctccacttagtgagGCgGCgaatgtgctgcagttg</p> <p>Reverse Primer: caactgcagcacattcGCcGCctcactaagtggagg</p>
pEF-MRTF-A RK70/71VQ	<p>Template: pEF-MRTF-A</p> <p>Change: RK70/71VQ</p> <p>Forward Primer: cctccacttagtgagGTgCagaatgtgctgcagttg</p> <p>Reverse Primer: caactgcagcacattcTGcACctcactaagtggagg</p>
pEF-MRTF-A S33A	<p>Template: pEF-MRTF-A</p> <p>Change: S33A</p> <p>Forward Primer: ctgtctgcgccccGCccccagagcgaagc</p> <p>Reverse Primer: gcttcgctctggggGCgggggcccgcagacag</p>
pEF-MRTF-A S33D	<p>Template: pEF-MRTF-A</p> <p>Change: S33D</p> <p>Forward Primer: ctgtctgcgccccGAcccccagagcgaagc</p> <p>Reverse Primer: gcttcgctctggggTCgggggcccgcagacag</p>
pEF-MRTF-A-B2A LSL46/47/48AAA	<p>Template: pEF-MRTF-A B2A</p> <p>Change: LSL46/47/48AAA</p> <p>Forward Primer: tgaactgcaggagGCgGccGCgcagcccagctga</p> <p>Reverse Primer: tcagctcgggctgcGCgGCcGCctcctgcagttca</p>
pEF-MRTF-A (2-204)- PK S33A	<p>Template: pEF-MRTF-A (2-204)-PK</p> <p>Change: S33A</p> <p>Forward Primer: ctgtctgcgccccGCccccagagcgaagc</p> <p>Reverse Primer: gcttcgctctggggGCgggggcccgcagacag</p>
pEF-MRTF-A (2-204)- PK S33A S98D	<p>Template: pEF-MRTF-A (2-204)-PK 98D</p> <p>Change: S33A</p>

	Forward Primer: ctgtctgcgggcccccGCCCCcagagcgaagc Reverse Primer: gcttcgctctgggggGCgggggcccgcagacag
MRTF-A (2-204)-PK S33D	Template: pEF-MRTF-A (2-204)-PK Change: S33D Forward Primer: ctgtctgcgggcccccGAcccccagagcgaagc Reverse Primer: gcttcgctctgggggTCgggggcccgcagacag
pEF-MRTF-A (2-204)- PK S33D S98A	Template: pEF-MRTF-A (2-204)-PK 98D Change: S33D Forward Primer: ctgtctgcgggcccccGAcccccagagcgaagc Reverse Primer: gcttcgctctgggggTCgggggcccgcagacag
pRev(1.4) 2-115 P94A	Template: pRev(1.4) 2-115 Change: P94A Forward Primer: agccaagggatcatgGCgcctttgaaaagcccc Reverse Primer: ggggcttttcaaaggcGCcatgatcccttggt
pRev(1.4) 2-115 P94S	Template: pRev(1.4) 2-115 Change: P94S Forward Primer: agccaagggatcatgTCgcctttgaaaagcccc Reverse Primer: ggggcttttcaaaggcGCcatgatcccttggt
pRev(1.4) 2-115 P94A L96A	Template: pRev(1.4) 2-115 Change: P94A L96A Forward Primer: agccaagggatcatgGCgcctGCgaaaagccccgctgc Reverse Primer: gcagcggggcttttcGCaggcGCcatgatcccttggt
pRev(1.4) 2-204 B2A xxx	Template: pRev(1.4) 2-204 xxx Change: KK152/154AA (B2A) Forward Primer: agccaagcagctgGCgctgGCgagagccaggctggc Reverse Primer: gccagcctggtctcGCcagcGCcagctgcttggt
pRev(1.4) 2-204 B3A xxx	Template: pRev(1.4) 2-204 xxx Change: KRK119/120/121AAA Forward Primer: accgaggactatttgGCAGCGCGatccgttccgctc Reverse Primer: gagcggaacggatCGCCGCTGCaaatagtccctcggt
pRev(1.4) 2-204 S98A	Template: pRev(1.4) 2-204 B2A Change: S98A Forward Primer: atgccgcctttgaaaGCCCCgctgcatttcat Reverse Primer: atgaaatgcagcggggGCTttcaaaggcggcat
pRev(1.4) 2-204 S98D	Template: pRev(1.4) 2-204 B2A

	<p>Change: S98D</p> <p>Forward Primer: TcatgccgcctttgaaaGAccccgctgcatttcatgag</p> <p>Reverse Primer: ctcatgaaatgcagcggggTCtttcaaaggcggcatgA</p>
pRev(1.4) 2-204 $\alpha 1^{AA}$	<p>Template: pRev(1.4) 2-204 B2A</p> <p>Change: $\alpha 1^{AA}$</p> <p>Forward Primer: gagcggaagaatgtgGCgcagttgaagGCCcagcagcggcggacc</p> <p>Reverse Primer: ggtccgcccgtgctggGCcttcaactgcGCcacattcttccgctc</p>
pRev(1.4) 2-204 S33A	<p>Template: pRev(1.4) 2-204 B2A</p> <p>Change: S33A</p> <p>Forward Primer: ctgtctgcccgcGCCCCcagagcgaagc</p> <p>Reverse Primer: gcttcgctctgggggGCgggggcccagacag</p>
pRev(1.4) 2-204 S33D	<p>Template: pRev(1.4) 2-204 B2A</p> <p>Change: S33D</p> <p>Forward Primer: ctgtctgcccgcGAccccagagcgaagc</p> <p>Reverse Primer: gcttcgctctgggggTCgggggcccagacag</p>
pET-41a-3C Δ 67-199 $\alpha 1^{AA}$	<p>Template: pET-41a-3CΔ 67-199</p> <p>Change: LL74/78AA</p> <p>Forward Primer: gagcggaagaatgtgGCgcagttgaagGCCcagcagcggcggacc</p> <p>Reverse Primer: ggtccgcccgtgctggGCcttcaactgcGCcacattcttccgctc</p>
pET-41a-3C Δ 67-199 12x	<p>Template: pET-41a-3CΔ 67-199</p> <p>Change: R169A</p> <p>Forward Primer: gaaaagattgcacagGCgcctggccccatggaa</p> <p>Reverse Primer: ttccatggggccaggcGCctgtgcaatcttttc</p>
pET-41a-3C Δ 67-199 S98A	<p>Template: pET-41a-3CΔ 67-199</p> <p>Change: S98A</p> <p>Forward Primer: atgccgcctttgaaaGCCccgctgcatttcat</p> <p>Reverse Primer: atgaaatgcagcggggGCtttcaaaggcggcat</p>
pET-41a-3C Δ 67-199 12x S98D	<p>Template: pET-41a-3CΔ 67-199 S98D</p> <p>Change: R169A</p> <p>Forward Primer: gaaaagattgcacagGCgcctggccccatggaa</p> <p>Reverse Primer: ttccatggggccaggcGCctgtgcaatcttttc</p>

pEF-Phactr1 _(MRTF) B1A	<p>Template: pEF-Phactr1_(MRTF)</p> <p>Change: RRR108/109/110AAA (B1A)</p> <p>Forward Primer: caccctgcccaccGCgGCgagcagtaagtttgcc</p> <p>Reverse Primer: ggcaacttactcgccGCcGCgatggcggggtg</p>
pEF-Phactr1 _(MRTF) B2A	<p>Template: pEF-Phactr1_(MRTF)</p> <p>Change: KK152/154AA (B2A)</p> <p>Forward Primer: aggccaagcagctgGCgctGGCGagagccaggctggc</p> <p>Reverse Primer: gccagcctggctctCGCCagCGCagctgcttggcct</p>
pEF-Phactr1 _(MRTF) B3A	<p>Template: pEF-Phactr1_(MRTF)</p> <p>Change: KRK119/120/121AAA</p> <p>Forward Primer: accgaggactatcttGCAGCGGCGatccgttcccggc</p> <p>Reverse Primer: gccgggaacggatCGCCGCTGCcfaatagtcctcggt</p>
pEF-Phactr1 _(MRTF) B1A B2A	<p>Template: pEF-Phactr1_(MRTF) B1A</p> <p>Change: KK152/154AA (B2A)</p> <p>Forward Primer: aggccaagcagctgGCgctgGCgagagccaggctggc</p> <p>Reverse Primer: gccagcctggctctcGCcagcGCcagctgcttggcct</p>
pEF-Phactr1 _(MRTF) B1A B3A	<p>Template: pEF-Phactr1_(MRTF) B1A</p> <p>Change: KRK119/120/121AAA</p> <p>Forward Primer: accgaggactatcttGCAGCGGCGatccgttcccggc</p> <p>Reverse Primer: gccgggaacggatCGCCGCTGCcfaatagtcctcggt</p>
pEF-Phactr1 _(MRTF) B1A xxx	<p>Template: pEF-Phactr1_(MRTF) xxx</p> <p>Change: RRR108/109/110AAA (B1A)</p> <p>Forward Primer: caccctgcccaccGCgGCgagcagtaagtttgcc</p> <p>Reverse Primer: ggcaacttactcgccGCcGCgatggcggggtg</p>
pEF-Phactr1 _(MRTF) B2A xxx	<p>Template: pEF-Phactr1_(MRTF) xxx</p> <p>Change: KK152/154AA (B2A)</p> <p>Forward Primer: aggccaagcagctgGCgctgGCgagagccaggctggc</p> <p>Reverse Primer: gccagcctggctctcGCcagcGCcagctgcttggcct</p>
pEF-Phactr1 _(MRTF) B3A xxx	<p>Template: pEF-Phactr1_(MRTF) xxx</p> <p>Change: KRK119/120/121AAA</p> <p>Forward Primer: accgaggactatcttGCAGCGGCGatccgttcccggc</p> <p>Reverse Primer: gagcgggaacggatCGCCGCTGCcfaatagtcctcggt</p>
pEF-Phactr1 _(MRTF) B1A B2A xxx	<p>Template: pEF-Phactr1_(MRTF) B1A xxx</p> <p>Change: KK152/154AA (B2A)</p> <p>Forward Primer: aggccaagcagctgGCgctgGCgagagccaggctggc</p> <p>Reverse Primer: gccagcctggctctcGCcagcGCcagctgcttggcct</p>
pEF-Phactr1 _(MRTF) B1A	<p>Template: pEF-Phactr1_(MRTF) B1A xxx</p>

B3A xxx	Change: KRK119/120/121AAA Forward Primer: accgaggactatattgGCAGCGGCGatccggttccgctc Reverse Primer: gagcggaaacggatCGCCGCTGCc aaatagtcctcggt
pEF-Phactr1 _(MRTF NT RPEL) B1A	Template: pEF-Phactr1 _(MRTF NT RPEL) Change: RRR108/109/110AAA (B1A) Forward Primer: caccctcgccatcGCgGCggcgagtaagtttgcc Reverse Primer: ggcaaaacttactcgccGCcGCgCgatgggcggggtg
pEF-Phactr1 _(MRTF NT RPEL) B2A	Template: pEF-Phactr1 _(MRTF NT RPEL) Change: KK152/154AA (B2A) Forward Primer: aggccaagcagctgGCgctGGCGagagccaggctggc Reverse Primer: gccagcctggctctCGCCagCGCagctgcttggcct
pEF-Phactr1 _(MRTF NT RPEL) B3A	Template: pEF-Phactr1 _(MRTF NT RPEL) Change: KRK119/120/121AAA Forward Primer: accgaggactatattgGCAGCGGCGatccggttcccggc Reverse Primer: gccgggaacggatCGCCGCTGCc aaatagtcctcggt
pEF-Phactr1 _(MRTF NT RPEL) B1A B2A	Template: pEF-Phactr1 _(MRTF NT RPEL) B1A Change: KK152/154AA (B2A) Forward Primer: aggccaagcagctgGCgctgGCgagagccaggctggc Reverse Primer: gccagcctggctctcGCcagcGCcagctgcttggcct
pEF-Phactr1 _(MRTF NT RPEL) B1A B3A	Template: pEF-Phactr1 _(MRTF NT RPEL) B1A Change: KRK119/120/121AAA Forward Primer: accgaggactatattgGCAGCGGCGatccggttcccggc Reverse Primer: gccgggaacggatCGCCGCTGCc aaatagtcctcggt
pEF-Phactr1 _(MRTF NT RPEL) B1A xxx	Template: pEF-Phactr1 _(MRTF NT RPEL) xxx Change: RRR108/109/110AAA (B1A) Forward Primer: caccctcgccatcGCgGCggcgagtaagtttgcc Reverse Primer: ggcaaaacttactcgccGCcGCgCgatgggcggggtg
pEF-Phactr1 _(MRTF NT RPEL) B2A xxx	Template: pEF-Phactr1 _(MRTF NT RPEL) xxx Change: KK152/154AA (B2A) Forward Primer: aggccaagcagctgGCgctgGCgagagccaggctggc Reverse Primer: gccagcctggctctcGCcagcGCcagctgcttggcct
pEF-Phactr1 _(MRTF NT RPEL) B3A xxx	Template: pEF-Phactr1 _(MRTF NT RPEL) xxx Change: KRK119/120/121AAA Forward Primer: accgaggactatattgGCAGCGGCGatccggttccgctc Reverse Primer: gagcggaaacggatCGCCGCTGCc aaatagtcctcggt
pEF-Phactr1 _(MRTF NT RPEL) B1A B2A xxx	Template: pEF-Phactr1 _(MRTF NT RPEL) B1A xxx Change: KK152/154AA (B2A)

	<p>Forward Primer: agccaagcagctgGCgctgGCgagagccaggctggc</p> <p>Reverse Primer: gccagcctggctctcGCcagcGCcagctgcttggcct</p>
<p>pEF-Phactr1_(MRTF NT RPEL) B1A B3A xxx</p>	<p>Template: pEF-Phactr1_(MRTF NT RPEL) B1A xxx</p> <p>Change: KRK119/120/121AAA</p> <p>Forward Primer: accgaggactatttgGCAGCGGCGatccggttccgctc</p> <p>Reverse Primer: gagcggaaacggatCGCCGCTGCaaatagtcctcggt</p>
<p>pRev(1.4) 2-115 PPS2/3/4AAA</p>	<p>Template: pRev(1.4) 2-115</p> <p>Change: PPS2/3/4AAA</p> <p>Forward Primer: ggaaccaaagaggatccaGccGctGccgtcattgctgtga</p> <p>Reverse Primer: tcacagcaatgacggCagCggCtggatcctctttggttcc</p>
<p>pRev(1.4) 2-115 VIA5/6/7AAA</p>	<p>Template: pRev(1.4) 2-115</p> <p>Change: VIA5/6/7AAA</p> <p>Forward Primer: gatccaccccccttccgCcGCtgcgtgtgaatgggctggacg</p> <p>Reverse Primer: cgtccagcccattcacagcaGCgGcggaaagggggtggatc</p>
<p>pRev(1.4) 2-115 VNG8/9/10AAA</p>	<p>Template: pRev(1.4) 2-115</p> <p>Change: VNG8/9/10AAA</p> <p>Forward Primer: ccttccgctcattgctgCgGCtgcgctggacggaggaggg</p> <p>Reverse Primer: ccctcctccgtccagcGcaGCcGcagcaatgacggaagg</p>
<p>pRev(1.4) 2-115 LDG11/12/13AAA</p>	<p>Template: pRev(1.4) 2-115</p> <p>Change: LDG11/12/13AAA</p> <p>Forward Primer: attgctgtgaatgggGCggCcgCaggaggggctggcgaa</p> <p>Reverse Primer: ttcgccagccccctcctGcgGccGCccattcacagcaat</p>
<p>pRev(1.4) 2-115 GGA14/15/16AAA</p>	<p>Template: pRev(1.4) 2-115</p> <p>Change: GGA14/15/16AAA</p> <p>Forward Primer: aatgggctggacggagCagCggctggcgaaaatgacgacg</p> <p>Reverse Primer: cgtcgctcattttcgccagccGctGctccgctccagcccatt</p>
<p>pRev(1.4) 2-115 GEN17/18/19AAA</p>	<p>Template: pRev(1.4) 2-115</p> <p>Change: GEN17/18/19AAA</p>

	<p>Forward Primer: gacggaggaggggctgCcgCaGCtgacgacgagccagtgc</p> <p>Reverse Primer: gcactggctcgtcgtcaGCtGcgGcagccctcctccgtc</p>
pRev(1.4) 2-115 DDE20/21/22AAA	<p>Template: pRev(1.4) 2-115 Change: DDE20/21/22AAA</p> <p>Forward Primer: ggggctggcgaaaatgCcgCcgGccagtgtcctgtctc</p> <p>Reverse Primer: gagacaggagcactggcGcgGcgGcattttcgcagcccc</p>
pRev(1.4) 2-115 PVL23/24/25AAA	<p>Template: pRev(1.4) 2-115 Change: PVL23/24/25AAA</p> <p>Forward Primer: gaaaatgacgacgagGcagCgGCcctgtctctgtctgcg</p> <p>Reverse Primer: cgcagacagagacaggGCcGctgCctcgtcgtcattttc</p>
pRev(1.4) 2-115 LSL26/27/28AAA	<p>Template: pRev(1.4) 2-115 Change: LSL26/27/28AAA</p> <p>Forward Primer: gacgagccagtgtcGCgGctGCgtctgcggccccagc</p> <p>Reverse Primer: gctgggggcccgcagacGCagCcGCgagcactggctcgtc</p>
pRev(1.4) 2-115 PSP32/33/34AAA	<p>Template: pRev(1.4) 2-115 Change: PSP32/33/34AAA</p> <p>Forward Primer: tctctgtctgcggccGccGCcGcccagagcgaagctggt</p> <p>Reverse Primer: aacagcttcgctctgggCgGCggCggccgcagacagaga</p>
pRev(1.4) 2-115 QSE35/36/37AAA	<p>Template: pRev(1.4) 2-115 Change: QSE35/36/37AAA</p> <p>Forward Primer: gcggccccagccccGCgGCcgCagctgttgccaatgaa</p> <p>Reverse Primer: ttcattggcaacagctGcgGCcGCggggctgggggcccgc</p>
pRev(1.4) 2-115 NEL41/42/43AAA	<p>Template: pRev(1.4) 2-115 Change: NEL41/42/43AAA</p> <p>Forward Primer: agcgaagctgttgccGCtgCaGCgcaggagctgtccctg</p>

	Reverse Primer: cagggacagctcctgcGcTgCaGCggcaacagcttcgct
pRev(1.4) 2-115 QEL44/45/46AAA	Template: pRev(1.4) 2-115 Change: QEL44/45/46AAA Forward Primer: gttgccaatgaactgGCggCgGCgtccctgcagcccagag Reverse Primer: ctcgggctgcagggacGCcGccGCcagttcattggcaac
pRev(1.4) 2-115 SLQ47/48/49AAA	Template: pRev(1.4) 2-115 Change: SLQ47/48/49AAA Forward Primer: gaactgcaggagctgGccGCgGCgccccgagctgactctag Reverse Primer: ctagagtcagctcgggcGCcGCggCcagctcctgcagttc
pRev(1.4) 2-115 PEL50/51/52AAA	Template: pRev(1.4) 2-115 Change: PEL50/51/52AAA Forward Primer: gagctgtccctgcagGccgCgGCgactctaggcctccat Reverse Primer: atggaggcctagagtcGCcGcggCctgcagggacagctc
pRev(1.4) 2-115 TLG53/54/55AAA	Template: pRev(1.4) 2-115 Change: TLG53/54/55AAA Forward Primer: ctgcagcccagagctgGctGCagCcctccatcctgggagg Reverse Primer: cctcccaggatggaggGctGCagCcagctcgggctgcag
pRev(1.4) 2-115 LHP56/57/58AAA	Template: pRev(1.4) 2-115 Change: LHP56/57/58AAA Forward Primer: gagctgactctaggcGCcGCtGctgggaggaacccaatt Reverse Primer: aattgggggttccctcccagCaGCgGCgcctagagtcagctc
pRev(1.4) 2-115 GRN59/60/61AAA	Template: pRev(1.4) 2-115 Change: GRN59/60/61AAA Forward Primer: ctaggcctccatcctgCgGCgGCcccccaatttacctccac Reverse Primer: gtggaggtaaatggggGCcGCcGcaggatggaggcctag

<p>pRev(1.4) 2-115 PNL62/63/64AAA</p>	<p>Template: pRev(1.4) 2-115 Change: PNL62/63/64AAA Forward Primer: catcctgggaggaacGccGCtGCacctccacttagtgagc Reverse Primer: gctcactaagtggaggtGCaGCggCgttcctcccaggatg</p>
<p>pRev(1.4) 2-115 PPL65/66/67AAA</p>	<p>Template: pRev(1.4) 2-115 Change: PPL65/66/67AAA Forward Primer: aggaacccccaatttaGctGcaGCtagtgagcggagaagaatg Reverse Primer: cattcttccgctcactaGCtgCagCtaaattggggttcct</p>
<p>Note: Substituted bases are shown in upper case</p>	

2.3.6.7 Site Directed Mutagenesis: Amino acid substitution using conventional restriction cloning

Two complementary primers were designed with the desired mutation in the centre and approximately 15 bases on either side. Fragments to be subcloned were generated in 3 PCR reactions. In the first PCR reaction, the forward mutagenesis primer and a reverse primer covering the closest restriction site (in the direction 3' of the forward primer) were used. In the second PCR reaction the reverse mutagenesis primer and a forward primer covering the closest restriction site (in the direction 3' of the forward primer) were used. In the third PCR reaction, the products from the previous reactions were purified and used in a PCR with the forward and reverse primers covering the restriction sites. The final product was purified and digested with the same restriction enzymes as the vector. Ligation was carried out as described in section 2.3.6.5.

Primers used for amino acid substitutions using conventional method	
Plasmid	Primers (5' to 3')
pEF-MRTF-A S98D	<p>Reaction1: gccatggccggatcccccccttcc (BamHI) and ctcatgaaatgcagcggggTCtttcaaaggcggcatga</p> <p>Reaction2: tcatgccgcctttgaaaGAccccgctgcatttcatgag and gtctctccaggatccggagcc (BamHI)</p> <p>Reaction3: gccatggccggatcccccccttcc (BamHI) and gtctctccaggatccggagcc (BamHI) and products from reactions 1 and 2.</p>
pET-41a-3CA 67-199 S98D	<p>Reaction1: cgaacgccagcacatggac (BamHI) and ctcatgaaatgcagcggggTCtttcaaaggcggcatga</p> <p>Reaction2: TcatgccgcctttgaaaGAccccgctgcatttcatgag and tgctagttattgctcagcgggt (XhoI)</p> <p>Reaction3: cgaacgccagcacatggac (BamHI) and tgctagttattgctcagcgggt (XhoI) and products from reactions 1 and 2.</p>
Note: Substituted bases are shown in upper case	

2.3.6.8 Site Directed Mutagenesis: Insertions

Primers were designed to be homologous to approximately 15 nucleotides of the fragment to be amplified. 5' to these nucleotides the appropriate restriction site was included, which itself was preceded by an extra 6 nucleotides to ensure efficient restriction enzyme digestion. Fragments were amplified by PCR, purified and digested as described in sections 2.3.6.1-2.3.6.4. Ligation was carried out as described in section 2.3.6.5, using a digested and 5' dephosphorylated vector.

Plasmid	Primers (5' to 3')
pRev(1.4) 30-60	Template: pEF-MRTF-A Forward Primer: TCTAGAGGATCCagcggccccagcccc (BamHI) Reverse Primer: TCTAGAACCGGTttcctcccaggatggag (AgeI)
pRev(1.4) 35-52	Template: pEF-MRTF-A Forward Primer: TCTAGAGGATCCacagagcgaagctggtg (BamHI) Reverse Primer: TCTAGAACCGGTgtcagctcgggctgcag (AgeI)
pRev(1.4) 85-104	Template: pEF-MRTF-A Forward Primer: TCTAGAGGATCCagaggaactggtgagcc (BamHI) Reverse Primer: TCTAGAACCGGTcgctccaggcttcttctc (AgeI)
pRev(1.4) 89-110	Template: pEF-MRTF-A Forward Primer: TCTAGAGGATCCaagccaaggatcatgc (BamHI) Reverse Primer: TCTAGAACCGGTtgcctcatgaaatgcagcg (AgeI)
pRev(1.4) 2-67	Template: pEF-MRTF-A Forward Primer: TCTAGAGGATCCaccccccttcgtc (BamHI) Reverse Primer: TCTAGAACCGGTctaagtggaggtaaa (AgeI)
pRev(1.4) 2-67 33A	Template: pEF-MRTF-A S33A Forward Primer: TCTAGAGGATCCaccccccttcgtc (BamHI) Reverse Primer: TCTAGAACCGGTctaagtggaggtaaa (AgeI)
pRev(1.4) 2-67 LSL46/47/48AAA	Template: pEF-MRTF-A LSL46/47/48AAA Forward Primer: TCTAGAGGATCCaccccccttcgtc (BamHI) Reverse Primer: TCTAGAACCGGTctaagtggaggtaaa (AgeI)
pRev(1.4) 2-67 33D	Template: pEF-MRTF-A S33D Forward Primer: TCTAGAGGATCCaccccccttcgtc (BamHI) Reverse Primer: TCTAGAACCGGTctaagtggaggtaaa (AgeI)
pRev(1.4) 2-115	Template: pEF-MRTF-A Forward Primer: TCTAGAGGATCCaccccccttcgtc (BamHI) Reverse Primer: TCTAGAACCGGTtctctcggtcctgg (AgeI)
pRev(1.4) 2-115 33D	Template: pEF-MRTF-A S33D Forward Primer: TCTAGAGGATCCaccccccttcgtc (BamHI) Reverse Primer: TCTAGAACCGGTtctctcggtcctgg (AgeI)
pRev(1.4) 2-115 $\alpha 1^{AA}$	Template: pEF-MRTF-A $\alpha 1^{AA}$ Forward Primer: TCTAGAGGATCCaccccccttcgtc (BamHI) Reverse Primer: TCTAGAACCGGTtctctcggtcctgg (AgeI)
pRev(1.4) 2-115 $\alpha 2^{AAA}$	Template: pEF-MRTF-A $\alpha 2^{AAA}$ Forward Primer: TCTAGAGGATCCaccccccttcgtc (BamHI)

	Reverse Primer: TCTAGAACCGGTtccctcggtcctgg (Agel)
pRev(1.4) 2-115 S33A	Template: pEF-MRTF-A S33A Forward Primer: TCTAGAGGATCCaccccccttccgtc (BamHI) Reverse Primer: TCTAGAACCGGTtccctcggtcctgg (Agel)
pRev(1.4) 2-115 R81A	Template: pEF-MRTF-A R81A Forward Primer: TCTAGAGGATCCaccccccttccgtc (BamHI) Reverse Primer: TCTAGAACCGGTtccctcggtcctgg (Agel)
pRev(1.4) 2-115 S98A	Template: pEF-MRTF-A S98A Forward Primer: TCTAGAGGATCCaccccccttccgtc (BamHI) Reverse Primer: TCTAGAACCGGTtccctcggtcctgg (Agel)
pRev(1.4) 2-115 S98D	Template: pEF-MRTF-A S98D Forward Primer: TCTAGAGGATCCaccccccttccgtc (BamHI) Reverse Primer: TCTAGAACCGGTtccctcggtcctgg (Agel)
pRev(1.4) 2-115 S96A	Template: pEF-MRTF-A S96A Forward Primer: TCTAGAGGATCCaccccccttccgtc (BamHI) Reverse Primer: TCTAGAACCGGTtccctcggtcctgg (Agel)
pRev(1.4) 2-115 LSL46/47/48AAA	Template: pEF-MRTF-A LSL46/47/48AAA Forward Primer: TCTAGAGGATCCaccccccttccgtc (BamHI) Reverse Primer: TCTAGAACCGGTtccctcggtcctgg (Agel)
pRev(1.4) 67-204	Template: pEF-MRTF-A Forward Primer: TCTAGAGGATCCacttagtgagcggaag (BamHI) Reverse Primer: TCTAGAACCGGTgaactgtctgctacc (Agel)
pRev(1.4) 67-204 B2A	Template: pEF-MRTF-A B2A Forward Primer: TCTAGAGGATCCacttagtgagcggaag (BamHI) Reverse Primer: TCTAGAACCGGTgaactgtctgctacc (Agel)
pRev(1.4) 2-204	Template: pEF-MRTF-A Forward Primer: TCTAGAGGATCCaccccccttccgtc (BamHI) Reverse Primer: TCTAGAACCGGTgaactgtctgctacc (Agel)
pRev(1.4) 2-204 xxx	Template: pEF-MRTF-A xxx Forward Primer: TCTAGAGGATCCaccccccttccgtc (BamHI) Reverse Primer: TCTAGAACCGGTgaactgtctgctacc (Agel)
pRev(1.4) 2-204 B2A LSL46/47/48AAA	Template: pEF-MRTF-A-B2A LSL46/47/48AAA Forward Primer: TCTAGAGGATCCaccccccttccgtc (BamHI) Reverse Primer: TCTAGAACCGGTgaactgtctgctacc (Agel)
pRev(1.4) 2-204 153A	Template: pEF-MRTF-A L153A Forward Primer: TCTAGAGGATCCaccccccttccgtc (BamHI)

	Reverse Primer: TCTAGA <i>ACCGGT</i> gaactgtctgctacc (Agel)
pRev(1.4) 2-204 153D	Template: pEF-MRTF-A L153D Forward Primer: TCTAGAGGATCCaccccccttccgtc (BamHI) Reverse Primer: TCTAGA <i>ACCGGT</i> gaactgtctgctacc (Agel)
pRev(1.4) 2-204 151/3AA	Template: pEF-MRTF-A LL151/153AA Forward Primer: TCTAGAGGATCCaccccccttccgtc (BamHI) Reverse Primer: TCTAGA <i>ACCGGT</i> gaactgtctgctacc (Agel)
Note: Restriction sites are shown in upper case italics, preceded by six bases to promote cleavage efficiency.	

2.3.7 Cloning using the In-Fusion HD Cloning Kit (Clontech Laboratories, Inc)

Primers were designed according to the manufacturer's recommendations. The 15 nucleotides at the 5' end of the primer were homologous to the DNA fragment to which it would be joined. The 3' end of the primer contained 15 nucleotides homologous to the target sequence to be amplified. The primers were used to amplify the desired fragment, which was then purified as described in section 2.3.6.4. The vector was linearised either by restriction digestion or by inverse PCR and purified. The recombinase based reaction was carried out according to the manufacturer's instructions, and a fraction of the reaction was used to transform TOP10 bacteria.

Plasmid	Primers (5' to 3')
pEF-MRTF-A Δ92	Template: pEF-MRTF-A Forward Primer: gccatggccGGATCCccgcctttgaaaagccccgctgca (BamHI) Reverse Primer: gggtgaattTCTAGActacaagcaggaatcccagtggag (XbaI) pEF-MRTF-A vector was digested with BamHI and XhoI
pEF-MRTF-A Δ92 STS544/545/549AAA	Template: pEF-MRTF-A STS544/545/549AAA Forward Primer:

	<p>gccatggccGGATCCccgcctttgaaaagccccgctgca (BamHI)</p> <p>Reverse Primer:</p> <p>gggtgaattTCTAGActacaagcaggaatcccagtgag (XbaI)</p> <p>pEF-MRTF-A vector was digested with BamHI and XhoI</p>
pEF-Phactr1 _(MRTF)	<p>Template: pEF-MRTF-A</p> <p>Insert Forward Primer:</p> <p>ttgtacaccagctcacttagtgagcggaagaatgtgctg</p> <p>Insert Reverse Primer:</p> <p>gtcttgggcatctgctgggtaatttacctggcccacaat</p> <p>Inverse PCR to linearise pEF-Phactr1 plasmid and delete Phactr1 RPEL:</p> <p>Forward Primer: gcagatgccaagactatg</p> <p>Reverse Primer: tgagctggtgtacaaagag</p>
pEF-Phactr1 _{(MRTF) XXX}	<p>Template: pEF-MRTF-A xxx</p> <p>Insert Forward Primer:</p> <p>ttgtacaccagctcacttagtgagcggaagaatgtgctg</p> <p>Insert Reverse Primer:</p> <p>gtcttgggcatctgctgggtaatttacctggcccacaat</p> <p>Inverse PCR to linearise pEF-Phactr1 plasmid and delete Phactr1 RPEL domain:</p> <p>Forward Primer: gcagatgccaagactatg</p> <p>Reverse Primer: tgagctggtgtacaaagag</p>
pEF-Phactr1 _(MRTF NT RPEL)	<p>Template: pEF-MRTF-A</p> <p>Insert Forward Primer:</p> <p>ttgtacaccagctcacccttccgctcattgctgtgaa</p> <p>Insert Reverse Primer:</p> <p>gtcttgggcatctgctgggtaatttacctggcccacaat</p> <p>Inverse PCR to linearise pEF-Phactr1 plasmid and delete Phactr1 RPEL domain:</p> <p>Forward Primer: gcagatgccaagactatg</p> <p>Reverse Primer: tgagctggtgtacaaagag</p>
pEF-Phactr1 _{(MRTF NT RPEL) XXX}	<p>Template: pEF-MRTF-A xxx</p> <p>Insert Forward Primer:</p> <p>ttgtacaccagctcacccttccgctcattgctgtgaa</p>

	<p>Insert Reverse Primer: gtcttggggcatctgctgggtaatttacctggccccacaat</p> <p>Inverse PCR to linearise pEF-Phactr1 plasmid and delete Phactr1 RPEL domain: Forward Primer: gcagatgccaagactatg Reverse Primer: tgagctggtgtacaaagag</p>
pET-41a-3CΔ 2-67	<p>Template: pEF-MRTF-A Forward Primer: caggggccc<i>GGATC</i>Ccccccttccgtcattgctgtgaat Reverse Primer: gtggtggtg<i>CTCGAGT</i>Taaagtggaggtaaattggggttcct</p> <p>pET-41a-3CΔ digested with BamHI and XhoI</p>
pET-41a-3CΔ 2-67 LSL46/47/48AAA	<p>Template: pEF-MRTF-A LSL46/47/48AAA Forward Primer: caggggccc<i>GGATC</i>Ccccccttccgtcattgctgtgaat Reverse Primer: gtggtggtg<i>CTCGAGT</i>Taaagtggaggtaaattggggttcct</p> <p>pET-41a-3CΔ digested with BamHI and XhoI</p>
pET-41a-3CΔ 2-115	<p>Template: pEF-MRTF-A Forward Primer: caggggccc<i>GGATC</i>Ccccccttccgtcattgctgtgaat Reverse Primer: gtggtggtg<i>CTCGAGT</i>tactcggtcctggcccgcctccagget</p> <p>pET-41a-3CΔ digested with BamHI and XhoI</p>
pET-41a-3CΔ 2-115 LSL46/47/48AAA	<p>Template: pEF-MRTF-A LSL46/47/48AAA Forward Primer: caggggccc<i>GGATC</i>Ccccccttccgtcattgctgtgaat Reverse Primer: gtggtggtg<i>CTCGAGT</i>tactcggtcctggcccgcctccagget</p> <p>pET-41a-3CΔ digested with BamHI and XhoI</p>
<p>Note: Restriction sites are shown in upper case italics.</p>	

2.3.8 Sequencing

All plasmids generated were confirmed by sequencing which was carried out by CRUK Equipment Park sequencing services.

2.4 Oligonucleotides

Primers were synthesised by Sigma-Aldrich. Lyophilised oligonucleotides were dissolved in TE buffer at 100 μ M for long-term storage and in water at 10 μ M for short storage (both stored at -20°C).

siRNA was purchased from Thermo Scientific Dharmacon. Lyophilised siRNAs were dissolved in 1x siRNA buffer (Thermo Scientific Dharmacon) to a final concentration of 20 μ M, aliquoted and stored at -20°C. All oligos, except for the non-targeting control and MRTF-A/B, were a pool of 4 siRNAs targeting different locations of the same target.

siRNA	
siRNA name	siRNA sequence
Non-targeting control	UUCUCCGAACGUGUCACGU
MRTF-A/B	UGGAGCUGGUGGAGAAGAA
CDC2L5	GAAGAAAGUCGCCAUUA UAACUAUGGUGGUAACUUA GCACGUAGUUUCAUUGGAA CUAACAAGGUCAUUACUUU
CLK2	GAUAACAAGUUGACACAUA GGAAGCAGCCCAGACUAGAA GAACACGAGUUGCCCUGAA CAAGAGCGAUUUGAAAUUG
CDK7	GGACAUAAGUCUAACAUUA GUACCGGGCUCCUGAGUUA UGUGUAGUCUCCCGAUUA CAAGGAAUAUUGCCCAAGA

CDK8	GAUCCCAUAUCCCAAACGA CAUCAUGACCUCCGACUAU GACCCAAUAAAGCGAAUUA UACAGAAGAAGAGCCUGA
CDK9	GGCCAAACGUAGACAAGUA CUACUCACUUGACGUCUAU AGACGGAAUUUGAACGUGU GCAGAGAUGUGGACUCGUA
CSNK1A1	GAAUUUGCCAUGUACUUA GUAUUGGGCGUCACUGUAA GCUCCAAGGCCGAAUUUAU CUAUGAAGACCGUACUUAU
DYRK1A	GAAAUCGACUCCUAAUAG GAAAUGAAGUACUACAUAG GAACCUAACACGAAAGUUU GGAUGUAUCUUGGUUGAAA
DYRK1B	CUGAUGAACCAGCAUGAUA CAACAGAGCCUACCGAUAC GACCAGAUGAGCCGUUUUG GGACAAAGGAACUCAGGAA
DYRK2	GGGACCAGCUGGCUUGUAU GGUCGAAGCAGUAUUAAAG GGACAAGGACAACACUAUG GUACAUCCAGUCACGCUUU
DYRK3	CAGGGAAGCGGGUAGUUAA UAGCAAGUCUACACCCAAA GGGAUAGCCAGUAAGCUUA UCCAGAAGGCUAAAUAUUA
DYRK4	CCAAGUCACUGUAAAGUU CCUCAAGCAUGCCUGGAUU AGUCGGAGGUUGAGAGUAA GAAUCAACCUGUAUGAGUU
HIPK1	UACAGAGAUCUAAUUUG UGACAUGGCUCAGGUAAAU

	GCAACCAGCUCAACACAGU GCUAUGAAGUCCUGGAGUU
HIPK2	GGACAAAGACAACUAGGUU UCAUUGACCUGUUAAGAA GAAGCAAGAAAGUACAUUU GCACGGAGAGCGCUGAUGA
HIPK3	GGAAGGAGGUGAUCUCUUG GAACAGGAGUAAUUCAUUG GGAAGGCGACUAUCAGUUA GAAAGAGGUUGAGGAAGUA
MKNK2	GGAAUAUGCUGUCAAGAUC GAACAGCUGUGCCAAAGAC CAUAGAAGGCGCCACUUUA GUUCGAAGAUGUCUAUCAG
NDR2	CAUGAAAGCUGGGAAGUUA ACAGAAACCUCACACAUAA GAAGGAGACUCUGGCAUUU GGACUUGAUUCUCAGAUUU
OSR1	CAAGAUCCCUAUCAGUCUA GAAGGGAUUUAGUAAUAGU AAACCGAUCUGUCACUUUC AUCCUAACAUUGUGUCUUA
PHKG2	GAAGGCCAAUAUCAGUUUA CAGAUACGCCUUUCAGAUU GUUCAAACACCGUCAAGA GUGCGGGACUCCAGGGUAU
PIM3	CACAGGACCUCUUCGACUU CAGAGUGGAUCCGAUAUCA CCAGAGUGCCAGCAGCUUA GAACUGUGACCUUCGGCUU
SNARK	GCAGCAAGAUUGUGAUUGU GCGUGAAUCUGGUUACUAC GCACAUACGGAGGGAGAUU CCGAAAGGCAUUCUCAAGA

TAK1	GGACAUUGCUCUACAAAU AAACACACAUGACCAAUAA GAUGGCGCCUGAAGUAUUU AAAUACAUCUCGUCUGGUA
TLK1	GAAAUCAAACCUCCUAUUA GCAAGAAACUACUUAUUGA GAAAGAAGCUCGGUCUAUU GAAAUUGGCAGCAUUAGAA
TLK2	GAGGAAAUCUUCAAACUUA GAAGCCCGAUCCAUAUUA CCAAAGAUCUCAAUAAAG UAGUGAAGCUGUAUGAUUA
ULK1	CCACUCAGGUGCACAAUUA UCACAAAGCCCUGCUAUUG GCAUGGACUUUGAUGAAUU UUACGGACCUGCUGCUUAA
ULK3	UGACCUGUCUCGCUUCAUU CAAGAAGGAUACUCGGGAA GCACGUACGCCACGGUGUA
YSK4	UAACAACUCUUGCCAAUUA GCCGAUGUGUCGUUAAUAA CAACGGACCAGGCAUCUAU GAUCCUAAGCUUUGUGAUU

2.5 Peptides

Peptides used in this study were synthesised and purified by the Peptide synthesis laboratory (CRUK). Phospho-acceptor sites are shown in bold.

Peptide name	Peptide sequence
KEMPtide	LRRAS L G
DYRKtide	RRRFRPAS P PLRGPPK
Peptide S33	RRLSLSAAPS P QSEAVA
Peptide S216	RREDSSDAL S PEQPASH
Peptide S231	RRESQGSV P SPLESRV
Peptide S248	RRLPSATS I SPTQVLSQ
Peptide T402	RRTPGSSAP T PSRSLST
Peptide S412	RRRSLSTSS S PSSGTPG
Peptide S414	RRLSTSSSP S SGTPGPS
Peptide S549	RRTGSTPPV S PTPSERS
Peptide T566	RRSTGDEN S T P GDADFGE
Peptide S587	RRTQLTLQAS P LQIVKE
Peptide S605	RRRAASCCL S PGARAE L
Peptide S785	RRQPLSQPG S PAPGPPA
Peptide S883	RRPPLTPQ P SPLSELPQ
Peptide S949	RRAILDHPP S PMDTSEL
RPEL1 (67-98) 5-FAM labelled	LSERKNVLQKLQQRRTREELVSQGIMPPL K S
RPEL1 (62-104) 5-FAM labelled	PNLPPLSERKNVLQKLQQRRTREELVSQGIMPPL K SPAAFHE
S33	SAAPS P QSEC
pS33	SAAP (p S) PQSEC
S1-R2	PPLKSPAAFHEQRRSLERARTEDYLKRKIRSRPERAELVRMHILEETSA
S1-R2 pS98	PPLK (p S) PAAFHEQRRSLERARTEDYLKRKIRSRPERAELVRMHILEETSA

2.6 Mammalian cell culture

Cell lines used in this thesis were the mouse embryonic fibroblasts NIH-3T3 (Treisman Laboratory, Cancer Research UK), NIH-TR3 that express Flag-MRTF-A

upon tetracycline treatment (generated by Dr F. Miralles), 3T3.3DA.18 stably transfected with the 3DA MRTF-A activity reporter and the TK-luciferase plasmid (generated by Dr R. Pawlowski), and the human cervical adenocarcinoma cell line HeLa.

All the cell lines were cultured in DMEM supplemented with 10% FCS and 1% Penicillin/Streptomycin (CRUK media production) and incubated at 37°C and 10% CO₂. To detach cells from dishes, two PBS washes were followed by incubation in trypsin/versene (CRUK media production) for approximately 5 minutes. Trypsin was inactivated by addition of 10% FCS DMEM and cells were seeded into new dishes.

2.7 siRNA transfection

siRNA was transfected using Lipofectamine RNAiMax transfection reagent (Life technologies) according to the manufacturer's instructions. siRNA transfections were carried out in a 24-well-plate format as follows:

1. Preparation of DNA and LipofectamineRNAiMax solutions (per well)
DNA mix: 50µL Opti-mem + siRNA (for final concentration of 25nM) Lipofectamine mix: 50µL Opti-mem + 0.6µL Lipofectamine RNAiMax
2. Incubation of transfection mixture
The DNA mixture and Lipofectamine mixture were combined, vortexed and incubated at room temperature for 20 minutes. The combined DNA/Lipofectamine mixture (100µL) was transferred to a well of a 24-well-plate.
3. Transfection
Cells were detached as described in section 2.6, counted and diluted to 35 000 cells per 400µL of 10% FCS DMEM. 400µL of the cell suspension were added to a well containing the transfection mixture, to give a final volume of 500µL. Cells were then incubated overnight.

2.8 Luciferase reporter assays

For luciferase assays cells were seeded in 24-well-plates. Cells were typically transfected with siRNA the previous day, as described in the previous section. The following day cells were transfected with the MRTF-A reporter plasmid, TK-Renilla plasmid and other plasmids according to the experiments, using Lipofectamine 2000 reagent. Transfection was carried out as follows:

<p>1. Preparation of DNA and Lipofectamine2000 solutions (per well)</p> <p>DNA mix: 50µL Opti-mem + 200ng DNA (8ng p3D.A-luc, 20ng ptkRL, 40ng SRF-VP16, different amounts of other plasmids according to experiment, up to 200ng with “empty” vector) (Typically a titration of 0.5 to 40ng per well was used; 5ng of plasmid lead to expression of MRTF-A at endogenous levels, as assessed by western blot).</p> <p>Lipofectamine mix: 50µL Opti-mem + 0.6µL Lipofectamine 2000</p>
<p>2. Incubation of transfection mixture</p> <p>The DNA mixture and Lipofectamine mixture were combined, vortexed and incubated at room temperature for 20 minutes.</p>
<p>3. Transfection</p> <p>Cells were washed twice in PBS and 100µL of Opti-mem was added. The combined DNA/Lipofectamine mixture was then added to the cells, for a final volume of 200µL. Cells were incubated at culture conditions for 2 hours. The transfection mixture was then replaced by 0.3% FCS DMEM and cells were starved overnight.</p>

The following day cells were treated and stimulated for 6 hours. Cells were lysed in 100µL 1x passive lysis buffer (Promega) and placed on a shaker for 10 minutes. 20µL of lysate were transferred to a flat-bottom 96-well plate (Matrix Technology). 50µL of luciferase assay reagent II (Promega) were added to the lysate and luminescence was measured using an EnVision Multilabel Reader (Perkin Elmer). Next, 50µL of Stop&Glo reagent was added, which quenches firefly

luciferase activity and elicits renilla luciferase activity. Luminescence generated by Renilla luciferase activity was measured as before.

Firefly luciferase values were normalised using renilla luciferase values. Where stated, normalised values were expressed as a percentage of activity of SRF-VP16.

Mammalian reporter plasmids	
p3D.A-luc	A 3D.ACAT SRF reporter derivative (Mohun et al., 1987), in which the CAT sequence was replaced by that of firefly luciferase. The promoter is composed of 3 copies of the <i>Fos</i> serum response element (SRE) with a <i>Xenopus</i> type 5 actin TATA box and transcription start site (Geneste et al., 2002). The SRE was modified, making the reporter unresponsive to TCF signalling. Firefly luciferase expression is therefore dependent on MRTF-A/SRF (Hill et al., 1995).
ptkRL	Renilla luciferase preceded by the thymidine kinase promoter (Geneste et al., 2002). The plasmid was used as an internal reference to control for transfection efficiency and non-specific activation of the p3D.A-luc reporter.

2.9 Quantitative real-time PCR

Cells were seeded at 30 000 cells per well in 24-well-plates unless they were transfected with siRNA the previous day (see section 2.7). After appropriate treatments, RNA was isolated using the GenElute Mammalian total RNA miniprep kit (Sigma-Aldrich) according to the manufacturer's protocol (250µL lysis buffer; 40µL elution buffer). Isolated RNA was treated with DNaseI to remove contaminating DNA. 0.5µg of RNA was reverse transcribed using the Superscript III First Strand synthesis system (Life Technologies). The reactions were set up as follows:

DNaseI treatment
1µg RNA 1µL DNaseI (2 units) 1µL 10x DNaseI buffer Top up to 7µL with water
10 min incubation at room temperature
1µL EDTA (25mM) and incubation at 65°C for 10 min to inactivate DNaseI

Priming reaction
0.5µg RNA 1µL random hexamers 1µL dNTPs (10mM) Top up to 10µL with water
5 min incubation at 65°C followed by 5 min incubation on ice
1µL of EDTA (25mM) and incubation at 65°C for 10 min to inactivate DNaseI

cDNA synthesis
10µL Priming reaction 2µL 10x RT buffer 4µL MgCl ₂ (25mM) 2µL DTT (0.1M) 1µL RNaseOUT (40U/µL) 1µL Superscript III reverse transcriptase
Incubation: 25°C 10 min, 50°C 50 min, 85°C 5 min, 4°C hold.
1µL RNase H, incubation at 37°C for 20 min.

cDNA was next used for qRT-PCR as follows:

qRT-PCR
Reaction set-up
1µL cDNA 1µL forward primer (10mM) 1µL reverse primer (10mM) 10µL SYBR Green reaction mix (Life Technologies) 7µL water

Thermal cycling		
95°C	10 min	 40 cycles
95°C	10 sec	
60°C	30 sec	

qRT-PCR primers		
Target	Primer sequence (5' to 3')	Notes
Itgb1	FW: GAGTGGAAGCCCTGAAGACATT RV: TTGCCTTTTCCTTATGACTGACAA	Intronic
Myh9	FW: CATTTCACATCGTGCTTCCTA RV: AGGGTTTTGGCACGTGTGA	Intronic
Vcl	FW: GATCCTGGTGTCTGTGCTTCT RV: TGAGCAAAATGCCCGAA	Intronic
Srf	FW: GTCAGGAATGGAGGATGGACAT RV: CCTTCTCGGACTAGCACAGGTA	Intronic
Dyrk1a	FW: GCTTGCACCGTCGTTCTCAT RV: GCATCTGTGCAGCCATCTGA	Exonic
Dyrk1b	FW: GTGTTTGAGCTGCTGTCTACAA RV: GACACCCCGAAAGTGTGTGT	Exonic
Dyrk2	FW: CACTGCCATGCACGTTTCT RV: GGCCGAAGGTTTCTGGTTA	Exonic
Dyrk3	FW: GCCCGGGTCTATGATCACAA RV: TCATTGCGCACCATTTTCA	Exonic
Dyrk4	FW: CCGATCCCCAGAGGTGATT RV: CCCAGGCTCCACATGTCAAT	Exonic
Egr1	FW: GACCCAAACGTCCAGTCCTTTC RV: CAAGACCCTGGAGCTGTGTGAA	Intronic
Mkl1 (MRTF-A)	FW: TCCGTCATTGCTGTGAATGG RV: TGGCTCGTCGTCATTTTCG	Exonic
Mkl2 (MRTF-B)	FW: CCAAGAATCCAAACGACAAACA RV: CTCGCGGTTTCGGATCTTT	Exonic
Gapdh	FW: TCTTGTGCAGTGCCAGCCT RV: CCATATGGCCAAATCCGTTCA	Exonic

Target abundance was quantitated using absolute quantification and a standard curve ranging from 0.1pg/ μ L to 10ng/ μ L.

2.10 Immunofluorescence microscopy

150 000 cells per well were seeded into 6-well-plates containing coverslips and transfected as follows:

1. Preparation of DNA and Lipofectamine2000 solutions (per well)
DNA mix: 100 μ L Opti-mem + 1 μ g DNA (50ng of pEF-MRTF-A derivatives, 20ng of pEF-PK derivatives, 100ng for pEF-chimera derivatives, 200ng of pRev derivatives, topped up to 1 μ g with “empty” vector)
Lipofectamine mix: 100 μ L Opti-mem + 3 μ L Lipofectamine 2000
2. Incubation of transfection mixture
The DNA mixture and Lipofectamine mixture were combined, vortexed and incubated at room temperature for 20 minutes.
3. Transfection
Cells were washed twice in PBS and 1mL of Opti-mem was added. The combined DNA/Lipofectamine mixture was then added to the cells, for a final volume of 1.2mL. Cells were incubated at culture conditions for 2 hours. The transfection mixture was then replaced by DMEM 0.3% FCS and cells were starved overnight.

The next day cells were treated accordingly and fixed with 4% paraformaldehyde (PFA) for 10 min at room temperature. After a PBS wash cells were permeabilised with 0.2% Triton-X in PBS for 10 min and blocked in blocking solution (10% FCS, 1% fish skin gelatin, 0.05% Triton-X in PBS) for 1 hour. Coverslips were then placed cell-side down on 50 μ L drops of blocking solution containing primary antibody and incubated for 1 hour. Coverslips were washed in PBS and transferred to 50 μ L drops of blocking solution containing secondary antibodies, as well as phalloidin and DAPI. After an hour incubation coverslips were washed twice in PBS, once in water and mounted on microscopy slides using 5 μ L

Mowiol. Imaging was carried out using a Zeiss Axiovert microscope. Cells were scored as predominantly nuclear, pancellular or predominantly cytoplasmic; 200 cells were counted per condition.

Antibodies used in immunofluorescence microscopy		
Antibody	Species	Dilution
Flag (F7425, Sigma-Aldrich)	rabbit	1:1000
AlexaFluor 488 IgG (H+L) (Molecular probes)	Donkey anti-rabbit	1:250

Other staining reagents		
DAPI	300nM	Stains DNA. Used to mark nucleus
Phalloidin Texas-Red-X (Molecular Probes)	1:200	Stains F-actin. Used to mark cytoplasm

2.10.1 Rev NES detection assay

80 000 cells per well were seeded in 6-well plates containing coverslips. Transfection was carried out as described in the section above, however at the end of the transfection 10% FCS DMEM was used to replace the transfection reaction. Cells were starved the next day as opposed to immediately after transfection.

After treatment and stimulation, cells were fixed with 4% PFA for 10 minutes, washed twice in PBS and incubated for 10 minutes in 300nM DAPI in PBS. After two PBS washes and one wash in water coverslips were mounted on microscope slides using 5µL Mowiol. Imaging and scoring was carried out as described above.

2.11 Protein Expression and Purification

2.11.1 Expression and purification of recombinant MRTF-A fragments

E. Coli Rosetta (DE3) pLysS (Novagen) (Genotype: F⁻ *ompT hsdS_B(r_B⁻ m_B⁻) gal dcm* (DE3) pLysSRARE (Cam^R) were transformed with the expression plasmid and plated on agar supplemented with the appropriate antibiotics. A single colony was then used to inoculate 100mL of LB media containing the appropriate antibiotics. The culture was incubated on a shaker at 37°C, 180rpm overnight. Next day, 5mL were used to inoculate 1L of LB media containing antibiotics. The culture was incubated as before, until it reached an OD₆₀₀ of 0.6, at which time expression was induced by adding 0.5mM IPTG. Induced cultures were incubated at 30°C for 5h or at 20°C for 18h. Bacteria were pelleted by centrifugation at 4000 xg for 15 minutes. Pellets were either frozen on dry ice for storage at -80°C or processed immediately.

GST fusion protein purification	
Bacterial lysis buffer	50mM Tris-HCl pH 7.5 300mM NaCl 1% TX-100 5mM DTT 10mM EDTA pH 8 1mM PMSF 15µg/mL Benzamidine
Wash buffer 1	50mM Tris-HCl pH 7.5 300mM NaCl 1mM DTT
Wash buffer 2	50mM Tris-HCl pH 7.5 500mM NaCl

	1mM DTT
Wash buffer 3	50mM Tris-HCl pH 7.5 50mM KCl 20mM MgCl ₂ 5mM ATP 1mM DTT
Equilibration buffer	50mM Tris-HCl pH 7.5 100mM NaCl 1mM DTT

Pellets were resuspended in lysis buffer (100mL/10g of pellet) and homogenised using a Dounce homogeniser on ice, before being passed through a French press until clear. Lysates were pelleted by centrifugation at 100 000 xg for 30 min, 4°C. Supernatants were then transferred to a new vessel containing 1.5mL of Glutathione Sepharose 4B (GE Healthcare) per 10g of pellet, and incubated for 2 hours at 4°C with gentle agitation.

The resin was then transferred to a column and washed with 150mL wash buffer 1, 300mL wash buffer 2, 150mL wash buffer 3 and equilibrated in equilibration buffer. The GST moiety was cleaved off by overnight incubation with 100µg GST-3C protease per mL of resin (purified by S. Guettler). The cleaved protein was eluted with 1mL per mL of resin, quantified and stored at -80°C.

2.11.2 Purification of Crm1

E. Coli BLR bacteria were transformed with the pH10zz-[TEV]-MmCrm1 plasmid (a gift from Thomas Guttler, Dirk Gorlich lab, Max Planck Institute for Biophysical Chemistry, Germany). A single colony was used to inoculate a pre-culture and was incubated overnight in the presence of 100µg/mL ampicillin. The following day, 5mL of pre-culture were used to inoculate 1L 2YT medium (2% w/v glycerol, 30mM K₂PO₄) supplemented with 100µg/mL ampicillin. The culture was incubated at 37°C until it reached OD₆₀₀ = 0.5, then cooled to 18°C and induced with 150µM IPTG for 20 hours.

Bacteria were pelleted by centrifugation at 4000 xg for 15 minutes and pellet were either frozen on dry ice for storage at -80°C or processed immediately. Pellets were resuspended in lysis buffer (100mL/10g of pellet) and homogenised using a Dounce homogeniser on ice, before being passed through a French press until clear. Lysates were pelleted by centrifugation at 100 000 xg for 30 min, 4°C.

Supernatants were then transferred to a new vessel containing 3mL of Complete His-Tag purification Resin (Roche) per 10g of pellet, and incubated for 2 hours at 4°C with gentle agitation. The resin was then transferred to a column and washed with 200mL wash buffer. Elution was carried out by incubating in 5mL elution buffer for 5 minutes. This was repeated 3-4 times, and eluates were pooled for a final volume of approximately 20mL. The eluate was concentrated to 5mL using a Vivaspin 20 concentrator (50kDa MWCO, Sartorius).

Using a HiPrep 26/10 Desalting column (GE Healthcare) mounted on an AKTA FPLC system, buffer was exchanged for desalting buffer. After concentrating to 5mL again, 100 units of Ac-TEV protease (His tagged, Life Technologies) were added to cleave off the His10-zz tag, and incubated overnight at 4°C on rollers. The eluate was collected and gel filtered in SEC buffer using a Superdex 200 16/60 column (GE Healthcare). Appropriate fractions (between 65-80mL elution volume) were pooled and concentrated to 10mg/mL. Purified Crm1 was aliquoted and stored at -80°C.

Crm1 purification buffers	
Lysis buffer	50mM Tris-HCl pH 7.5 500mM NaCl 1mM EDTA 2mM Imidazole 1mM PMSF 5mM DTT
Wash buffer	50mM Tris-HCl pH 7.5 500mM NaCl 1mM EDTA 2mM Imidazole 1mM PMSF 5mM DTT 100mM KCl 10mM Mg(OAc) ₂ 2mM ATP
Elution buffer	50mM Tris-HCl pH 7.5 500mM NaCl 1mM EDTA 300mM Imidazole 1mM PMSF 5mM DTT
Desalting buffer	50mM Tris-HCl pH 7.5 200mM NaCl 1mM EDTA 1mM DTT

2.11.3 Purification of Ran Q69L

E. Coli BLR bacteria were transformed with the pH10zz-[TEV]-HsRan(1-180) Q69L plasmid (a gift from Thomas Guttler, Dirk Gorlich lab). The expression and lysis procedure was identical to that of Crm1 (see above).

The clarified bacterial lysate was incubated with 3mL of Complete His-Tag purification Resin (Roche) per 10g of pellet, and incubated for 2 hours at 4°C with gentle agitation. The resin was then transferred to a column and washed with 200mL lysis buffer. Elution was carried out by incubating in 5mL elution buffer for 5 minutes. This was repeated 3-4 times, and eluates were pooled for a final volume of approximately 20mL. The eluate was concentrated to 2mL using a Vivaspin 6 concentrator (30kDa MWCO, Sartorius) and dialysed against 1L dialysis buffer overnight, in the presence of 100 units Ac-TEV. The next day the solution was incubated with 3mL of fresh Complete His-Tag purification Resin, which was previously equilibrated in dialysis buffer, for 1 hour. The eluate was concentrated to 3.5mL and subjected to gel filtration in dialysis buffer, on a Superdex 75 16/60 column (GE Healthcare). Appropriate fractions were pooled and concentrated to 1.8 mg/mL (90µM).

Ran concentration was measured using an extinction coefficient $\epsilon_{280}=34\ 820\ \text{M}^{-1}\text{cm}^{-1}$ to correct for the presence of GTP, whose absorption spectrum overlaps with that of proteins.

RanQ69L purification buffers	
Lysis buffer	50mM K-Phosphate pH 7 500mM NaCl 5mM Mg(OAc) ₂ 1mM EDTA pH 8 2mM Imidazole 1mM PMSF 5mM DTT 30µM GTP

Elution buffer	50mM K-Phosphate pH 7 500mM NaCl 1mM EDTA pH 8 300mM Immidazole 1mM PMSF 5mM DTT 30µM GTP
Dialysis buffer	50mM K-Phosphate pH 7 200mM NaCl 1mM EDTA 1mM DTT 20µM GTP

2.11.4 Purification of rabbit skeletal muscle actin

Actin was purified from rabbit skeletal muscle as previously described (Spudich and Watt, 1971). The following procedure was carried out at 4°C unless stated otherwise. Approximately 500g of rabbit leg tissue was minced until homogenous and mixed vigorously in 4L of the following solutions. Between washing steps muscle tissue was drained using gauze.

10mM KCl	10 min
50mM NaHCO ₃	10 min
1mM EDTA	10 min
The following steps are per 250g of initial rabbit muscle	
Deionised water	5 min
Deionised water	5 min, then bring to room temperature
Cold acetone	As briefly as possible
500mL Acetone	10 min room temperature
500mL Acetone	10 min room temperature
500mL Acetone	10 min room temperature

After a final draining through gauze the homogenate was spread over 3MM Whatman paper in a fume hood to dry overnight. The following day the acetone powder was stored as 10g aliquots at -80°C , and used for actin extraction and purification.

The following quantities are for 10-12g of acetone powder. Acetone powder was rehydrated to 200mL with ice cold Ca^{2+} G-buffer supplemented with 0.15mM PMSF for 1h at 4°C , while stirring. The homogenate was drained and this step was repeated three times. The filtrates were pooled and centrifuged for 90 min at 27 000 xg, 4°C . The clarified filtrate was transferred to a beaker and actin polymerisation was induced by adjusting final concentrations to 1mM ATP, 2mM MgCl_2 , 50mM KCl. Actin was polymerised under gentle stirring for 2 hours. 4.1g of solid KCl/100mL were then added directly to bring KCl to 600mM under fast stirring. Polymerised actin was next pelleted at 100 000 xg for 90 min and resuspended in 30mL Ca^{2+} G-buffer supplemented with 0.5mM ATP and 1mM DTT, using a Dounce homogeniser on ice. Homogenisation was carried out carefully to avoid introduction of air. Actin was dialysed for 2 days in 4L of Ca^{2+} G-buffer with twice daily changes of buffer. ATP concentration of the dialysis buffer was gradually decreased from 0.5mM to a final 0.2mM ATP. After dialysis, insoluble material was pelleted by centrifugation at 100 000 xg for 30 min, 4°C .

A second round of polymerisation and dialysis was repeated to increase actin purity. After the final dialysis step, actin at $100\mu\text{M}$ (4.2 mg/mL) was aliquoted and stored at -80°C . For Latrunculin B-bound actin, which is rendered unable to polymerise, a 5-fold molar excess of Lat-B (50mM stock in DMSO, Calbiochem) was slowly added under continuous stirring. After overnight incubation, actin polymerisation was induced using 20x polymerisation buffer as before. Insoluble material was pelleted at 200 000 xg for 15 min, 4°C and the supernatant was dialysed in Mg^{2+} G-buffer. Lat-B G-actin was aliquoted and stored at -80°C .

Actin concentration was measured at 290nm using a molar extinction coefficient of $\epsilon_{290}=26\ 600\ \text{M}^{-1}\text{cm}^{-1}$, because measurement at A_{280} is affected by ATP present in the buffer.

Actin extraction and purification buffers	
Ca ²⁺ G-buffer	5mM Tris-HCl pH 8.0 0.2mM CaCl ₂ 0.2mM ATP 0.5mM DTT
20x Polymerisation buffer	2M NaCl 60mM MgCl ₂ 10mM ATP
Mg ²⁺ G-buffer	2mM Tris-HCl pH 8 0.3 mM MgCl ₂ 0.2mM EGTA 0.2mM ATP 0.5mM DTT

2.12 Protein analysis

2.12.1 GST affinity pull-down assays

The GST-MRTF-A fragments used as bait in the Crm1 and ERK pull-down assays were prepared as described in section 2.11.1, but were not cleaved off the resin. The resin was washed in pull-down buffer. The conditions for the reactions are shown below:

Pull down buffer
50mM Tris-HCl pH 7.5 100mM NaCl 10mM MgCl ₂ 0.05% NP-40

Pull-down reactions	
Crml	ERK2
25µL resin	12.5µL resin
2µL Crml (10 mg/mL)	3µL ERK2 (5.5mg/mL)
2µL RanQ69L (1.8 mg/mL)	-
Final volume 200µL	Final volume 200µL

Reactions were incubated for 3 hours at 4°C on a shaker. The resin was then washed with 1mL pull-down buffer 5 times. The proteins were eluted with SDS-loading buffer, resolved by SDS-PAGE and analysed either by coomassie staining or Western blotting.

2.12.2 RhoGTP pull-down assay

RhoGTP pull-downs were performed using the Rho activation assay kit (Merck Millipore) with a modified protocol. Cells were grown in 15cm dishes and stimulated according to the experiment. After treatment cells were washed twice in ice-cold TBS placed slanted on ice. TBS was completely removed and cells were scraped in 400µL 2x lysis buffer (supplemented with 16% glycerol). Samples were snap-frozen as they were collected.

Samples were next thawed on ice, made up to 800µL using ice-cold water and insoluble material was pelleted at maximum speed on a refrigerated bench top centrifuge. 20µL of the supernatant were retained and mixed with SDS loading buffer; the rest was incubated with 20µL GST-Rhotekin resin for 45 min at 4°C. The resin was next washed 3 times with 1mL 1x Lysis buffer (supplied with the kit) and proteins were eluted by addition of SDS loading buffer. Active Rho levels were assessed by Western blotting using RhoA antibody (Cell Signalling, 67B9, 1:1000).

2.12.3 SDS-PAGE

Proteins were resolved according to their size by sodium dodecyl sulfate polyacrylamide electrophoresis (SDS-PAGE) on 4-12% gradient gels (Life

Technologies). Usually SDS-PAGE was carried out in MOPS buffer, unless better resolution was desired for the smaller molecular weights, in which case MES buffer was used. For assessment of changes in MRTF-A electrophoretic mobility 7% tris-acetate gels (Life Technologies) were run with tris-acetate running buffer. Electrophoresis was performed at 150V.

2.12.4 Protein detection

2.12.4.1 Coomassie Staining

Following SDS-PAGE gels were incubated in Coomassie staining solution for 30-60 minutes on a shaker. Gels were then destained after multiple washes with destaining solution. For rapid staining/destaining, incubations were preceded by microwaving for 1 min.

Staining solution	0.1% Coomassie brilliant blue 50% methanol 10% acetic acid 40% water
Destaining solution	10% Methanol 10% acetic acid 80% water

2.12.4.2 Western blotting

After SDS-PAGE, proteins were transferred to nitrocellulose or PVDF membranes (Whatman). PVDF required activation by a 1-minute incubation in methanol. The gel and membrane were sandwiched between 3MM Whatman paper. Transfers were performed in Mini Trans-Blot Cell (Biorad) filled with transfer buffer, at 250mA for 75 minutes.

Membranes were then blocked by incubation in blocking solution for 45 minutes at room temperature on a shaker. Membranes were incubated with primary antibodies diluted in blocking solution overnight at 4°C or at room temperature for 1

hour. Next, the membranes were washed 3 times in PBS-Tween for 10 minutes, and incubated in HRP-conjugated secondary antibodies for 45 minutes. After three washes in PBS-Tween, HRP activity was detected using ECL Western blotting detection reagents (GE Healthcare) and ECL Hyperfilm (GE Healthcare).

Western blotting buffers	
Transfer buffer	192mM Glycine 25mM Tris base 10% Methanol
PBS-Tween	PBS 0.1% Tween 20 (Sigma-Aldrich)
Blocking buffer	PBS-Tween 4% dry milk powder

Primary Antibodies	
Name	Working dilution
MRTF-A (C-19, Santa Cruz)	1:1000
Flag (F7425, Sigma-Aldrich)	1:1000
RhoA (67B9, Cell Signalling)	1:1000
Phospho-ERK1/2 (Cell Signalling)	1:1000
panERK (BD Biosciences)	1:10 000
HA-12CA5 (Abcam plc)	1:1000
MRTF-A phospho-specific antibodies	1-2 μ g/mL
Secondary Antibodies	
Name	Working dilution
Rabbit IgG-HRP (DAKO)	1:2000
Mouse IgG-HRP (DAKO)	1:2000
Goat IgG-HRP (DAKO)	1:2000

2.13 Fluorescence polarisation assay

Fluorescence polarisation (FP) assays were carried out as described in (Guettler et al., 2008), in 384-well-flat-bottom black polystyrene plates with a non-binding surface (Corning Inc) and a final volume of 10 μ L. Peptides were dissolved in FP assay buffer to a concentration of 0.5 μ M. Lat-B actin was added at a concentration ranging from 1nM to 60 μ M. Reactions were incubated for at least 5 hours at room temperature to allow attainment of binding equilibrium.

Measurements were made using a Safire² microplate reader (Tecan). Using the fluorescence polarisation mode the following settings were selected:

FP-assay settings	
Excitation	470nm
Emission	525nm
Excitation bandwidth	20nm
Emission bandwidth	20nm
Time between move and flash	10ms
Integration time	40 μ s
Lag time	0
Automatically determined z-position	
Optimal gain	
10 reads	

Anisotropies were calculated by the Magellan software. Dissociation constants were calculated using the GraphPad Prism6 software by non-linear regression and using the equation: $Y = ((A_b - A_f) * (X / (K_D + X))) + A_f$, where Y is total anisotropy; A_b is anisotropy from bound ligand; A_f is anisotropy from free ligand; X is a protein concentration; K_D is the dissociation constant (Heyduk and J. C. Lee, 1990).

2.14 Analytical gel filtration

20 μ L of 100 μ M LatB-actin was mixed with a 3-fold molar excess of peptide or purified MRTF-A RPEL domain in a total volume of 110 μ L, using GF buffer to top up. The mixture was incubated for 5 minutes at room temperature and then subjected to size exclusion chromatography on an equilibrated S200 10/300 column (GE Healthcare). The entire sample was injected into a 100 μ L loop. Elution of proteins was followed by absorption at 215nm and 280nm. The column was calibrated using a gel filtration standard (Biorad).

GF-Buffer	2mM Tris-HCl pH 8 100mM NaCl 3mM MgCl ₂ 0.2mM EGTA 0.3mM TCEP 5% w/v glycerol
-----------	---

2.15 IP/Kinase assay

Cells were seeded into 10cm dishes at 1x10⁶ cells per dish and incubated overnight in 10% FCS DMEM. The next day, cells were transfected with either empty vector, DYRK1A or DYRK1B as follows:

1. Preparation of DNA and Lipofectamine2000 solutions (per well)
DNA mix: 500 μ L Opti-mem + 4 μ g DNA (pEF, DYRK1A or DYRK1B)
Lipofectamine mix: 500 μ L Opti-mem + 12 μ L Lipofectamine 2000
2. Incubation of transfection mixture
The DNA mixture and Lipofectamine mixture were combined, vortexed and incubated at room temperature for 20 minutes.

3. Transfection

Cells were washed twice in PBS and 4mL of Opti-mem was added. The combined DNA/Lipofectamine mixture was then added to the cells, for a final volume of 5mL. Cells were incubated at culture conditions for 2 hours. The transfection mixture was then replaced by 0.3% FCS DMEM and cells were starved overnight.

After a 15 minute serum stimulation, cells were washed twice in PBS and then scraped in 500µl lysis buffer. Lysates were brought to 1mL using lysis buffer and incubated on ice for 20 minutes. The lysates were next sonicated (two 10 second pulses) and insoluble material was pelleted by centrifugation at maximum speed in a refrigerated bench top centrifuge.

Supernatants were then transferred to fresh tubes containing 20µL of HA-agarose beads (Sigma-Aldrich) and incubated for 1.5 hours at 4°C on a rotating mixer. The beads were next washed three times in 1mL IP wash buffer and used for kinase assays.

IP lysis buffer	50mM HEPES pH 7.4 1% NP-40 150mM NaCl 2mM EDTA 30mM Sodium pyrophosphate 25mM NaF 1mM Na ₃ VO ₄ 1mM PMSF 2µg/mL aprotinin 2µg/mL leupeptinin 1µg/mL pepstatin
IP wash buffer	50mM HEPES (pH7.4) 150mM NaCl 2mM EDTA

Kinase Buffer	25mM HEPES pH 7.4 5mM MgCl ₂ 5mM MnCl ₂ 0.5mM DTT 200μM γ- ³² P ATP (100-150μCi/mL) 200μM substrate peptide
---------------	---

Kinase reactions were initiated by addition of 20μL kinase buffer to 10μL of beads with immobilised kinase. Reactions were incubated at 30°C for 20 minutes. 8μL of the reaction were spotted onto P81 paper and allowed to dry. P81 paper was then washed extensively with 5% Phosphoric acid and activity was measured using a scintillation counter.

When full-length MRTF-A was used as a substrate the reaction was resolved by SDS-PAGE and transferred to nitrocellulose membrane. The membrane was then scanned using a Typhoon FLA 7000 Phosphorimager and subsequently immunoblotted.

2.16 λ-phosphatase assay

NIH-TR3 cells were seeded in 10cm dishes at 1×10^6 cells per dish in the presence of 1μg/mL tetracyclin, to induce Flag-MRTF-A expression. After treatment and stimulation, cells were scraped in 500μL RIPA buffer and incubated on ice for 15 minutes. Lysate volume was brought to 1mL using RIPA buffer and insoluble material was pelleted by centrifugation at maximum speed in a refrigerated bench top centrifuge. The supernatant was transferred to a fresh tube containing 30μL Flag-beads (Sigma-Aldrich) and incubated for 1 hour at 4°C on a rotating shaker. The beads were next washed 3 times with 1mL RIPA buffer and 3 times with phosphatase buffer. The beads were then split in two and made up to 30μL with phosphatase buffer.

1000 units of λ-phosphatase (NEB) were added to one of the tubes. The reaction was carried out at 30°C for 30 minutes. Beads were washed three times in phosphatase buffer and then 50μL of SDS-loading buffer was added to the beads. The samples were subsequently resolved by SDS-PAGE on a 7% Tris-Acetate gel.

RIPA buffer	50mM Tris-HCl 150mM NaCl 0.1% SDS 0.5% Sodium Deoxycholate 1% Triton X-100 1mM PMSF
Phosphatase buffer	50mM HEPES 100mM NaCl 2mM DTT 0.01% Brij 35 1mM MgCl ₂

Chapter 3. Characterisation of MRTF-A phosphorylation

3.1 Aims

Serum stimulation leads to MRTF-A nuclear accumulation and target gene activation. Simultaneously, MRTF-A is also multiply phosphorylated suggesting a positive regulatory role, especially since the C-terminal part containing the transactivation domain is phosphorylated. In this chapter I aim to gain further insight into the determinants of MRTF-A phosphorylation and how phosphorylation impinges on MRTF-A activity.

3.2 MRTF-A phosphorylation correlates with the onset of activity

The observation that activated MRTF-A is also phosphorylated is reminiscent of other transcription factors, such as Elk1, where phosphorylation of its transactivation domain switches it to the active state (Cruzalegui et al., 1999). If the case for MRTF-A phosphorylation is analogous, then phosphorylation should precede target gene activation, assuming that all phosphorylation positively regulates activity. I therefore sought to look at the kinetics of phosphorylation in more detail and compared these to the kinetics of target gene activation.

After FCS stimulation, transcription of representative MRTF/SRF targets sharply increased and peaked within 30 minutes, as assessed by qRT-PCR (Figure 3.1A). Induction was transient and returned to baseline after 2 hours. FCS stimulation also led to a sharp decrease in electrophoretic mobility in SDS-PAGE, which reached a maximum within 10 minutes (Figure 3.1B). Maximum

phosphorylation persisted for an hour and began to decrease after 2 hours, by which time target gene transcription was already back to baseline.

As the initial kinetics of the events correlate, it is possible that phosphorylation could be required for target gene activation, like in the case of Elk1. However the lack of correlation between phosphorylation and transcription shut off suggests that other regulatory mechanisms must be involved. One explanation could be that MRTF-A dissociates from SRF within 2 hours and that dephosphorylation is not involved in the shut down of transcription.

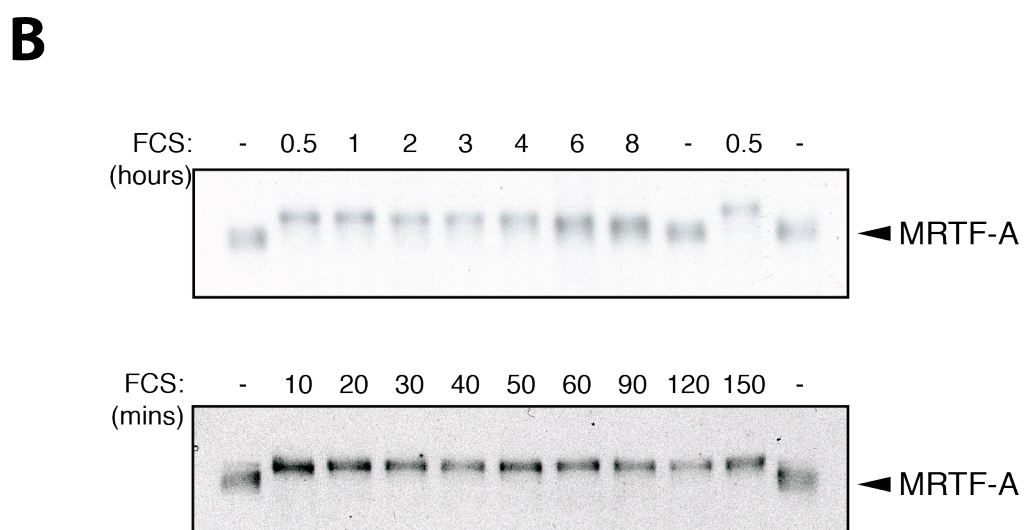
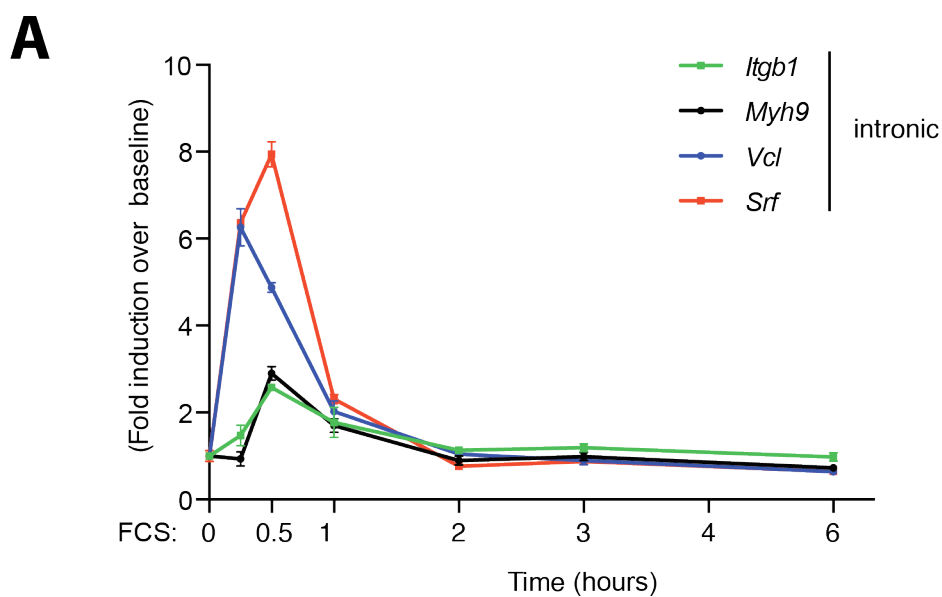


Figure 3.1 MRTF-A phosphorylation correlates with the onset of transcriptional activity

A. MRTF-A target gene transcription kinetics. NIH 3T3 cells maintained on 0.3% FCS overnight were stimulated with 15% FCS and RNA was extracted at indicated times. MRTF-A target genes expression was analysed by qPCR using intronic probes. Target gene abundance was normalised to GAPDH and data are expressed relative to starved conditions (fold change). Error bars represent standard error of the mean (SEM) from at least two independent experiments. **B.** Kinetics of gross MRTF-A phosphorylation. NIH 3T3 cells were starved in 0.3% serum overnight and stimulated with 15% FCS for indicated times. Cell lysates were resolved on a 7% polyacrylamide gel. Endogenous MRTF-A was detected by immunoblotting.

3.3 Actin dissociation and ERK activation lead to MRTF-A phosphorylation

Serum induced phosphorylation is sensitive to inhibition of MEK and Rho activity, using U0126 and C3-transferase respectively (Fig 3.2A) and (Miralles et al., 2003)). Actin dissociation is required for MRTF-A activation, but it is unknown whether this is sufficient for MRTF-A phosphorylation. In addition the sensitivity to MEK1/2 inhibitor U0126 once again (Muehlich et al., 2008) suggests MRTF-A is an ERK target.

To investigate the role of ERK in MRTF-A phosphorylation, tetradecanoyl phorbol acetate (TPA) was used as an alternative way to activate ERK. TPA activates ERK in a PKC dependent manner (Marquardt et al., 1994). Treatment of cells with TPA resulted in partial phosphorylation and MEK1/2 inhibition using U0126 completely blocked this effect (Figure 3.2B). Since ERK is the only known MEK1/2 substrate, this result suggests that active ERK either directly phosphorylates MRTF-A or lies upstream of the kinases that could, for example Mnks or Rsk. The complete block of phosphorylation by U0126 precludes PKCs from being the kinases that directly phosphorylate MRTF-A after TPA stimulation.

CD disrupts F-actin, but its binding to actin is mutually exclusive with RPELs, and so CD activates MRTF-A (Sotiropoulos et al., 1999). Treatment of cells with CD also led to MRTF-A phosphorylation (Figure 3.2B). This phosphorylation was not U0126 sensitive excluding the possibility that basal ERK activity is sufficient once actin is dissociated. In addition this demonstrates that kinases other than ERK are able to phosphorylate MRTF-A. CD and TPA co-stimulation resulted in reduction of electrophoretic mobility equivalent to that with FCS stimulation, suggesting that disruption of the actin-MRTF interaction and simultaneous ERK activation are sufficient for full phosphorylation.

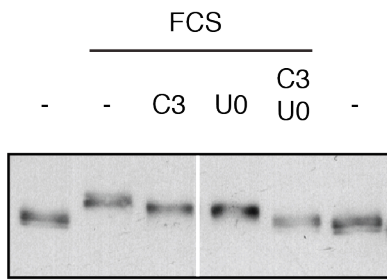
The Rho component of MRTF-A phosphorylation could be due to depletion of G-actin, activation of downstream kinases or nuclear accumulation per se. G-actin depletion using constitutively active mDia1*, was sufficient for MRTF-A phosphorylation (Figure 3.2C), however positive feedback from mDia to RhoA has been reported (Kitzing et al., 2007). CD treatment circumvents this issue by making actin incapable of binding to MRTF-A. However it is still possible that F-actin disruption by CD could activate kinases, such as LATS (Reddy et al., 2013) or PKD (Eiseler et al., 2009; 2007; Higuchi et al., 2009).

MRTF-A^{xxx}, that does not bind actin, was constitutively nuclear and phosphorylated in starved cells (Figure 3.2C), suggesting that actin binding inhibits MRTF-A phosphorylation. Co-transfection of Dia1 did not further decrease electrophoretic mobility, confirming that actin dissociation per se is sufficient for partial phosphorylation. Serum stimulation was then able to further increase phosphorylation, presumably due to activation of the MAPK pathway.

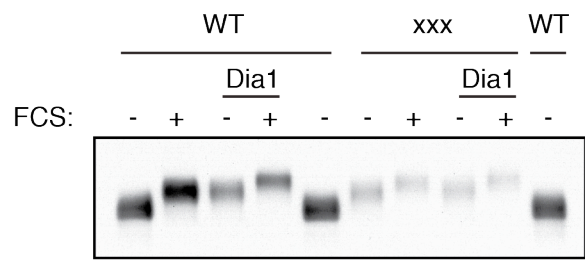
If phosphorylation positively regulates MRTF-A activity, then the relative levels of phosphorylation caused by TPA, CD and FCS stimulations could correlate with the relative MRTF-A activity. TPA and CD which induce partial phosphorylation induced the SRF/MRTF target genes *Vcl* and *Srf* less effectively than FCS, which leads to full phosphorylation, suggesting that phosphorylation correlates with initial transcriptional activation (Figure 3.2D).

Taken together these data show that actin dissociation per se is sufficient for MRTF-A phosphorylation, that this phosphorylation can be potentiated by MAPK pathway activity and that the extent of phosphorylation correlates with levels of target gene activation.

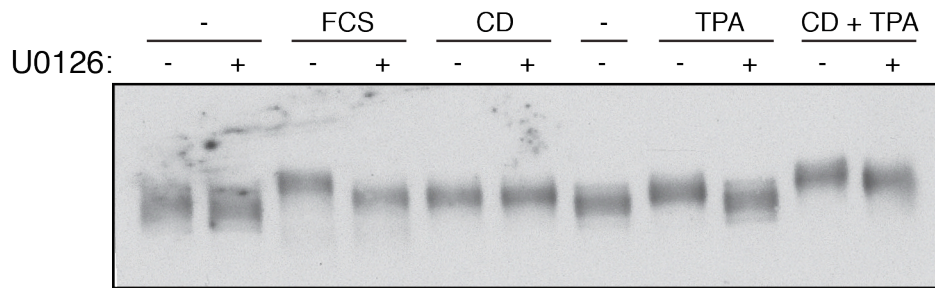
A



C



B



D

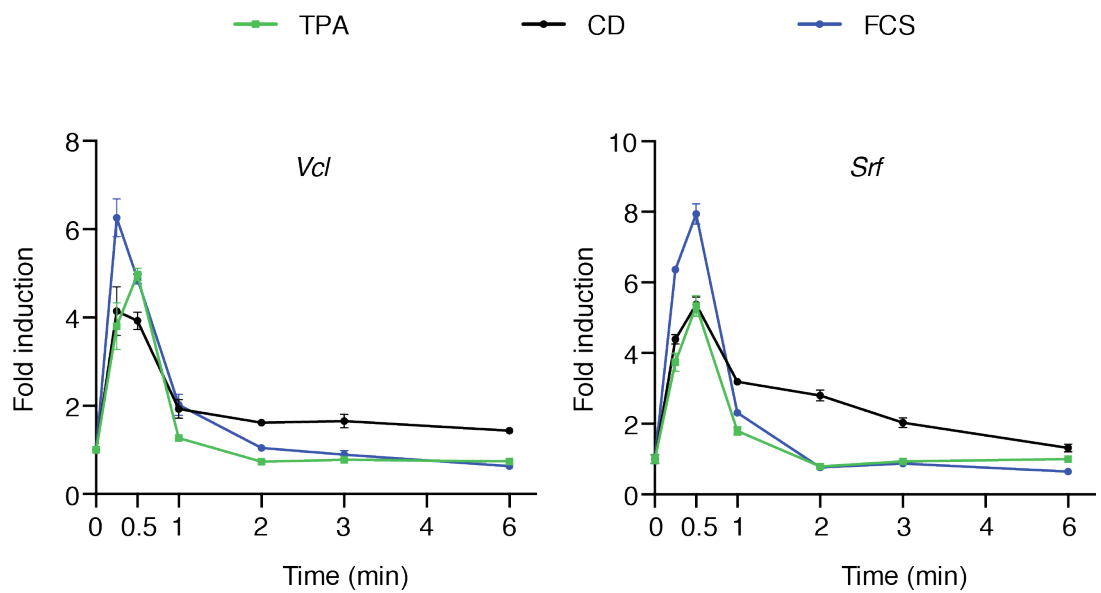


Figure 3.2 Serum induced MRTF-A phosphorylation depends on an intact RhoA and MAPK pathway

A. NIH-3T3 cells transfected with empty vector or C3-transferase were starved overnight and stimulated with 15% FCS in the presence or absence of U0126. Cell lysates were resolved on a 7% polyacrylamide gel. Endogenous MRTF-A was detected by immunoblotting (experiment performed by F. Miralles). **B.** NIH-3T3 cells were transfected with indicated MRTF-A derivatives and co-transfected with constitutively active Dia1 where indicated. After overnight starvation cells were stimulated with 15% FCS for 30 min. Cell lysates were resolved on a 7% polyacrylamide gel and MRTF-A derivatives were detected by immunoblotting. MRTFxxx does not bind actin. **C.** NIH 3T3 cells were starved overnight and stimulated for 45 min with either 15% FCS, 2 μ M CD, 100ng/mL TPA or CD and TPA simultaneously, in the presence of 10 μ M U0126 where indicated. Cell lysates were resolved on a 7% gel. Endogenous MRTF-A was detected by immunoblotting. **D.** NIH-3T3 cells were starved overnight and stimulated with 15% FCS, 2 μ M CD or 100ng/mL TPA. RNA extracted at indicated times was analysed by qPCR using intronic probes against MRTF target genes. Target gene abundance was normalised to GAPDH and data are expressed relative to unstimulated conditions (fold change). Error bars represent standard error of the mean (SEM) from at least two independent experiments.

3.4 Nuclear localisation is required but not sufficient for full MRTF-A phosphorylation

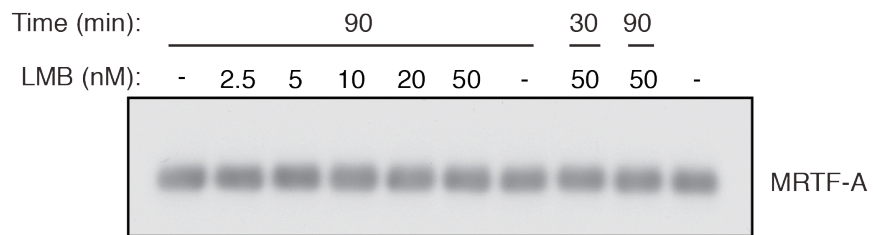
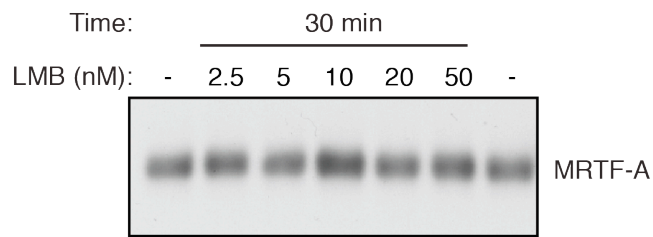
FCS induced target gene expression requires MRTF-A nuclear localisation. Both phosphorylation and nuclear localisation are coupled, as both are dependent on actin. Previous studies have shown that an NLS defective MRTF-A mutant that is unable to accumulate in the nucleus was also only partially phosphorylated after FCS treatment and this partial phosphorylation was U0126 sensitive (R. Pawlowski, unpublished). Furthermore CD treatment did not lead to any phosphorylation of this mutant. These observations indicate that ERK dependent phosphorylation does not

require nuclear accumulation, but the phosphorylation resulting from actin dissociation does.

Since actin dissociation leads to simultaneous nuclear accumulation and phosphorylation, the question arises whether actin dissociation is really a requirement for phosphorylation or simply nuclear accumulation. LMB treatment blocks MRTF-A export and leads to rapid nuclear entrapment of MRTF-A, without detectably changing the MRTF-A/actin interaction as measured by FRET (Vartiainen et al., 2007). To test whether nuclear accumulation was sufficient for MRTF-A phosphorylation cells were incubated with increasing amounts of LMB for 30 minutes and there was no reduction in electrophoretic mobility (Figure 3.3A). It was a possibility that while bound to actin phosphorylation could still occur but less efficiently. Phosphorylation was not detected even after a longer LMB treatment of 90 minutes. Changes in MRTF-A electrophoretic mobility reflect changes in total phosphorylation with low resolution. A small panel of phospho-specific antibodies was used to probe for any small changes in phosphorylation at specific sites. Again, no phosphorylation was detected upon LMB treatment (Figure 3.3B).

Nuclear accumulation is therefore not sufficient for MRTF-A phosphorylation but is required for full phosphorylation, provided that actin dissociation occurs.

A



B

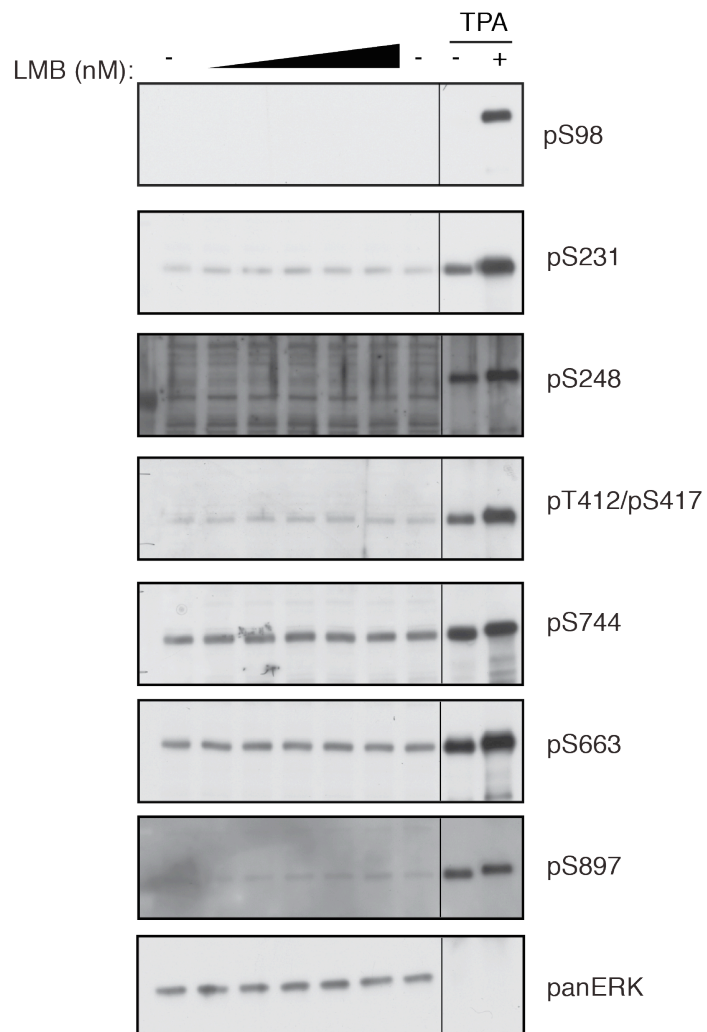


Figure 3.3 Nuclear localisation is not sufficient for MRTF-A phosphorylation

A. Gel shift assay after LMB treatment. NIH-3T3 cells stably transfected with a tetracyclin inducible MRTF-A expression vector, were starved and treated with tetracyclin overnight. Cells were then treated with indicated concentrations of LMB for 30 or 90 min. Cell lysates were resolved on a 7% polyacrylamide gel and MRTF-A was detected by immunoblotting with a specific antibody. **B.** Lysates prepared as explained in (A), were resolved on 4-12% polyacrylamide gradient gels and immunoblotting was carried out using antibodies that recognise specific phosphorylation sites on MRTF-A. Immunoprecipitated MRTF-A from TPA stimulated cells was loaded as a positive control. LMB concentrations used were: 2.5, 5, 10, 20, 50nM.

3.5 MRTF-A dimerisation and binding to SRF are dispensable for phosphorylation

Transcriptional cyclin dependent kinases (Cdks), including Cdk7, Cdk8 and Cdk9, are so called because of their association with transcriptional machinery at gene promoters (Lim and Kaldis, 2013). Previous work in our lab, shows that MRTF-A phosphorylation is sensitive to Cdk inhibition using the pan-Cdk inhibitor Purvalanol A. It was therefore hypothesised that association of MRTF-A with SRF could lead to phosphorylation by the transcriptional Cdks.

Biochemical and functional assays have demonstrated that interaction with SRF *in-vivo* is abolished by the Y330A mutation (Zaromytidou et al., 2006), while dimerisation is dependent on the leucine zipper motif (Miralles et al., 2003). In MRTF-A depleted cells, rescue experiments are frequently complicated by dimerisation with residual endogenous MRTF-A (Vartiainen, 2008; Pawłowski et al., 2010). To test whether binding to SRF is required for MRTF-A phosphorylation the Y330A and leucine zipper deletion Δ LZ were combined.

The activity of the abovementioned MRTF-A derivatives was measured in an MRTF-A luciferase reporter assay, in order to assess the effectiveness of the mutations (Figure 3.4). Cells were depleted of endogenous MRTF-A/B and then transfected with the MRTF-A derivatives and reporters. Reporter activity in cells

transfected with the Y330A mutants was very low in all conditions tested, consistent with their inability to bind SRF. In agreement with previous studies the Δ LZ mutant which was SRF binding competent was less able to induce reporter activity (Pawłowski et al., 2010; Zaromytidou, 2007), especially after TPA stimulation.

The MRTF-A derivatives were next tested for their ability to be phosphorylated (Figure 3.5A). After serum or CD stimulation, MRTF-A Y330A showed no defect in phosphorylation, as observed by a reduction in electrophoretic mobility identical to that of wild type MRTF-A (Figure 3.5B). MRTF-A Y330A Δ LZ did exhibit faster electrophoretic mobility than MRTF-A Y330A, however this was not due to the inability to bind SRF. The faster electrophoretic mobility was also seen in the Δ LZ mutant indicating that this was a consequence of the dimerisation defect. The leucine zipper deletion decreases the predicted molecular weight of MRTF-A from 108kDa to 104kDa, and it is therefore unlikely that the differences seen were due to the deletion. In addition, there are no identified phosphorylation sites within the leucine zipper and the mutant has no defect in its ability to accumulate in the nucleus (Figure 3.5D).

Because of its poor activity in the reporter assay, MRTF-A Δ LZ was further tested for its ability to be phosphorylated. Despite normal nuclear accumulation, MRTF-A Δ LZ demonstrated faster electrophoretic mobility than WT in all conditions (Figure 3.5C). Just like WT was partially phosphorylated in response to CD and TPA treatments with respect to its maximum with FCS stimulation. Sensitivity to U0126 was like that of WT. λ -phosphatase treatment revealed that deletion of the LZ leads to an apparent molecular weight reduction that can be resolved by SDS-PAGE (Figure 3.5E).

Taken together, the data show that MRTF-A phosphorylation is not dependent on SRF binding or MRTF-A dimerisation.

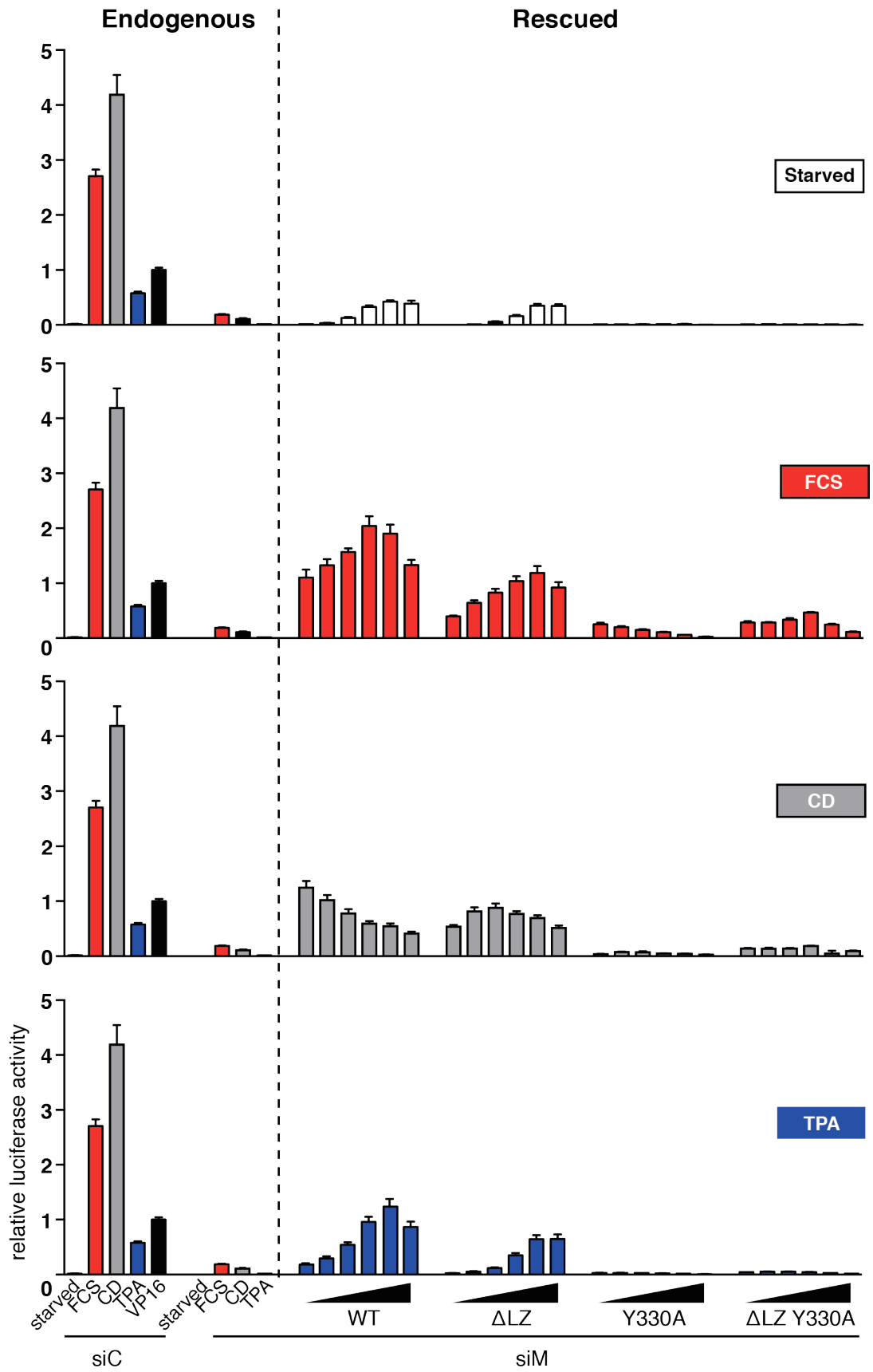


Figure 3.4 Activation potential of dimerisation defective and SRF binding defective MRTF-A

NIH-3T3 cells were transfected with the p3D.A and ptkRL luciferase reporters (see section 2.8) as well as the indicated MRTF-A derivatives. VP16 indicates cells transfected with the fusion protein SRF-VP16 which constitutively activates activity of the p3D.A reporter. The cells were starved overnight and stimulated with 15% FCS, 2 μ M CD or 100ng/mL TPA for 6 hours. Cell extracts were then assessed for luciferase activity. Error bars represent standard error of the mean (SEM) from at least two independent experiments.

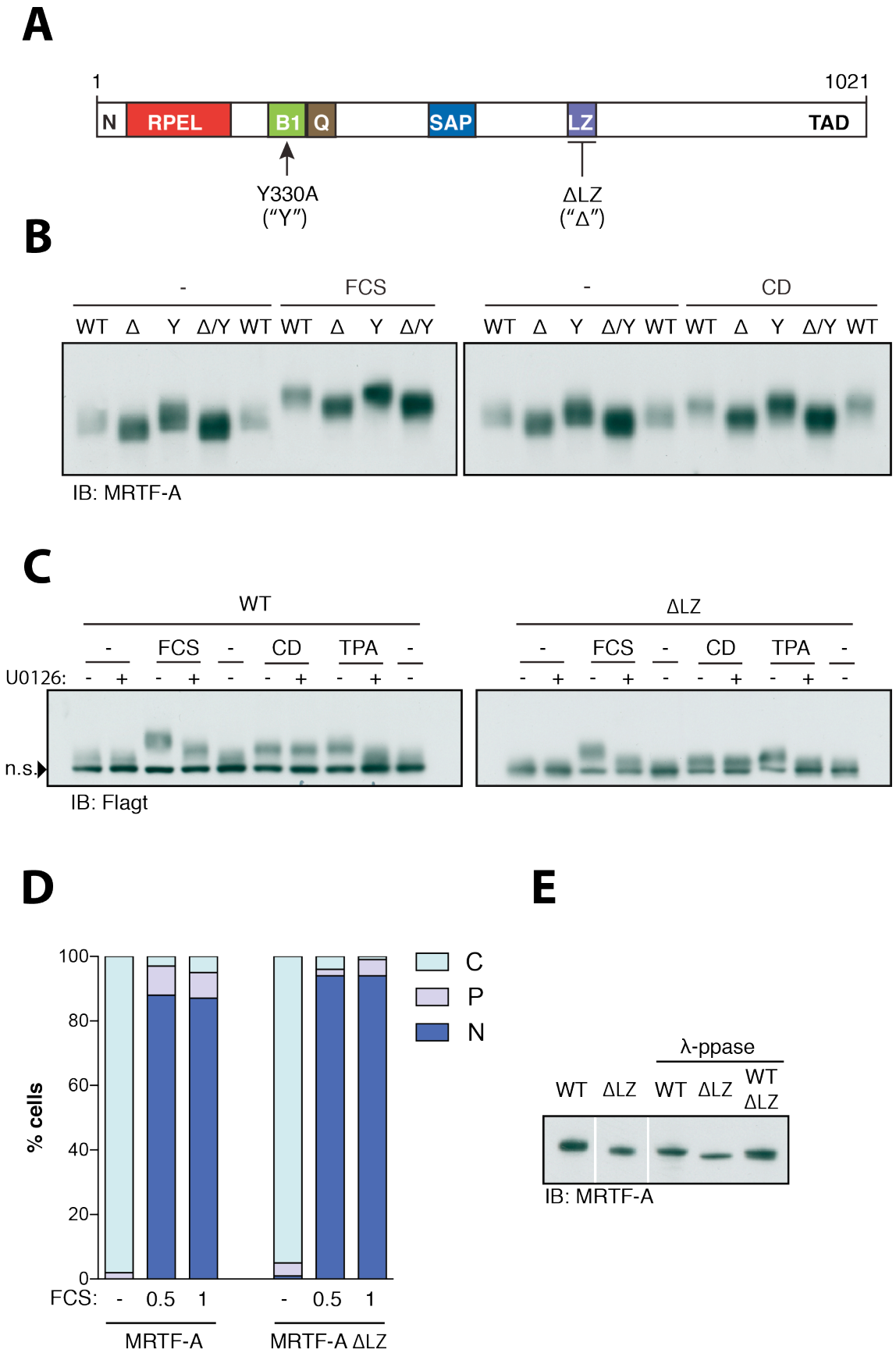


Figure 3.5 Ternary complex formation and dimerisation are dispensable for MRTF-A phosphorylation

A. Schematic representation of MRTF-A showing the regions affected by the Y330A point mutation and the LZ deletion. The resulting MRTF-A mutants cannot bind SRF and cannot dimerise, respectively. **B.** Gel shift assay of MRTF-A mutants. NIH-3T3 cells were transfected with the indicated MRTF-A derivatives, starved overnight and stimulated with 15% FCS or 2 μ M CD. Cell lysates were run on a 7% polyacrylamide gel and MRTF-A was detected by immunoblotting. **C.** NIH-3T3 cells were transfected with WT MRTF-A or the Δ LZ mutant which cannot dimerise and starved overnight. The cells were subsequently stimulated with 15% FCS, 2 μ M CD or 100ng/mL TPA. Cell lysates were resolved on a 7% polyacrylamide gel and MRTF-A was detected by immunoblotting with an anti-Flag antibody. An arrow head marks a non specific band. **D.** Cells were transfected with MRTF-A WT or Δ LZ, maintained in 0.3% FCS overnight and stimulated with 15% FCS. MRTF-A localisation was assessed by immunofluorescence using an anti-Flag antibody. At least 100 cells were counted and localisation was scored as predominantly nuclear (navy blue), pancellular (lilac) or predominantly cytoplasmic (light blue). **E.** Cells were transfected with the indicated constructs and extracts were used for immunoprecipitating MRTF-A. λ -phosphatase treatment was carried out where indicated.

3.6 Phosphorylation is required for full activity

Our lab and others have identified multiple phosphorylation sites on MRTF-A, all of which are S/T-P sites and spread throughout the protein (Figure 3.6A). The S/T-P sites were substituted to alanine residues by F Miralles to generate a derivative for use in determining the role of phosphorylation of MRTF-A (Figure 3.6B). This mutant, named “E3”, was able to accumulate in the nucleus normally, but exhibited reduced transcriptional activity in response to serum stimulation.

Further analyses, including validation using specific antibodies led to a set of 26 residues that are reproducibly phosphorylated upon MRTF-A activation by serum. Based on this set of 26 phospho-acceptor sites, additional 6 residues were

mutated to alanine on E3, while 6 residues were repaired back to serines or threonines because they were subsequently shown to remain unphosphorylated. The resulting derivative named “26ST/A” lacks all phosphorylation sites observed *in-vivo* (Figure 3.6C). The strategy followed for the generation of 26ST/A is shown in Figure 3.6D.

All intermediate derivatives obtained during the generation of 26ST/A from E3 were tested in a reporter assay to assess whether a particular residue substitution had a drastic effect on activity. Cells were depleted of endogenous MRTF-A and transfected with the various ST/A mutant intermediates. The FCS and CD induced maxima were all lower than that of MRTF-A WT, but did not fluctuate significantly as alterations were made. The baseline activity, however, fluctuated with some mutations. After the last alteration was made, the final product, 26ST/A appeared identical to the E3 with respect to activity in all conditions tested (Figure 3.6E).

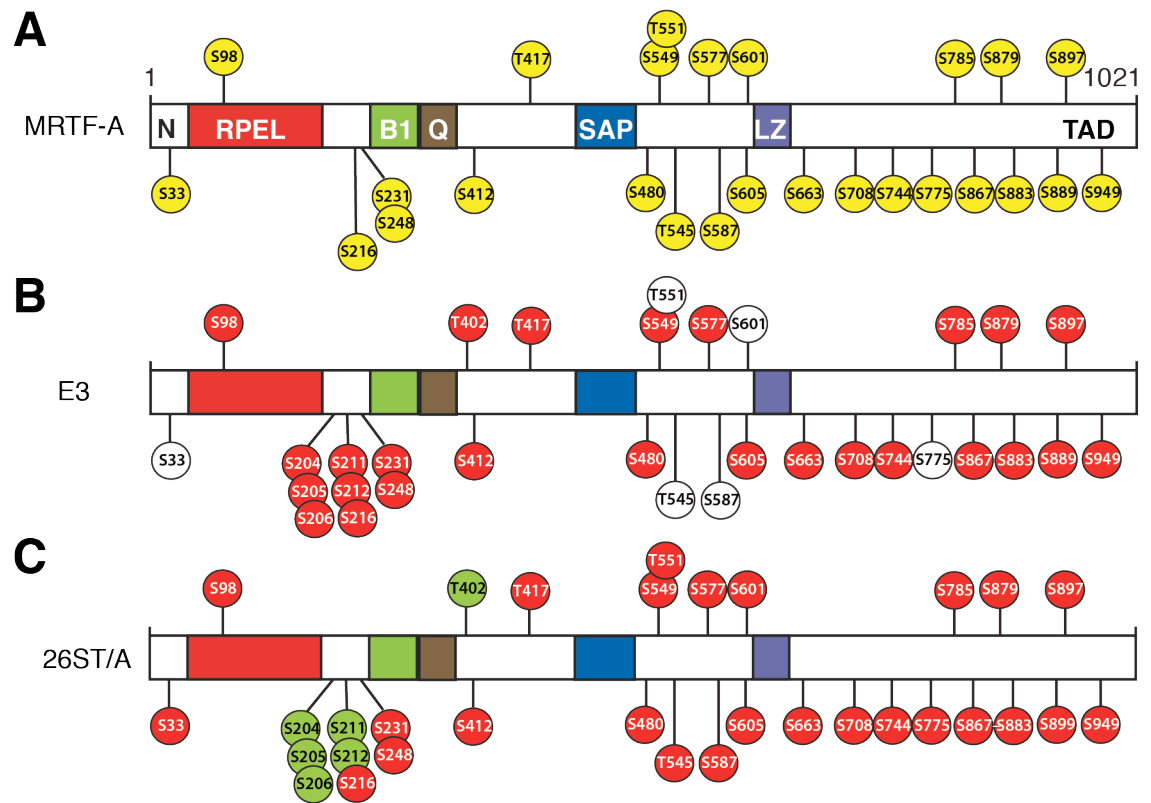
During the correction process alanine substitution of S33 (ST/A_c) appeared to cause a significant change in baseline activity. To validate this, the assay was repeated, comparing E3, ST/A_c and 26ST/A. Indeed, ST/A_c was as active as the E3 and 26ST/A mutants in stimulated conditions, but more active in starved conditions (Figure 3.7A). The increased activity in unstimulated conditions suggests that the S33A modification affects MRTF-A regulation, in a way that is redundant after stimulation. In addition, it appears that in the low ranges of the titration, FCS or CD induced activity is not different between WT and ST/As. One explanation could be that there is enough endogenous MRTF-A to dimerise with the ectopically expressed and is possibly sufficient to induce activity. Once enough ectopic MRTF-A is expressed, endogenous MRTF is titrated out and significant amounts of ectopic MRTF-A dimers begin to form. It is at this point that MRTF-A WT dimers continue to provide more activity, whereas the ST/A mutant dimers cannot and defects begin to be seen.

Both E3 and 26ST/A exhibited similar mobility in SDS-PAGE, which did not detectably change upon stimulation with FCS or CD (Figure 3.7B). In addition, neither E3 nor 26ST/A were defective in their ability to accumulate in the nucleus after FCS stimulation (Figure 3.7C). To gain more insight into the reduced activity observed with 26ST/A, the 26ST/A mutant was rendered unable to bind actin. In the absence of any actin binding localisation would not be regulated. In addition,

since stimulation would be unnecessary, any remaining endogenous MRTF-A would be sequestered in the cytoplasm or at least in the inactive state.

Cells were therefore depleted of endogenous MRTF and wild type MRTF-A , MRTF-A xxx or 26ST/A xxx were titrated in. As previously seen, titrating in the wild type protein increased baseline activity in starved conditions. Titrating in MRTF-A xxx led to a dose dependent increase in reporter activity, while ST/A xxx was significantly less effective but not completely inactive (Figure 3.8). In this experimental setup, the inability to become phosphorylated appears to have a more drastic effect on reporter activation. It would be interesting to see if deletion of the leucine zipper would lead to a complete loss of activity in this context.

Taken together these data show that phosphorylation of MRTF-A is required for full transcriptional activity.



D

Strategy for revision of E3 to make 26ST/A

Construct	a	b	c	d	f	g	h	i	j
Residues	204 205 206	211 212	33	402	545	551	587	601	775
Change to	S	S	A	T	A	A	A	A	A

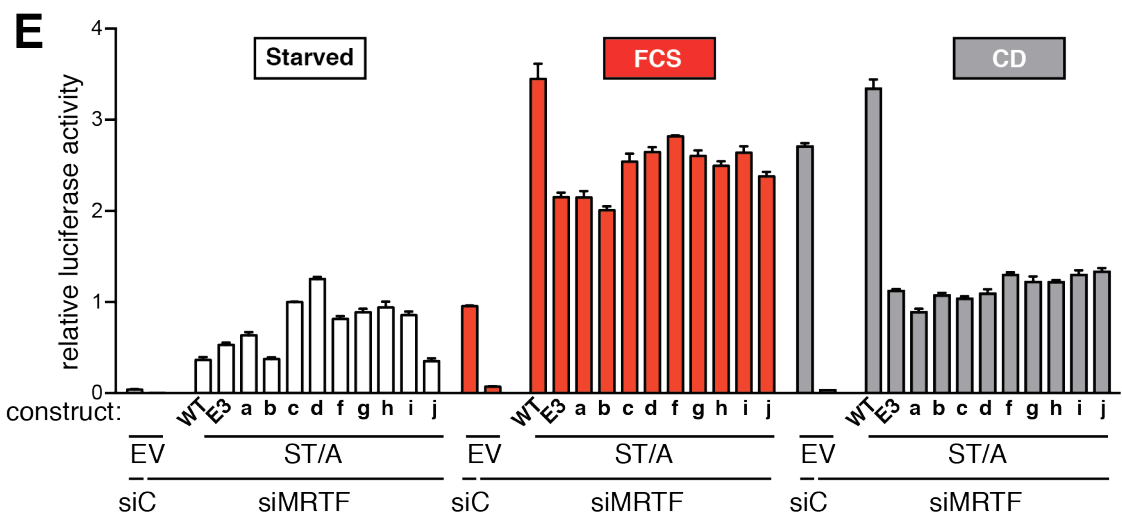


Figure 3.6 Generation of a non phosphorylatable MRTF-A derivative

A-C. Schematic representation of MRTF-A. Top shows all confirmed phosphorylation sites. Middle shows a mutant (E3) in which the phosphorylation sites shown in red were mutated to alanines. In white are confirmed phosphorylation sites that were not known at the time the mutant was made. Bottom shows the revised ST/A construct (26ST/A) in which only validated phosphorylation sites are mutated to Alanine (red) while some others, mutated in E3, were repaired (green). **D.** Strategy followed to generate the revised MRTF-A ST/A. Starting with E3 residues were sequentially mutated or repaired to generate the 26ST/A derivative. Changes were cumulative; each progressive derivative includes the changes in the previous ones. **E.** Cells were transfected with the luciferase reporter plasmids (p3D.A for MRTF-A activity, ptkRL for normalisation) and 20ng of different ST/A MRTF-A mutants (a to j, explained in part D) and their activity assayed by luciferase assay after stimulation with 15% FCS, 2 μ M CD or 100ng/mL TPA for 6 hours. Error bars represent standard error of the mean (SEM) from at least two independent experiments.

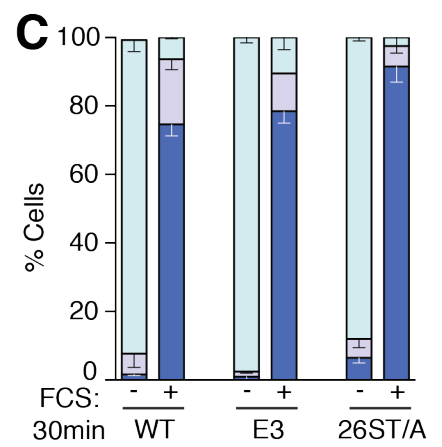
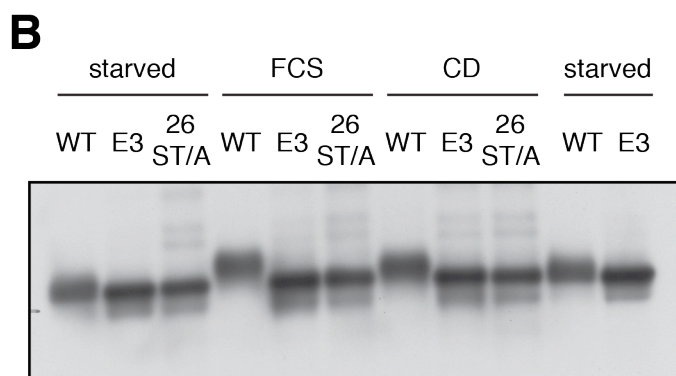
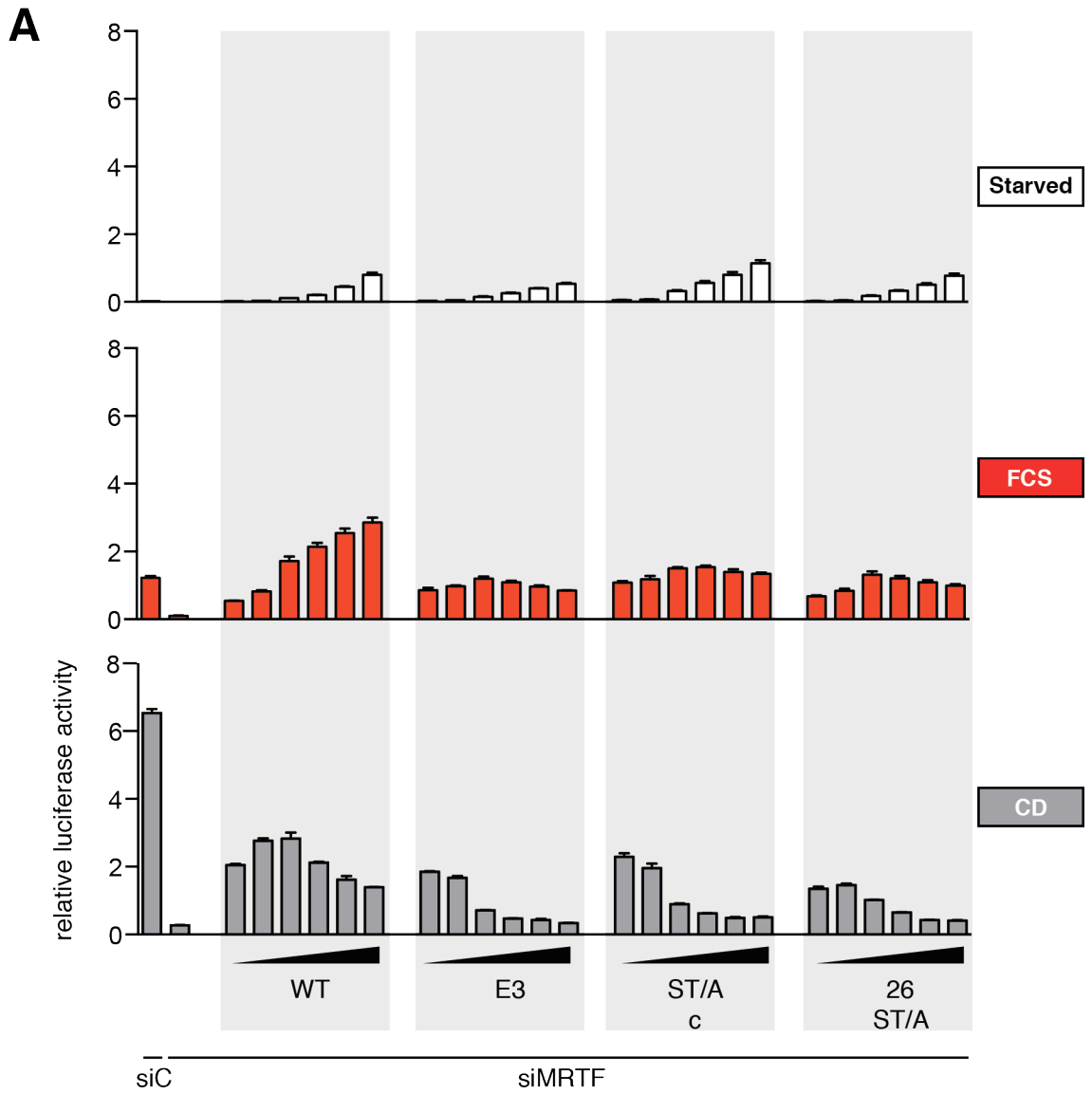


Figure 3.7 MRTF-A phosphorylation is required for full activity

A. MRTF-A activity reporter assay. NIH-3T3 cells depleted of endogenous MRTF-A using siRNA, were transfected with luciferase reporter plasmids and the indicated MRTF-A derivatives (0.5, 1, 5, 10, 20, 40ng of derivatives). After overnight starvation, the cells were stimulated with 15% FCS or 2 μ M CD. Cell extracts were then assessed for luciferase activity. **B.** Gel shift assay. NIH 3T3 cells transfected with the indicated MRTF-A derivatives were starved and stimulated with 15% FCS or 2 μ M CD for 30 min. Lysates were resolved on a 7% polyacrylamide gel and MRTF-A derivatives were detected by immunoblotting. **C.** Cells were transfected with MRTF-A WT, E3 or 26ST/A, maintained in 0.3% FCS overnight and stimulated with 15% FCS. MRTF-A localisation was assessed by immunofluorescence using an anti-Flag antibody. At least 100 cells were counted and localisation was scored as predominantly nuclear (navy blue), pancellular (lilac) or predominantly cytoplasmic (light blue). Error bars represent standard error of the mean (SEM) from at least two independent experiments.

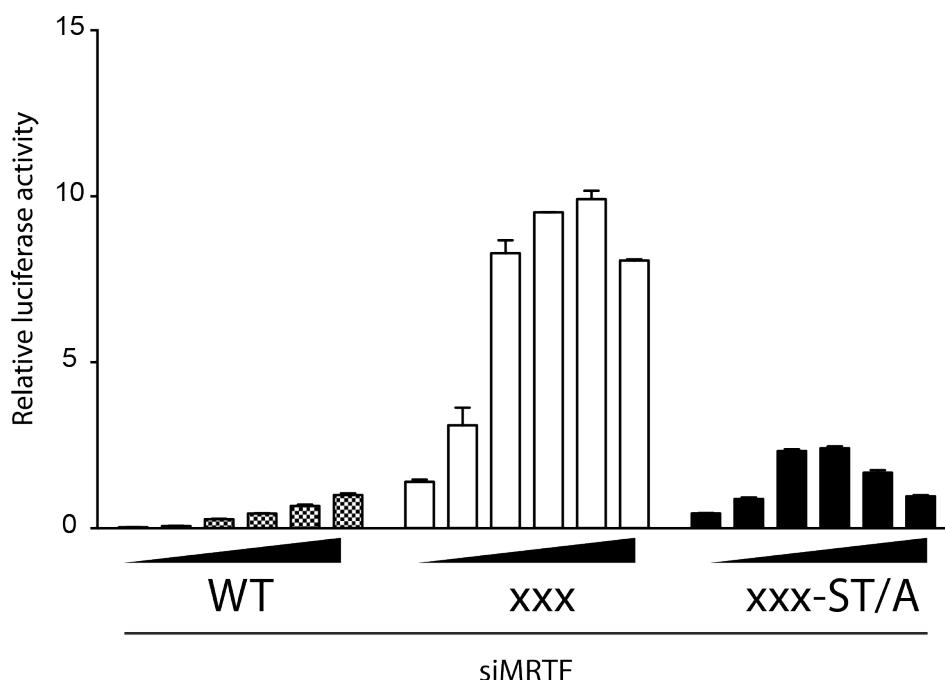


Figure 3.8 The defect in ST/A activity is actin binding independent

MRTF-A activity reporter assay. NIH-3T3 cells depleted of endogenous MRTF-A using siRNA, were transfected with luciferase reporter plasmids and the indicated MRTF-A derivatives (0.5, 1, 5, 10, 20, 40ng). After incubation in 0.3% FCS overnight, cell extracts were prepared and assessed for luciferase activity.

3.7 Kinase siRNA screen

To identify the kinases responsible for MRTF-A direct phosphorylation R Pawlowski carried out a small molecule inhibitor screen using “Protein kinase inhibitor libraries I, II and III” (Calbiochem). The screen included 288 cell-permeable, reversible protein kinase inhibitors, most of which were ATP competitive. The outline of the strategy followed is shown in Figure 3.9.

A cell line stably expressing an MRTF-A reporter gene was used to identify inhibitors from the library that blocked FCS or CD induced MRTF activity. Effects on MRTF-A nuclear accumulation were assessed by immunofluorescence. 14 inhibitors that blocked both FCS and CD induced MRTF-A activity, without affecting nuclear accumulation, were next tested for their ability to inhibit MRTF-A phosphorylation.

Three inhibitors blocked MRTF-A phosphorylation: PI3K inhibitor VIII, 5-iodotubercidin and indirubin derivative. A subsequent ligand immobilised affinity binding assay against a panel of 442 kinases, was then carried out to determine the specificity. A small siRNA library against the 20 most promising targets was compiled. Criteria used included degree of inhibition by the above inhibitors, whether the kinase is constitutively active and is nuclear or pancellular.

The aim of my studies was to investigate the potential role of these targets in MRTF-A regulation. The 20 siRNAs were tested in the MRTF-A reporter assay. Out of the 20 siRNA pools, 8 impaired both FCS and CD induction of the reporter (Figure 3.10). However, none of those 8 siRNA pools blocked phosphorylation of MRTF-A in any of the conditions tested, suggesting that none of the siRNA targeted kinases directly phosphorylate MRTF-A (Figure 3.11). siRNA pools against CLK2 and CK1a (CSNK1A1), which increased reporter activity, were also tested, and depletion of those led to an increase in MRTF-A phosphorylation. I did not however investigate those candidates further since I was interested in kinases that would directly phosphorylate MRTF-A.

Depletion of no single kinase, from the panel tested, is sufficient to block MRTF-A phosphorylation. Taken together, the data suggest that MRTF-A phosphorylation induced by either serum or CD, involves multiple kinases.

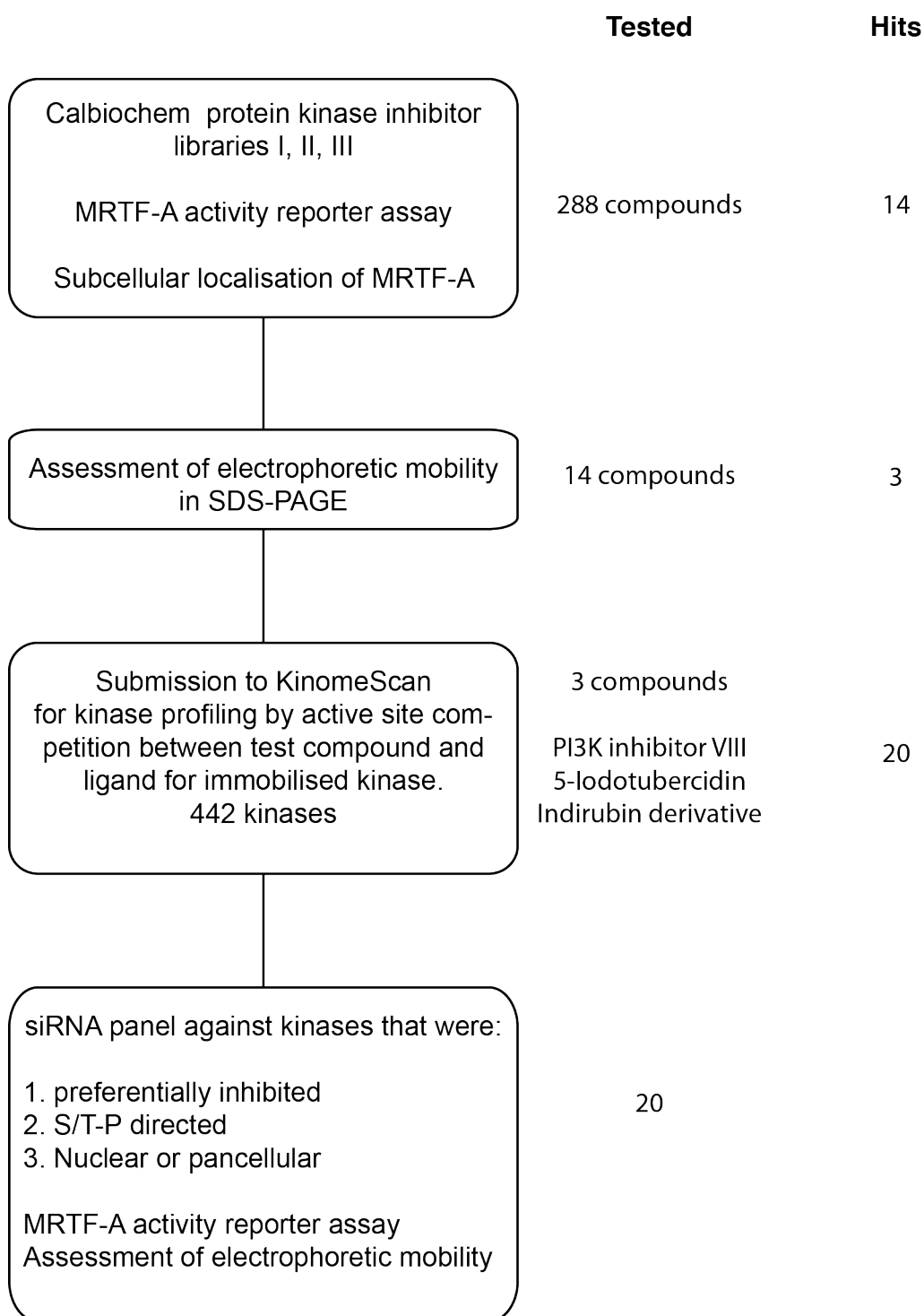


Figure 3.9 Strategy for identification of kinases that phosphorylate MRTF-A

Outline of the strategy followed to identify kinases that directly phosphorylate MRTF-A. See text for details.

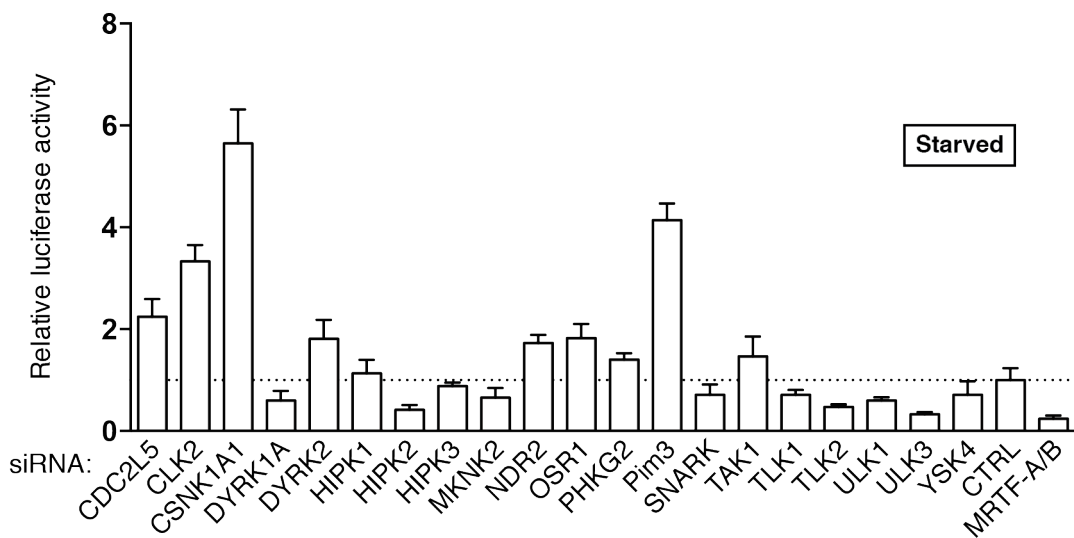
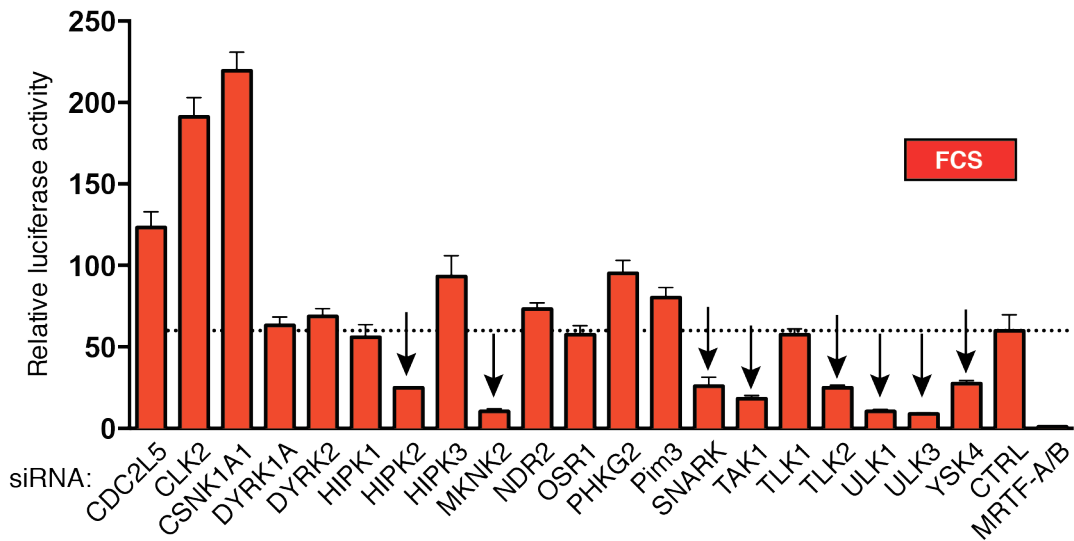
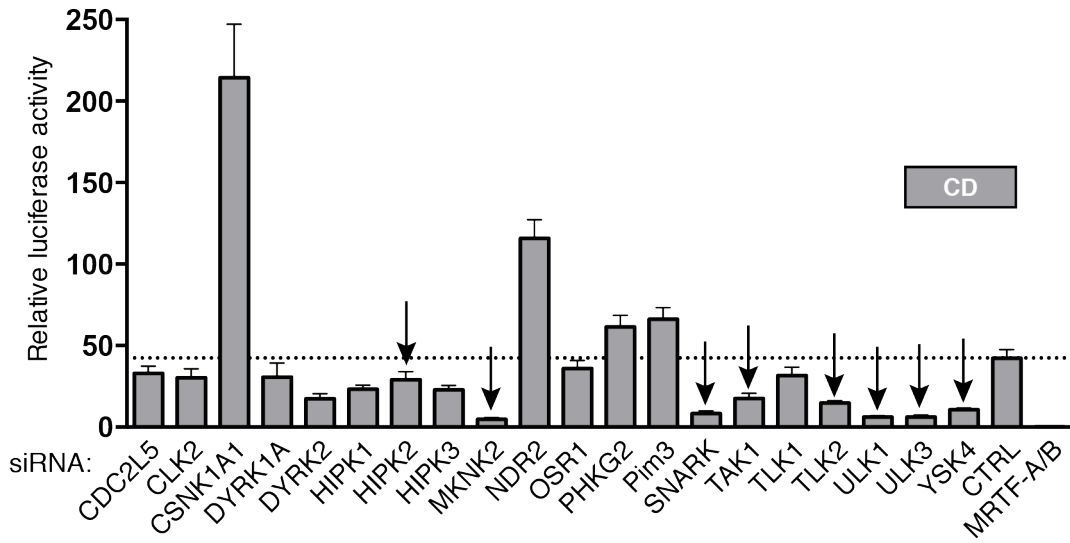
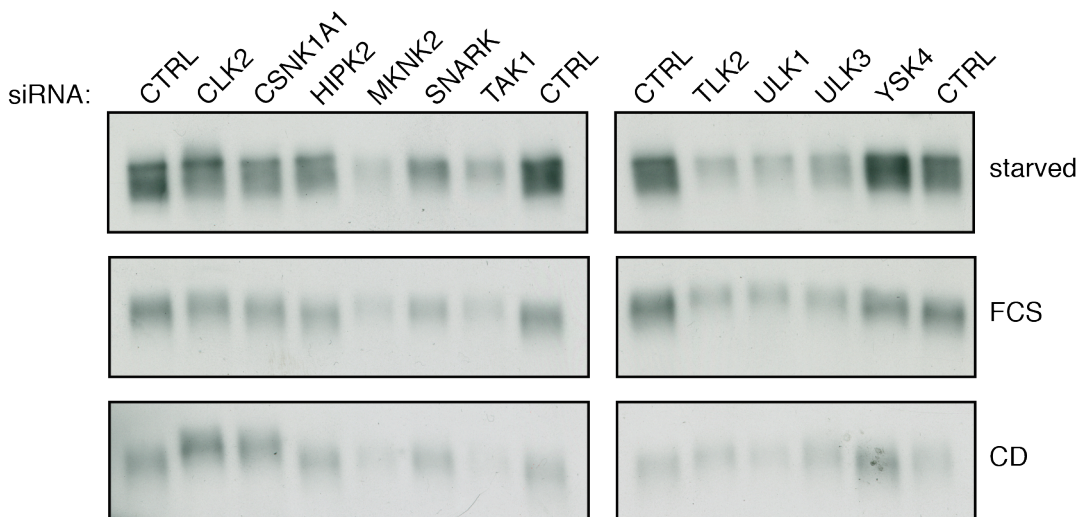


Figure 3.10 Kinase siRNA screen

NIH-3T3 cells stably transfected with the MRTF-A activity reporter were transfected with siRNA against the indicated kinases. After starving overnight, cells were stimulated with 15% FCS or 2 μ M CD. Firefly luciferase activity was normalised to renilla luciferase activity and plotted as fold change relative to control in starved conditions (the dotted line indicates the activity of the control). Arrows indicate the eight siRNAs that led to a block in both FCS and CD activation. Error bars represent standard error of the mean (SEM) from at least two independent experiments.

**Figure 3.11 MRTF-A phosphorylation after kinase knockdown**

NIH-3T3 cells were transfected with non-targeting siRNA (CTRL), or siRNA against indicated kinases, maintained in 0.3% FCS overnight and stimulated with 15% FCS or 2 μ M CD. Lysates were resolved by SDS-PAGE on a 7% polyacrylamide gel and MRTF-A was detected by immunoblotting.

3.8 Are DYRK kinases involved in MRTF-A regulation?

Previous work in the lab, using the small molecule inhibitor DMAT, implicated dual-specificity tyrosine-phosphorylated and regulated kinases (DYRKs) in MRTF-A regulation. Since two members of the DYRK family were also targeted in the 20 siRNA screen, I decided to investigate them in more detail.

Using siRNA each family member was depleted (DYRK1A, 1B, 2, 3, 4) and MRTF activity was followed by qRT-PCR analysis of expression of the target genes Vcl and Srf. Only depletion of DYRK1A moderately hindered activation of both target genes, after both FCS and CD stimulation (Figure 3.12). Since there is a possibility of redundancy, especially between DYRK1A and DYRK1B (Leder et al., 1999), I also depleted DYRK family members in pairs. All combinations that included DYRK1A, except when paired with DYRK4, caused the greatest inhibition in all MRTF-A target genes tested and after both FCS and CD stimulation (Figure 3.13). The data suggest there is redundancy between DYRK family members with respect to MRTF-A regulation. Expression levels could be a contributing factor, and only once two family members are depleted MRTF-A activity is impaired.

I next tested Harmine, a low nanomolar potency inhibitor of DYRK1A and DYRK1B (*in-vitro* IC₅₀ of 33nM and 166nM respectively; over 1 μ M for other DYRKs) (Göckler et al., 2009). 10 μ M Harmine treatment, led to 50% attenuation of Vcl induction but had a weaker effect on Srf (20% and 35% attenuation after FCS and CD respectively) (Figure 3.14).

To test whether overexpression of DYRKs could potentiate MRTF-A activity cells were transfected with either wild type or kinase dead versions of DYRK1A or DYRK1B (Kinase dead versions are mutated in the ATP binding site). Overexpression had no effect on MRTF-A target gene transcription in starved or stimulated conditions (Figure 3.15).

To confirm that the expressed kinases were functional, they were immunoprecipitated from transfected cells for use in kinase assays. First I confirmed that an optimal DYRK substrate peptide called DYRKtide could be specifically phosphorylated. The DYRKtide was successfully phosphorylated only by anti-HA conjugated resin incubated with lysates from cells transfected with HA-DYRK1A (Figure 3.16A). Appropriate controls were included to ensure that

detected activity was not due to kinases non-specifically bound to the resin. In addition DYRK1A did not phosphorylate the PKA substrate KEMPTide, indicating its specificity.

DYRK1B phosphorylated the DYRKtide with 30% the efficiency of DYRK1A under the assay conditions used (Figure 3.16B). In addition, the kinase dead versions did not display any activity, confirming that they are indeed inactive and detected activity was dependent on the DYRK kinase domain.

The immunoprecipitated complexes were also used to test whether they could phosphorylate a panel of 15 residue peptides corresponding to MRTF-A segments that include validated phosphorylation sites. These sites were predicted to be DYRK targets by the GPS 2.0 prediction tool (Xue et al., 2008). One peptide, which contains the S949 phospho-acceptor site, was phosphorylated when incubated with DYRK1A but not DYRK1B (Figure 3.17A). This phosphorylation site is conserved between MRTF family members and throughout vertebrates, and is located in the transactivation domain of MRTF-A. Phosphorylation of this peptide was 5-fold over background but only 7% of the positive control. A phospho-specific antibody that recognises pS949 was not available to confirm this result. The immunoprecipitated kinases were also incubated with recombinant MRTF-A. DYRK1A but not DYRK1B was able to weakly phosphorylate MRTF-A, however the residue(s) concerned was not identified (Figure 3.17B). It is not clear why harmine did not inhibit DYRK activity in this *in vitro* assay. Because harmine is an ATP competitive inhibitor, the ATP concentration of the kinase reaction could be lowered and higher concentrations of harmine could be tested.

The data suggest that DYRK kinases are involved in MRTF-A regulation, but further work is required to determine whether they directly phosphorylate MRTF-A. An S949A derivative could be used in a kinase assay to determine whether S949 is a DYRK1A substrate and whether there are more residues phosphorylated.

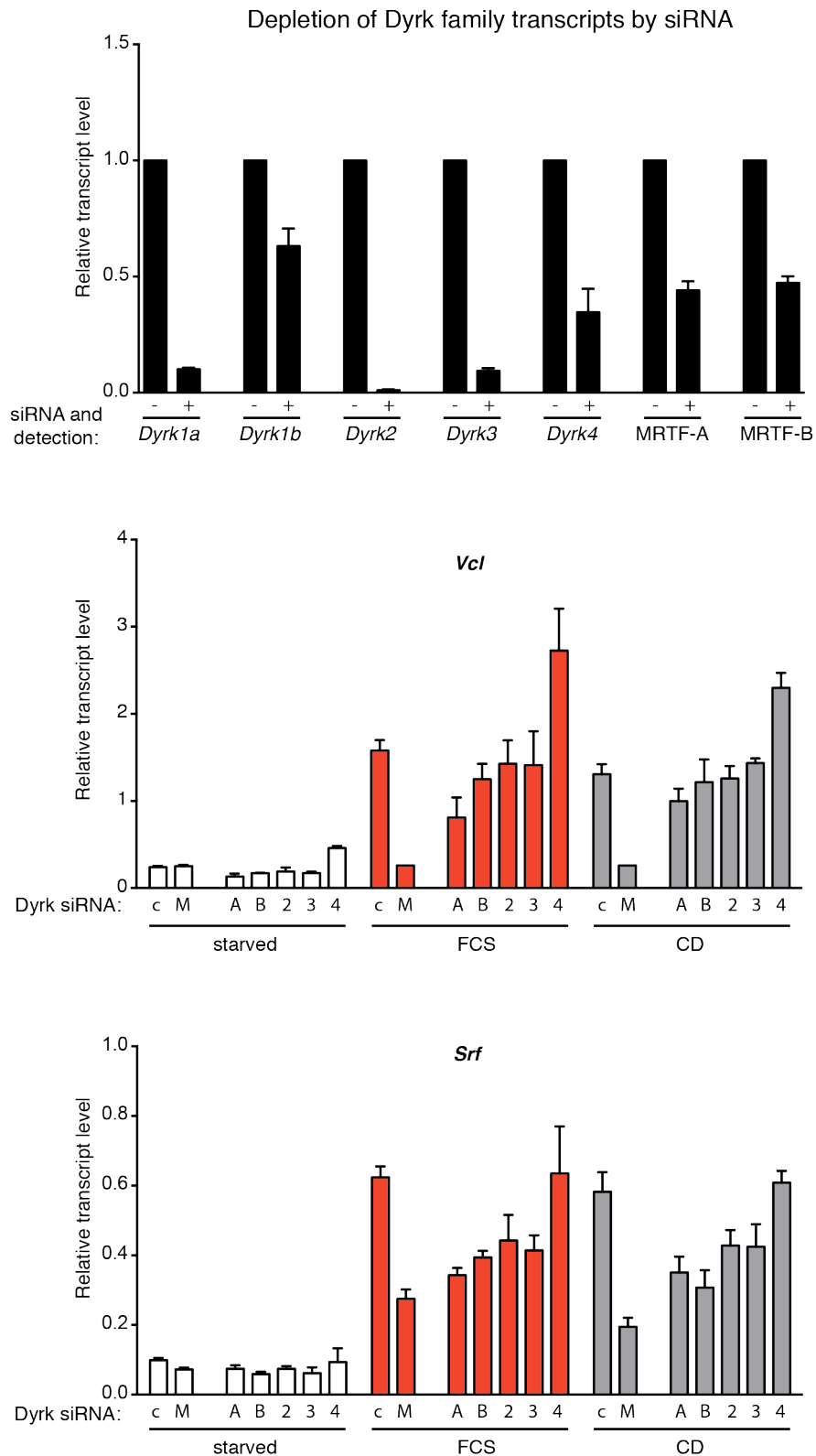


Figure 3.12 Effect of DYRK knockdown on MRTF-A target genes

NIH-3T3 cells were transfected with siRNA against the indicated kinases, starved overnight and stimulated with 15% FCS or 2 μ M CD. Extracted RNA was used to

make cDNA, which was analysed by qRT-PCR analysis of MRTF-A target gene expression, using intronic probes. Data presented as target gene/GAPDH abundance. For the top panel exonic probes were used to assess depletion of siRNA targets and data are presented as fold change relative to before knockdown. For the middle and bottom panels intronic probes were used. c is control, M is MRTF-A, A is DYRK1A, B is DYRK1B and 1-4 are DYRK1-4 respectively. Error bars represent standard error of the mean (SEM) from at least two independent experiments.

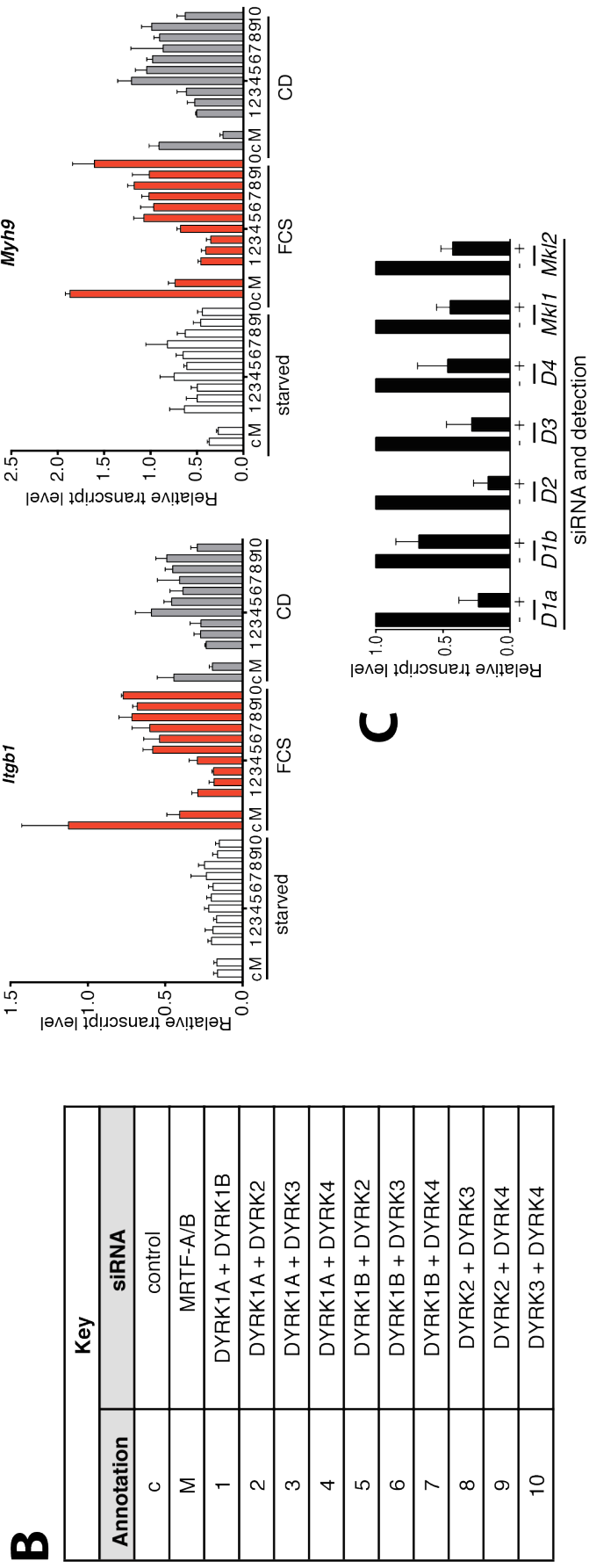
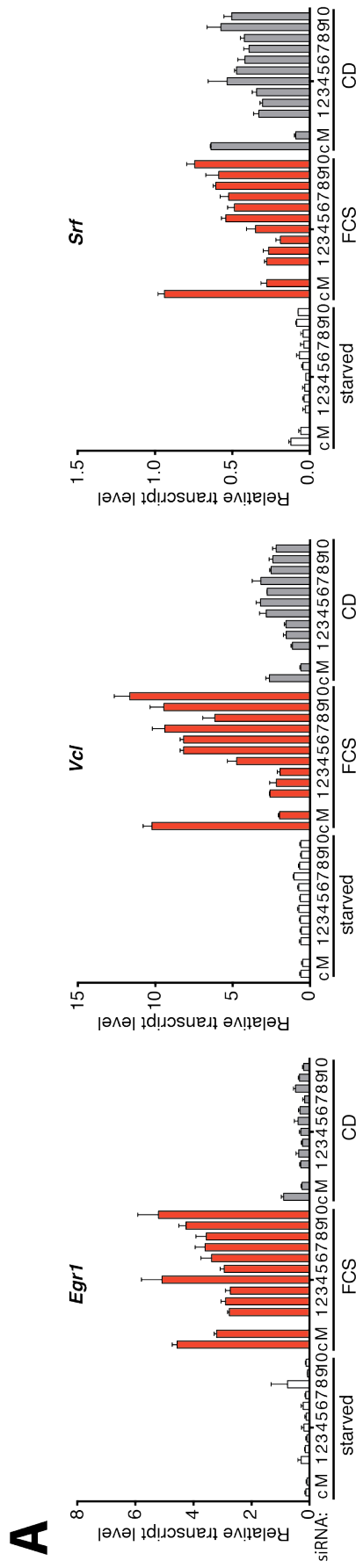


Figure 3.13 Combination knockdowns of DYRK family members

A. Cells were treated as described in Figure 12. Combinations of siRNA are explained in **B.** Efficiency of siRNA depletion of the DYRK target transcripts is shown in **C.** Error bars represent standard error of the mean (SEM) from at least two independent experiments.

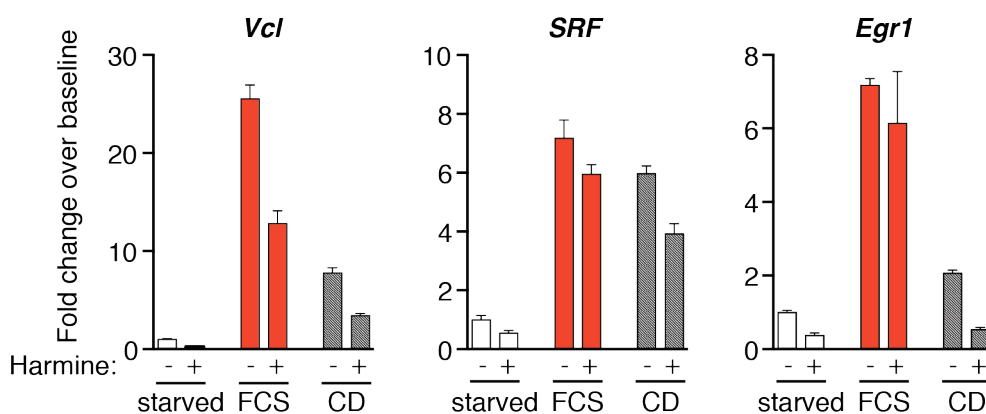


Figure 3.14 DYRK inhibitor Harmine attenuates MRTF-A target gene induction

NIH-3T3 cells were maintained in 0.3% FCS overnight and treated for 15 minutes with 10 μ M Harmine before stimulation with 15% FCS or 2 μ M CD. Extracted RNA was used to synthesise cDNA, which was analysed by qRT-PCR for expression of MRTF target genes using intronic probes. Error bars represent standard error of the mean (SEM) from at least two independent experiments.

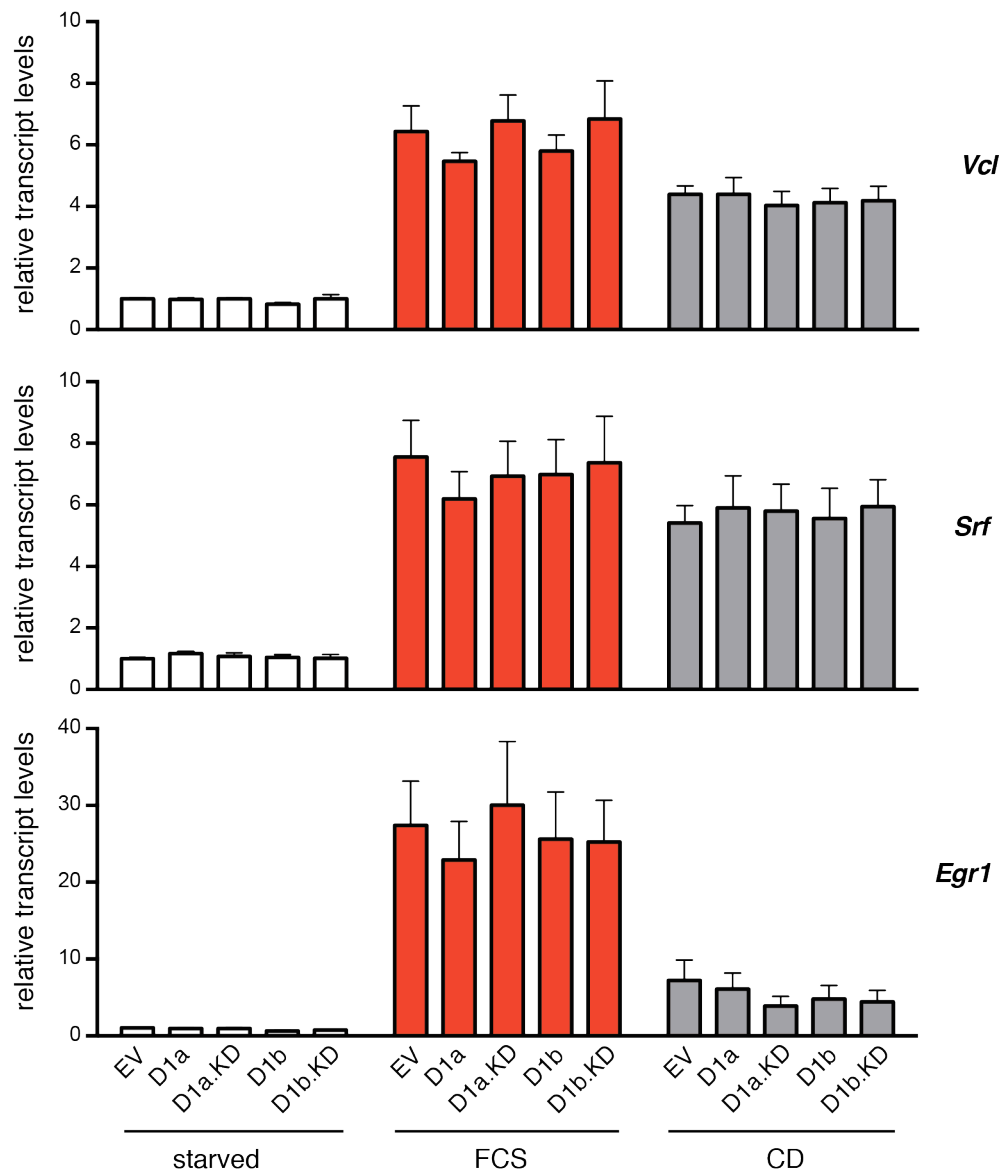
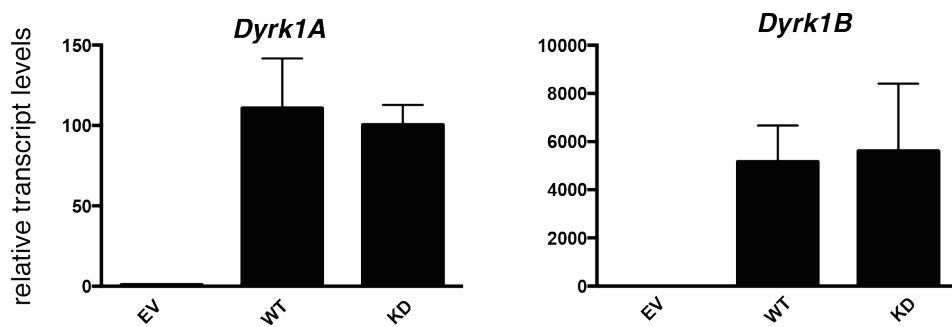
A**B**

Figure 3.15 Effect of DYRK overexpression on MRTF-A target gene expression

A. NIH-3T3 cells were transfected with wild type or kinase dead (KD) DYRK1A or DYRK1B. Cells were starved overnight and stimulated with 15% FCS or 2 μ M CD for 30 min. RNA extracts were used to synthesise cDNA for qRT-PCR analysis of MRTF target genes using intronic probes. **B.** DYRK overexpression was confirmed using exonic primers. EV is empty vector. Error bars represent standard error of the mean (SEM) from at least two independent experiments.

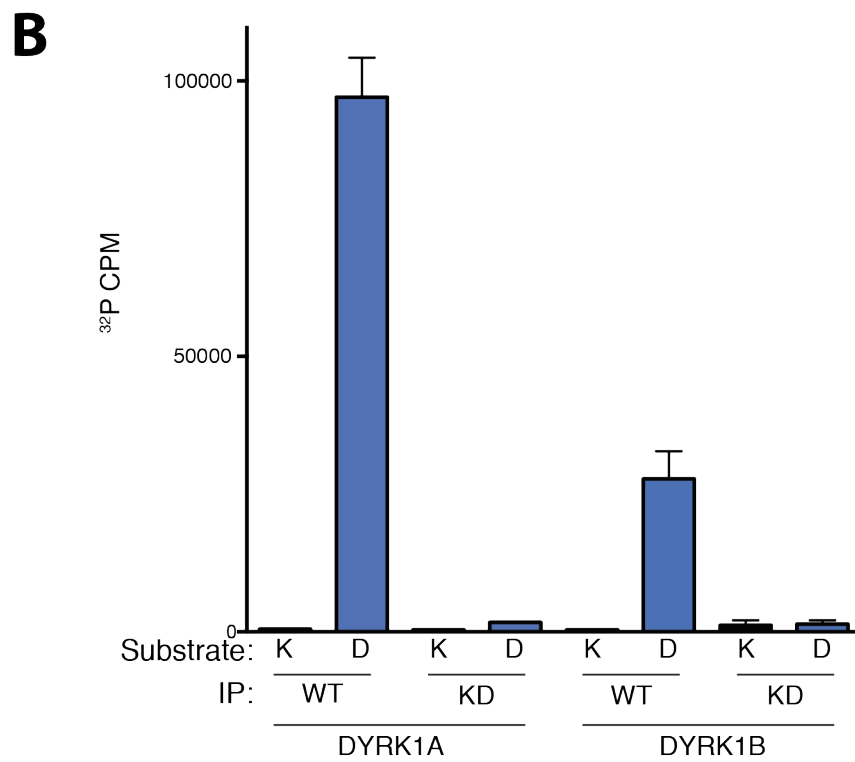
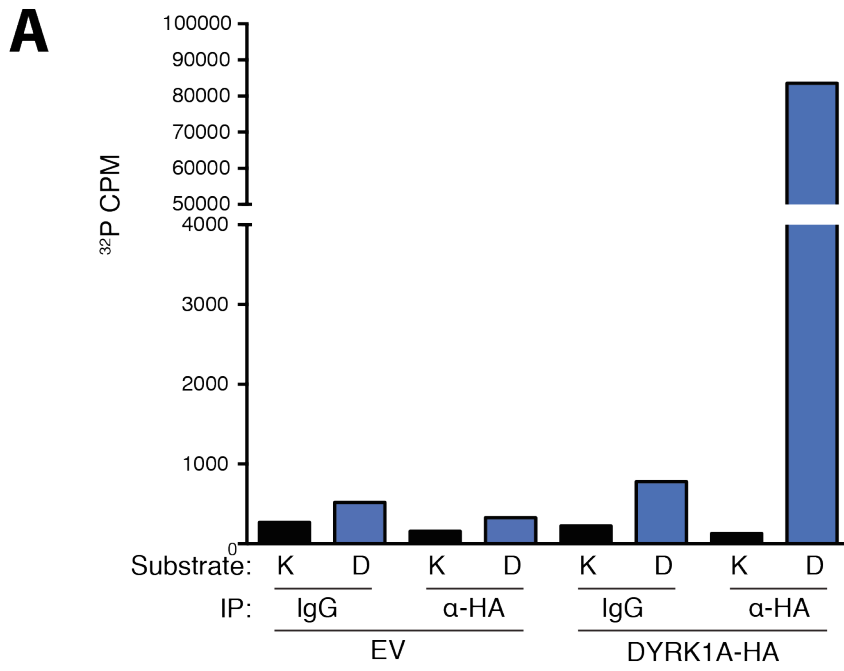


Figure 3.16 Expressed DYRK1A and DYRK1B are functional kinases

A. NIH-3T3 cells were transfected with HA-tagged DYRK1A. The kinase was then immunoprecipitated using anti-HA from the extracts of the FCS stimulated cells. Immune complexes were then tested for their ability to phosphorylate either the KEMPtide peptide (K, AMPK substrate) or the DYRKtide peptide (D, DYRK substrate) in the presence of ATP γ ³²P. A fraction of the reaction was spotted on P81 paper and activity measured using a scintillation counter. **B.** Cells were transfected with either HA-tagged DYRK1A or DYRK1B wild type or kinase inactive (KD). Immune complexes were tested in kinase assays, as in (A).

A

Substrate	Peptide sequence	D1A	D1B
KEMPtide	LRRASLG	< 500	< 500
DYRKtide	RRRFRPASPLRGPPK	42000	8500
S33	RRLSLSAAPSQSEAVA	< 500	< 500
S216	RREDSSDALSPSEQPASH	< 500	< 500
S231	RRESQGSVSPLESRVVS	< 500	< 500
S248	RRLPSATSISPTQVLSQ	< 500	< 500
T402	RRTPGSSAPTPSRSLST	< 500	< 500
S412	RRRSLSTSSSPSSGTPG	< 500	< 500
S414	RRLSTSSSPSSGTPGPS	< 500	< 500
S549	RRTGSTPPVSPTPSERS	< 500	< 500
T566	RRSTGDENSTPGDAFGE	< 500	< 500
S587	RRTQLTLQASPLQIVKE	< 500	< 500
S605	RRRAASCCLSPGARAEL	< 500	< 500
S785	RRQPLSQPGSPAPGPPA	< 500	< 500
S883	RRPPLTPQPSPLSELPO	< 500	< 500
S949	RRAILDHPPSPMDTSEL	3200	<500

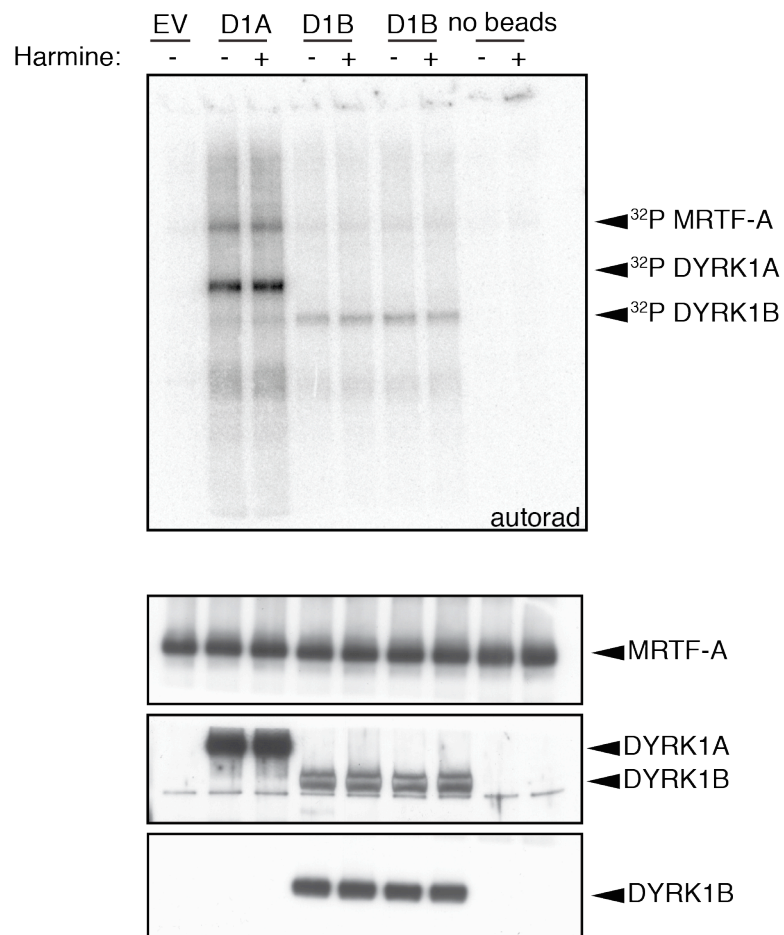
B

Figure 3.17 DYRK and MRTF-A kinase assay

A. DYRK1A and DYRK1B immunoprecipitates were prepared as described in Figure 16 and incubated with peptides corresponding to regions of MRTF that include a phosphorylation site. Sites tested were predicted DYRK targets (Xue et al., 2008). Predicted phospho-acceptor residue is in red. The two amino-terminal arginines shown in blue were added to ensure adsorption to the P81 phosphocellulose paper. A fraction of the reaction was spotted onto P81 phosphocellulose paper and incorporation of ^{32}P was measured using a scintillation counter. **B.** Immunoprecipitates were incubated with purified MRTF-A in the presence of $\text{ATP}\gamma\text{-}^{32}\text{P}$ and where indicated 10 μM Harmine. Reactions were then resolved by SDS-PAGE, transferred and developed using a phosphorimager (Top panel) or used in immunoblotting (Bottom panel). The reaction with DYRK1B was done in duplicate. MRTF-A, DYRK1A and DYRK1B were detected using specific antibodies.

3.9 Are cyclin dependent kinases involved in MRTF-A regulation?

Previous work in the lab using Purvalanol A implicated CDKs in MRTF-A regulation. siRNA depletion of CDK7, CDK8 or CDK9 did not block MRTF-A activity in the reporter assay (Figure 3.18A). Flavopiridol is a panCDK inhibitor, regarded as a CDK9 inhibitor due to its strong potency towards CDK9. Flavopiridol treatment resulted in a dose dependent inhibition of MRTF-A phosphorylation (Figure 3.18B). In addition there was a dose dependent decrease in MRTF-A activity in the reporter assay (Figure 3.19). Flavopiridol also inhibited transcription of the constitutively expressed TK-renilla luciferase construct, as expected, since CDKs are part of the basal transcription machinery. Expression of the MRTF-A reporter however was exceptionally sensitive to Flavopiridol compared to TK-renilla luciferase, as reporter activity was completely blocked at 400nM Flavopiridol while TK-renilla luciferase was inhibited by 40%. These data warrant further investigation into the role of CDKs in MRTF-A regulation.

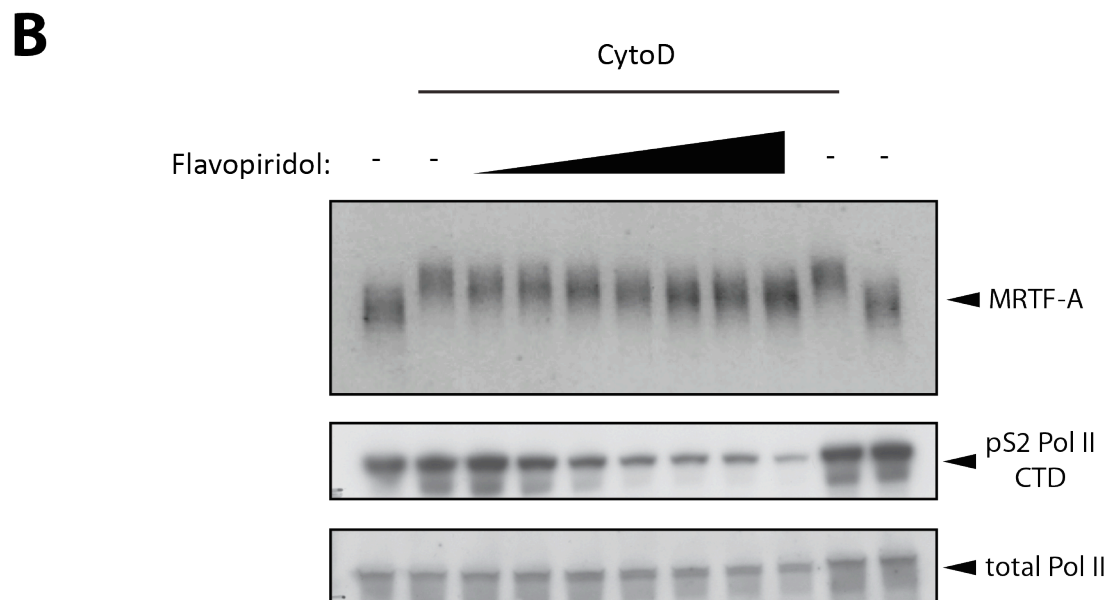
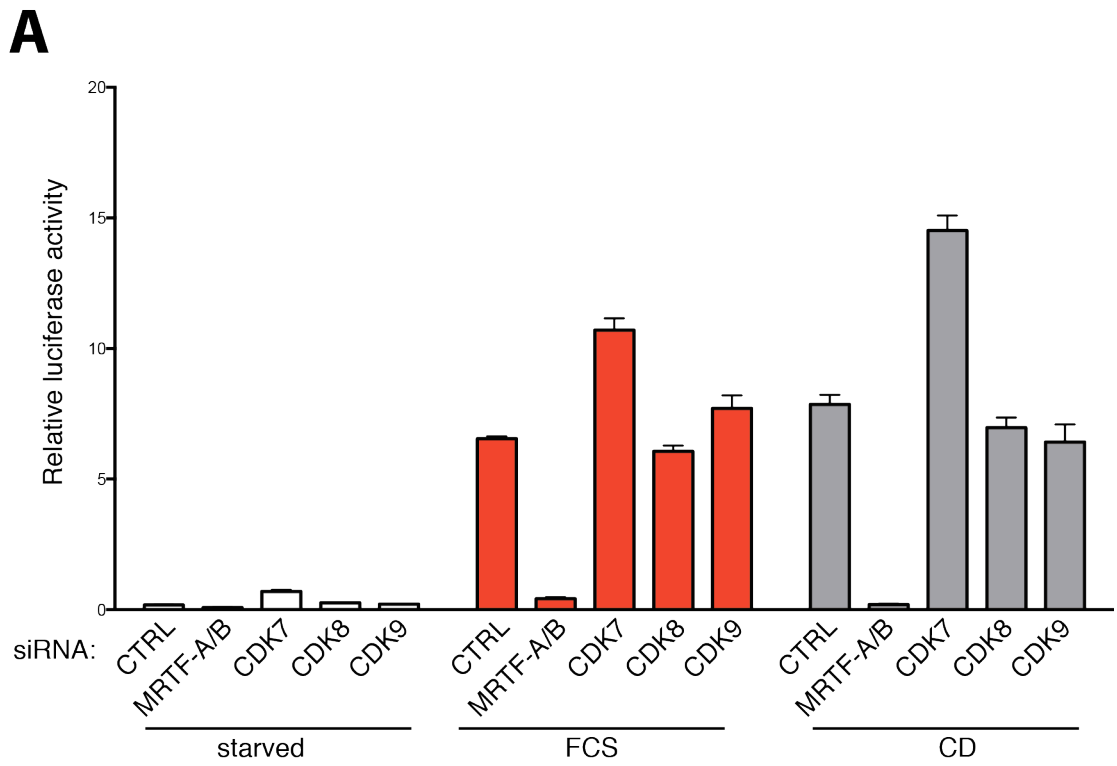


Figure 3.18 CDK knockdown does not impair MRTF-A reporter activation

A. NIH-3T3 cells stably expressing the MRTF-A activity reporter were transfected with siRNA against the indicated CDKs. Conditions for efficient knockdown of CDKs were optimised in a separate experiment. After overnight incubation in 0.3% FCS, cells were stimulated with 15% FCS or 2 μ M CD for 6 hours. Firefly luciferase activity was normalised to renilla luciferase activity. Error bars represent standard error of the mean (SEM) from at least two independent experiments. **B.** Cells were starved overnight and then stimulated with 2 μ M CD for 45 min, in the presence of increasing amounts of Flavopiridol (50, 100, 200, 400, 600, 1000, 2000nM). Lysates were resolved by SDS-PAGE and MRTF-A, pSer2 of Pol II C-terminal domain (CTD) and total Pol II were detected using specific antibodies.

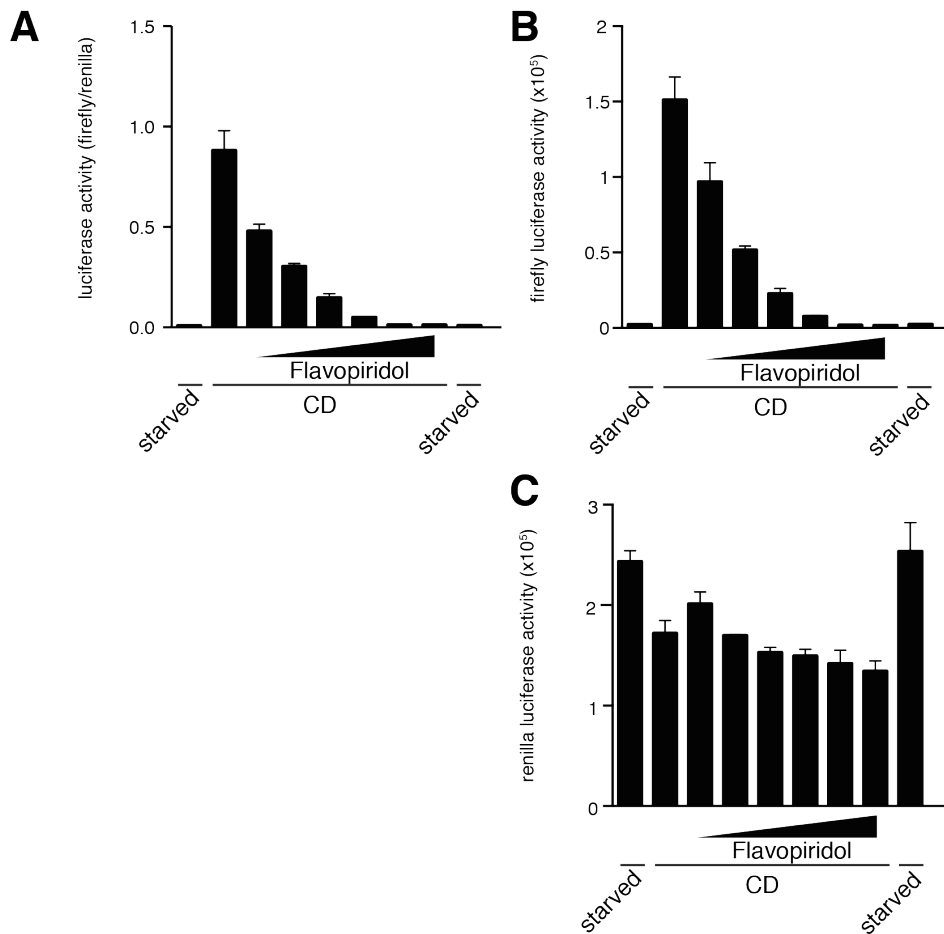


Figure 3.19 Flavopiridol blocks MRTF-A reporter activation

NIH-3T3 cells were transfected with the MRTF-A activity reporter, starved overnight and stimulated with $2\mu\text{M}$ CD for 6 hours in the presence of increasing amounts of flavopiridol. Cell extracts were then assessed for luciferase activity. (Flavopiridol: 50, 100, 200, 400, 800, 1000nM). **A.** Data are presented as firefly/luciferase **B.** firefly luciferase activity. **C.** renilla luciferase activity.

3.10 Summary

The evidence presented in this chapter shows that MRTF-A phosphorylation is required for full activity. MRTF-A phosphorylation can occur upon MAPK pathway activation, possibly by ERK itself. Actin keeps MRTF-A in a low stoichiometry phosphorylation in part by cytoplasmic sequestration. By an unknown mechanism, even when MRTF-A is trapped in the nucleus, actin is able to inhibit phosphorylation. In the absence of stimulation, actin dissociation is sufficient for phosphorylation of MRTF-A suggesting that nuclear constitutively active kinases are responsible. For high stoichiometry phosphorylation actin dissociation and MAPK pathway activation are required. I have presented evidence for the involvement of CDKs and DYRKs, but also that there is probably a high degree of redundancy.

Chapter 4. Regulation of MRTF-A by the MAPK pathway

4.1 Aims

MRTF-A has previously been reported to be regulated in response to ERK signalling. In neurones ERK activation was reported to lead to phosphorylation of MRTF-A and activation of MRTF-A/SRF target genes (Kalita et al., 2006). In HeLa cells ERK activation was reported to lead to phosphorylation and subsequent export of MRTF-A (Muehlich et al., 2008). In our system, using NIH-3T3 fibroblasts, we also have evidence for ERK signalling to MRTF-A. Treatment with MEK1/2 inhibitor U0126 affects MRTF-A phosphorylation and binding to SRF (Miralles et al., 2003; Esnault et al., 2014). Tetradecanoyl phorbol acetate (TPA) is widely used as a means to activate the MAPK pathway and this activation occurs in a PKC dependent manner (Griner and Kazanietz, 2007). Unpublished data from R. Pawlowski demonstrated that in 3T3 fibroblasts TPA treatment leads to nPKC mediated downregulation of RhoA activity and a subsequent increase in G-actin concentration. This negative effect of TPA on Rho/actin signalling makes MRTF-A refractory to FCS activation.

In the following chapter I investigate the consequences of ERK signalling on MRTF-A and how the MAPK pathway contributes to MRTF-A regulation.

4.2 ERK signalling activates MRTF-A

To ask whether ERK activation was sufficient to activate MRTF-A, cells were stimulated and MRTF-A/SRF target gene expression was monitored by qRT-PCR using intronic probes (Figure 4.1A). Transcription of *Srf*, *Vcl* and *Itgb1*, which depend on MRTF-A for activation, was induced upon TPA treatment, together with

the TCF dependent *Egr1* gene used as a control. Induction was largely sensitive to the MEK1/2 inhibitor U0126. Residual activity after U0126 treatment was similar to that of the ERK/TCF regulated *Egr1* suggesting incomplete inhibition of ERK rather than the contribution of other transcription factors. To confirm this observation I additionally tested the TPA treatment on cells transiently transfected with an MRTF-A reporter gene. Expression of the reporter gene is entirely dependent on MRTF-A and TPA stimulation of the reporter occurred only in the presence of MRTF-A (Figure 4.1B).

In 3T3 cells TPA treatment downregulates Rho activity and increases G-actin concentration, which creates inhibitory conditions for MRTF-A (Figure 4.2A). Using the Rho-GTP binding domain of Rhotekin active Rho was precipitated from cells stimulated by either FCS or TPA. Indeed, as opposed to FCS treatment, TPA led to a reduction of available RhoGTP, as judged by recovery of Rho in the Rhotekin pulldown experiment (Figure 4.2B). Hence the MRTF-A dependent activity observed is occurring despite TPA induced increase in G-actin concentrations. These results suggest that TPA influences MRTF-A subcellular localisation by mechanisms other than G-actin depletion. The presence of an ERK phosphorylation site, S98, within the RPEL domain suggests that this might occur through a decrease in the affinity of the RPEL domain towards actin.

S98 exhibits little phosphorylation in resting conditions and is rapidly phosphorylated after TPA stimulation in a U0126 sensitive manner (Figure 4.3). Other phosphorylation sites tested exhibited baseline phosphorylation and some were induced by TPA. The large change in S98 phosphorylation, and its presence within the actin binding RPEL domain, suggested that it might provide a way to regulate the actin binding properties of MRTF-A and therefore its localisation.

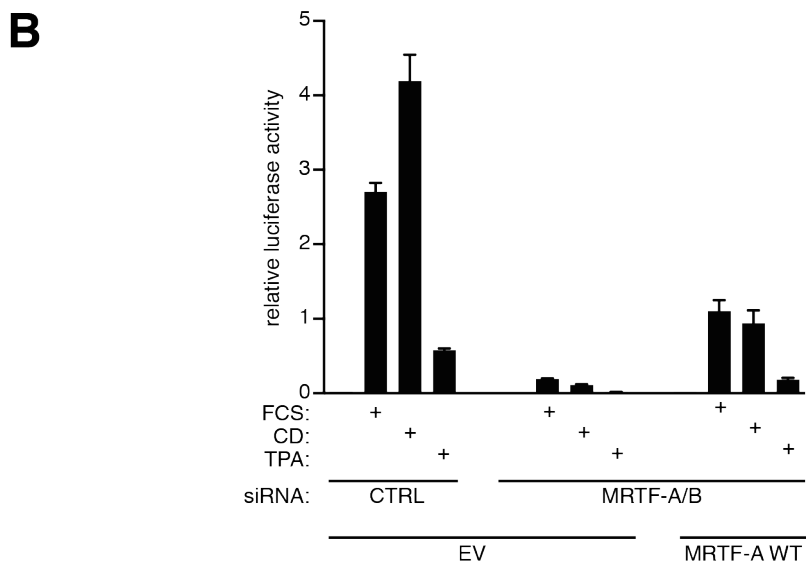
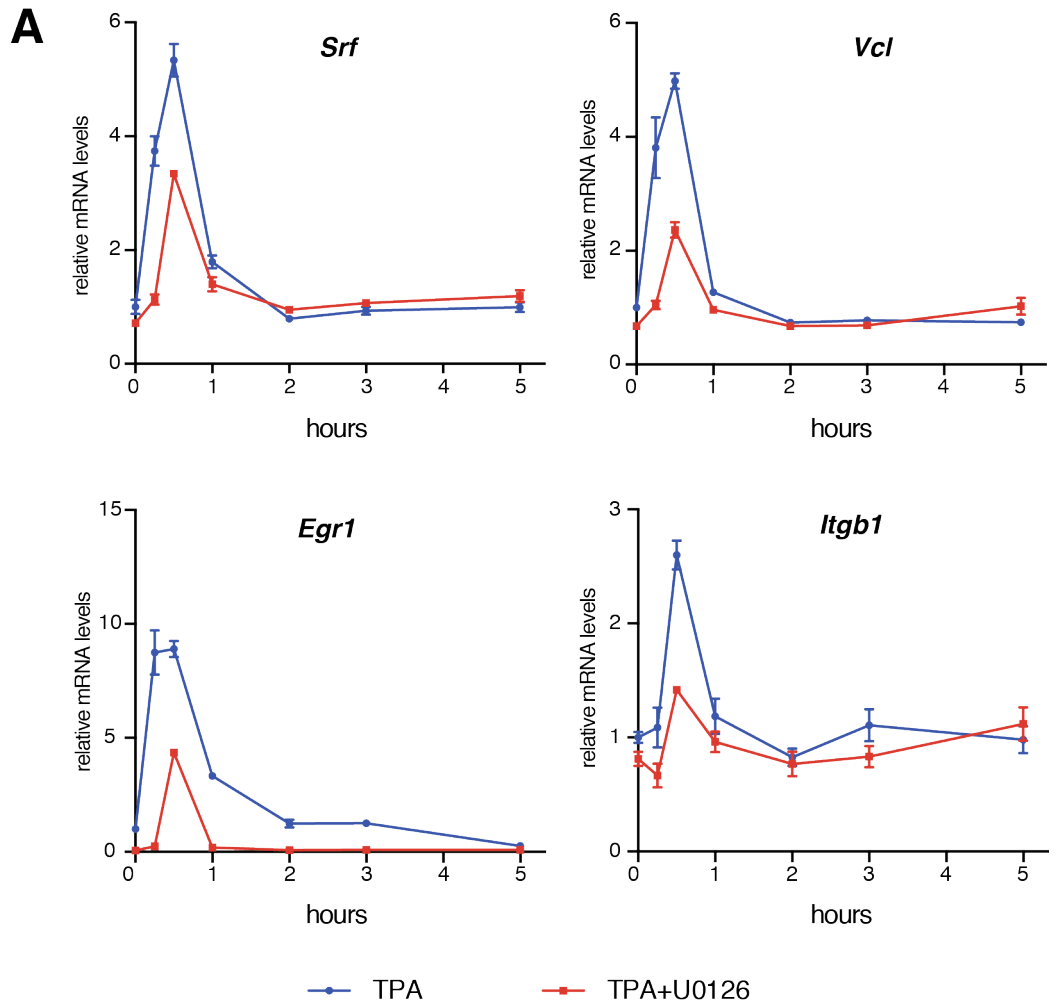


Figure 4.1 TPA induces MRTF-A target gene activation

A. NIH-3T3 cells were maintained in 0.3% FCS overnight and stimulated with 100ng/mL TPA for the indicated times, in the presence or absence of 10 μ M U0126 . RNA extracts were used for qRT-PCR analysis of MRTF-A target gene expression using intronic probes. **B.** MRTF-A activity reporter assay. NIH-3T3 cells depleted of endogenous MRTF-A using siRNA were transfected with luciferase reporter plasmids and 3ng/well MRTF-A. After overnight starvation cells were stimulated with 15% FCS, 2 μ M CD or 100ng/mL TPA for 6 hours. Error bars represent standard error of the mean (SEM) from at least two independent experiments.

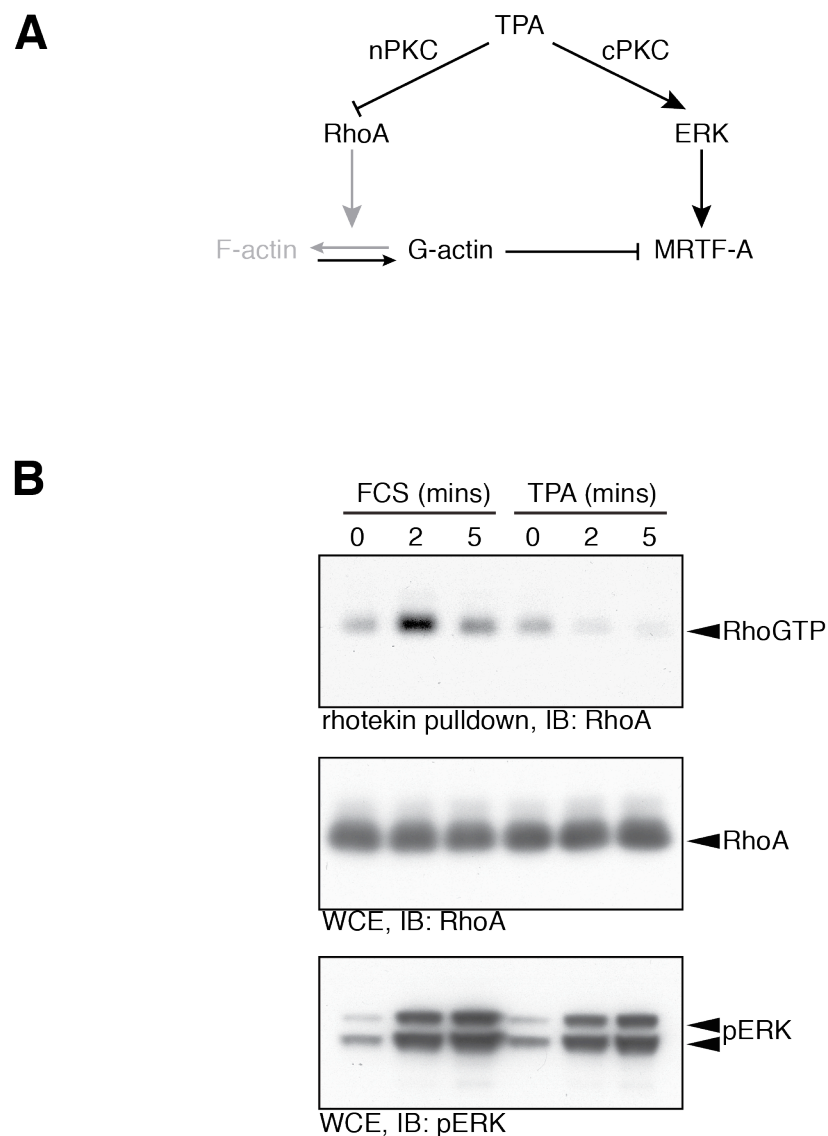


Figure 4.2 TPA treatment downregulates Rho activity in 3T3 cells

A. Schematic depicting the effects of TPA on ERK and RhoA signalling in 3T3 cells (R. Pawlowski, unpublished). **B.** Starved NIH-3T3 cells were treated with 15% FCS or 100ng/mL TPA for indicated times. RhoGTP was pulled down on bead-immobilised GST-rhotekin RBD. Precipitates were resolved by SDS-PAGE and probed with an anti RhoA antibody. Whole cell extracts were immunoblotted with anti RhoA as a loading control and anti phospho ERK for ERK activation.

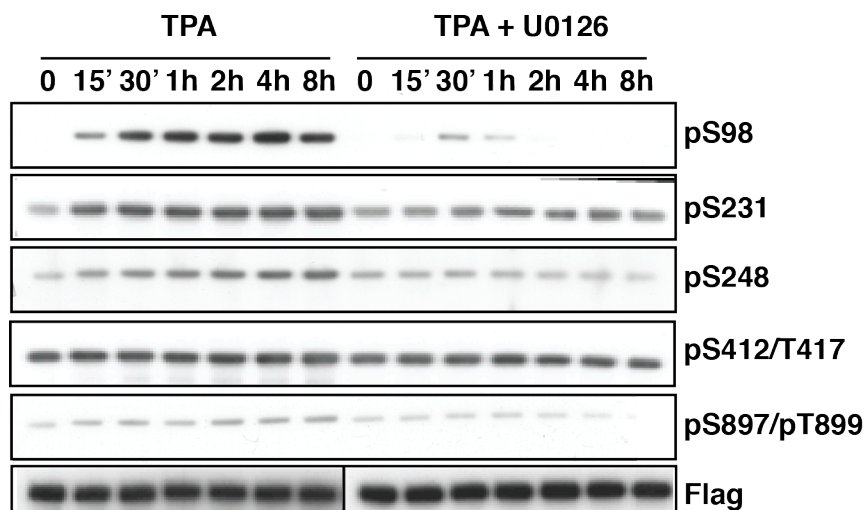


Figure 4.3 TPA leads to MRTF-A phosphorylation

NIH-3T3 cells stably transfected with a tetracyclin inducible MRTF-A expression vector, were starved and treated with tetracyclin overnight. The cells were next treated with 100ng/mL TPA for the indicated times in the presence or absence of 10 μ M U0126. Lysates were resolved by SDS-PAGE and MRTF-A was detected using an anti flag antibody or the indicated phospho-specific antibodies.

4.3 ERK directly binds MRTF-A and phosphorylates S98

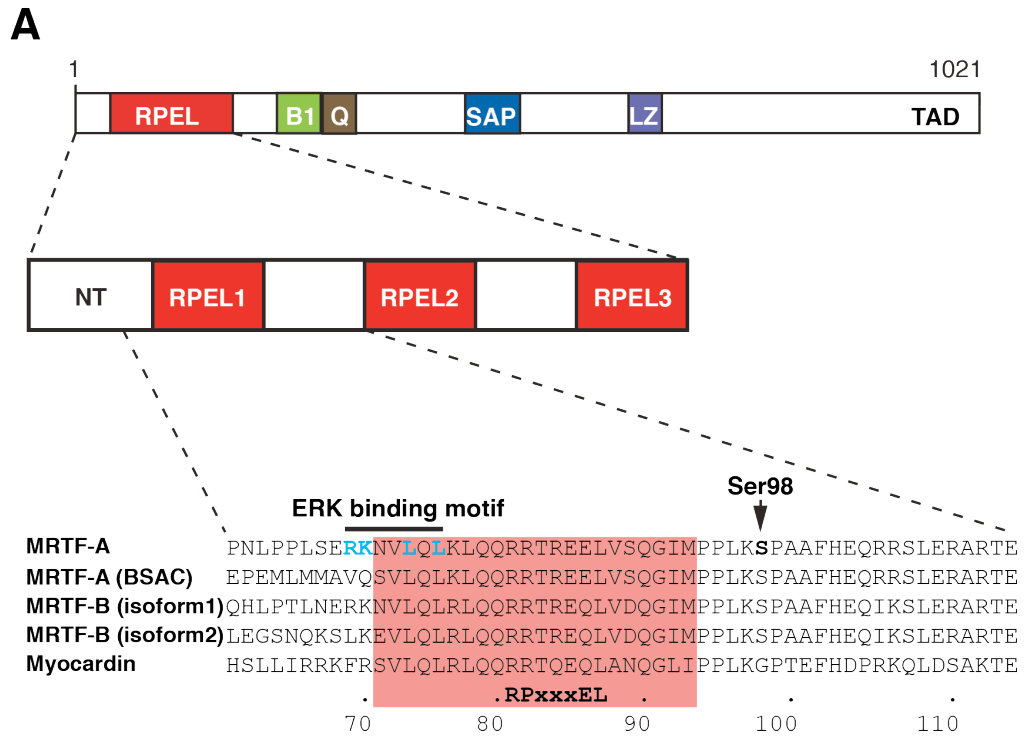
S98 is located at the N-terminal end of Spacer1 (Figure 4.4A). A sequence which closely resembles an ERK binding motif (Figure 4.4B) (Sharrocks et al., 2000) is present N-terminal to this, overlapping RPEL1. The motif is composed of the two positive residues RK 70/71, followed by a two-residue spacer and LQL 74/75/76 (Figure 4.4A). The motif overlaps with RPEL1, sharing the highly conserved Leucine 74 that is involved in actin binding.

To determine whether this putative ERK binding motif was required for phosphorylation of S98, I mutated either the basic or the hydrophobic residues of the motif (Figure 4.4C). Because it was previously seen that BSAC is not phosphorylated on its S98 equivalent position (F. Miralles, unpublished), I exchanged the positive residues in MRTF-A to those found in BSAC (VQ) or to

alanine (AA). This analysis showed that S98 phosphorylation was dependent on the motif for phosphorylation. Upon serum stimulation, S98 was phosphorylated and mutation of the positive residues to AA greatly reduced phosphorylation (Figure 4.4C). Indeed phosphorylation of the serine was not detected in BSAC and in MRTF-A RK/VQ S98 phosphorylation was substantially reduced. No phosphorylation was detected upon mutation of Leucines 74/76 of the ERK binding motif.

I next wanted to confirm whether ERK could directly interact with MRTF-A using purified components. I used immobilised GST MRTF-A 2-115 as bait and successfully precipitated purified ERK2. The interaction was dependent on the integrity of both the positive and hydrophobic residues of the ERK binding motif (Figure 4.4D).

Combined these results show that activated ERK directly binds MRTF-A via the ERK binding motif to phosphorylate S98 within the RPEL domain.



B

Protein	Sequence
MRTF-A	LSE RKNV LQLKL
hElk1	KGRKPRDLELPL
hSAP1	RS KKPKGL LAP
mNet	KG KKPKGLEI SA
MKK4	GKRKALKLN FAN
MEF2A	SRKPDLRV VIPP
MKK1	PKKKPTPIQLNP

$\Psi(1-3)-x(1-7)-\Phi-x-\Phi$

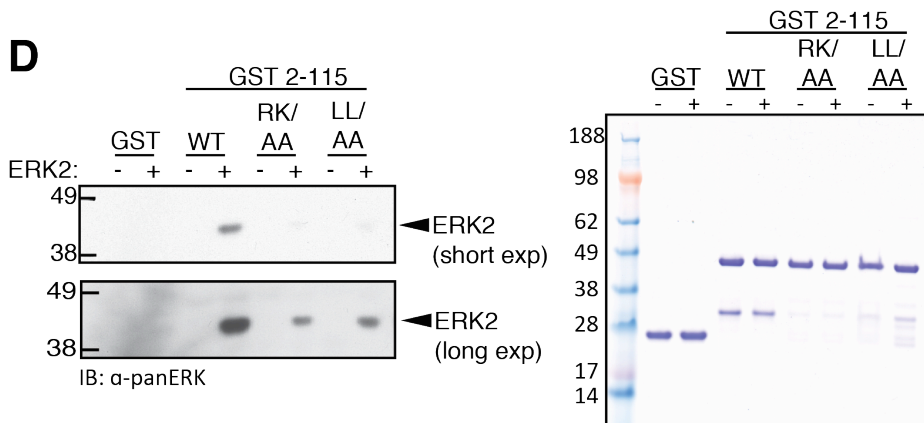
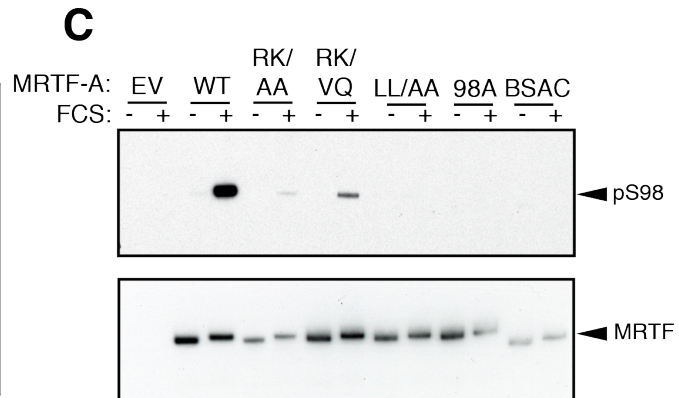


Figure 4.4 ERK directly binds MRTF-A and phosphorylates Ser98

A. Schematic representation of MRTF-A. Expanded region containing the ERK binding motif (D-domain) and S98 is aligned with that of other MRTF family members. RPEL1 is enclosed in a red box and the conserved R, P, E and L residues of the RPEL motif are indicated below. Conserved positions of the D-domain are colored blue. **B.** The MRTF-A D-domain, aligned with other known D-domains is presented and the consensus sequence is shown below ('Multiple docking sites on substrate proteins form a modular system that mediates recognition by ERK MAP kinase', n.d.; Garai et al., 2012). Conserved positions are shown in blue. Ψ is either Arg or Lys (basic), Φ is Leu, Val, Iso, Phe or Met (hydrophobic). **C.** Cells were transfected with either MRTF-A WT or derivatives where key positions of the D-domain were mutated or BSAC, an MRTF-A isoform in which the D-domain is divergent. After stimulation, the overexpressed proteins were probed for S98 phosphorylation using a phospho-specific antibody against pS98. **D.** ERK2 pull down using immobilised GST-MRTF-A (2-115) as bait. GST-MRTF-A (2-115) and derivatives with mutated D-domains were immobilised on resin and tested for their ability to interact with ERK2. Left: Immunoblot using an anti-ERK antibody. Right: coomassie stained gel to show that equal amounts of bait were used. ERK2 protein amounts were not sufficient for coomassie staining.

4.4 S98 phosphorylation affects actin binding by the RPEL domain

The RPEL domain forms a compact complex with actin (Mouilleron et al., 2011) and it might be expected that introduction of a negatively charged phosphate moiety at S98 would affect complex assembly. I first tested whether S98 phosphorylation would affect actin binding to RPEL1, which is just N-terminal to S98, using the fluorescence anisotropy assay. The assay allows accurate measurements of binding affinity, the basic principle of the technique is shown in Figure 4.5A. In a previous study, N-terminally fluorophore-labeled peptides corresponding to RPEL1 ± 5 residues (residues 67-98) and purified actin-LatB were

used (Mouilleron et al., 2008). For comparison, S98 phosphorylation was first studied in this context (Figure 4.5B). The K_d of WT RPEL1 was $1.1\mu\text{M}$. The K_d of the $\alpha 1^{\text{AA}}$ peptide in which the $\alpha 1$ -helix contact points were mutated could not be determined due to very low or no binding. The K_d of phospho-S98 and S98A peptides, were $0.6\mu\text{M}$ and $1.7\mu\text{M}$ respectively (Figure 4.5C). Phosphorylation of S98 does not appear to appreciably affect actin-binding affinity. For example the “weak” R81A mutation in RPEL1 results in a K_d of $17.7\mu\text{M} \pm 2.4$ (Guettler et al., 2008).

Since S98 was the terminal residue of the 67-98 peptides, longer peptides were also used (62-104), in which S98 was followed by an authentic α -carbon chain. Again the phosphorylated S98 residue did not affect the K_d of the RPEL1-actin interaction. There was no difference between the shorter and longer peptides (Figure 4.5D). Thus S98 phosphorylation does not affect actin binding in the context of the isolated RPEL1.

I next tested whether S98 phosphorylation affected actin binding to Spacer1. Previously, size exclusion chromatography experiments showed that the Spacer1-RPEL2 peptide can form a complex with 2 actins and that actin binding to Spacer1 cannot occur in the absence of RPEL2 (Mouilleron et al., 2011). This was a suitable context to investigate the effect of S98 phosphorylation for two reasons. First, if S98 phosphorylation affected actin binding to spacer1 there would be a distinct change in the complex mass. Second, the resulting complex would be easily monitored. This is because the actin would grant the complex good absorption at A280, as opposed to peptide alone. Actin alone eluted as a single peak at an elution volume corresponding to an apparent MW of 42.4 kDa; the mass of 1 actin (Figure 4.6). The deduced MW of the complex formed between S1-R2 was 70.9 kDa, corresponding to one peptide and 1.5 actins. This apparent stoichiometry did not significantly change with the phosphorylated S98 peptide or the S98D derivative. Phospho-S98 was therefore unable to affect actin binding to Spacer1, at least in the context of the S1-R2 peptide.

The RPEL domain binds actin cooperatively to form a 3:1 complex with actin bound to RPEL1-Spacer1-RPEL2. This complex is stable enough in solution and for size exclusion chromatography. A 5:1 complex can form, but this complex can only be detected under conditions where actin is constantly present during separation (Mouilleron et al., 2011). Actin interaction with Spacer2 and RPEL3 is

not strong enough to survive the process of SEC. I therefore next investigated whether S98 phosphorylation can destabilise the 3:1 complex and lead to a lower stoichiometry.

As previously observed a 3:1 complex formed between actin and the wild type MRTF RPEL domain (Figure 4.7A). The S98D derivative however, formed a 2:1 complex, indicating that 98D was somehow affecting binding of one of the actins. To determine whether RPEL1 was the affected actin-binding element, I compared the RPEL domain x23, which cannot bind actin via RPEL1, to the RPEL x23 S98D. In this case the 98D mutation was first tested as a potential phosphomimetic substitution. Both derivatives bound 2 actins; there was no further change in actin binding upon aspartate substitution of S98. This suggests that 98D abolishes actin binding to RPEL1 (Figure 4.7A).

To ensure that the stable trimer formed was by actin binding to RPEL1, Spacer1 and RPEL2 and that the only change with S98D was loss of actin from RPEL1, I looked at the effect of the S98D substitution in the context of RPEL 12x, an RPEL domain derivative which is unable to bind actin through Spacer2 and RPEL3. This would preclude the possibility that S98D causes a rearrangement of the RPEL-actin complex. RPEL 12x formed a 3:1 complex, and the S98D substitution led to the loss of one actin. The results confirmed that S98D abolished actin from RPEL1, leaving actin bound to Spacer1 and RPEL2 (Figure 4.7B).

Because of the compact assembly formed by the RPEL domain and actin, I hypothesised that the integrity of S98 itself could be required for formation of the stable complex. In order to investigate this I asked whether RPEL S98A would be impaired in actin binding. The S98A derivative formed a trimeric complex with actin suggesting the alanine substitution did not affect actin binding properties and that integrity of S98 is not required (Figure 4.7C).

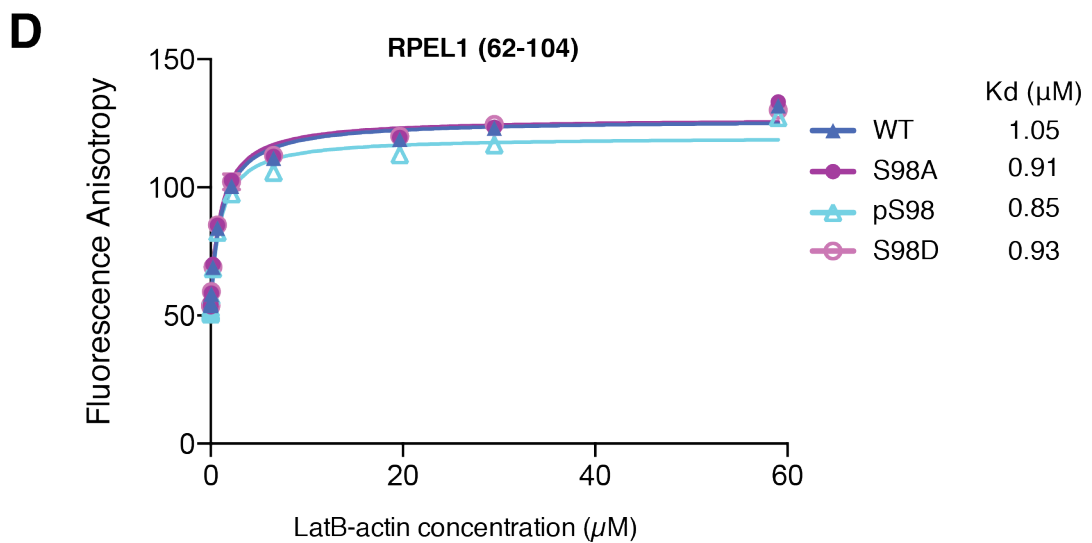
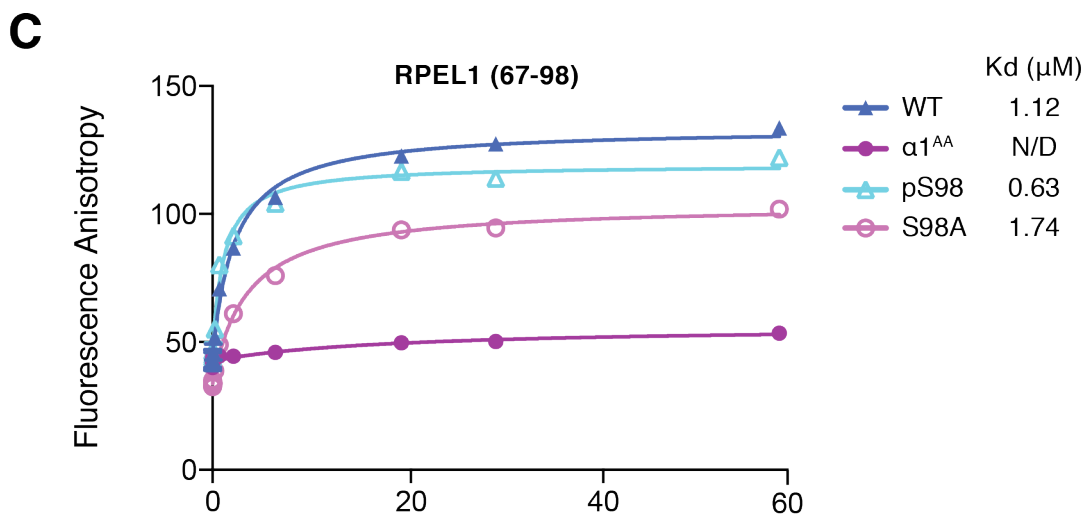
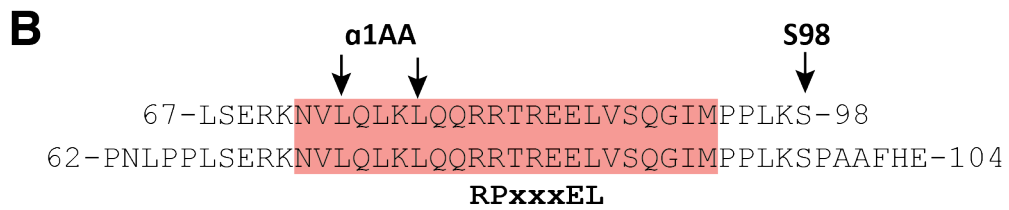
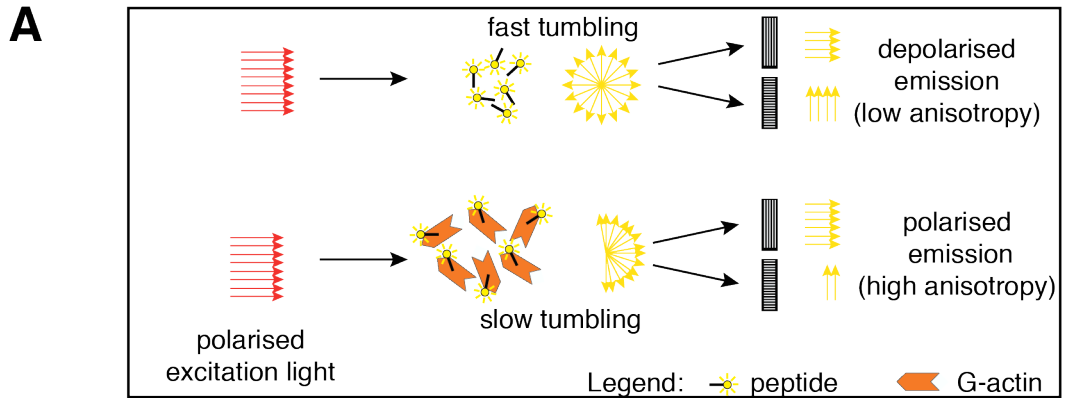


Figure 4.5 S98 phosphorylation does not affect actin binding in the context of the RPEL1 peptide alone

A. Schematic representation of how the affinity of a peptide for actin can be quantified in the fluorescence polarisation assay. Actin is shown in orange and labeled peptides are black with yellow fluorophores. Polarised light is used to excite the peptide-coupled fluorophores into a high-energy state. Small, highly mobile peptides change orientation before returning to ground state and re-emitting light. As a consequence of changing orientation, emitted light is depolarised. Binding to actin reduces mobility of peptides and hence the light emitted remains more polarized compared to the free peptide. Degree of polarisation is proportional to amount of complex formation (Heyduk et al., 1996) **B.** The short and longer RPEL1 containing peptides used in the fluorescence polarisation assay are shown. Residues altered in the derivatives tested are shown with arrows, RPEL1 is enclosed in a red box and the conserved RPEL residues are shown below. **C and D.** Anisotropy of indicated FAM labeled RPEL1 peptides measured over a range of LatB-actin concentrations. Error bars represent standard error of the mean (SEM) from at least two independent experiments.

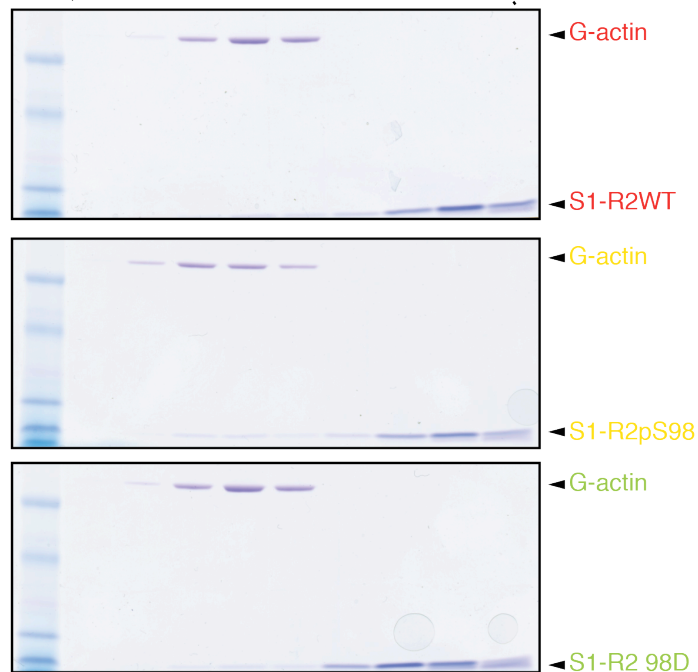
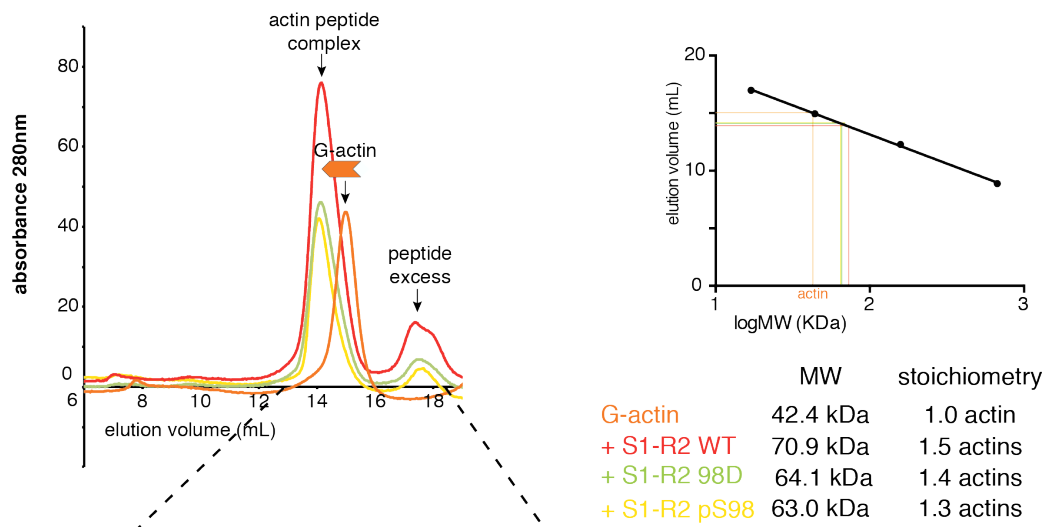
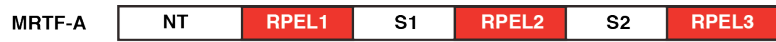


Figure 4.6 S98 phosphorylation does not affect actin binding to Spacer1

Peptides corresponding to Spacer1-RPEL2 of the RPEL domain were incubated with purified actin and analysed by size exclusion chromatography. The elution volumes of the complexes, determined by the peaks, were converted to apparent molecular weight using the calibration curve (right). Bottom: Coomassie gels show the major peaks corresponding to the actin-peptide complexes, and excess peptide.

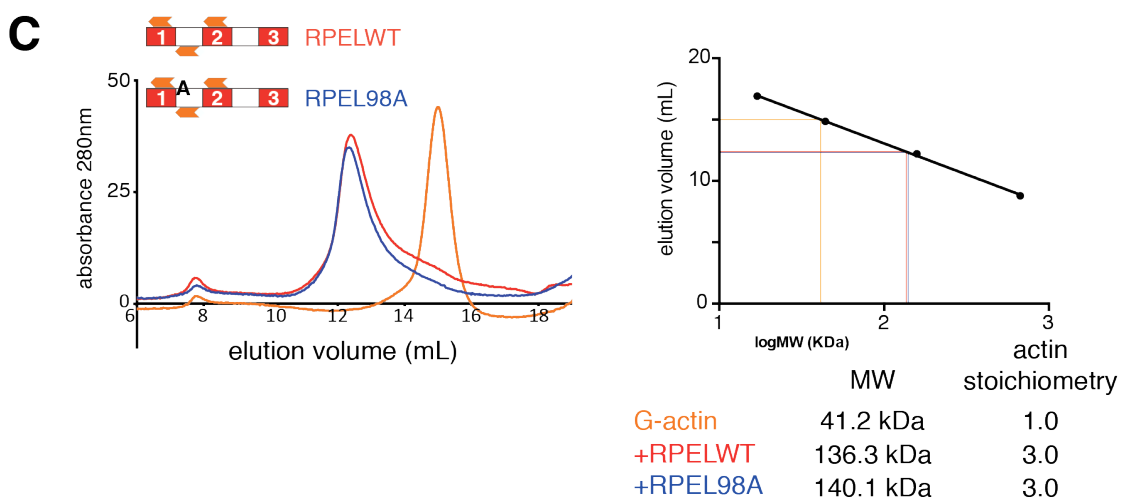
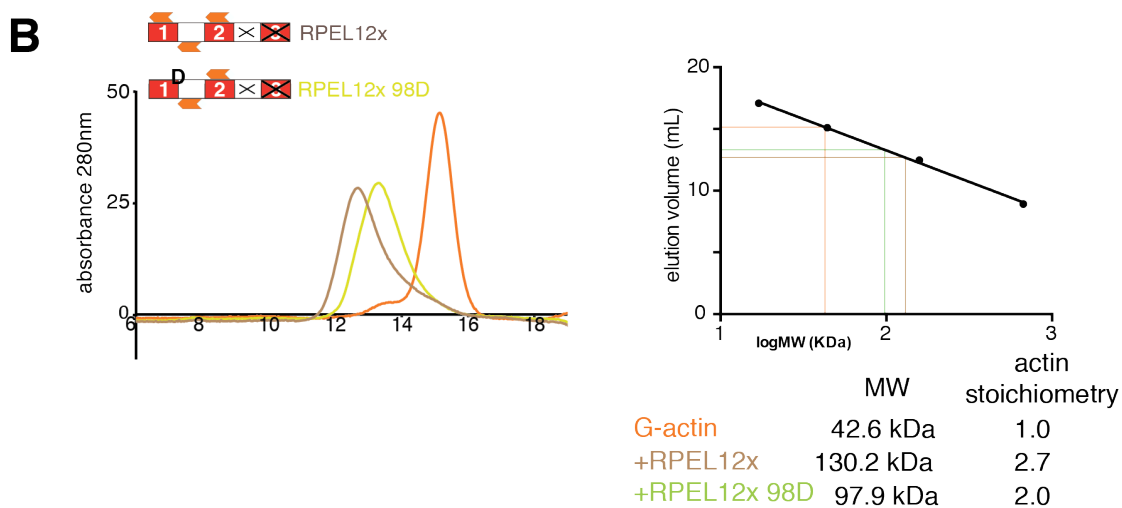
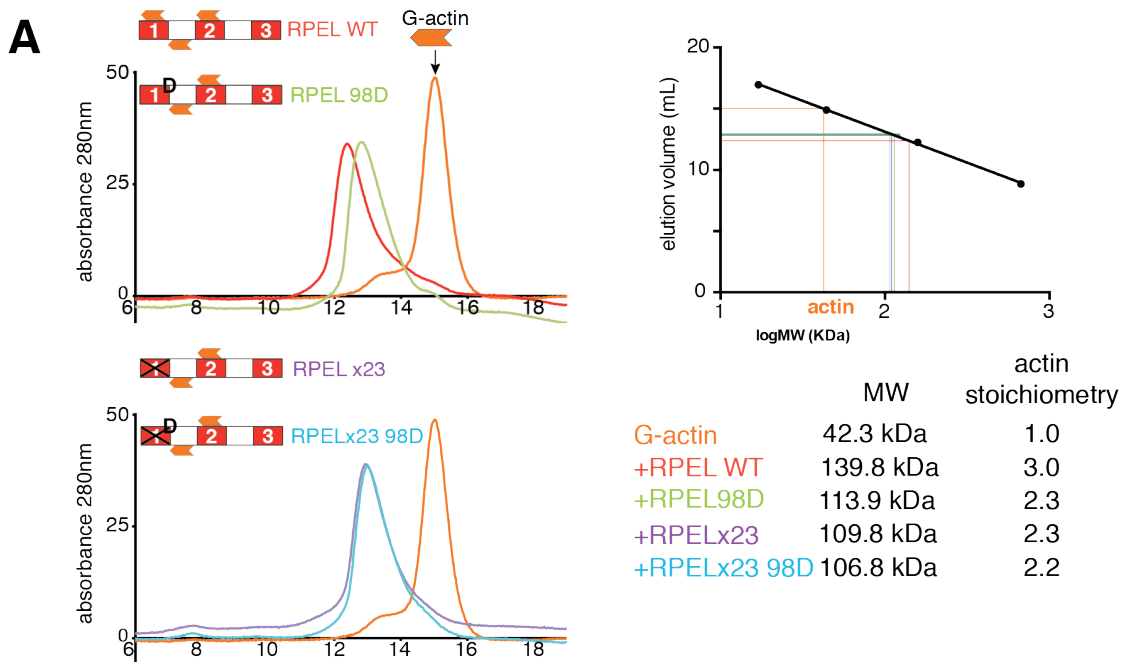


Figure 4.7 S98 phosphorylation blocks actin binding to RPEL1 in the context of the RPEL domain

Recombinant RPEL domain and the indicated derivatives were incubated with actin and complexes were analysed by size exclusion chromatography. Separate sample runs are superimposed in different colours. Conversion of elution volumes to apparent molecular weight is shown on the right, along with the corresponding apparent stoichiometry of each complex.

4.5 ERK promotes MRTF-A nuclear accumulation through S98 phosphorylation.

Actin binding to the RPEL domain regulates MRTF-A shuttling. Because ERK activation leads to S98 phosphorylation, which in turn affects actin binding, I tested whether TPA induced MRTF-A activation is dependent on S98. To do this I examined the effect of S98A mutation both in MRTF-A and the fusion protein MRTF-A (2-204) PK.

TPA treatment led to transient nuclear accumulation of MRTF-A (Figure 4.8A), however, this was not entirely dependent on S98. MRTF-A S98A exhibited only a slight impairment in TPA induced nuclear accumulation. The S98D derivative, which mimics S98 phosphorylation, exhibited elevated nuclear accumulation in resting cells, which was potentiated upon TPA treatment. These results suggest that phosphorylation of S98 promotes nuclear accumulation, but is not the only event contributing to TPA induced nuclear accumulation. It is possible that the peak of nuclear localisation in the case of S98D is lower, because the aspartate substitution does not faithfully mimic a phospho-serine. TPA induced nuclear accumulation can be attributed to ERK activation, because it was blocked by the MEK1/2 inhibitor U0126 (Figure 4.8B).

Previous studies suggest other phosphorylation sites (S544, T545, S549) impinge on MRTF-A regulation (Muehlich et al., 2008). The N-terminal region of MRTF-A, including the N-terminus and RPEL domain is sufficient to confer MRTF-

A like shuttling when fused to the normally cytoplasmic pyruvate kinase (Guettler et al., 2008).

Use of the MRTF-A (2-204) PK fusion allowed investigation of S98, independently from the other phosphorylation events. The MRTF-A (2-204) PK fusion and its S98A derivative accumulated in the nucleus upon TPA treatment indicating that S98 phosphorylation is not required (Figure 4.8C). Accumulation was not completely blocked by U0126 (Figure 4.8D) indicating that TPA induced nuclear localisation is not accomplished solely through ERK activation. S98 phosphorylation by ERK is therefore not required for TPA induced nuclear accumulation, however, the S98D derivative is predominantly nuclear indicating that S98 phosphorylation is sufficient.

TPA activates other pathways besides ERK, and inhibits Rho activation, as shown above. I therefore induced ERK activation by making use of RafER. RafER is a fusion between the Raf kinase domain and the estrogen binding domain of the estrogen receptor. The fusion is kept inactive by binding to HSP90 and can be activated by tamoxifen (Samuels et al., 1993). Upon tamoxifen addition, an increase in S98 and total phosphorylation of MRTF-A was observed, which was sensitive to MEK1/2 inhibition (Figure 4.9A). The time dependent increase was reflected by nuclear accumulation of either full length MRTF-A or MRTF-A (2-204) PK (Figure 4.9B). Together, these experiments show that selective activation of the MAPK pathway is sufficient for MRTF-A phosphorylation and nuclear accumulation, and suggest that this occurs through phosphorylation of S98.

To confirm that nuclear accumulation was occurring via ERK and S98 I co-transfected cells with constitutively active MEK (MEK^{R4F}) and the S98 derivatives of MRTF-A (2-204) PK. In the presence of MEK^{R4F}, the fusion was substantially more nuclear, as with TPA (Figure 4.9C). The S98A derivative did not respond to constitutive MEK-ERK signalling, in contrast to treatment. This supports the notion that TPA induced nuclear accumulation was not simply down to S98 phosphorylation. Thus S98 phosphorylation can promote nuclear accumulation at least in the context of the RPEL domain. The observation that the S98D derivative showed relatively high nuclear accumulation in starved conditions, which was not TPA or MEK^{R4F} responsive, suggests that S98 phosphorylation is not only necessary but also sufficient to promote nuclear accumulation.

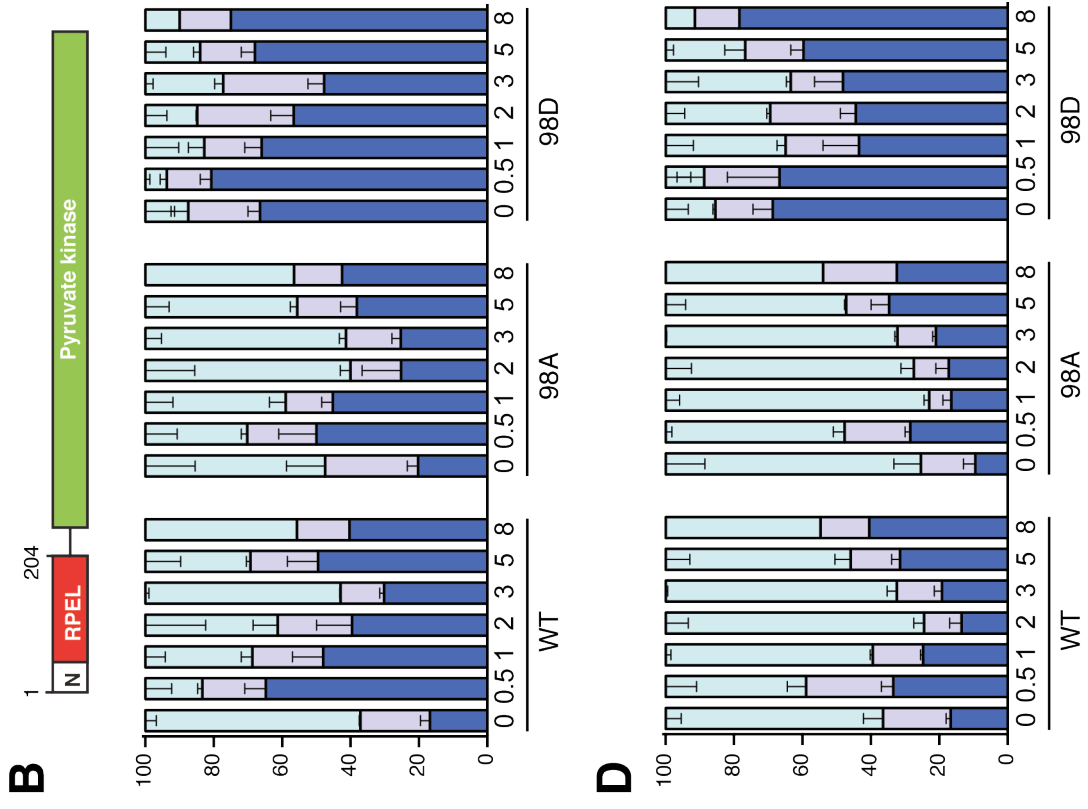
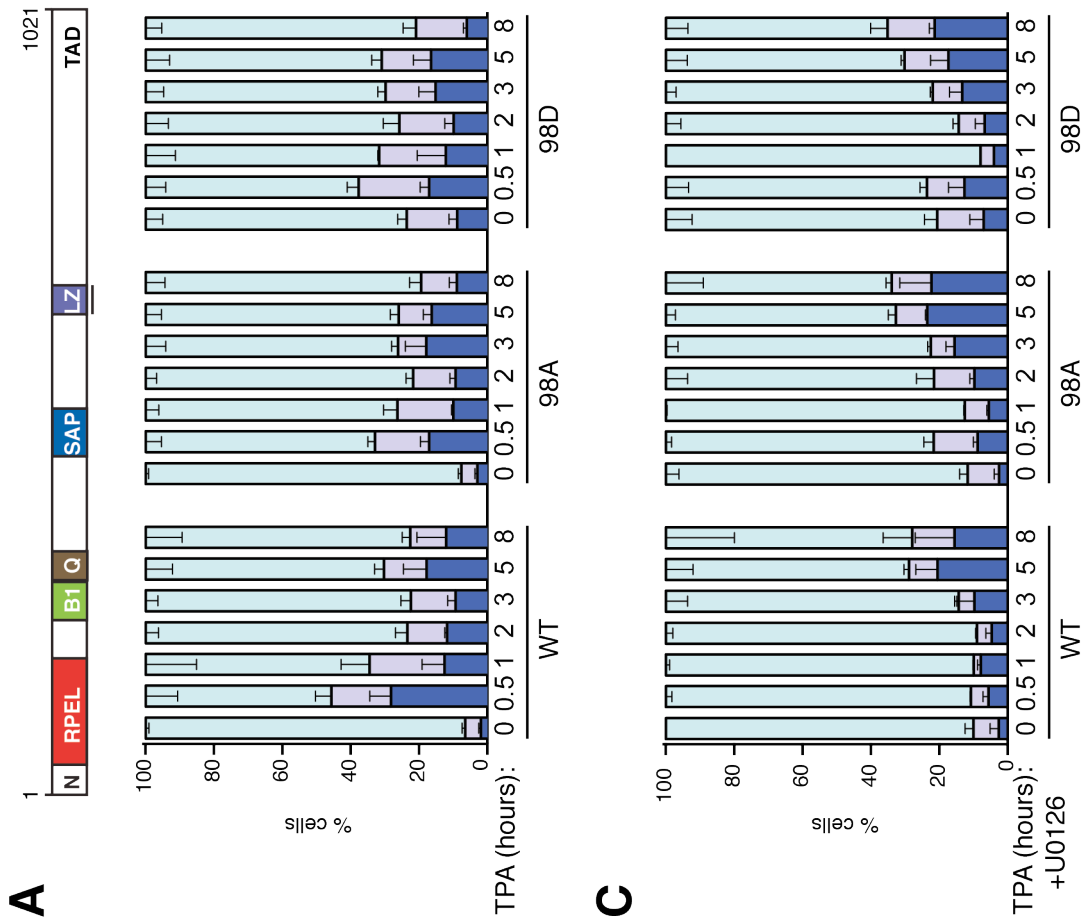


Figure 4.8 TPA leads to MRTF-A nuclear localisation

NIH-3T3 cells were transfected with wild type, S98A or S98D derivatives of either full length MRTF-A (**A and B**) or MRTF-A-PK fusion protein (**C and D**). Following overnight starvation, cells were stimulated with 100ng/mL TPA for the indicated times in the presence or absence of 10 μ M U0126. Localisation was determined by immunofluorescence using an anti flag antibody. At least 100 cells were counted and localisation was scored as predominantly nuclear (navy blue), pancellular (lilac) or predominantly cytoplasmic (light blue). Error bars represent standard error of the mean (SEM) from at least two independent experiments.

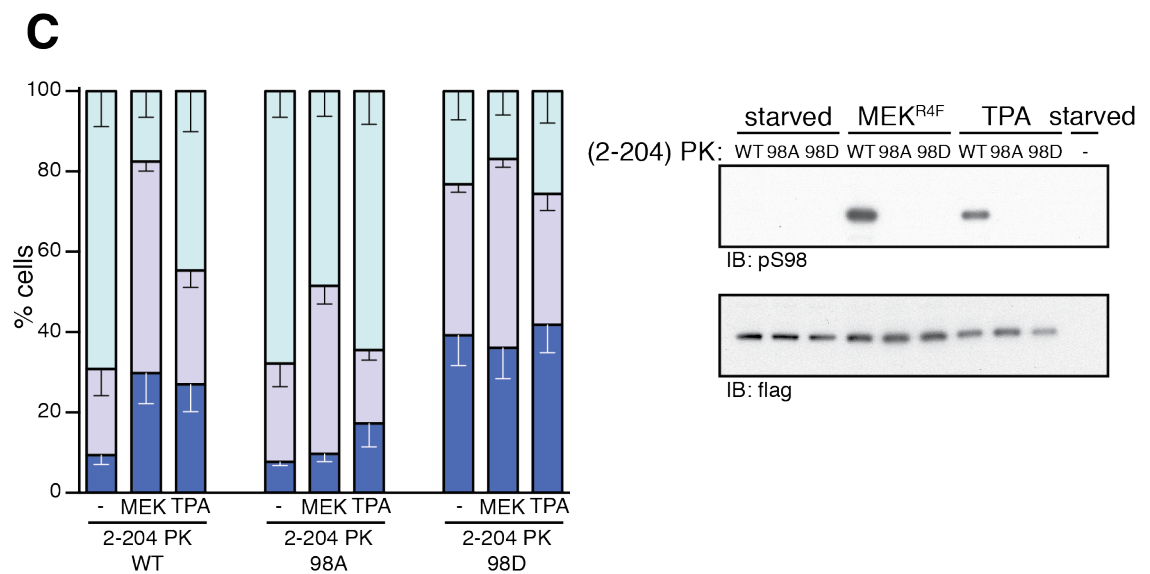
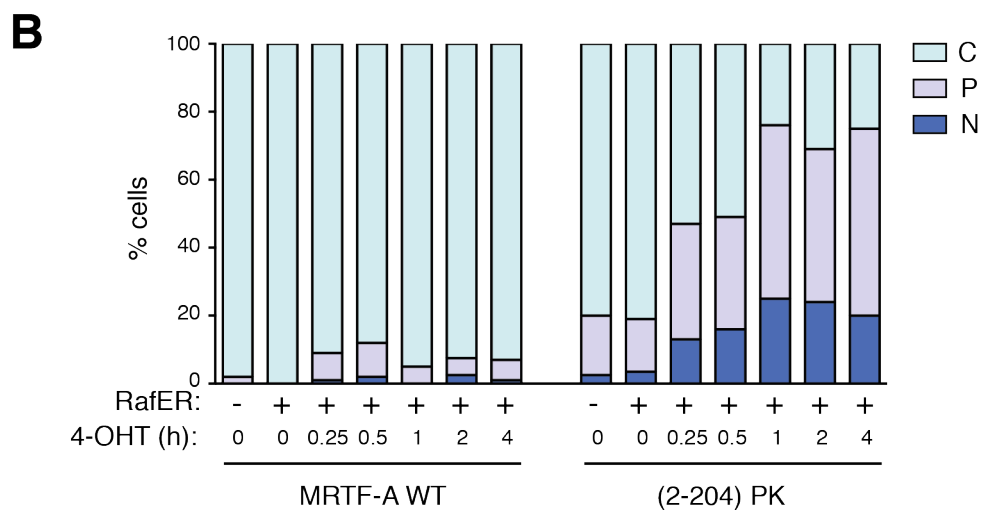
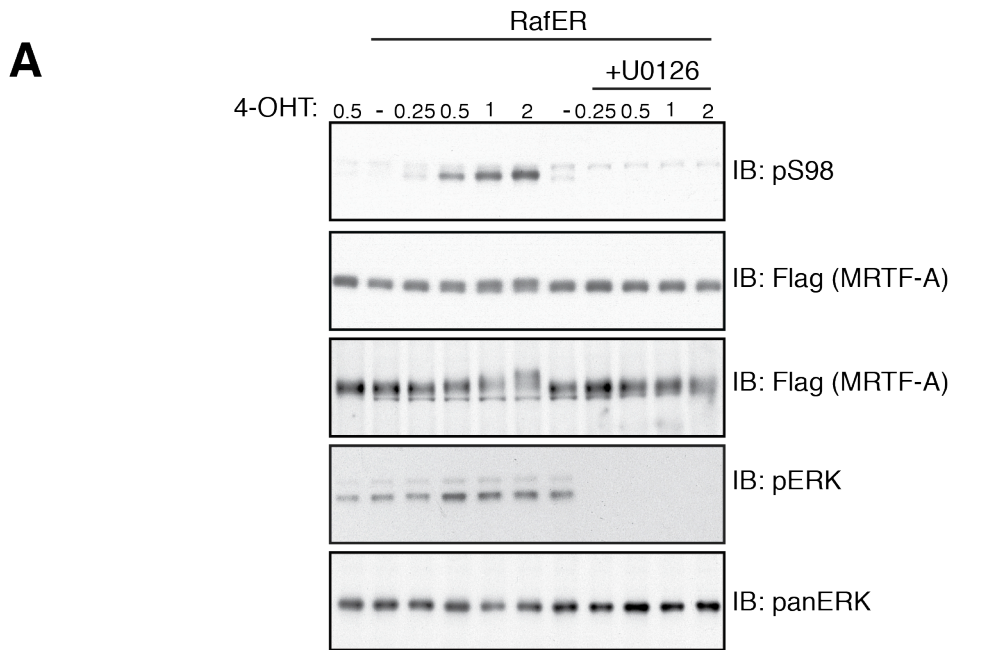


Figure 4.9 Activation of the MAPK pathway promotes S98 phosphorylation and nuclear accumulation

A. Cells transfected with RafER were starved overnight and treated with tamoxifen for indicated times in the presence or absence of 10 μ M U0126. Lysates were then resolved by SDS-PAGE and analysed by immunoblot using the indicated antibodies. **B.** Cells were co-transfected with RafER and MRTF-A or MRTF-A (2-204) PK fusion, starved overnight and treated with tamoxifen for the indicated times. Localisation was determined by immunofluorescence using an anti flag antibody. At least 100 cells were counted and localisation was scored as predominantly nuclear (navy blue), pancellular (lilac) or predominantly cytoplasmic (light blue). **C.** Left: Cells were co-transfected with MRTF-A (2-204) PK fusion and MEK^{R4F}, starved overnight and stimulated with 100ng/mL TPA as indicated. Localisation was determined by immunofluorescence using an anti flag antibody. At least 100 cells were counted and localisation was scored as predominantly nuclear (navy blue), pancellular (lilac) or predominantly cytoplasmic (light blue). Right: Cells were co-transfected with MRTF-A (2-204) PK and constitutively active MEK (MEK^{R4F}), starved overnight and stimulated with TPA where indicated. Lysates were resolved by SDS-PAGE and S98 phosphorylation was determined using the specific antibody. Error bars represent standard error of the mean (SEM) from at least two independent experiments.

4.6 Ser33 is basally phosphorylated

Although MEK^{R4F} and RafER transfections provided more specific MAPK pathway activation to investigate S98 phosphorylation, TPA treatment uncovered the potential for a further regulatory element within the N-terminal region. Because TPA could still affect MRTF-A (2-204) PK S98A localisation, S33 was investigated. Like S98, S33 is followed by a proline and is in close proximity to the ERK binding site, making it a candidate for the remaining regulation observed.

In order to confirm and characterise S33 phosphorylation, a peptide corresponding to residues 29-37, which contain S33, was synthesised in its phospho-S33 form and used in the immunisation of 3 rabbits (Figure 4.10A).

Serum from each rabbit was incubated with resin-immobilised non-phosphopeptide, thereby removing antibodies reactive against epitopes irrelevant to the phosphate moiety of the antigen. To test reactivity towards pS33, each depleted serum was tested in immunoblotting. All three depleted sera recognised MRTF-A S33A indicating incomplete depletion (Figure 4.10B). Their reactivity against MRTF-A was therefore tested in the presence of excess non-phosphorylated antigen, to block any remaining reactivity against non-phosphorylated S33. In the presence of excess non-phosphorylated antigen serum1, but not serum 2 or 3, recognised MRTF-A only when S33 was intact and presumably phosphorylated (Figure 4.11C).

To confirm the reactivity observed was indeed against phosphorylated S33, the sera were tested in the presence of the phosphorylated form of the antigen (Figure 4.11D). The phosphorylated antigen should sequester phospho-specific antibodies. In the case of Serum1 the pS33 peptide prevented any detection of immunoprecipitated MRTF-A, confirming that Serum1 was suitable for detection of pS33 on MRTF-A.

Serum1 could therefore be used, in the presence of excess non-phosphopeptide, to assess S33 phosphorylation. As shown in Figure 4.10A (top panel), S33 is phosphorylated in resting conditions and phosphorylation increases by approximately 3-fold after serum stimulation and 2-fold after TPA stimulation.

Because induction of pS33 appeared poor after stimulation I carried out a timecourse to investigate the phosphorylation kinetics of S33 after FCS stimulation. The data from the timecourse confirm that S33 phosphorylation does not dramatically change after stimulation, suggesting it may already be highly phosphorylated (Figure 4.11A). The FCS induced increase in pS33 was sensitive to ERK inhibition, but not dependent on the identified ERK binding motif (Figure 4.11 B,C).

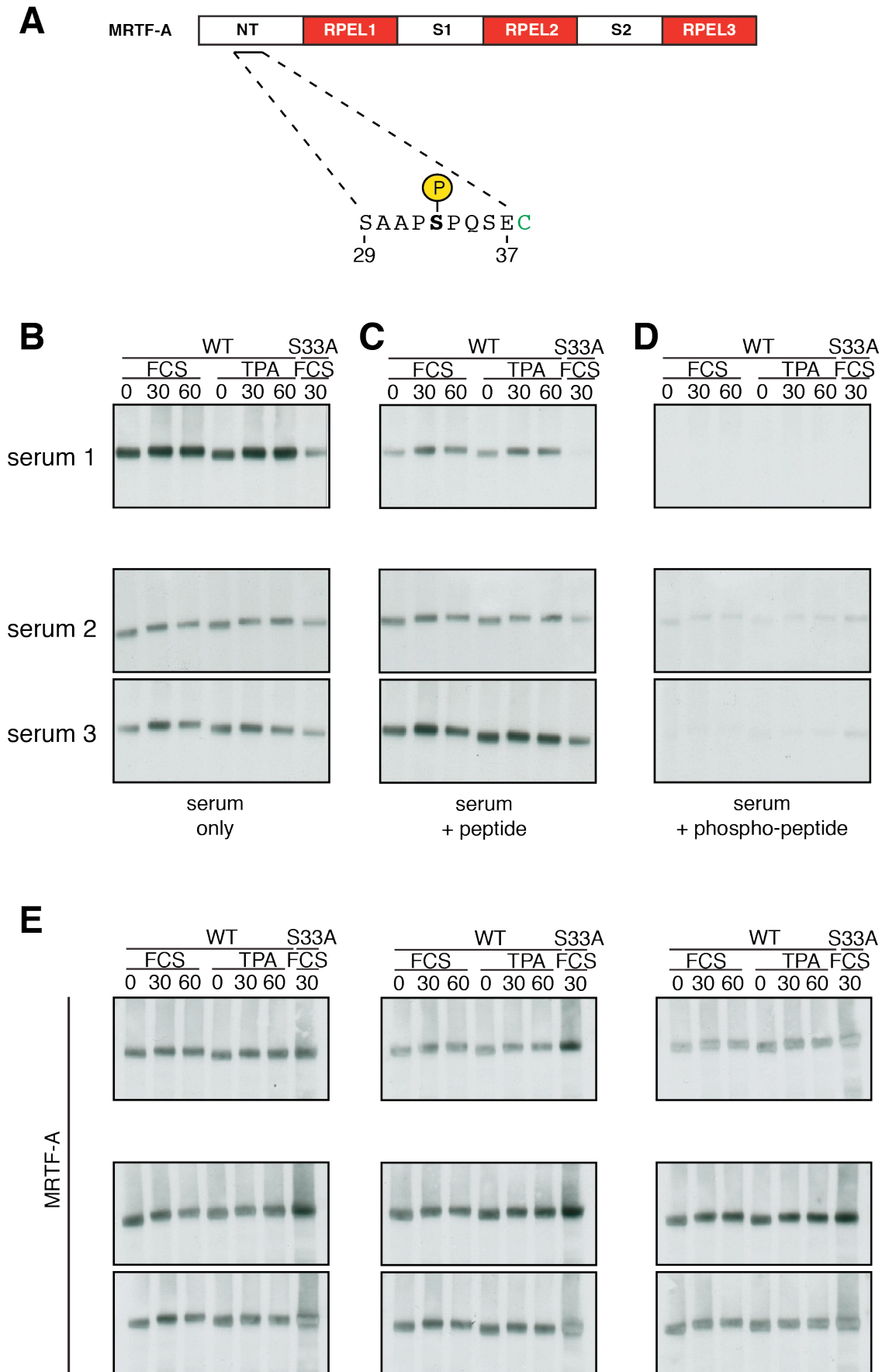


Figure 4.10 Generation of a pSer33 specific antibody

A. Schematic representation of the peptide sequence used for the generation of pS33 reactive serum. The C-terminal cysteine, shown in green, was used for crosslinking and immobilisation of the peptide. **B.** Cells were transfected with Flag-MRTF-A or the S33A derivative, starved and then stimulated with 15% FCS or 100ng/mL TPA for indicated times. Anti-Flag immunoprecipitates were resolved by SDS-PAGE. Sera from 3 immunised rabbits, were passed over resin with immobilised non-phospho peptide, in order to deplete the serum of antibodies which recognise the non-phosphorylated form of the peptide. The depleted sera were then tested for reactivity against the abovementioned samples. Each depleted serum was tested alone, or **C.** in the presence of non-phospho peptide or **D.** phospho-peptide, to assess specificity. **E.** Membranes were probed with an anti-MRTF-A antibody to assess loading.

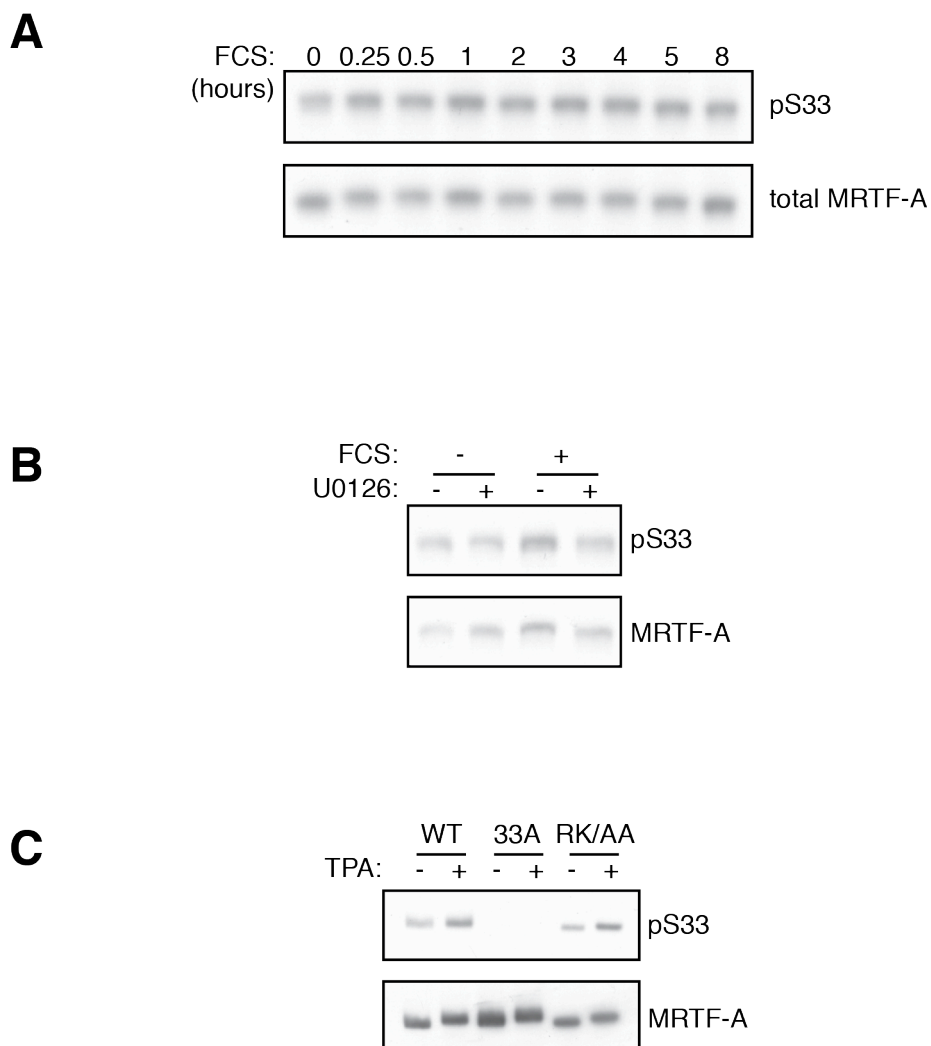


Figure 4.11 S33 phosphorylation

A. Cells transfected with MRTF-A were starved overnight and stimulated with 15% FCS for the indicated times. MRTF-A was immunoprecipitated using an anti-Flag antibody. pS33 and total MRTF-A were then detected by immunoblot analysis. **B.** Cells were treated as in (A) but also with U0126 where indicated. **C.** Cells were transfected with MRTF-A, the S33A derivative or the ERK binding motif mutant RK/AA. Cells were starved overnight and treated with 100ng/mL TPA for 30 minutes. Extracts were then resolved by SDS-PAGE and analysed by immunoblot analysis using specific antibodies.

4.7 S33 phosphorylation prevents nuclear accumulation

To determine how S33 phosphorylation affects shuttling of MRTF-A (2-204) PK, S33 and S98 were cotransfected with RafER. Alanine substitution of S33 led to an increase in nuclear localisation, which is further potentiated by ERK activity (Figure 4.12). In contrast the S33D derivative was more cytoplasmic in resting conditions and refractory to ERK induced nuclear accumulation. These results suggest that S33 phosphorylation prevents nuclear accumulation. In agreement with previous data S98D promotes nuclear accumulation. The S33A mutation appears to potentiate S98D and RafER induced nuclear accumulation, while S33D appears to make MRTF-A (2-204) PK refractory to nuclear accumulation, consistent with the observations that S33 is basally phosphorylated but can also be phosphorylated further. Together these data show a functionally antagonistic effect of pS33 against pS98 on MRTF-A(2-204) PK localisation. In addition these data support the previous observation that S33 is basally phosphorylated.

The observation that ERK mediated phosphorylation of MRTF-A promotes its cytoplasmic localisation is in accordance with the findings of Muehlich et al. In their view ERK mediated phosphorylation of residues S544, T545 and S549 is required for MRTF-A nuclear export by promoting association with actin (Muehlich et al., 2008). They showed that TPA treatment does not activate MRTF-A, but rather makes MRTF-A refractory to subsequent activation by FCS. In our lab, Rafal Pawlowski has shown using PKC and MEK1/2 inhibitors, that ERK activity was dispensable for the inhibitory effect of TPA, which is instead caused by nPKC mediated RhoA down-regulation (R. Pawlowski, unpublished data).

Since the observations with pS33 provide evidence for phosphorylation having a negative role on nuclear accumulation I sought to determine whether the reported phosphorylation sites co-operate with S33 to promote export. Muehlich et al. used human MALmet, which lacks the 92 N-terminal residues including the N-terminus and RPEL1, but state that similar behaviour was observed for full length MRTF-A. The reported residues were therefore substituted to alanines in the context of full length MRTF-A and a truncated version (Δ 92) that was generated to mimic their MALmet (Figure 4.13A).

In our system, using NIH-3T3 cells, alanine substitution of the reported residues did not cause constitutive nuclear accumulation in starved conditions; instead it looked almost identical to wild type MRTF-A (Figure 4.13B). The truncated version designed to mimic their construct, exhibited a baseline that was slightly increased in combination with the alanine mutations. Finally, in an attempt to replicate their findings, the experiment was carried out in HeLa cells but similar results with 3T3 cells were obtained (Figure 4.13C).

Taken together, the data show that S33 is basally phosphorylated and promotes cytoplasmic localisation of MRTF-A, presumably by promoting export. The idea that phosphorylation promotes export has also been reported by others, however I cannot replicate their findings and S33 phosphorylation cannot explain the effects reported. Since MRTF-A shuttling is regulated at the level of export, in the next chapter I address how S98 and S33 impinge on MRTF-A export.

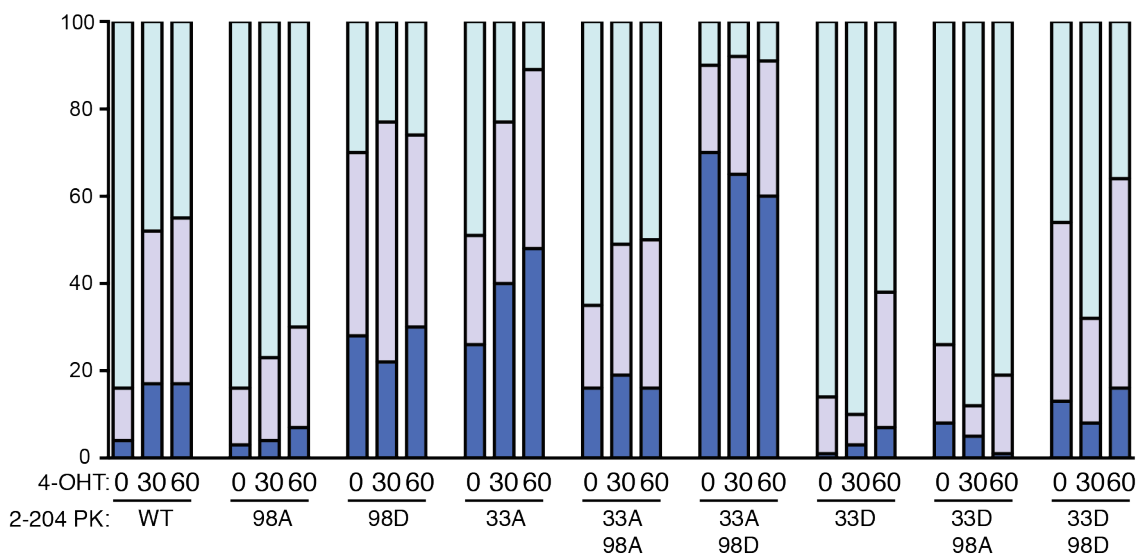
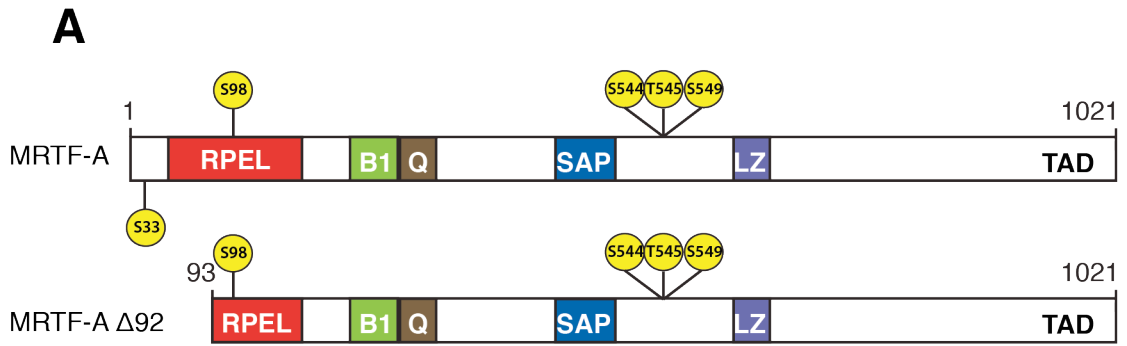
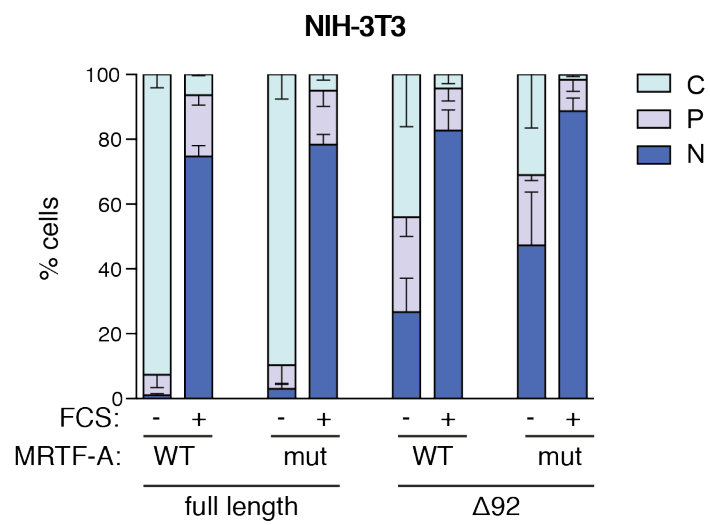


Figure 4.12 MAPK activation leads to MRTF-A nuclear accumulation through S98 phosphorylation

Cells were co-transfected with RafER and the indicated MRTF-A (2-204) PK fusion derivatives. After overnight starvation cells were treated with tamoxifen for 30 or 60 min. MRTF-A (2-204) PK localisation was determined by immunofluorescence using an anti-Flag antibody. At least 100 cells were counted and localisation was scored as predominantly nuclear (navy blue), pancellular (lilac) or predominantly cytoplasmic (light blue).



B



C

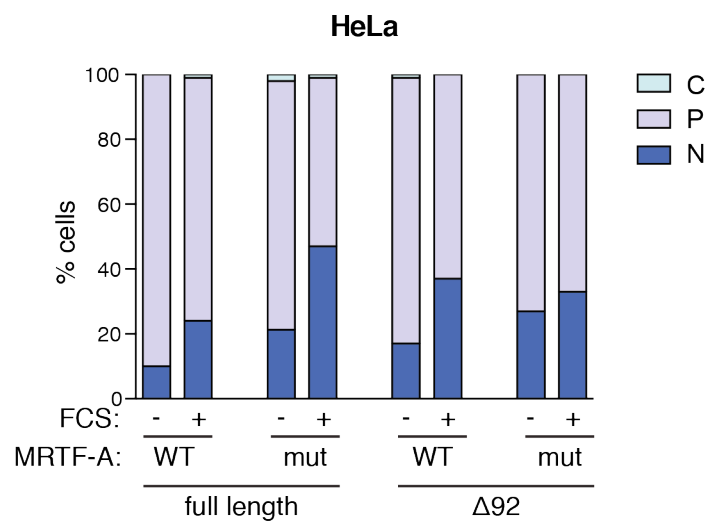


Figure 4.13 Alanine substitution of STS544/545/549 does not block export

A. Schematic of MRTF-A showing derivatives used in this experiment. **B.** 3T3 cells were transfected with wild type MRTF (WT) or STS544/545/549AAA (mut) in the context of full length or N-terminally truncated MRTF-A. Cells were then starved overnight and stimulated with 15% FCS for 30 minutes. Localisation was determined by immunofluorescence using an anti-Flag antibody. At least 100 cells were counted and localisation was scored as predominantly nuclear (navy blue), pancellular (lilac) or predominantly cytoplasmic (light blue). Error bars represent standard error of the mean (SEM) from at least two independent experiments. **C.** Same as in (B) but using HeLa cells.

Chapter 5. Identification of a Crm1 NES in the N-terminus of MRTF-A

5.1 Aims

MRTF-A nuclear localisation is regulated primarily at the level of export. Decreases in cellular G-actin concentrations result in reduced actin-MRTF-A interaction leading to its nuclear accumulation. In the fibroblast model import of MRTF-A appears to be constant, as it is not affected by growth factors, although it is inhibited in very high G-actin concentrations. MRTF-A export is mediated by Crm1 and is dependent on actin binding. Therefore depletion of the actin pool results in decreased export rates (Vartiainen et al., 2007). In this chapter I identify a Crm1 dependent export signal within the MRTF-A N-terminus, and investigate how S33 and S98 may be involved in its regulation.

5.2 Multiple export signals in MRTF-A

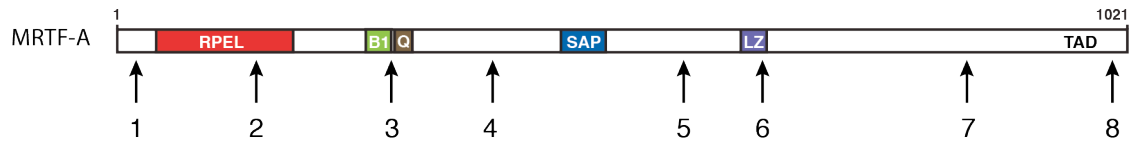
I first analysed the MRTF-A primary sequence using the prediction software NetNES (<http://www.cbs.dtu.dk/services/NetNES/>) (la Cour et al., 2004). This algorithm takes into account previously identified export signals and their similarity to the sequence in question, integrating the apparent high specificity of the hidden Markov model (HMM) and the apparent sensitivity of the Neural network (NN) to detect potential NES elements. The output returned after submission of a sequence shows both scores individually and generates a combined score (which is a function of the two) which ranges from 0 – 2.1. A default threshold of 0.5 is set. Sequences that score below the 0.5 threshold, have a greater than 0.1 false discovery rate.

Within the MRTF-A sequence eight regions are given a score by NN, HMM or both. The regions identified are shown in Figure 5.1. Two of these regions, putative NES 3 and 6, receive a score above the threshold. NES2 was the only NES detected within the RPEL domain and also received the lowest score. It is still possible that some true NESs receive a low score. Muehlich et al have confirmed NES 3 but not NES 6 as a functional NES in MRTF-A (Muehlich et al., 2008). In addition, Hayashi et al. have also identified NES3 (Hayashi and Morita, 2013), as well as a region overlapping with RPEL1 and the ERK binding motif shown in chapter 4.

Previous experiments in the lab showed that gross deletions encompassing single or pairs of these NESs did not completely block MRTF-A export. This suggested that multiple NES contribute to MRTF-A export, but the mechanism was not analysed in detail (R. Pawlowski, unpublished data).

The N-terminal region of MRTF-A has been shown to be sufficient to confer MRTF-A-like shuttling when fused to the normally cytoplasmic protein pyruvate kinase (Guettler et al., 2008). In addition R. Pawlowski has shown that the N-terminal region (residues 2-261) is also able to interact with Crm1 *in-vitro*. Therefore the RPEL domain, and the 66 aminoacids that precede it must contain both an import signal, which is known (Pawlowski et al., 2010), and at least one export signal.

In the following sections I will address (i) whether Crm1 mediated export is a property of the RPEL domain and (ii) where the Crm1 binding sequences are.



putative NES	Sequence	peak NES score (arbitrary)
1	37-EAVANE LQ E L SL-48	< 0.5
2	142-AE P S LQ AK Q L K L-153	< 0.5
3	355-L Q Q Q L F L Q L Q I-366	> 0.5
4	445-MK V A E L K Q E L K L-456	< 0.5
5	573-EM V T S P L T Q L T L-584	< 0.5
6	638-K Q Q L VE L L R L Q L-649	> 0.5
7	835-S Q H M DD L F D I L I-846	< 0.5
8	1004-S M D F LD G H D L Q L-1015	< 0.5

NES consensus: $\Phi^1-(x)_{2-3}-\Phi^2-(x)_{2-3}-\Phi^3-x-\Phi^4$
 $\Phi = L, I, V, F, M$
 x is preferentially charged, polar or small

Figure 5.1 MRTF-A possesses multiple putative classical export sequences

Schematic representation of MRTF-A. Arrows point at the locations that resemble the classical nuclear export signal consensus. Regions detected by NetNES prediction software, are aligned below. Coloured in red are the key residues that conform to the classical NES consensus shown at the bottom.

5.3 The MRTF-A and Phactr1 RPEL domains are not interchangeable

Phactr1, like MRTF-A, possesses an RPEL domain and accumulates in the nucleus upon serum stimulation (Wiezlak et al., 2012). The MRTF-A and Phactr1 RPEL domains both contain an embedded NLS and three highly homologous RPEL motifs, separated by spacer sequences (Figure 5.2). It is not known if Phactr1 continuously shuttles through the nucleus, however, a Phactr1 mutant containing an RPEL domain that cannot bind actin is constitutively nuclear. However Phactr1 is not dependent on Crm1 for export, suggesting that although both proteins rely on actin binding through similar RPEL domains for their localisation they rely on different export machinery.

While the Phactr1 RPEL domain can form a trivalent complex by binding one actin on each RPEL motif, the MRTF-A RPEL domain can form a pentavalent complex by also binding actins via its slightly longer spacers. Despite this difference, the actins bound by the RPEL motifs in each RPEL/actin complex share near identical relative orientation and proximity to each other (Mouilleron et al., 2011; 2012). The different dependence of Phactr1 and MRTF-A on Crm1 allowed investigation into the relationship between Crm1 and the RPEL domain.

When the MRTF-A RPEL domain was transferred to Phactr1, the resulting chimera Phactr1_(MRTF-R) (Figure 5.3A, top), accumulated in the nucleus after FCS stimulation, but LMB treatment had no effect (Figure 5.3B). LMB sensitivity was not transferred along with the RPEL domain, suggesting that it is context specific. Phactr1_(MRTF-R) exhibited increased nuclear localisation in starved conditions compared to wild type Phactr1. This may reflect the introduction of the strong MRTF-A NLS in place of the weaker Phactr1 NLS. Although the two NLS were not directly compared, the B2 NLS embedded in the Phactr1 RPEL domain plays a secondary role relative to the Phactr1 B1 NLS (Wiezlak et al., 2012). Therefore upon transplanting the MRTF-A RPEL the weaker Phactr1 B2 NLS is replaced by the stronger NLS of MRTF-A (Pawłowski et al., 2010; Wiezlak et al., 2012).

Conversely, when the Phactr1 RPEL domain was transferred to MRTF-A, the resultant chimera, MRTF_(Phactr-R), was completely cytoplasmic in starved, FCS stimulated and LMB treated conditions (Figure 5.3B). It is possible that concomitant

replacement of the strong MRTF-A NLS for the weak Phactr1 NLS results in very inefficient import and so upon FCS treatment or LMB mediated inactivation of Crm1, the MRTF_(Phactr-R) chimera is very inefficient in nuclear import.

Taken together, the data show that MRTF-A and Phactr1 RPEL domains are not functionally interchangeable, and that Crm1 dependence for export is not a property of the MRTF-A RPEL domain itself. However, through actin binding, the RPEL domain can affect the function of other elements that define subcellular localisation and the mechanism appears to be context specific. MRTF-A regulation is at the level of Crm1 mediated export. In Phactr1_(MRTF-R), it could be regulation of non-Crm1 dependent export, or cytoplasmic anchoring.

To gain further insight into the chimeras' mechanism of shuttling I studied their dependence on actin and previously mapped NLS elements. As shown in Figure 5.4 A, multiple elements contribute to this chimera's nuclear import. Serum regulation of Phactr1 is abolished by mutation of its B1 element (Wiezlak et al., 2012). The RPEL motif adjacent to the B1 region was shown to have a minor contribution in maintaining cytoplasmic localisation of Phactr1. Cytoplasmic localisation of Phactr1 is in fact dependent on its RPEL domain (Wiezlak et al., 2012). MRTF-A regulation is heavily dependent on the B2B3 elements embedded within the RPEL domain (Pawłowski et al., 2010), however MRTF-A shuttling is regulated at the level of export in fibroblasts (Vartiainen et al., 2007).

Phactr1_(MRTF-R) xxx, which cannot bind actin, is constitutively nuclear indicating that actin binding is required for cytoplasmic localisation, either by promoting export or inhibiting import (Figure 5.4B-2). Inactivation of the MRTF B2 NLS element within the RPEL domain, led to cytoplasmic localisation, indicating that the B2 element contributes to import in starved conditions leading to the high levels of nuclear localisation observed (Figure 5.4B-3). Serum regulation is retained, indicating that regulation of Phactr1_(MRTF-R) is not solely determined on the B2 NLS. Moreover, the observation that the derivative lacking B2, which cannot bind actin, is constitutively nuclear indicates that cytoplasmic localisation is not solely the result of actin inhibition of the B2 element (Figure 5.4B-4).

Because of the possibility of an NES overlapping the B2 region (NES2 in Figure 3.1) B3 was mutated instead, which would diminish import activity contributed by the RPEL domain without compromising the putative NES. Mutation

of the B3 element also decreased import but again regulation was maintained (Figure 5.4B-5).

Mutation of the B1 NLS did not abolish serum regulation (Figure 5.4C-1). Regulation in the absence of B1 is still actin dependent, since additional mutation of the RPEL domain led to constitutive nuclear accumulation (Figure 5.4C-2). Inactivation of B1 in combination with either B2 or B3 NLSs did not abolish regulation, confirming that serum induced nuclear accumulation of Phactr1_(MRTF-R) is not achieved by changes in import (Figure 5.4C-3 & 5).

Regulation of the Phactr1_(MRTF-R) chimera is therefore dependent on actin binding to the RPEL domain, however the mechanism is not as simple as competition between importin and actin binding to the MRTF-A RPEL domain. Although the RPEL embedded NLSs do contribute to nuclear import of Phactr1_(MRTF-R) they are not required for actin regulation. Actin binding is therefore not only masking the NLSs but also impinges on the function of elements outside the RPEL domain, to regulate subcellular localisation.

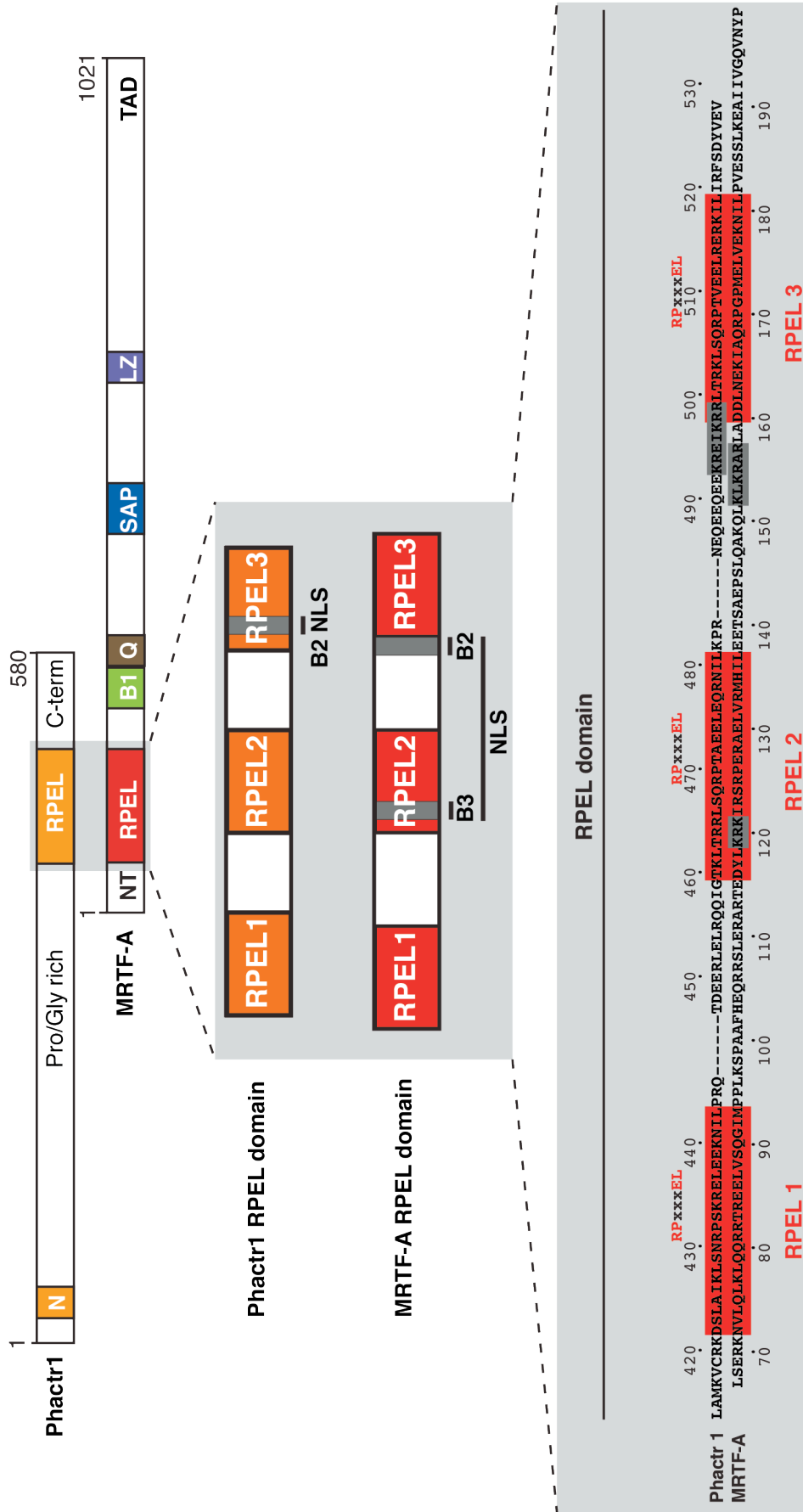
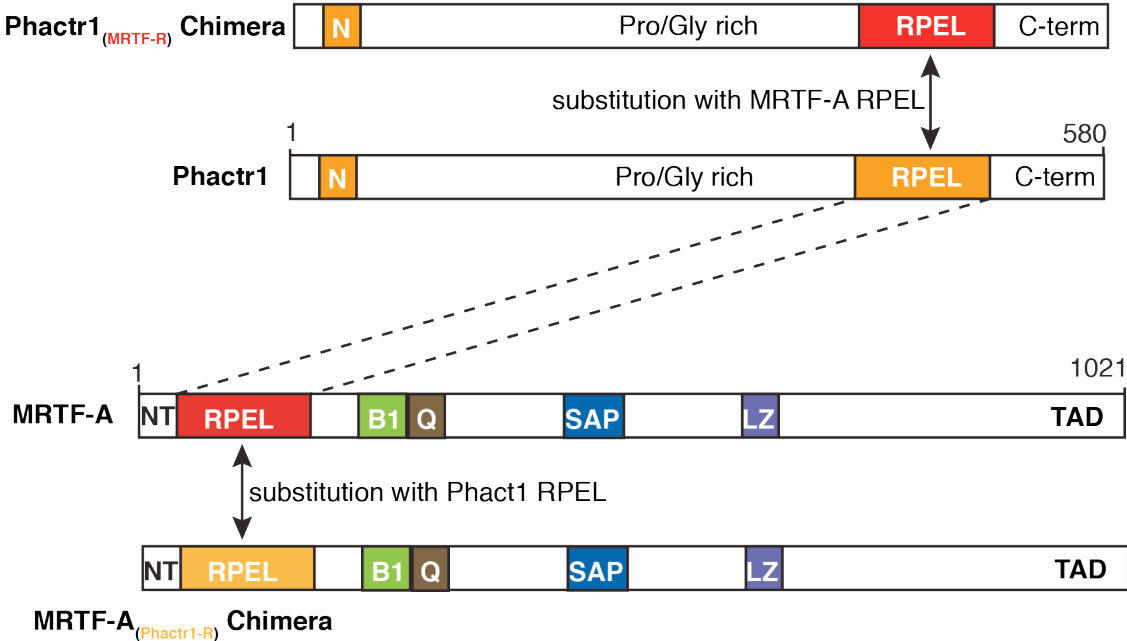


Figure 5.2 Alignment of MRTF-A and Phactr1 RPEL domains

Top: Schematic representation and domain structure of MRTF-A and Phactr1 proteins. Middle: schematic showing the main elements of the MRTF-A and Phactr1 RPEL domains. Bottom: Alignment of the MRTF-A and Phactr1 RPEL domain primary sequences. RPEL motifs are enclosed in red boxes and the basic elements comprising the NLS of each protein are in grey. Note the shorter spacer elements of Phactr1 compared to MRTF-A.

A



B

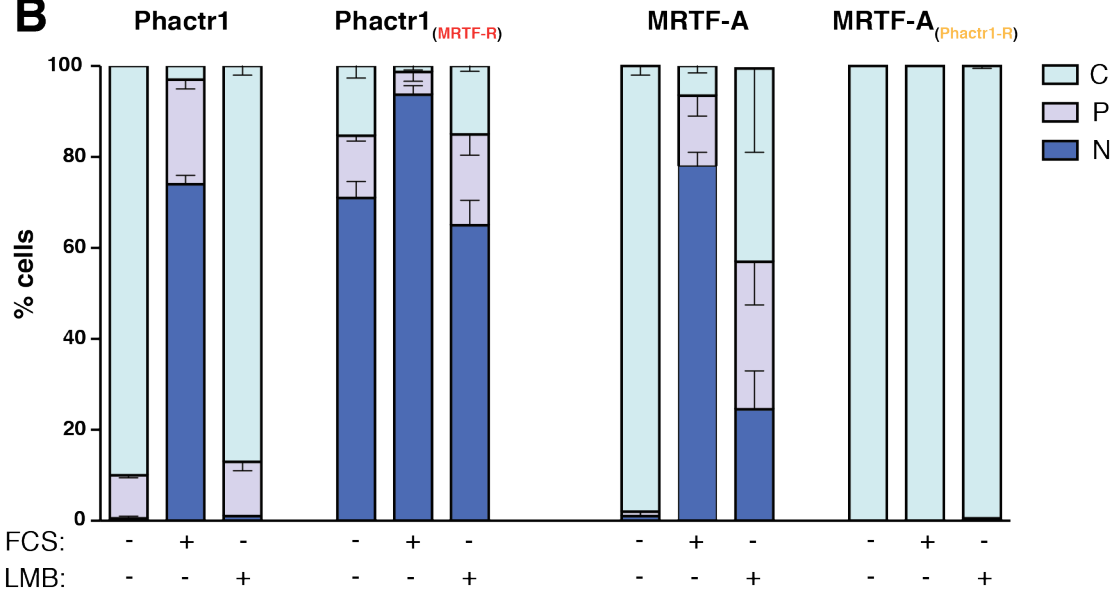


Figure 5.3 The RPEL domains of MRTF-A and Phactr1 are not functionally interchangeable

A. Top: Schematic depicting the replacement of the Phactr1 RPEL domain with that of MRTF-A to generate the Phactr1_(MRTF-R) chimera; junctions are: N-terminal (Phactr1) ...ASLYTSS//LSERKNV...(MRTF-A), C-terminal: (MRTF-A)...VGQVNYP//ADAQDYD...(Phactr1) . Bottom: replacement of the MRTF-A RPEL domain with that of Phactr1 to generate the MRTF-A_(Phactr-R) chimera; junctions are: N-terminal (MRTF-A) ...RNPNLPP//LAMKVCR... (Phactr1), C-terminal (Phactr1) ...FSDYVEV//IIVGQVN... (MRTF-A). **B.** Cells were transfected with MRTF-A, Phactr1 and the chimeras, starved overnight and treated with 15% FCS or 50nM LMB for 30 min. Localisation of each protein was determined by immunofluorescence using an anti-Flag antibody. At least 100 cells were counted and localisation was scored as predominantly nuclear (navy blue), pancellular (lilac) or predominantly cytoplasmic (light blue). Error bars represent standard error of the mean (SEM) from at least two independent experiments.

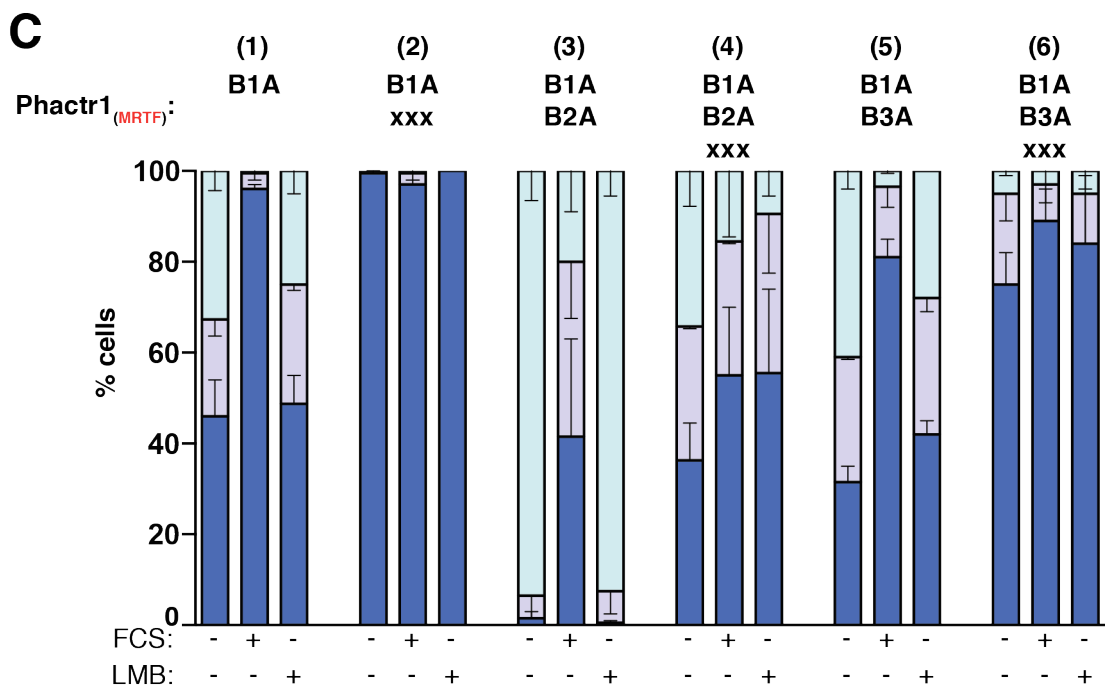
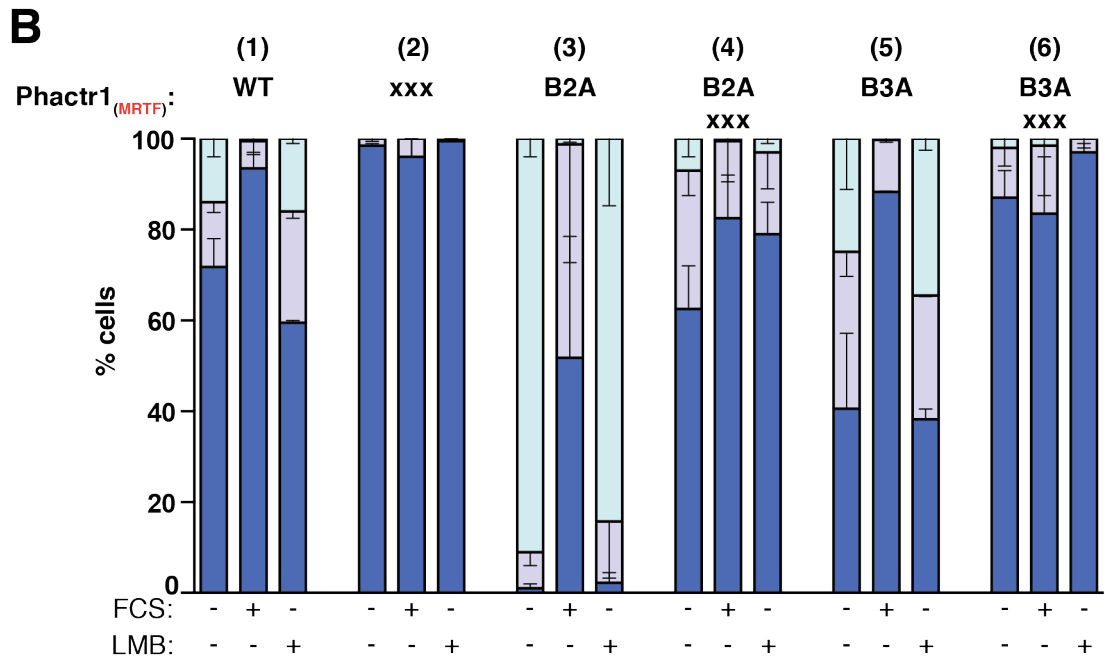
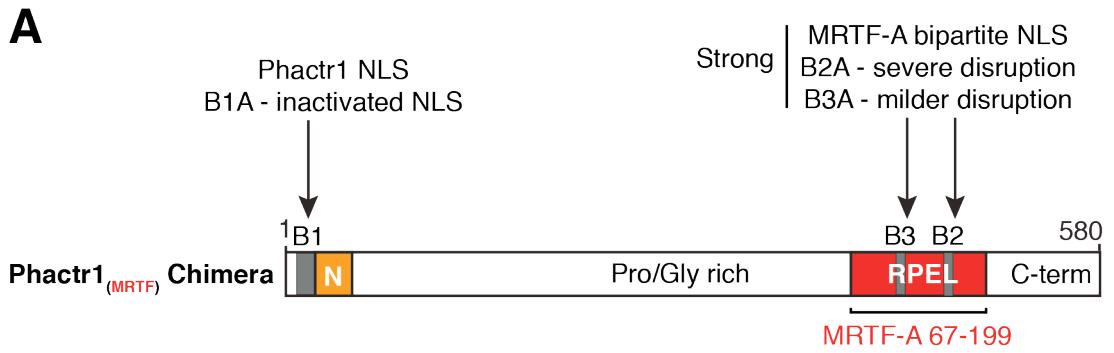


Figure 5.4 Cellular localisation of the chimera is determined by actin dependent export

A. Schematic representation of the Phactr1_(MRTF-R) chimera with arrows indicating the basic elements present, which contribute to nuclear import of the chimera. **B and C.** Cells were transfected with the indicated chimera derivatives, starved overnight and stimulated with 15% FCS for 30 min or 50nM LMB for 2 hours. Localisation of each protein was determined by immunofluorescence using an anti-Flag antibody. B1A: inactivation of the Phactr1 N-terminal NLS by alanine substitution of R108, R109 and R110. B2A and B3A: inactivation of the basic elements that constitute the bipartite MRTF-A NLS. At least 100 cells were counted and localisation was scored as predominantly nuclear (navy blue), pancellular (lilac) or predominantly cytoplasmic (light blue). Error bars represent standard error of the mean (SEM) from at least two independent experiments.

5.4 The MRTF-A N-terminus contains a Crm1 dependent export signal

Previous work showed that residues 2-204 contain an LMB sensitive export signal (Guettler et al., 2008). I therefore tested whether the N-terminus (2-67) would confer LMB sensitivity to Phactr1_(MRTF-R) (Figure 5.5A).

Phactr1_(MRTF-NR) was more cytoplasmic than Phactr1_(MRTF) in starved conditions and accumulated in the nucleus after serum stimulation. It also accumulated in the nucleus after LMB treatment, indicating that it contains a Crm1 NES (Figure 5.5B-1, compare with Figure 5.4B-1). In addition, its nuclear accumulation was actin dependent as the actin binding deficient mutant Phactr1_(MRTF-NR) xxx was completely nuclear in unstimulated cells (Figure 5.5B-2).

As with Phactr1_(MRTF-R), nuclear accumulation of Phactr1_(MRTF-NR) was strongly dependent on the MRTF NLS elements B2 and B3 (Figure 5.5B-3 & 5). However its cytoplasmic localisation was actin dependent (Figure 5.5B-2). Mutants incompetent to bind actin were still sensitive to LMB, indicating that in this context actin binding is not required for Crm1 function (Figure 5.5B-4).

Interestingly, although the RPEL domain cannot bind actin in this derivative, serum regulation was retained, suggesting the Phactr1 N-terminal RPEL motif might be regulating B1. Consistent with this idea, additional inactivation of B1, to generate Phactr1_(MRTF-NR) B1A B2A xxx abolished serum regulation but retained LMB sensitivity (Figure 5.5C-4).

Alternatively, the apparent loss of serum regulation could be due to insufficient NLS activity to counter the actin independent Crm1 mediated export activity. Phactr1_(MRTF-NR) B1A B3A xxx, which is less impaired in import activity is also not serum regulated (Figure 5.5C-6), further supporting that actin regulates import, at least in part through the B1 element. However, Phactr1_(MRTF-NR) B1A is regulated in response to serum stimulation, indicating that the B1 element is not required for serum regulation (Figure 5.5C-1).

Taken together these data suggest that the N-terminus of MRTF-A contains a Crm1 dependent export signal, however, in the context of the Phactr1_(MRTF-NR) chimera residues 2-204 do not exhibit actin dependent Crm1 mediated export.

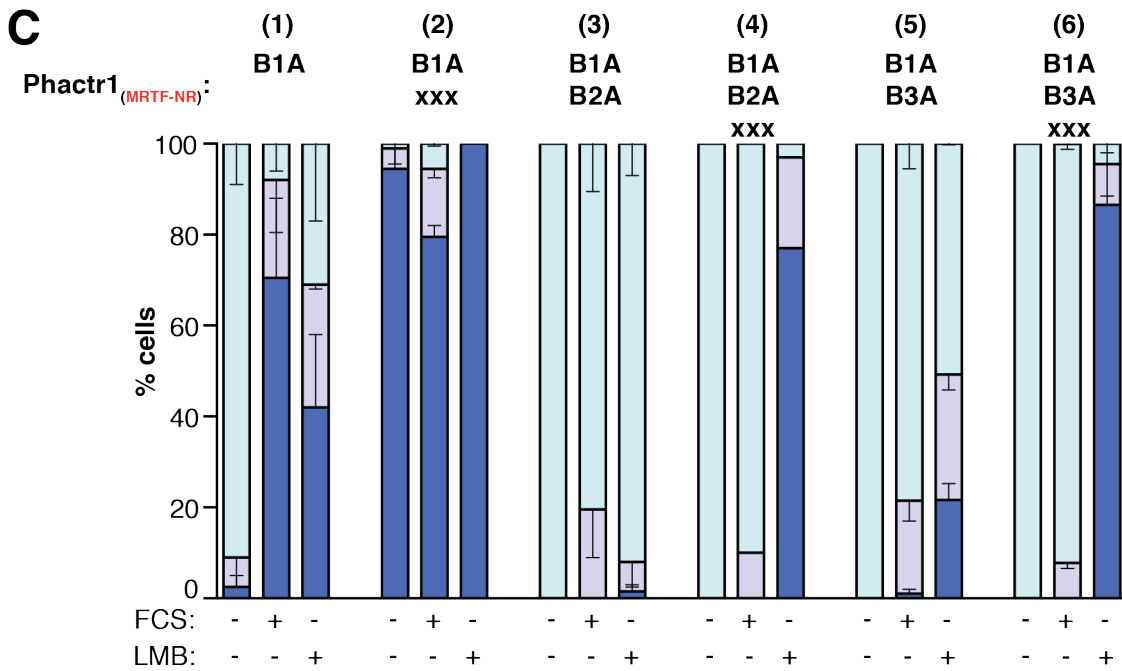
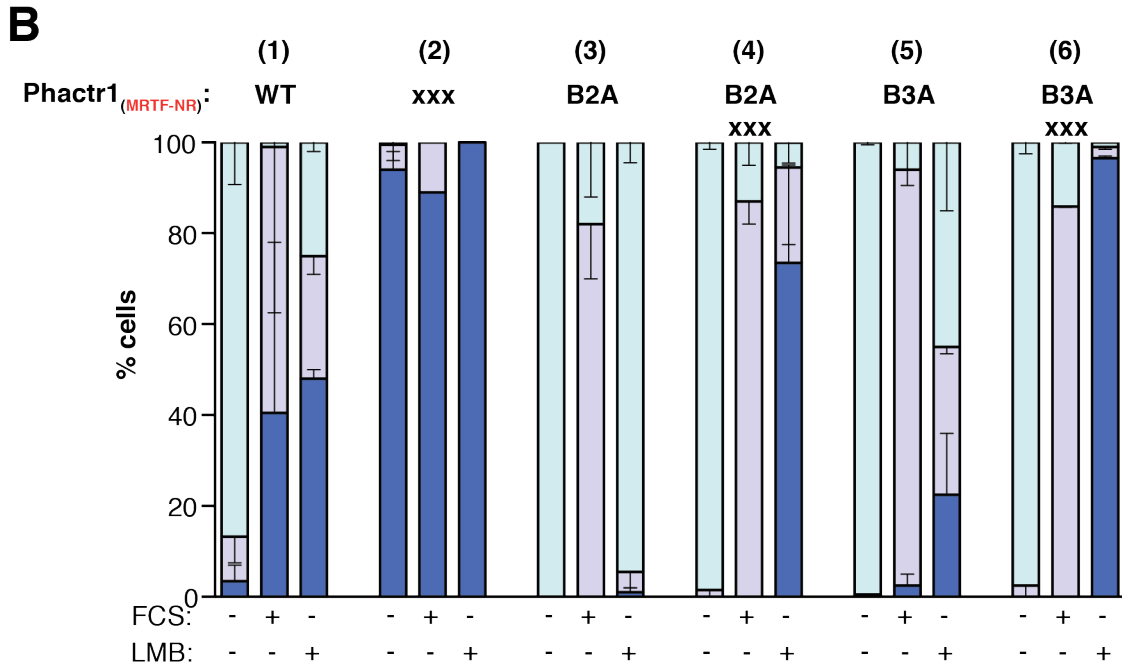
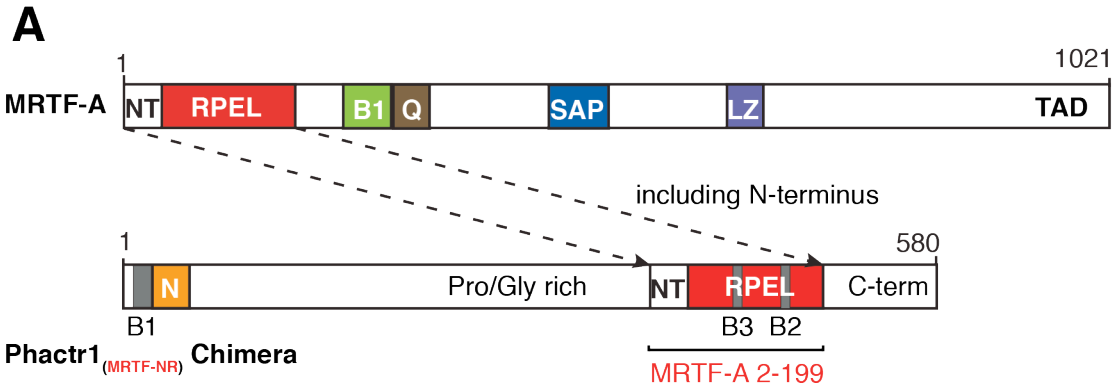


Figure 5.5 The MRTF-A N-terminus confers Crm1 mediated export

A. Schematic representation of the Phactr1_(MRTF-NR) chimera showing the replacement of the Phactr1 RPEL domain with the N-terminus and RPEL domain of MRTF-A. **B and C.** Cells were transfected with Phactr1_(MRTF-NR) chimera and the indicated derivatives. After overnight starvation the cells were treated with 15% FCS for 30 min or 50nM LMB for 2 hours. Localisation of each protein was determined by immunofluorescence using an anti-Flag antibody. At least 100 cells were counted and localisation was scored as predominantly nuclear (navy blue), pancellular (lilac) or predominantly cytoplasmic (light blue). Error bars represent standard error of the mean (SEM) from at least two independent experiments.

5.5 RPEL domain sequences cooperate with the N-terminus for export activity

To investigate the N-terminal export signal in more detail, a NES detection assay was used (B. R. Henderson and Eleftheriou, 2000). The assay is based on the HIV protein Rev, which shuttles between the cytoplasmic and nucleus, where it accumulates in nucleoli. Rev is imported via importin-beta interaction with its arginine rich NLS (B. R. Henderson and Percipalle, 1997) and exported via a Crm1 dependent NES (Fornerod et al., 1997). Rev shuttling ceases upon inactivation of its NES resulting in nuclear accumulation. Henderson et al. exploited this observation to map NES elements, by insertion of sequences into a NES-inactivated Rev-GFP derivative (hereafter Rev Δ) (Figure 5.6A,B). I used this approach to determine the exact location of the N-terminal NES and investigate the mechanism that underlies its dependency on actin for Crm1 mediated export.

Insertion of the MRTF-A RPEL domain alone did not relocalise Rev Δ (figure 5.6D). This domain also contains additional NLS elements, B2 and B3, one of which overlaps with a putative NES (NES2, see Figure 5.1). The combined import conferred by the Rev Δ NLS and B2B3 NLS could mask potential export activity. Mutation of either the B2 or B3 NLS element did not result in detectable export activity (Figure 5.6D). This result supports the notion that there is no effective NES within the RPEL domain.

In contrast, inclusion of the MRTF N-terminus, resulted in significant relocalisation suggesting that it contains an NES (Figure 5.6E). In addition export activity was reduced upon FCS and LMB treatment, consistent with regulated Crm1 dependent export. To test whether nuclear accumulation is regulated at the level of export and not import, the B2 and B3 NLS elements embedded in the RPEL domain were inactivated, yielding derivatives where import was driven only by the Rev Δ NLS. Inactivation of the B2 NLS element resulted in almost entirely cytoplasmic localisation in starved conditions, but allowed accumulation in the nucleus after FCS stimulation, showing that depletion of G-actin levels reduced its export activity. Therefore export is promoted by G-actin. Sensitivity of Rev (NT+RPEL) B2A to LMB treatment indicated Crm1 mediated export.

The partial regulation observed, evident by the weak nuclear accumulation after FCS, suggests that export is not entirely blocked by actin depletion. Evidence for actin independent mediated export of MRTF-A has been reported previously (Guettler et al., 2008). FLIP analysis showed that although MRTF-A (2-204) xxx-2GFP was nuclear, it was still exported.

Rev (NT+RPEL) xxx, that cannot bind actin, is entirely nuclear in resting conditions (Figure 5.6F). Upon mutation of the B2 element export activity was detected indicating that actin independent export was indeed occurring. LMB treatment confirmed that Crm1 mediated export could occur in the absence of actin. Regulation in response to FCS stimulation was lost however, in agreement with the previous observation that actin promotes export (Figure 5.6E).

Rev (NT+RPEL) B2A xxx nuclear accumulation is more efficient than that of its actin binding equivalent, Rev (NT+RPEL) B2A, suggesting that actin binding is regulating import in this context.

Taken together, the data suggest that the N-terminus contains an NES. Export activity exhibited by residues 2-204 of MRTF-A (N-terminus+RPEL) is actin independent, and can be potentiated by actin binding to the RPEL domain.

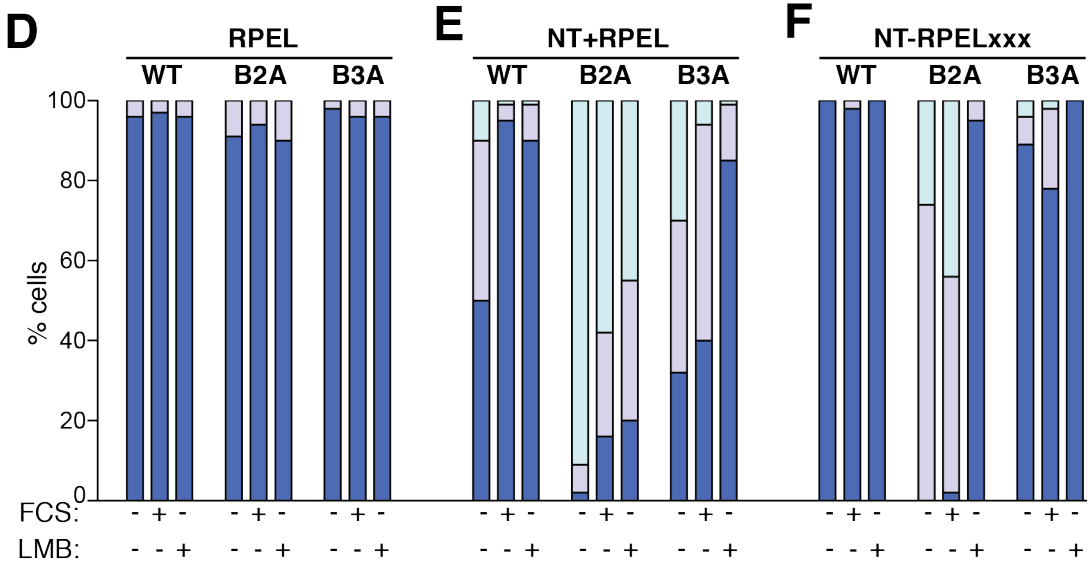
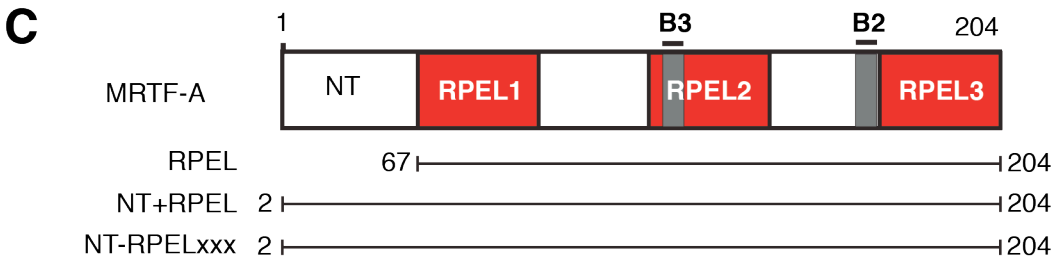
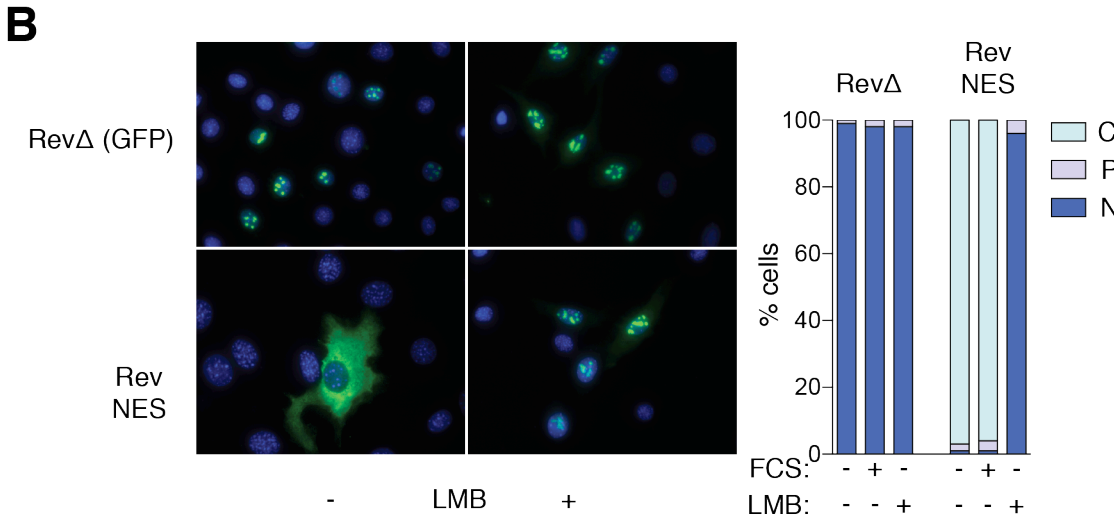


Figure 5.6 The N-terminus and RPEL domain together provide Crm1 dependent and actin regulated export

A. Rev export assay: The schematic shows the Rev-GFP (Rev Δ) construct used as an export signal reporter. The Rev NLS is shown in a dark grey box and the location of the inactivated Rev NES is shown in a yellow box crossed out. The site of insertion of a putative NES to be tested is shown by dotted lines. **B.** Left: immunofluorescence images of cells transfected with Rev Δ or the positive control where the intact NES of Rev is inserted to provide Crm1 mediated export. Right: quantification of the localisation of the negative and positive controls. At least 100 cells were counted and localisation was scored as predominantly nuclear (navy blue), pancellular (lilac) or predominantly cytoplasmic (light blue). **C-F.** Cells were transfected with Rev constructs in which either the MRTF-A RPEL domain was inserted, or the RPEL domain including the N-terminus (NT+RPEL), or NT-RPEL xxx, which doesn't bind actin. Following serum starvation cells were stimulated with 15% FCS for 30 min or 50nM LMB for 2 hours.

5.6 Mapping the N-terminal NES

The previous data suggest Crm1 mediated export is independent of actin in MRTF-A N-terminal sequences. To test this directly, residues 2-67 were inserted into Rev Δ . Rev (2-67) exhibited Crm1 dependent export (Figure 5.7B, construct B), confirming the N-terminus contains an autonomous NES. However, export activity exhibited by Rev (2-67) was markedly lower than Rev (2-204) B2A, suggesting that the RPEL domain enhances export activity. Although residues 67-115 did not confer export, they enhanced export activity of the N-terminal residues 2-67 (Figure 5.7B, construct C and D respectively).

In the Rev assay, weak NESs can restore shuttling but not cause relocalisation, as this requires the NES activity to be sufficient to overcome the rate of import. Actinomycin D (ActD), prevents nucleolar accumulation of Rev by an unclear mechanism that involves nucleolar dissociation (B. R. Henderson and Eleftheriou, 2000). ActD therefore lowers the threshold for NES detection. Nevertheless, after ActD treatment, residues 67-115 did not exhibit export activity,

suggesting that they do not contain an additional autonomous NES (Figure 5.7C construct C). In contrast, residues 67-204, corresponding to the RPEL domain, relocalised Rev to the cytoplasm in the presence of ActD (Figure 5.7C, construct A). Export activity however, was not LMB sensitive. Together, the results suggest that a non-Crm1 dependent NES is present between residues 115-204 of the RPEL domain.

The capacity of the above RPEL domain fragments to bind actin complicates interpretation of the results. I attempted to map minimal sequences within the N-terminal region. Surprisingly, while residues 2-67 confer export activity, 40-70 and 30-60 showed no activity, but 35-52 were active (Figure 5.8 construct A,B,C). Again, these results were more pronounced in the presence of ActD. Together these results suggest that there is a Crm1-dependent export signal within 2-67 and the minimal core for this is 35-52.

Because previous data from a peptide array implicated Spacer1 sequences in Crm1 binding, residues 85-110 and 89-104 were also tested for export activity. No export activity was detected with or without ActD (Figure 5.8B construct D and E), in agreement with the data presented in figure 5.7C.

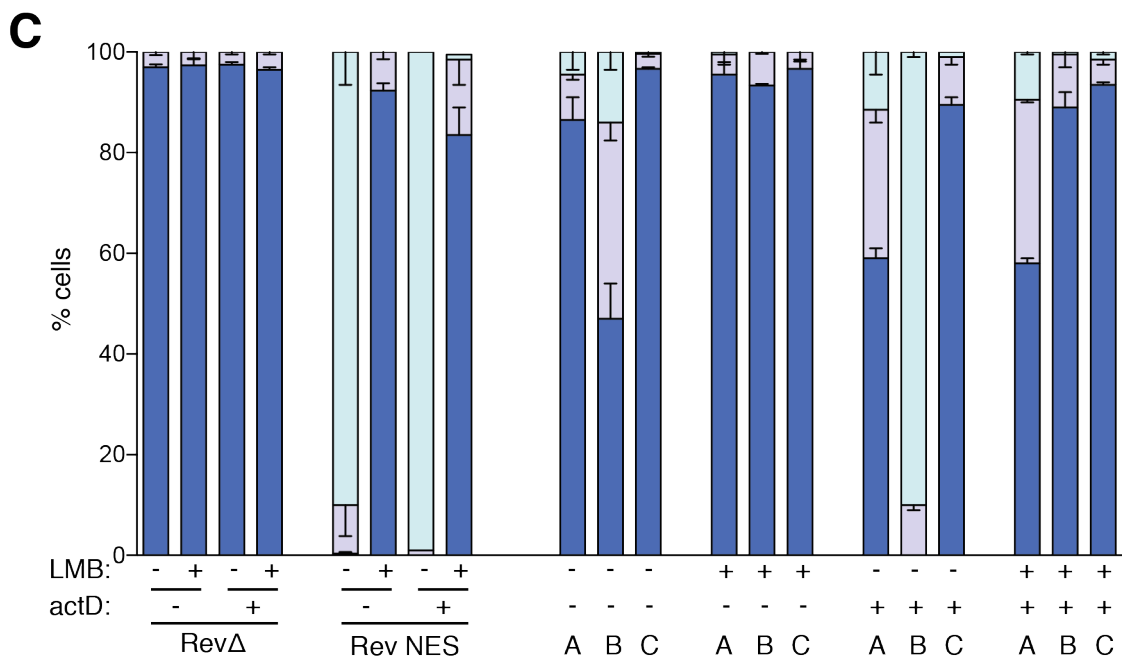
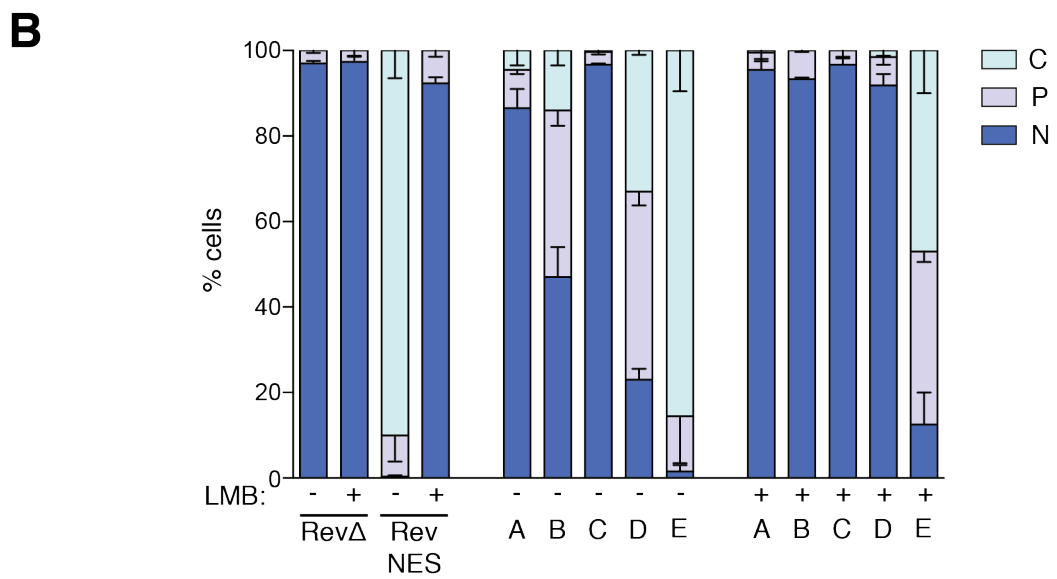
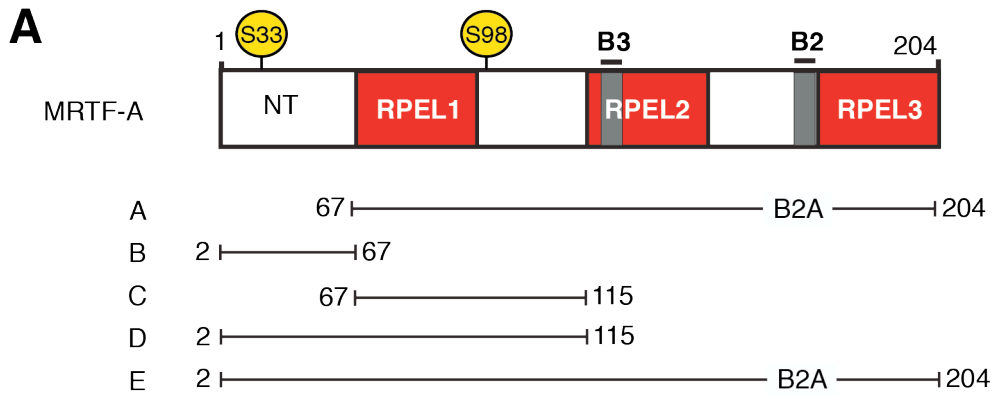


Figure 5.7 The RPEL domain potentiates the export activity of the N-terminus

A. Schematic showing the MRTF-A N-terminus + RPEL domain and a summary of the different segments tested in the Rev assay. **B.** Rev assay carried out as described for Figure 6, to test the various RPEL fragments for NES activity. Where indicated cells were treated with 50nM LMB for 2 hours. At least 100 cells were counted and localisation was scored as predominantly nuclear (navy blue), pancellular (lilac) or predominantly cytoplasmic (light blue). **C.** Rev assay testing the indicated segments. Where indicated, cells were treated with actinomycin D to decrease the activity of the Rev NLS and increase the assay sensitivity to NES activity. Error bars represent standard error of the mean (SEM) from at least two independent experiments.

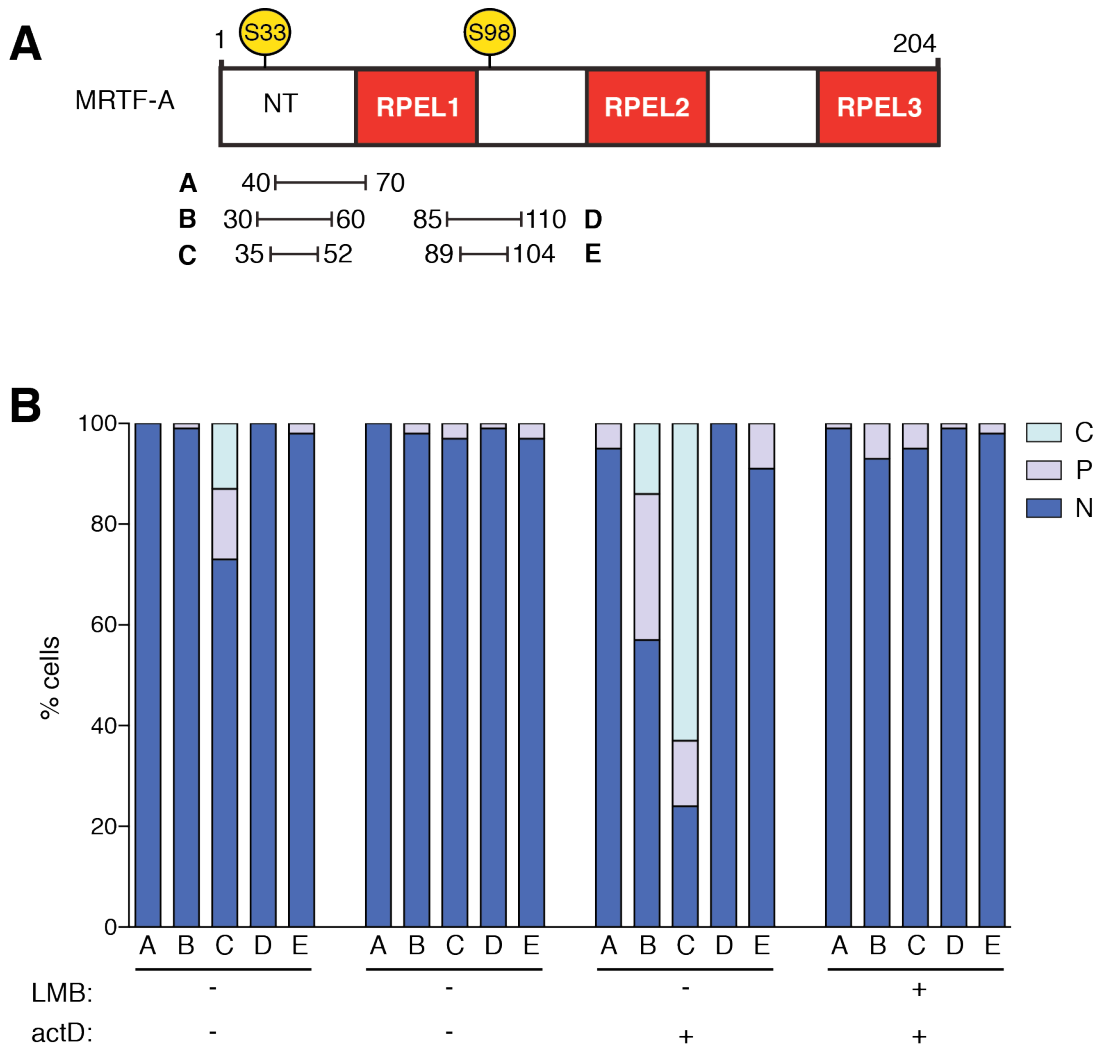


Figure 5.8 A short sequence containing the N-terminal NES is sufficient for export

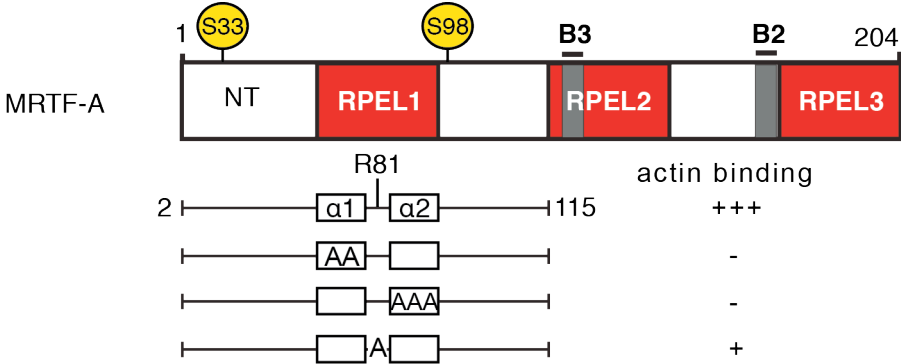
A. Summary of RPEL segments tested in the Rev export assay. B. Cells were transfected with the indicated derivatives and starved overnight. Actinomycin D was added for 6 hours where indicated. LMB was added during the last two hours of the experiment. At least 100 cells were counted and localisation was scored as predominantly nuclear (navy blue), pancellular (lilac) or predominantly cytoplasmic (light blue).

5.7 Actin binding to RPEL1 may facilitate export

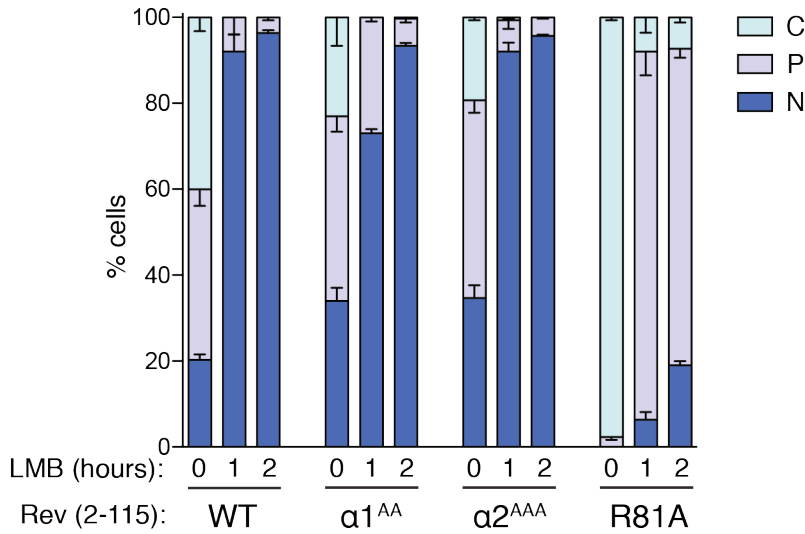
RPEL1-Spacer1 (67-115) might facilitate the export conferred by the N-terminus (2-67) either by enhancing interaction with Crm1 or through its ability to bind actin. To determine whether actin binding to RPEL1 was important three different ways to perturb actin binding by RPEL1 were employed. Previous studies showed that loss of contact mutations in α 1-helix and α 2-helix in RPEL1, α 1^{AA} and α 2^{AAA} respectively, severely affect the actin binding capacity of RPEL1. Both mutations lead to partial nuclear accumulation of full length MRTF-A. In contrast, although mutation of R81 in the R-loop between the two helices, decreases affinity of the RPEL1 for actin, it deregulates shuttling of MRTF-A to a lesser extent compared to the α -helix mutations (Mouilleron et al., 2008).

The α 1^{AA} and α 2^{AAA} mutations led to a small decrease in export of Rev (2-115), suggesting that actin binding only weakly promotes export in this context. Unexpectedly, the weaker R81A mutation led to an increase in export activity (Figure 5.9A). There is therefore no simple correlation with ability to bind actin.

Because RPEL1-R81A can still bind actin, I tested whether increasing G-actin levels would promote actin binding and restore the regulation back to that of Rev (2-115). Expression of C3-transferase, which inhibits Rho function and increases the proportion of G-actin (Posern et al., 2004), did not however have an effect (Figure 5.9B). Further experiments are required to determine if the increased export caused by the R81A mutation is due to a change in actin binding or the arginine residue per se. An alternative approach could be to co-transfect increasing amounts of non-polymerisable actin R62D.



A



B

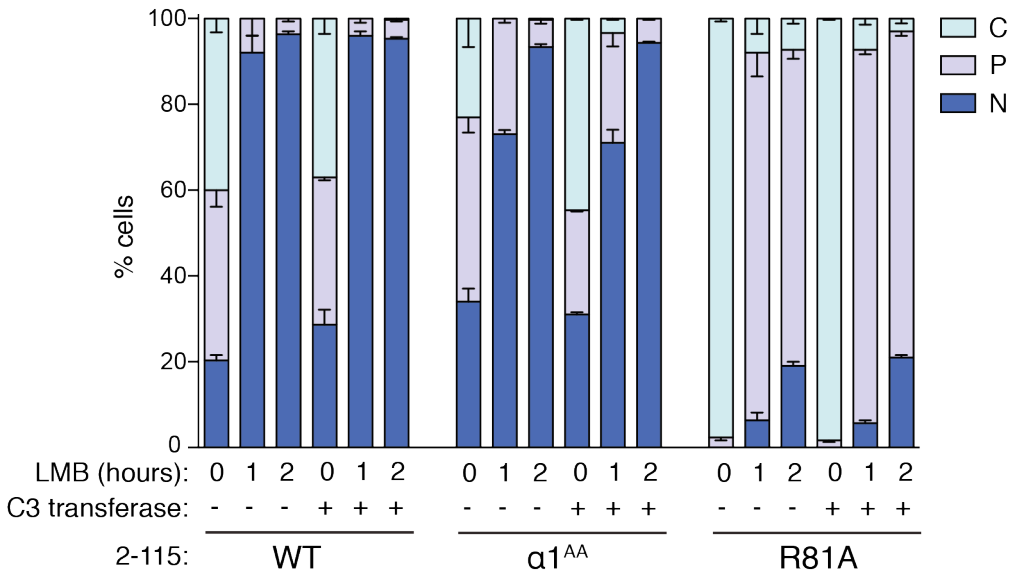


Figure 5.9 Presence of RPEL1-Spacer1 potentiates NES activity of the N-terminus

A. Rev export assay: Cells were transfected with the indicated Rev constructs, starved overnight and treated with 50nM LMB for 1 or 2 hours. **B.** Cells were co-transfected with the indicated Rev constructs and C3-transferase. After overnight starvation cells were treated for 1 or 2 hours with 50nM LMB. At least 100 cells were counted and localisation was scored as predominantly nuclear (navy blue), pancellular (lilac) or predominantly cytoplasmic (light blue). Error bars represent standard error of the mean (SEM) from at least two independent experiments.

5.8 Leucine rich NES in the N-terminus directly binds Crm1

To map the residues that define the N-terminal NES in detail I carried out an alanine substitution scan, moving across the N-terminus in triplets (Figure 5.10A). The Rev (2-115) construct was used, as it was the simplest construct exported efficiently enough to have a good range.

The scan revealed that the three mutants spanning residues 41-49, each of which contained sequences of the putative NES, did not exhibit export activity (Fig 5.10B), consistent with the tested minimal sequence 35-52 in Figure 5.8. This sequence, which corresponds to the predicted NES1 in Figure 5.1, resembles a typical leucine-rich export signal, although it scored below threshold in the prediction. Other residues appeared to affect export, including a triplet of acidic residues DDE in positions 20-22 and PPL in positions 65-67.

I next investigated whether Crm1 directly interacts with the sequence identified. Using purified recombinant proteins GST pulldowns were performed with the N-terminus (residues 2-67), the better-exported NT-RPEL1-Spacer1 (residues 2-115) and the RPEL domain (residues 67-199) (Figure 5.11). Reactions were carried out with or without RanGTP, which is required for Crm1-cargo interaction (see chapter 1.2). The N-terminus alone was sufficient to interact with Crm1. Mutation of residues LSL 46-48, the NES anchor point ($\phi x \phi$) (Güttler et al., 2010) to alanine, abolished this interaction. GST-2-115 recovered Crm1 more efficiently and

the interaction was again entirely dependent on the integrity of residues LSL 46-48. GST-67-199 was unable to efficiently interact with Crm1 but did indeed recover some Crm1 in a RanGTP dependent manner. The efficiencies with which the GST-baits bind Crm1 reflect their performance in the Rev assay.

The role of the sequence identified was examined in the context of shorter or longer constructs in the Rev assay (Figure 5.12A). In agreement with the alanine scanning results, both 2-67 and 2-115 are completely dependent on NES core residues 46-48 for export (Figure 5.12 B). Moreover, these residues are required for Crm1 dependent export of Rev (2-204) B2A.

I have shown previously that the RPEL domain alone (67-204) does not show Crm1 dependent export, but promotes export activity of the N-terminal sequences and enable actin regulation. Ablation of the N-terminal NES reduced export of Rev (2-204) B2A revealing residual Crm1-independent export in agreement with Figure 5.7C (construct A). However residual export was not serum regulated, suggesting that it is also actin independent, suggesting that actin-regulated export required the N-terminal NES in this context.

In summary, these results confirm that a leucine rich export signal within the N-terminus of MRTF-A is required for direct interaction with Crm1. This interaction is enhanced in the presence of RPEL1-Spacer1 and further enhanced by the entire RPEL domain (67-204), which also enables regulation by actin. Rev (2-204) B2A exhibits both Crm1 dependent and independent export. A caveat in this context is that the B2A mutation, which is necessary for enabling assessment of changes in export, possibly affects an overlapping export signal.

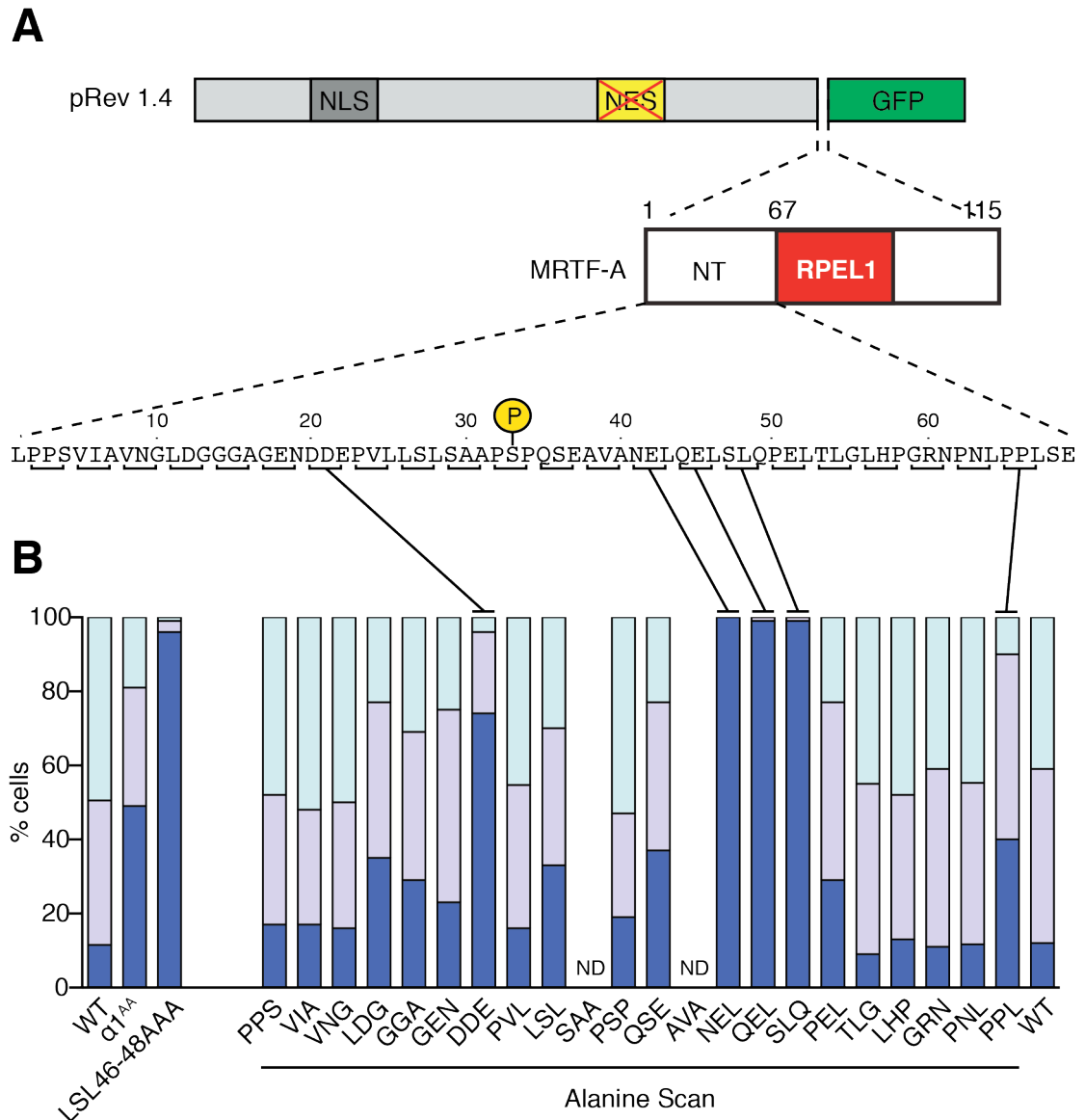


Figure 5.10 Classical NES element in the N-terminus of MRTF-A

A. Schematic representation of the Rev-MRTF-A (2-115)-GFP derivative used in the alanine scan. The N-terminus is expanded to show the residues across which the alanine scan was carried out. Consecutive triplets of residues mutated are indicated with brackets below; the location of Ser33 is indicated with a phosphate symbol. **B.** Cells were transfected with the various Rev-MRTF-A-(2-115)-GFP derivatives and starved overnight. At least 200 cells were counted and localisation was scored as predominantly nuclear (navy blue), pan-cellular (lilac) or predominantly cytoplasmic (light blue).

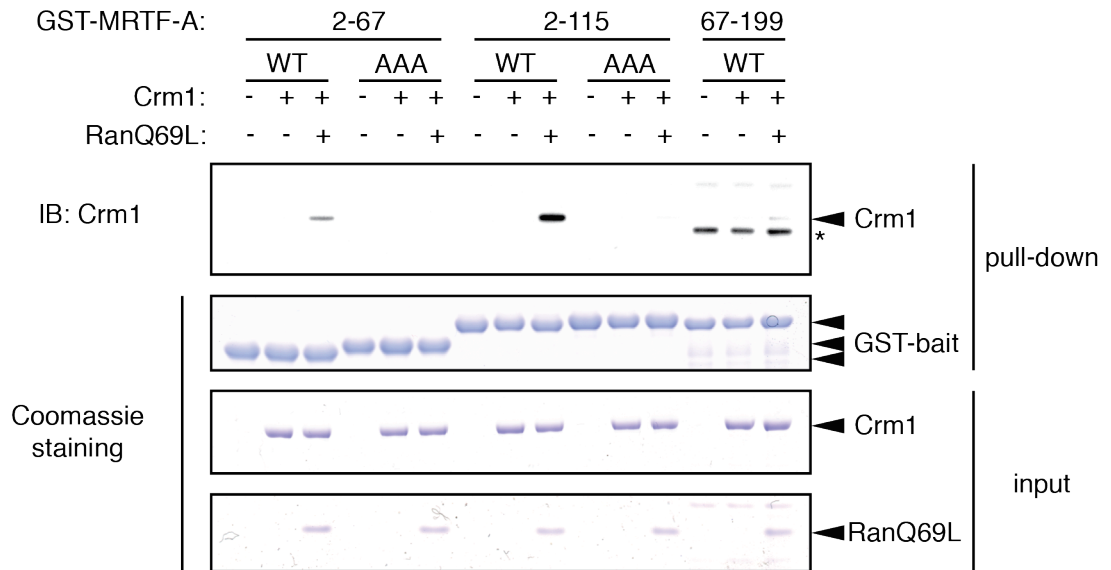


Figure 5.11 Crm1 directly interacts with the MRTF-A N-terminus

Recombinant GST MRTF-A segments were used in a pulldown with Crm1. AAA represents LSL46-48AAA mutation of the N-terminal NES. Top panel is an immunoblot using an anti-Crm1 antibody. Bottom three panels are Coomassie stained gels showing the GST baits, Crm1 input and RanQ69L input.

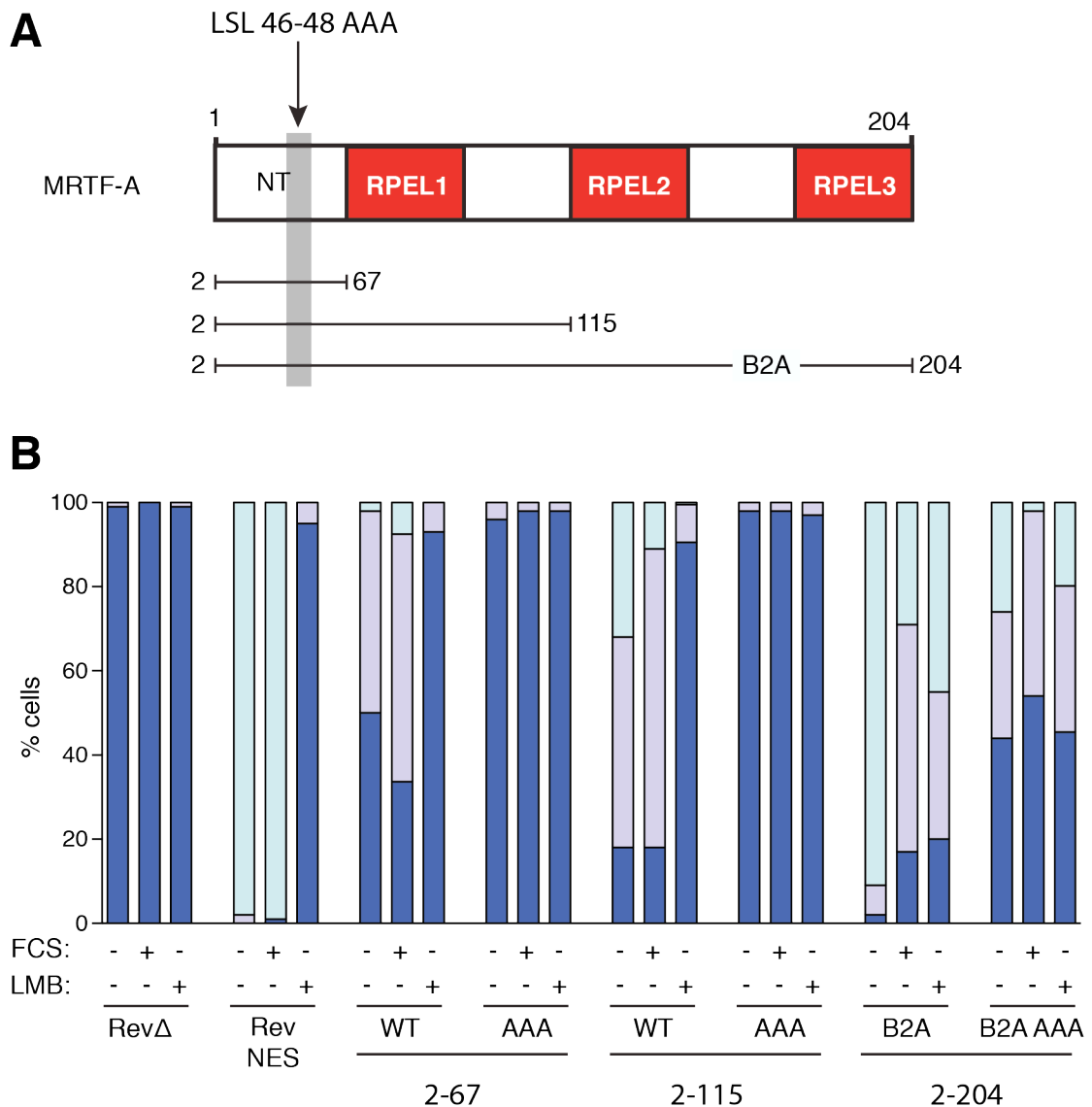


Figure 5.12 RPEL domain enhances N-terminal NES activity

A. Summary of the RPEL segments used in the Rev export assay. The location of the alanine substitutions intended to inactivate the NES is shown in a grey box. **B.** Cells were transfected with the indicated constructs, starved overnight and treated with 15% FCS or 50nM LMB for 30 min and 2 hours respectively. At least 200 cells were counted and localisation was scored as predominantly nuclear (navy blue), pancellular (lilac) or predominantly cytoplasmic (light blue).

5.9 Probing Spacer1 for an export signal

The spacers in the MRTF-A RPEL domain, and their ability to bind actin are important for MRTF-A localisation (Mouilleron et al., 2011). In data presented so far, spacer1 alone did not demonstrate export activity but was present in the sequences that enhanced export activity of NES1 in the Rev assay and Crm1 interaction in the pull down. This region bears similarity to a structure based consensus for Crm1 binding (Figure 5.13A) described by (Güttler et al., 2010). In addition, the presence of S98 in the sequence makes it tempting to speculate that its phosphorylation may inactivate the export signal.

To investigate whether a NES is present, Rev 2-115 was used. The residues reported to be important for the putative NES were substituted to alanine (Figure 5.13). Alanine substitution of P94 or L96 individually or in combination, had no effect on localisation. Positions of the hydrophobic residues are not all equally important, particularly if other hydrophobic residues are sufficiently strong. The alanine substitutions may therefore be tolerable. (Güttler et al., 2010) show that in certain cases alanine substitutions of each residue does not necessarily abolish Crm1 binding. Upon exchange of the critical proline to a serine, a small increase in nuclear accumulation was observed. The data therefore do not support the presence of an NES in Spacer1.

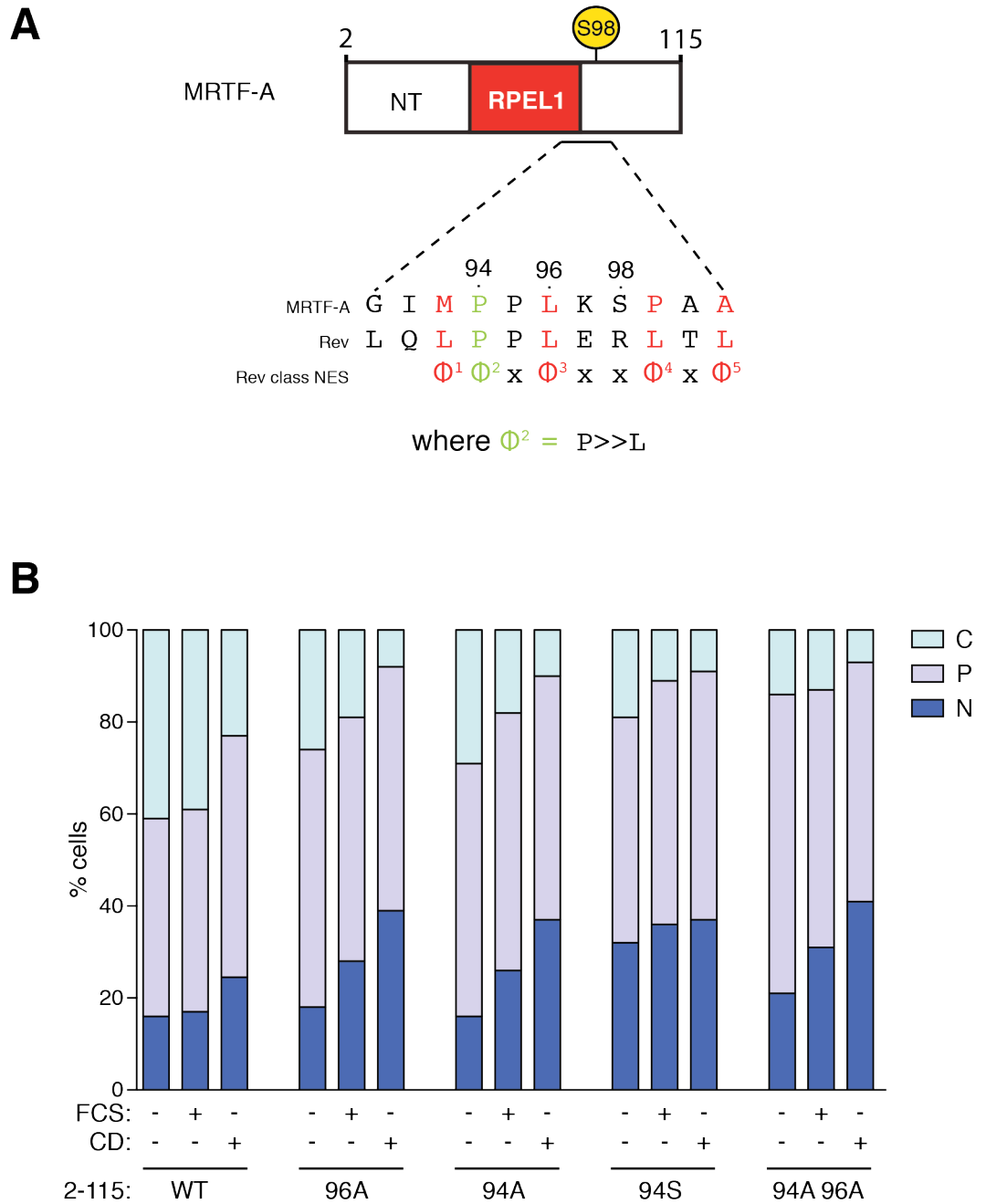


Figure 5.13 Probing Spacer1 for an export signal

A. Alignment of a putative NES in spacer1 with the Rev-like non-canonical NES. **B.** Cells were transfected with the various Rev constructs with point mutations intended to disrupt the putative non-canonical NES. At least 200 cells were counted and localisation was scored as predominantly nuclear (navy blue), pancellular (lilac) or predominantly cytoplasmic (light blue).

5.10 Probing Spacer 2 for an export signal

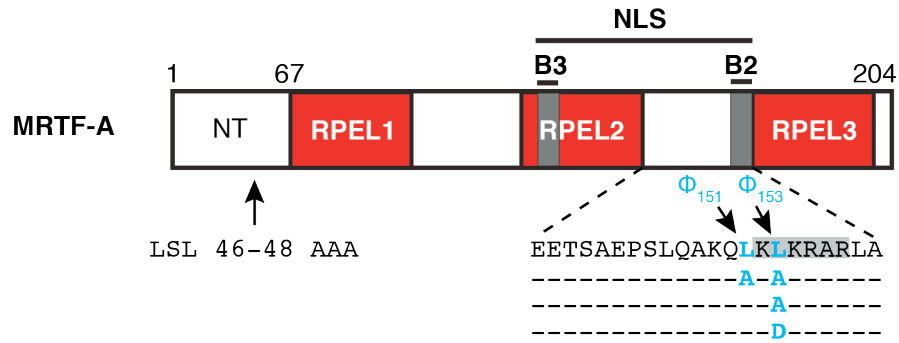
Overlapping the NLS B2 region within spacer2, is a set of leucine residues which resemble a Crm1 consensus site (Figure 5.14A). This sequence was detected by the prediction algorithm but scored significantly below the threshold (NES2 in Figure 5.1). Alanine substitution of the anchor point leucines, L151 and L153 led to nuclear localisation of the MRTF-PK fusion (R. Pawlowski, preliminary data).

Alanine or aspartate substitution of L153, results in opposite effects on full length MRTF-A-(2-204)-PK localisation. L153A increases nuclear localisation without affecting import (Mouilleron et al., 2011). L153D decreases nuclear localisation by affecting import rate and additionally affecting actin binding to spacer2. To gain further insight alanine or aspartate derivatives of L153 were tested using the Rev assay.

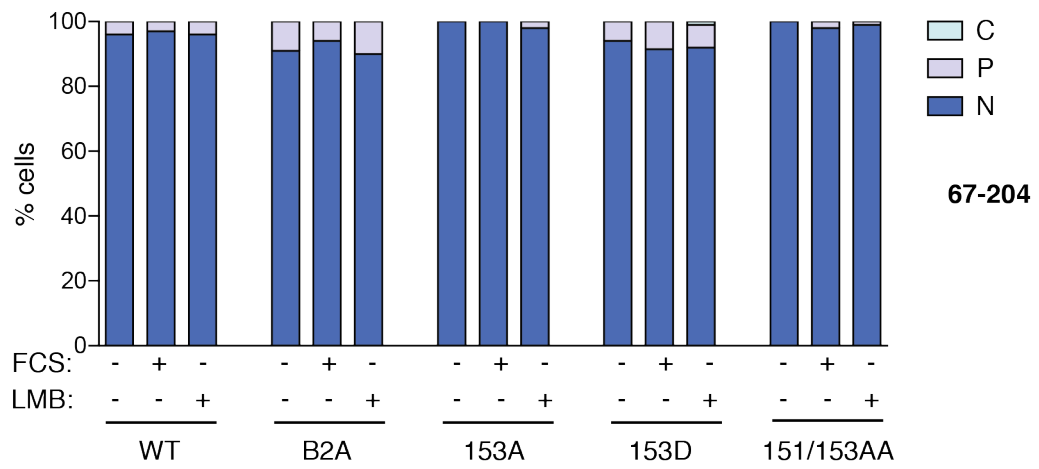
Rev 67-204 was nuclear and neither B2A nor 153D affected this localisation (Figure 5.14B). In Rev 2-204 the 153A mutation led to nuclear accumulation (Figure 5.14C). Since the 153A mutation does not affect import, nuclear localisation may be a result of diminished export. It is not clear whether it is through direct disruption of the putative NES or indirectly through affecting actin binding to spacer2. The 153D mutation led to a small decrease in nuclear accumulation, because the acidic substitution is in the NLS and may be affecting importin binding. The small defect may reflect a simultaneous loss of export activity.

To gain further insight into the effect of L153A, RPEL3 mutated derivatives could be used. Actin binding to spacer2 is RPEL3 dependent. Preventing actin binding to spacer2 could reveal whether 153A perturbs NES activity.

A



B



C

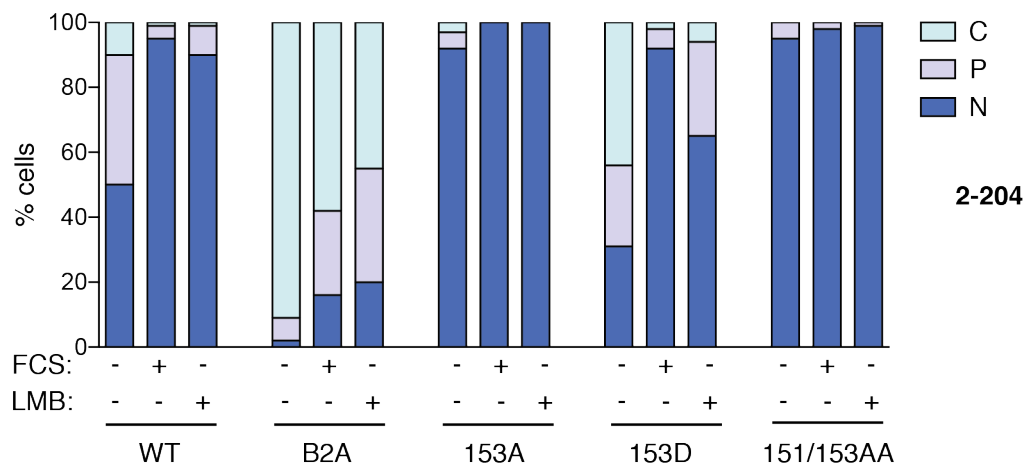


Figure 5.14 Probing Spacer 2 for an export signal

A. Schematic of MRTF-A RPEL domain. Spacer 2 is expanded to show the residues mutated in the following experiment. Spacer 2 mutations were tested in the context of the RPEL domain or N-terminus + RPEL as indicated. AAA indicates mutation of the NES in the N-terminus. **B and C.** Rev export assay. Cells were transfected with the indicated constructs, starved overnight and treated with 15% FCS or 50nM LMB for 30 min and 2 hours respectively. At least 200 cells were counted and localisation was scored as predominantly nuclear (navy blue), pancellular (lilac) or predominantly cytoplasmic (light blue).

5.11 The role of S33 and S98 in regulation of export

As shown in Chapter 4, S33 that is basally phosphorylated blocked nuclear accumulation of MRTF-A (2-204) PK. S98 is not phosphorylated in resting conditions and its phosphorylation is required for nuclear accumulation of MRTF-A (2-204) PK in response to ERK signalling. To investigate how S33 and S98 affect export, derivatives were tested in the context of Rev (2-67) and Rev (2-204). In both contexts S33D promoted export, while S33A made export less efficient, suggesting that phosphorylated S33 facilitates the function of the NES (Figure 5.15A).

Substitutions of S98 were less clear. In the context of 2-115, mutations of S98 did not affect export (Figure 5.15B). However I have shown that in this context S98 is not able to affect actin binding to RPEL1.

The effects of S33 and S98 were also investigated in the context of Rev (2-204) B2A (figure 5.15C). As observed with 2-115, in this context S33A was more nuclear. S33D did not appear to have an effect, however it appears to be at the lower detection limits of the assay. Rev (2-204) B2A is already cytoplasmic in the majority of cells and it is possible that higher export levels cannot be detected.

The S98A and S98D mutations caused a small increase in nuclear localisation despite the fact that one mimics phosphorylation and the other is phospho-deficient. This may be due to a requirement for serine in that position.

Since aspartate substitution of S98 abolished actin binding from RPEL1 *in-vitro*, it could be expected to cause nuclear localisation comparable to that of the mutant that cannot bind actin on RPEL1 ($\alpha 1^{AA}$) (Figure 5.15 C). One explanation for the difference between $\alpha 1^{AA}$ and S98D is that under starved conditions, when G-actin concentrations are relatively high, RPEL1 can still bind actin even with the disruption by S98D. Mutation of the RPEL1 α -helix appears to be a more severe disruption.

Together the data show that S33 phosphorylation promotes export activity of the N-terminal NES and that it is phosphorylated in the absence of stimulation, in accordance with the findings in Chapter 4. The effect of S33 is more likely to be direct, for example by forming a better substrate for Crm1. The small decrease in export observed with S98D is likely to be indirect through affecting actin loading of the RPEL domain.

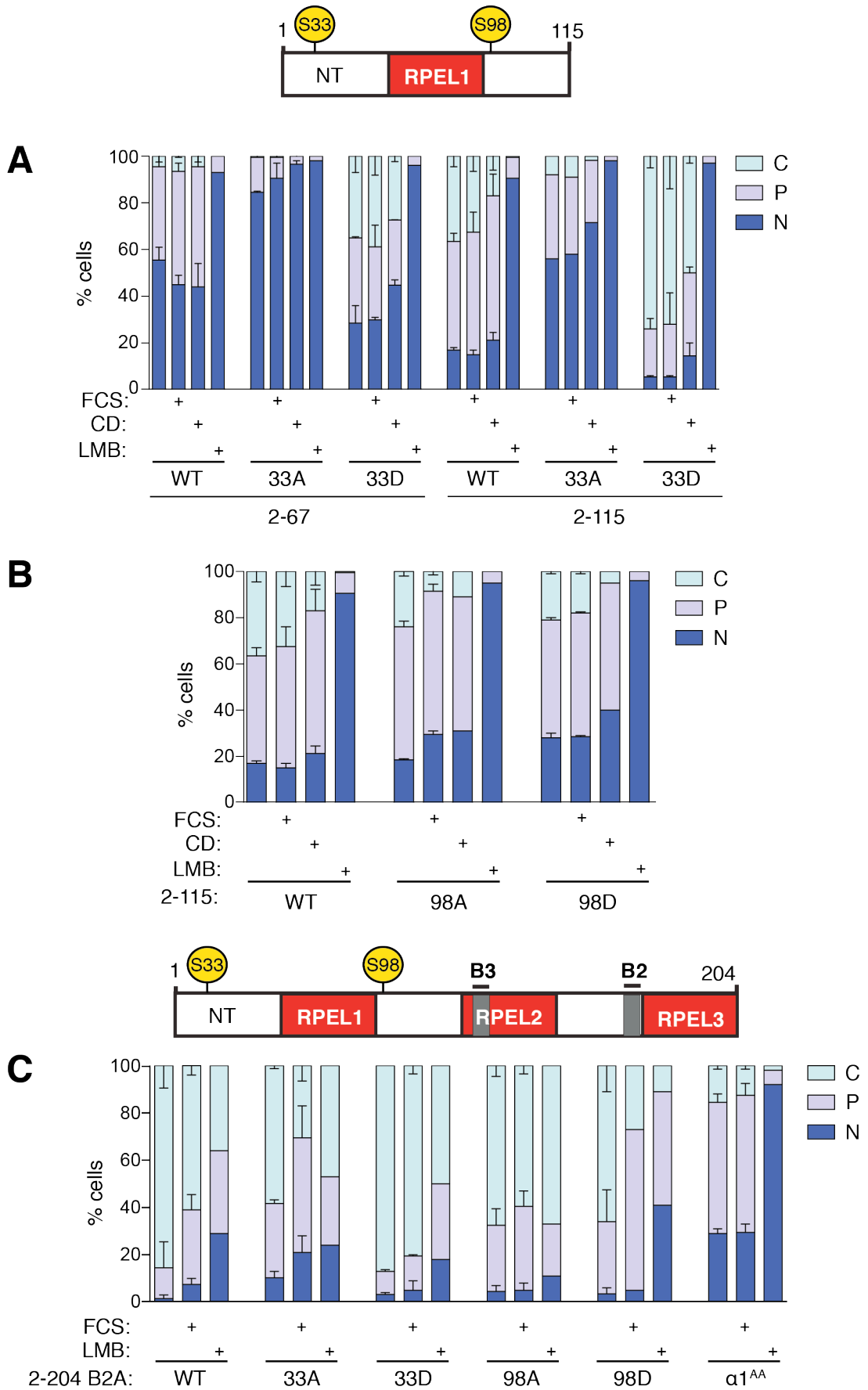


Figure 5.15 The role of S33 and S98 in MRTF-A export

A. Cells were transfected with Rev-MRTF-A-(2-67)-GFP or Rev-MRTF-A-(2-115)-GFP S33 mutants, starved overnight and treated with 15% FCS or 50nM LMB for 30 min and 2 hours respectively. **B.** Cells were transfected with Rev-(2-115)-S98 derivatives and treated as above. **C.** Cells were transfected with Rev-MRTF-A-(2-204)-GFP derivatives and treated as in A. At least 100 cells were counted and localisation was scored as predominantly nuclear (navy blue), pancellular (lilac) or predominantly cytoplasmic (light blue). Error bars represent standard error of the mean (SEM) from at least two independent experiments.

Chapter 6. Discussion

6.1 Outline

In the present thesis I have analysed the role of phosphorylation as a regulatory mechanism of MRTF-A. MRTF-A is phosphorylated on multiple serine and threonine residues upon ERK activation or G-actin depletion. I have shown that overall phosphorylation of MRTF-A is required for its full capacity to activate transcription.

Although the phosphorylation sites are spread throughout MRTF-A, S98 is the only one located within the RPEL domain. I have shown that S98 is phosphorylated by ERK, which promotes MRTF-A nuclear accumulation by blocking actin binding to RPEL1. S98 therefore provides a means for ERK signalling to affect the ability of MRTF-A to sense Rho-actin signalling.

Not all phosphorylation positively regulates MRTF-A function. S33 is located in the N-terminus of MRTF-A, close to the RPEL domain, and phosphorylation of S33 promotes MRTF-A export. The mechanism by which pS33 promotes MRTF-A export is likely to involve an adjacent leucine rich region shown to directly bind Crm1 and mediate MRTF-A export. This leucine rich region is an NES that cooperates with the RPEL domain to confer actin dependent nucleocytoplasmic shuttling.

In the following sections, the impact of MRTF-A phosphorylation on its function will be discussed. In addition, evidence will be presented on how S33 and S98 phosphorylation impacts how the N-terminus of MRTF-A regulates its nucleocytoplasmic shuttling.

6.2 Rho and MEK-ERK signalling converge on MRTF-A

FCS stimulation leads to MRTF-A phosphorylation that can be visualised as a reduction in electrophoretic mobility. Inhibition of either Rho signalling using C3-transferase, or MEK-ERK signalling using U0126, attenuates FCS-induced MRTF-A phosphorylation. Inhibition of both signalling pathways effectively blocks MRTF-A phosphorylation (Miralles et al., 2003). Therefore in addition to sensing Rho-actin signalling, MRTF-A is also responsive to MAPK signalling.

MRTF-A thus appears to integrate signalling from the two pathways, which can be seen at the level of phosphorylation and activity. Levels of MRTF-A transcriptional activity correlate with phosphorylation levels. SRF/MRTF-A target gene activity, measured by qRT-PCR, is higher when both pathways are activated compared to when each pathway is active alone. MRTF-A phosphorylation levels are also highest when both pathways are activated and partial when only one pathway is activated.

MAPK-mediated MRTF-A phosphorylation in the actin-sensing domain provides a mechanism by which the MAPK pathway can cooperate with Rho signalling, for MRTF-A regulation.

Measuring reduction of electrophoretic mobility does not allow for quantitative measurement of phosphorylation, in part because not all phosphorylations lead to a reduction in electrophoretic mobility and because the average of a cell population of cells is taken into account. Using stable isotope labelling by amino acids in cell culture (SILAC) would enable quantitative measurements and determination of the phosphorylation kinetics of individual sites. It could therefore be possible to distinguish between early (possibly activating) phosphorylation events and later (possibly inactivating) ones.

6.3 Actin controls phosphorylation

Phosphorylation of MRTF-A is regulated by actin binding to the RPEL domain. Rho activates multiple downstream effectors, however three lines of

evidence agree that it is G-actin depletion that results in MRTF-A phosphorylation. First, coexpression of an activated form of the formin mDia1, which induces F-actin nucleation, is sufficient to cause MRTF-A phosphorylation. Second, direct disruption of the actin-MRTF-A interaction by CD is also sufficient for partial phosphorylation. Third, MRTF-A xxx, that does not bind actin, is constitutively phosphorylated. Constitutive phosphorylation of MRTF-A xxx, in the absence of any manipulations of actin, suggests that actin suppresses MRTF-A phosphorylation.

Because actin regulates MRTF-A nuclear export, actin dissociation leads to MRTF-A phosphorylation but also simultaneous nuclear accumulation. This raises the issue of whether phosphorylation reflects actin dissociation or nuclear localisation. However nuclear accumulation without compromising actin binding, achieved by LMB treatment, is not sufficient for MRTF-A phosphorylation. Considering that the import defective derivative MRTF-A B2A does not become phosphorylated after CD treatment, then a nuclear kinase or kinases must target MRTF-A.

Actin can therefore regulate MRTF-A phosphorylation by spatially separating MRTF-A from the nuclear kinases and either (i) by blocking access of the kinase to MRTF-A or (ii) promoting interaction with a phosphatase that continuously dephosphorylates MRTF-A.

6.4 What are the kinases that phosphorylate MRTF-A?

MRTF-A is phosphorylated by ERK, as well as other kinases, which are constitutively active and nuclear. Given that all phosphorylation sites on MRTF-A are S/T-P sites, these kinases should be proline-directed kinases. Experiments presented in this thesis implicate the Cdk family in MRTF-A phosphorylation. While depletion of single Cdk family members did not affect MRTF-A activity, pharmacological inhibition of multiple Cdks resulted in inhibition of MRTF-A activity. These observations suggest redundancy between the Cdks that phosphorylate MRTF-A.

Depletion or pharmacological inhibition of DYRK family members had gene specific effects on MRTF-A target genes and also affected transcription of the non-MRTF-A target *Egr1*. Although DYRKs phosphorylated full length MRTF-A *in-vitro*, it is not necessarily the case *in-vivo*. It is therefore unlikely that DYRKs directly regulate MRTF-A activity.

ERKs, Cdks and DYRKs belong to the CMGC kinase group and within the family ERKs and Cdks are more closely related (Manning et al., 2002). Although not the only determinant of substrate specificity, the three kinase families share similar phosphorylation consensus sequences. ERK: Px(S/T)P, DYRK1A: RPx(S/T)P, DYRK2/3: Rx(S/T)P and Cdks: (S/T)Px(K/R) (ERK and Cdk: (Pinna and Ruzzene, 1996; Songyang et al., 1994; 1996) DYRKs: (Himpel et al., 2000; Aranda et al., 2011)). It has previously been reported that Cdks and ERK can phosphorylate the same residues on a protein (Aoki et al., 2013; Brumbaugh et al., 2014; Voong et al., 2008).

Both Cdks and ERK1/2 have been shown to regulate transcription through phosphorylation of the C-terminal domain (CTD) of RNA Pol II (Bonnet et al., 1999; Eick and Geyer, 2013). I have shown that ternary complex formation is not required for MRTF-A phosphorylation, suggesting that MRTF-A can interact with its kinase(s) independently of SRF or promoter association. In addition, inhibition of Cdks using flavopiridol, blocked CD-induced phosphorylation of MRTF-A and reporter activation. It is therefore conceivable that MRTF-A recruits Cdks to the promoters of target genes, and is also phosphorylated by Cdks itself.

In support of this notion, unpublished data by F. Gualdrini showed that Cdk-dependent Ser2 phosphorylation of the C-terminal domain of Pol II and productive transcription of MRTF/SRF targets require actin dissociation from MRTF-A. A similar scenario has been reported for NF- κ B, which is required for recruitment of Cdk9/CyclinT to the IL-8 gene for TNF α induced transcription (Barboric et al., 2001).

To investigate whether MRTF-A can directly associate with Cdks, coimmunoprecipitation and pull-down experiments could be carried out. However these approaches would not provide information on whether MRTF-A recruits the kinases to promoters.

6.5 The role of phosphorylation in MRTF transcriptional activity

To assess the potential role of MRTF-A phosphorylation on transcriptional activation of its target genes, an MRTF-A activity reporter was used. The MRTF-A activity reporter used contains 3 copies of the *Fos* SRF binding site that drive transcription of the luciferase enzyme. The *Fos* derived sequences are modified so that they are not sufficient for TCF binding (Hill et al., 1995), and thus transcription of luciferase is dependent on MRTF-A/SRF signalling. Transcriptional activation of the MRTF-A reporter gene by the phosphorylation-deficient derivative E3, in which most but not all phosphorylation sites were replaced by alanine, was impaired. The 26ST/A derivative, in which all phosphorylation sites were replaced by alanine, was no more defective, suggesting that there may be a threshold stoichiometry, beyond which MRTF-A activity is potentiated. Phosphorylation of MRTF-A on multiple sites is therefore required for full transcriptional activation.

Although the reporter specifically allows measurement of MRTF-A activity, the assay has certain limitations that should be considered. Transcriptional activation of MRTF targets, measured by qRT-PCR of introns, is transient and occurs over a period of 2 hours after stimulation. In the reporter assay activity is quantified indirectly by measuring the amount of luciferase protein produced. The measurement is therefore one of the combined processes of transcription and translation. As opposed to endogenous targets, the coding sequence in the reporter is intronless and is therefore subject to fewer regulatory processes that can affect the rate and minimum requirements of transcription (Lynch, 2006). In addition, the transiently transfected reporter is not necessarily in a bona fide chromatin context and may not be subjected to all regulatory processes that need to be overcome in the case of endogenous target genes. For example if MRTF-A promotes transcription activation through recruitment of chromatin remodellers, the process will be redundant in the reporter context.

After depletion of MRTF-A/B, FCS or CD stimulation resulted in effectively no reporter activity. Subsequent transfection of MRTF-A led to increased baseline activity, which could be a result of titrating out negative regulators. There was no appreciable difference between MRTF-A and 26ST/A in unstimulated conditions,

suggesting that the two proteins exhibit similar activity in conditions under which MRTF-A is basally phosphorylated. Differences in activity were observed in stimulated conditions, when MRTF-A would be phosphorylated at high stoichiometry. However the 26ST/A derivative was not completely inactive. Remaining activity could be a consequence of dimerisation with residual endogenous MRTF-A, which can heterodimerise with 26ST/A.

It was previously reported that after siRNA depletion, residual MRTF-A can dimerise with transfected derivatives and contribute to reporter activation (Pawłowski et al., 2010). It is especially apparent when comparing the MRTF-A Y330A (SRF binding deficient) with or without the leucine zipper (Figure 3.4). MRTF-A Y330A appears to act in a dominant negative manner, only when it can dimerise with the residual endogenous MRTF-A.

Interpretation is further complicated by the presence of multiple phosphorylation sites, which can affect different regulatory processes, for example localisation (Muehlich et al., 2008), transactivation and SRF binding. At least two sites, S33 and S98, not only affect localisation, but also exert opposite effects. 26ST/A xxx, is not regulated at the level of localisation and was considerably less able to stimulate reporter activity.

In the context of xxx, regulation of phosphorylation is uncoupled from nuclear accumulation. The possibility of dimerisation however remains and it would therefore be interesting to test whether deletion of the leucine zipper would abolish the remaining activity of 26ST/A xxx. Partially phosphorylated MRTF-A xxx, can be further phosphorylated by activation of the MAPK pathway (Figure 6.1A). Preliminary data show that activation of the MAPK pathway potentiates MRTF-A xxx activity (Figure 6.1B).

Phosphorylation therefore promotes MRTF-A activity. Further work is required to determine whether phosphorylation is essential for transcriptional activity rather than merely enhancing it. To avoid heterodimerisation with endogenous MRTF-A, MRTF-A/B KO MEFs could be transfected with MRTF-A xxx or 26ST/A xxx. In the absence of possible heterodimerisation, a defect in endogenous gene activity in 26ST/A xxx transfected cells, would strongly support a positive regulatory role for phosphorylation. In addition, chromatin immunoprecipitation can be carried out, to assess whether phosphorylation affects ternary complex formation.

In this study, comparison between different MRTF-A derivatives involved transient transfection. This approach leads to a population of cells expressing different levels of MRTF-A derivatives, which are pooled before transcriptional activity is assessed. The importance of MRTF-A abundance in target gene expression is evident in Figures 3.4 and 3.7. Future work should involve generation of cell lines stably expressing comparable levels of MRTF-A derivatives. This can be accomplished by fluorescence assisted cell sorting (FACS) after which cells can be grouped according to expression of MRTF-A GFP. Additionally complications arising from cell heterogeneity can be circumvented using single cell analysis, such as single cell RNA sequencing.

6.6 Regulation of MRTF-A nuclear accumulation by ERK

Activation of ERK by TPA treatment leads to MRTF-A nuclear accumulation, phosphorylation, and activation of MRTF-A. The data presented in this thesis show that MRTF-A accumulates in the nucleus upon TPA treatment, despite elevated G-actin levels. The nuclear accumulation observed, at least in part, required ERK mediated phosphorylation of S98 in the RPEL domain. In the MRTF-A-(2-204)-PK fusion protein, the N-terminus of MRTF-A including the RPEL domain, can be studied separately from the other phosphorylation sites and regulatory elements in the rest of the protein. This allowed investigation of the mechanism by which ERK signalling affects how the N-terminus contributes to MRTF-A shuttling. Specific activation of ERK, using the constitutively active MEK derivative MEK R4F or the tamoxifen-inducible RafER fusion protein, resulted in S98-dependent nuclear accumulation of MRTF-A-(2-204)-PK. Phosphorylation of S98 blocks actin binding to RPEL1 and promotes nuclear accumulation of MRTF-A.

TPA treatment also leads to a two-fold increase in S33 phosphorylation, however S33 phosphorylation promotes export of MRTF-A from the nucleus. S33 is basally phosphorylated in unstimulated conditions. Substitution to alanine promotes nuclear accumulation, while aspartate substitution prevents nuclear accumulation by potentiating export.

It has previously been shown that TPA stimulation leads to MRTF-A phosphorylation (Muehlich et al., 2008). In contrast to the data presented in this thesis, Muehlich et al. proposed that phosphorylation promotes export through increased actin binding. The authors showed that MRTF-A STS544/545/549AAA, in which the three residues they mapped were substituted to alanine, was constitutively nuclear. According to their view, phosphorylation of these sites is required for actin association and nuclear export. This implies that basal phosphorylation of these sites is involved in the maintenance of cytoplasmic localisation of MRTF-A in unstimulated cells. The relevance of their findings to signalling is therefore unclear. Because the experiments presented were carried out in HeLa cells, we wanted to confirm this observation in our NIH-3T3 system.

Contrary to their observations, I found that MRTF-A STS544/545/549AAA was cytoplasmic in starved conditions and accumulated in the nucleus after

stimulation both in 3T3 and HeLa cells. The experiments presented by Muehlich et al. were carried out using an N-terminally truncated MRTF-A, MRTF-A(met), starting at Spacer1 (Muehlich et al., 2008). I therefore generated an analogous derivative by deletion of the first 92 residues (N-terminus + RPEL1) of full length MRTF-A. The truncation itself led to an increase in nuclear accumulation, consistent with the loss of the N-terminal Crm1-dependent MRTF-A nuclear export signal described below. However, again, nuclear accumulation was not further increased by alanine substitution of S544, T545 and S549.

Muehlich and colleagues also reported that in 3T3 cells TPA treatment blocks reporter activation by subsequent FCS stimulation (Muehlich et al., 2008). In their view, this reflects ERK-mediated phosphorylation of S544, T545 and S549, leading to heightened nuclear export, and therefore antagonising the effects of serum (Muehlich et al., 2008). In contrast, other work (R Pawlowski), found that blockade of ERK signalling does not relieve the blockade of the serum response and that instead TPA blocked FCS activation because of PKC-mediated downregulation of RhoA activity and consequent high G-actin levels.

In this thesis I present evidence that ERK activity impinges on MRTF-A regulation, by phosphorylating S98 in the RPEL domain, which is the major regulatory domain in MRTF-A. In addition ERK can also phosphorylate other sites in MRTF that contribute to full activity of MRTF-A.

6.7 S98 phosphorylation affects actin binding to RPEL1

MRTF-A shuttling is controlled by actin, which is sensed via the N-terminally located RPEL domain (Miralles et al., 2003; Vartiainen et al., 2007). The RPEL domain however, is not the only element contributing to MRTF-A shuttling, as deletions of C-terminal sequences affect MRTF-A localisation (Miralles et al., 2003). Gene fusion experiments showed that the MRTF-A N-terminal sequences and RPEL domain are sufficient to confer MRTF-A-like shuttling (Guettler et al., 2008; Mouilleron et al., 2008). Data presented in this thesis show that, at least in the context of these fusions, S98 phosphorylation affects shuttling conferred by the

RPEL domain. Since S98 is located within the RPEL domain itself, I investigated the effect of S98 phosphorylation on actin binding.

Size exclusion chromatography and fluorescence polarisation assays showed that phosphorylation of S98 did not alter actin binding to the isolated RPEL1 or Spacer1-RPEL2 peptides, but instead prevented recruitment of actin to RPEL1 in complexes formed with the intact RPEL domain. The aspartate substitution can at least in part mimic phosphorylation of S98.

Although RPEL3 exhibits a low affinity for G-actin, its mutation results in severe deregulation of MRTF-A, indicating that the interaction is crucial for MRTF-A regulation. However the contribution of RPEL3 to regulation of MRTF-A by actin, is dependent on actin binding to RPEL1, Spacer1 and RPEL2 (Mouilleron et al., 2011; Guettler et al., 2008; Mouilleron et al., 2008).

Direct destabilisation of actin binding to RPEL1 through mutation of actin contact residues results in partial deregulation of MRTF-A (Guettler et al., 2008; Mouilleron et al., 2008). S98 phosphorylation would provide a subtle way of altering the regulatory properties of MRTF-A. Indeed, the BSAC isoform of MRTF-A lacks both the N-terminal NES and the ERK docking site that is required for S98 phosphorylation.

By lowering affinity of the RPEL domain for actin, S98 phosphorylation could increase the threshold at which RPEL/actin assembly occurs. S98 phosphorylation, could therefore act as a timer, by making MRTF-A refractory to actin reassociation, thereby prolonging nuclear accumulation and activity. A similar case is that of WASp activation. WASp activation involves release from an autoinhibitory conformation by initial binding of Cdc42 and PIP2 (Rohatgi et al., 2000). Subsequent phosphorylation of Y291 by Src family kinases acts as a mechanism of molecular memory, prolonging WASp activity (Torres and Rosen, 2003).

The mechanism by which actin binding to RPEL1 is inhibited, is likely to involve occlusion of RPEL1, that requires sequences that are only present in the context of the whole RPEL domain. Introduction of a negative charge may cause intramolecular rearrangements that cause occlusion of RPEL1 thereby preventing actin binding.

Phosphorylation of serine or threonine residues can have strong effects on the conformation and function of a protein, primarily through two types of interaction, (i) interaction of the negatively charged phosphoryl group with the main

chain nitrogens at the beginning of a polar alpha helix and (ii) interaction of the phosphate group with the side chain of arginine residues which form strong electrostatic interactions (L. N. Johnson and Lewis, 2001).

S98 is in close proximity to the $\alpha 2$ helix of RPEL1. A simple model for how S98 inhibits actin binding would be that phospho-S98 coordinates with the RPEL1 $\alpha 2$ helix, thereby disrupting the sharp turn in spacer1 and destabilising the interaction with actin. Alternatively, phospho-S98 could coordinate to the arginines of the RPEL1 motif making it inaccessible to actin. However, if either case were true, loss of actin binding would have been observed with the RPEL1 and RPEL1-Spacer1 peptides.

Instead, the observation that inhibition of actin binding can occur in the context of the whole RPEL domain supports a model where sequences required for RPEL1 occlusion are downstream of Spacer1. It is possible that S98 phosphorylation enables additional contacts with actin bound to RPEL2 (See Figure 6.2), thereby preventing the RPEL1 motif from adopting the necessary orientation to bind actin.

Because the S98D derivative of the RPEL domain formed a stable complex with two actin molecules *in-vitro*, it appears that actin binding downstream of RPEL1 is unaffected. Actin binding by Spacer2 and RPEL3 is not stable enough to endure the separation process in size exclusion chromatography (SEC). It therefore remains possible that the S98 phosphorylation affects formation of the pentameric complex. For detection of the pentameric complex by SEC, actin needs to be present in the running buffer during the separation (Mouilleron et al., 2011) and it would be interesting to evaluate the effects of phospho-S98 or S98D in this assay.

In cells, inability to form the import defective pentameric assembly could result in MRTF-A activity in conditions that would normally be inhibitory. For example MRTF-A import is blocked at tensional homeostasis and it has been proposed that the block is a result of a high G/F actin ratio (McGee et al., 2011). Because MRTF-A is itself part of the homeostatic loop, it would be interesting to test whether in the presence of higher basal MAPK activity homeostasis is achieved at higher tension (Salvany et al., 2014; Esnault et al., 2014).

A simple way to test whether S98 phosphorylation raises the threshold for pentameric complex assembly, would be to test MRTF-A (2-204)-PK serum

induced nuclear accumulation, against a gradient of G-actin. MRTF-A (2-204)-PK-S98A, which cannot be phosphorylated, would be more susceptible to import blockade, and nuclear accumulation should be blocked at a lower concentration compared to wild type MRTF-A (2-204)-PK.

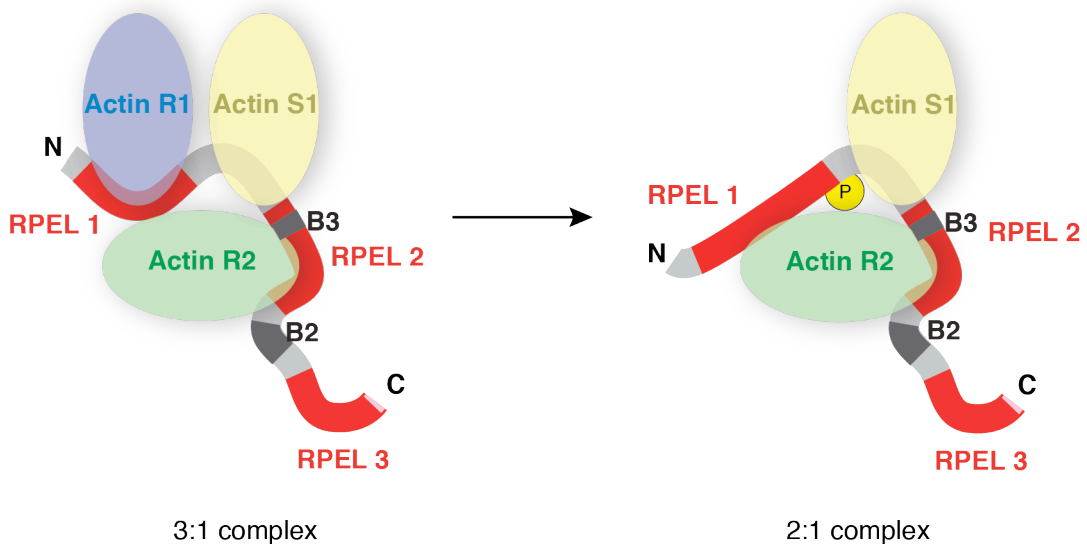


Figure 6.2 Potential mechanism by which S98 phosphorylation blocks actin binding to RPEL1

S98 phosphorylation blocks actin binding to RPEL1 only in the context of the entire RPEL domain. Addition of the phosphate moiety may promote conformational changes that inhibit RPEL1 from adopting the necessary conformation to bind actin.

6.8 MRTF-A export

While disruption of actin binding by CD or RPEL mutations, substantially reduces MRTF-A export, as measured by FLIP, it does not completely block it (Vartiainen et al., 2007). These observations have led to the idea that actin functionally cooperates with Crm1, but the NES involved and the mechanism of cooperativity have not been described.

N-terminal sequences of MRTF-A are sufficient for regulation, but C-terminal sequences also contribute to MRTF-A localisation. Miralles et al. showed that

deletion of the C-terminus (leaving MRTF-A 1-563) renders MRTF-A constitutively nuclear, indicating that sequences that promote export are present in the C-terminus. In addition, deletion of the N-terminus (leaving MRTF-A 200-1021) also led to constitutive nuclear accumulation, suggesting that export-promoting sequences are also present in the first 200 residues (Miralles et al., 2003). Muehlich et al. have reported a NES in the Q-box (residues 356 -377), mutation of which leads to constitutive nuclear localisation (Muehlich et al., 2008). Hayashi et al. reported two regions, one within the α 1 helix of RPEL1 (residues 73-78) and another in the Q-box (residues 356 -377) (Hayashi and Morita, 2013). They show that both regions individually bind Crm1 and mutation of both reduces Crm1 association by 80% (Hayashi and Morita, 2013).

MRTF-A subcellular localisation is therefore defined by the net effect of multiple sequences that affect import and export. Regulation of shuttling however is managed by actin binding to the RPEL domain.

6.9 The MRTF-A RPEL domain is not sufficient for Crm1-mediated export

Phactr1 subcellular localisation, like MRTF-A, is regulated by actin binding to its RPEL domain and in both cases actin competes with importins for binding to the RPEL domain (Wiezlak et al., 2012). Phactr1 however, is not exported by Crm1. Structural analysis and comparison of how the two RPEL domains bind actin revealed that the difference is that the 6-residue-shorter spacers of Phactr cannot bind actin. Otherwise, the relative orientation and distances between the actins bound to RPEL1, 2 and 3 of each RPEL domain, are almost identical (Mouilleron et al., 2012). Since in both proteins a triple RPEL repeat is required for regulation, they allowed investigation of the relationship between Crm1 dependence and the RPEL domain.

In agreement with previous observations (Maria W, unpublished), when the RPEL domain of MRTF-A was replaced with that of Phactr1, the resulting chimera was cytoplasmic and did not accumulate in the nucleus after serum stimulation or LMB treatment, even for prolonged periods of time. While this shows that the RPEL

domain of Phactr1 cannot functionally replace that of MRTF-A, it remains unclear whether the failure of the chimera to respond to Crm1 blockade reflects the weaker Phactr1 NLS or a true functional difference.

The reciprocal exchange, replacing the Phactr1 RPEL by that of MRTF-A, allowed greater insight. The chimera showed greater basal levels of nuclear accumulation compared to Phactr1, which could be reduced by mutation of the NLS elements, without loss of regulation. Export however was Crm1 independent. The RPEL domain alone therefore is not sufficient to confer Crm1 mediated export.

The Phactr1 chimera containing the N-terminus + RPEL domain was indeed LMB sensitive, suggesting that an NES is present in the N-terminus. The chimera was dependent on actin for cytoplasmic localisation, however Crm1 mediated export was independent of actin.

6.10 A nuclear export signal in the N-terminus

The inability of the RPEL domain alone to confer Crm1 mediated export suggested that the N-terminus (2-67) contained an NES. The Phactr1 chimera containing the N-terminus + RPEL domain was indeed LMB sensitive, consistent with the presence of an NES in the N-terminus.

Analysis of the MRTF-A amino acid sequence using the NES prediction software NetNES suggested the presence of an NES in the N-terminus of MRTF-A, between residues 37-48. Being located on a terminal unstructured region of a protein is also a characteristic of NES sequences (Moulleron et al., 2011; Güttler et al., 2010). An Alanine scan across the N-terminus of MRTF-A revealed an NES, the minimal core of which is amino acids 35-52. In the context of amino acids 2-67 the NES exhibited more efficient export, probably due to the presence of S33 that promotes export. The phospho-specific pS33 antibody could be used to test whether S33 is phosphorylated in Rev 2-67 and not Rev 30-60. The export activity exhibited by the Rev 2-67 was entirely dependent on the integrity of the leucine rich sequence.

Consistent with these data, GST-2-67 was able to directly bind Crm1 in a Ran-dependent manner in-vitro and the Crm1 interaction was abolished by

mutation of the leucine rich sequence. Since the N-terminus does not bind actin (Vartiainen et al., 2007), its function must be affected by the RPEL domain, which does bind actin.

6.11 The N-terminus and RPEL domain cooperate to confer actin regulated shuttling

Insertion of the N-terminus, (2-67) into Rev Δ , conferred Crm1 dependent export, which was enhanced by inclusion of C-terminal sequences extending into the RPEL domain. To investigate how the RPEL domain promotes export and allows regulation by actin, a variety of MRTF-A sequences were inserted into the Rev construct. In some experiments, the NLS of MRTF-A was inactivated, eliminating the possibility of actin regulated import.

Although residues 67-115 that correspond to RPEL1-Spacer1, did not exhibit any export activity, they potentiated that of residues 2-67. In agreement with this, GST-2-115 associated better with Crm1 compared to GST-2-67 *in-vitro*, in the absence of actin. These results suggest that the N-terminal NES interacts with the hydrophobic groove of Crm1 and the sequences C-terminal can form additional contacts with Crm1. Such additional interactions were previously reported in the case of Snurportin/Crm1 binding (Monecke et al., 2009). Furthermore, in a subsequent study Snurportin (residues 15-360) was fused to the PKI NES, which stabilised interaction between the NES and the hydrophobic groove of Crm1 (Güttler et al., 2010).

Consistent with the observation that RPEL sequences per se enhance interaction with Crm1 *in-vitro*, loss of contact mutations in RPEL1 did not abolish the enhancement in export activity, as assessed in the context of Rev (2-115) GFP. Interestingly, mutation of R81 enhanced export activity.

The R81A mutation lowers affinity of RPEL1 for actin (Guettler et al., 2008), but resulted in an opposite effect to that of the other mutations which abolish actin binding. The data suggest that weaker actin binding to RPEL1 promotes Crm1 binding.

The RPEL domain is unstructured in solution and forms transient α -helices (Mizuguchi et al., 2014; Mouilleron et al., 2008). Actin binding stabilises formation of the helices observed in the actin-RPEL motif structures (Mouilleron et al., 2008). Actin binding to RPEL1 may occlude the sequences that potentiate Crm1 binding, but promote presentation of the N-terminal NES and stabilise the conformation required to enhance Crm1 binding. Less stable actin binding to RPEL1 may allow more efficient exchange of those sequences between actin and Crm1 (Figure 6.3).

While residues 67-115 enhanced export activity of the N-terminus, 67-204 B2A enhanced export activity even further. In addition, fusion of 67-204 B2A to the N-terminal NES enabled regulation of export activity by actin. Therefore, actin regulation of Crm1-dependent export requires all actin-binding elements of the entire RPEL domain.

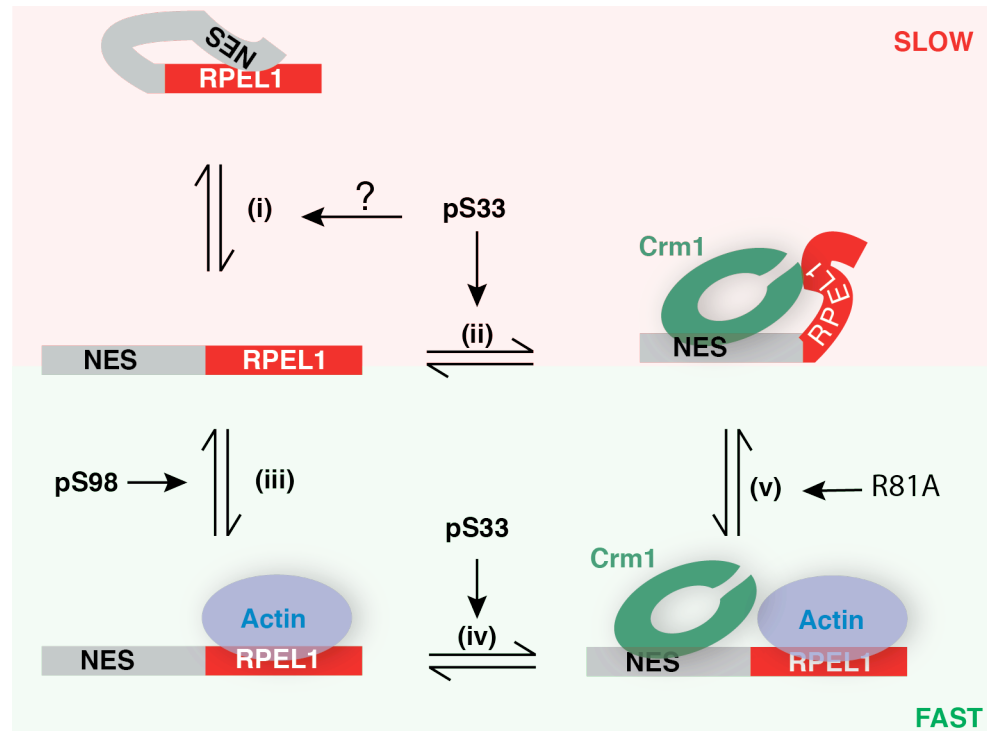


Figure 6.3 Binding of Crm1 to the N-terminal NES is facilitated by RPEL1-Spacer1

The N-terminal NES can autonomously bind Crm1 but C-terminal sequences facilitate binding. Based on this and other observations described in this thesis, the following model can be proposed. (i) In the absence of actin, the N-terminus switches between an open and closed conformation by association with RPEL1 sequences. (ii) In the open conformation Crm1, shown in green, is able to bind the NES and mediate export. The process can be “catalysed” by actin. (iii) Actin binding to RPEL1 stabilises the open conformation (iv) thereby making the NES more readily accessible to Crm1. (v) In a second step actin is displaced from RPEL1 and additional contacts are formed between Crm1 and RPEL, leading to formation of a stable export complex. The steps that could be affected by S33 and S98 phosphorylation are indicated. The R81A mutation, which weakens affinity of the RPEL1-actin interaction, could promote exchange of the RPEL1 sequences from actin to Crm1.

6.12 The role of phosphorylation in the N-terminal region of MRTF-A

S98 phosphorylation promotes MRTF-A nuclear accumulation in response to ERK signalling. Nuclear accumulation observed after TPA stimulation or RafER-mediated activation of ERK is more pronounced in the context of the isolated N-terminus compared to the full-length protein. This is due to the fact that in the full length protein the relative contribution of the RPEL domain is smaller than in the MRTF-A-(2-204)-PK fusion.

TPA stimulation leads to increased G-actin levels, which may mask the effects of S98 phosphorylation. However when RafER was used to activate ERK, nuclear accumulation of full length MRTF-A was also weak. In starved cells G-actin levels are relatively high because of low Rho activity. It is therefore possible that G-actin concentration was too high for phosphorylation of S98 to exert an effect.

It would be interesting to test this hypothesis by comparing localisation of MRTF-A-(2-204)-PK and MRTF-A-(2-204)-PK S98D across a range of G-actin levels. By lowering the affinity of the RPEL domain for actin, pS98 may allow MRTF-A nuclear accumulation at higher G-actin levels, enabling MRTF-A to be activated in response to smaller decreases in cellular G-actin levels (Figure 6.4). In addition S98 phosphorylation could impair formation of the pentameric MRTF-A/actin complex, thereby preventing import inhibition at G-actin concentrations that normally would be inhibitory.

As described in section 1.3.7, nuclear actin dynamics can be regulated. A change in the F/G actin ratio could differentially affect actin binding proteins in the nucleus, depending on their affinity for actin. For example, a brief change in nuclear G-actin may not affect a protein stably bound to an actin monomer. One may speculate that ERK activity could increase the presence of MRTF-A in the nucleus, and in a brief, transient decrease in nuclear G-actin levels, more MRTF-A would be readily activated.

In a recent publication, Aoki et al. showed that cell density affects stochastic ERK activity pulses (Aoki et al., 2013). Sequencing of RNA from cells subjected to pulsatile ERK activity revealed an enrichment in SRF binding sites in pulse-induced genes. One could therefore speculate that ERK activity pulses could activate MRTF

in two ways. ERK could phosphorylate S98 and promote actin dissociation and nuclear accumulation. In addition, ERK could phosphorylate other phosphorylation sites on MRTF-A thereby potentiating activation of target gene expression.

In the absence of stimulation, MRTF-A is nuclear in a small proportion of cells. Because cell density was shown to be inversely related to ERK activity pulses, I tested whether cell density could affect the proportion of nuclear scoring cells. Preliminary data show that indeed the proportion of cells with nuclear MRTF-A-(2-204)-PK decreases as cell density increases (Figure 6.5). In addition MRTF-A-(2-204)-PK S98D is unaffected by cell density. However, nuclear localisation of MRTF-A-(2-204)-PK S98A is affected, suggesting that ERK activity is not the only determinant of localisation of the fusion. Further investigation is needed to determine whether this is solely an effect of ERK pulses and why the S98A derivative is affected. For example, immunofluorescence experiments can be carried out to test for coincident ERK activity and MRTF-A-(2-204)-PK nuclear accumulation. In addition S33 phosphorylation should also be taken into account. Furthermore, if the increase in MRTF-A-(2-204)-PK nuclear accumulation is ERK dependent, it should be tested for U0126 sensitivity.

S33 is also present in the N-terminal region of MRTF-A, in close proximity to the NES. S33 is phosphorylated in starved conditions and promotes MRTF-A export. The mechanism by which pS33 promotes MRTF-A export was not determined. However, since S33 mutants had affected export in the context of the isolated N-terminus (2-67) in the Rev assay, it is likely that S33 directly enhances Crm1 binding to the N-terminal NES. Alanine substitution of S33 led to moderate nuclear accumulation, in agreement with the observation that S33 is phosphorylated. S33A also potentiated nuclear accumulation of S98 phosphorylation, suggesting that the mechanism of how S98 affects steady state involves accessibility of Crm1 to the N-terminal NES.

Multiple studies have shown that proteins such as ERF (Le Gallic et al., 2004) , HIF1 α (Mylonis et al., 2006) and CIITA (Voong et al., 2008) depend on ERK-mediated phosphorylation for promotion or inhibition of Crm1-mediated export. However it was not determined whether phosphorylation directly affected Crm1 binding to the NES, or whether conformational changes led to masking/unmasking.

The finding that phosphorylation of MRTF-A promotes export, is in agreement with Muehlich and colleagues (Muehlich et al., 2008). However S33 was

not present in the MRTF-A derivative used in their studies and cannot be involved in their observations. In addition, in the context of MRTF-A-(2-204)-PK where pS33 affects localisation, their proposed sites (S544, T545, S549) are absent.

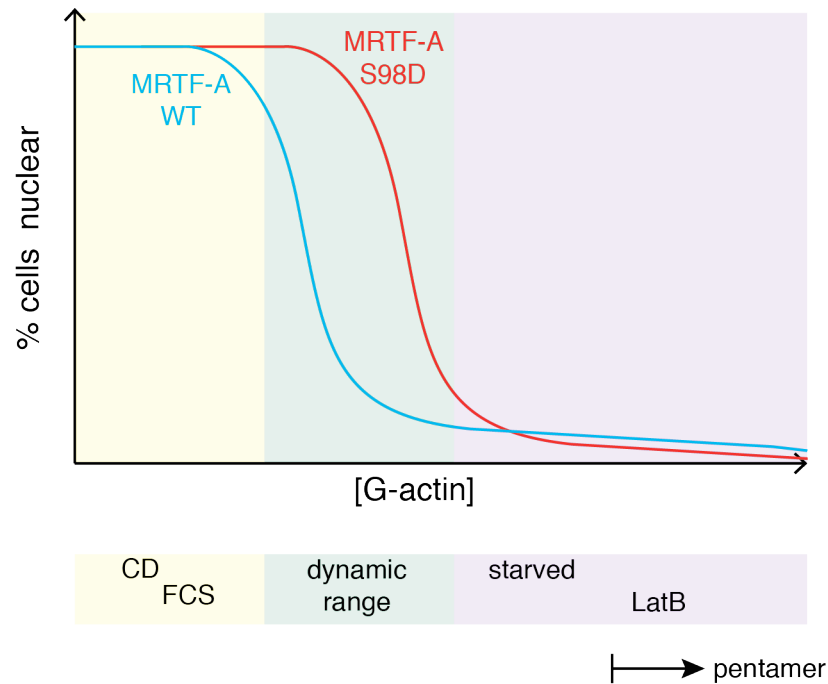


Figure 6.4 Effect of S98 phosphorylation on regulation of MRTF-A localisation

S98 phosphorylation blocks actin binding to RPEL1, which could affect the overall affinity of the RPEL domain for actin. Lowering the affinity of the RPEL domain for actin would allow for nuclear accumulation of MRTF-A at higher G-actin concentrations. Thus, the MAPK pathway can affect sensitivity of MRTF-A to Rho-actin signalling.

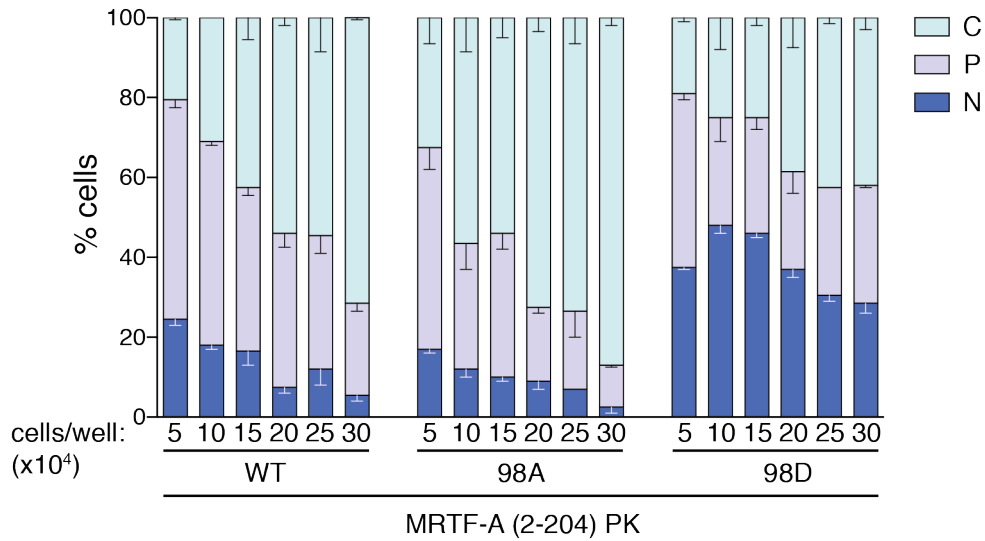


Figure 6.5 Effect of cell density on MRTF-A (2-204) PK localisation

NIH-3T3 cells, seeded at different confluencies were transfected with wild type, S98A or S98D derivatives of MRTF-A (2-204) PK fusion protein. Localisation was determined by immunofluorescence using an anti flag antibody. At least 100 cells were counted and localisation was scored as predominantly nuclear (navy blue), pancellular (lilac) or predominantly cytoplasmic (light blue). Error bars represent standard error of the mean (SEM) from at least two independent experiments.

6.13 Conclusions

In this thesis, I have shown that MRTF-A is subject to regulatory phosphorylation, which impinges on at least two levels: localisation and transactivation efficiency. Phosphorylation on multiple sites is required for maximal MRTF-A activity. Amongst 26 phosphorylation sites, scattered across MRTF-A, S33 and S98 are located in the N-terminus and RPEL domain respectively.

S98 phosphorylation abolishes actin binding to RPEL1 and promotes nuclear accumulation. S98 is phosphorylated by ERK, which requires an ERK docking site located N-terminal to S98. Thus, S98 represents a mechanism by which ERK signalling can affect how MRTF-A senses Rho signalling; the major regulatory pathway of MRTF-A.

In contrast, S33 phosphorylation promotes MRTF-A export, probably by enhancing the interaction between Crm1 and the leucine rich NES which was identified in this study. Although the mechanism by which actin promotes MRTF-A export was not elucidated, I have shown that the RPEL domain itself does not possess a Crm1-dependent NES, but is able to cooperate with the N-terminal NES to confer actin and Crm1 dependent export.

Reference List

- Ahn, N. G. et al. (1992) Current Opinion in Cell Biology | Vol 4, Iss 6, Pgs 919-1092, (December 1992) | ScienceDirect.com. *Current opinion in cell biology*. 4 (6), 992–999.
- Alber, F. et al. (2007) The molecular architecture of the nuclear pore complex. *Nature*. [Online] 450 (7170), 695–701.
- Allen, N. P. C. et al. (2002) Deciphering networks of protein interactions at the nuclear pore complex. *Molecular & cellular proteomics : MCP*. 1 (12), 930–946.
- Allen, P. B. et al. (2004) Phactrs 1-4: A family of protein phosphatase 1 and actin regulatory proteins. *Proceedings of the National Academy of Sciences of the United States of America*. [Online] 101 (18), 7187–7192.
- Anderson, N. G. et al. (1990) Requirement for integration of signals from two distinct phosphorylation pathways for activation of MAP kinase. *Nature*. [Online] 343 (6259), 651–653.
- Ando, R. et al. (2004) Regulated fast nucleocytoplasmic shuttling observed by reversible protein highlighting. *Science (New York, N.Y.)*. [Online] 306 (5700), 1370–1373.
- Andrade, M. A. et al. (2001) Comparison of ARM and HEAT protein repeats. *Journal of molecular biology*. [Online] 309 (1), 1–18.
- Anon (n.d.) Multiple docking sites on substrate proteins form a modular system that mediates recognition by ERK MAP kinase.
- Aoki, K. et al. (2012) Stable expression of FRET biosensors: a new light in cancer research. *Cancer science*. [Online] 103 (4), 614–619.
- Aoki, K. et al. (2013) Stochastic ERK Activation Induced by Noise and Cell-to-Cell Propagation Regulates Cell Density-Dependent Proliferation. *Molecular cell*. [Online] 52 (4), 529–540.
- Aranda, S. et al. (2011) DYRK family of protein kinases: evolutionary relationships, biochemical properties, and functional roles. *FASEB journal : official publication of the Federation of American Societies for Experimental Biology*. [Online] 25 (2), 449–462.
- Aravind, L. & Koonin, E. V. (2000) SAP - a putative DNA-binding motif involved in chromosomal organization. *Trends in biochemical sciences*. 25 (3), 112–114.
- Askjaer, P. et al. (1999) RanGTP-regulated interactions of CRM1 with nucleoporins and a shuttling DEAD-box helicase. *Molecular and cellular biology*. 19 (9), 6276–6285.

- Attwood, P. V. (2013) Histidine kinases from bacteria to humans. *Biochemical Society Transactions*. [Online] 41 (4), 1023–1028.
- Baarlink, C. et al. (2013) Nuclear Actin Network Assembly by Formins Regulates the SRF Coactivator MAL. *Science (New York, N.Y.)*. [Online]
- Ballestrem, C. et al. (2000) Actin-dependent lamellipodia formation and microtubule-dependent tail retraction control-directed cell migration. *Molecular biology of the cell*. 11 (9), 2999–3012.
- Barboric, M. et al. (2001) NF-kappaB binds P-TEFb to stimulate transcriptional elongation by RNA polymerase II. *Molecular cell*. 8 (2), 327–337.
- Bayliss, R. et al. (2000) Structural basis for the interaction between FxFG nucleoporin repeats and importin-beta in nuclear trafficking. *Cell*. 102 (1), 99–108.
- Belaya, K. (2006) FLIPing heterokaryons to analyze nucleo-cytoplasmic shuttling of yeast proteins. *RNA*. [Online] 12 (5), 921–930.
- Biggs, W. H. et al. (1999) Protein kinase B/Akt-mediated phosphorylation promotes nuclear exclusion of the winged helix transcription factor FKHR1. *Proceedings of the National Academy of Sciences*. [Online] 96 (13), 7421–7426.
- Bischoff, F. R. & Görlich, D. (1997) RanBP1 is crucial for the release of RanGTP from importin beta-related nuclear transport factors. *FEBS letters*. 419 (2-3), 249–254.
- Bischoff, F. R. & Ponstingl, H. (1991a) Catalysis of guanine nucleotide exchange on Ran by the mitotic regulator RCC1. *Nature*. [Online] 354 (6348), 80–82.
- Bischoff, F. R. & Ponstingl, H. (1991b) Mitotic regulator protein RCC1 is complexed with a nuclear ras-related polypeptide. *Proceedings of the National Academy of Sciences of the United States of America*. 88 (23), 10830–10834.
- Bischoff, F. R. et al. (1995) Co-activation of RanGTPase and inhibition of GTP dissociation by Ran-GTP binding protein RanBP1. *The EMBO journal*. 14 (4), 705–715.
- Boggon, T. J. & Eck, M. J. (2004) Oncogene - Abstract of article: Structure and regulation of Src family kinases. *Oncogene*.
- Bohnsack, M. T. et al. (2006) A selective block of nuclear actin export stabilizes the giant nuclei of *Xenopus* oocytes. *Nature cell biology*. [Online] 8 (3), 257–263.
- Bonner, W. M. (1975a) Protein migration into nuclei. I. Frog oocyte nuclei in vivo accumulate microinjected histones, allow entry to small proteins, and exclude large proteins. *The Journal of cell biology*. 64 (2), 421–430.
- Bonner, W. M. (1975b) Protein migration into nuclei. II. Frog oocyte nuclei accumulate a class of microinjected oocyte nuclear proteins and exclude a class of microinjected oocyte cytoplasmic proteins. *The Journal of cell biology*.

- Bonnet, F. et al. (1999) Transcription-independent phosphorylation of the RNA polymerase II C-terminal domain (CTD) involves ERK kinases (MEK1/2). *Nucleic acids research*. 27 (22), 4399–4404.
- Boulton, T. G. et al. (1990) An insulin-stimulated protein kinase similar to yeast kinases involved in cell cycle control. *Science (New York, N.Y.)*. 249 (4964), 64–67.
- Boulton, T. G. et al. (1991) ERKs: a family of protein-serine/threonine kinases that are activated and tyrosine phosphorylated in response to insulin and NGF. *Cell*. 65 (4), 663–675. [online].
- Breeuwer, M. & Goldfarb, D. S. (1990) Facilitated nuclear transport of histone H1 and other small nucleophilic proteins. *Cell*. 60 (6), 999–1008.
- Brennan, D. F. et al. (2011) A Raf-induced allosteric transition of KSR stimulates phosphorylation of MEK. *Nature*. [Online] 472 (7343), 366–369.
- Brumbaugh, J. et al. (2014) NANOG Is Multiply Phosphorylated and Directly Modified by ERK2 and CDK1 In Vitro. *Stem cell reports*. [Online] 2 (1), 18–25.
- Brunet, A. et al. (1999) Akt Promotes Cell Survival by Phosphorylating and Inhibiting a Forkhead Transcription Factor. *Cell*. [Online] 96 (6), 857–868.
- Campellone, K. G. & Welch, M. D. (2010) A nucleator arms race: cellular control of actin assembly. *Nature reviews. Molecular cell biology*. [Online] 11 (4), 237–251.
- Carrier, M. F. (1991a) Actin: protein structure and filament dynamics. *The Journal of biological chemistry*. 266 (1), 1–4.
- Carrier, M. F. (1991b) Nucleotide hydrolysis in cytoskeletal assembly. *Current opinion in cell biology*. 3 (1), 12–17.
- Chaudhary, A. et al. (2000) Phosphatidylinositol 3-kinase regulates Raf1 through Pak phosphorylation of serine 338. *Current biology : CB*. 10 (9), 551–554.
- Chen, R. H. et al. (1992) Nuclear localization and regulation of erk- and rsk-encoded protein kinases. *Molecular and cellular biology*.
- Chi, N. C. et al. (1995) Sequence and characterization of cytoplasmic nuclear protein import factor p97. *The Journal of cell biology*. 130 (2), 265–274.
- Chuderland, D. & Seger, R. (2005) Protein-protein interactions in the regulation of the extracellular signal-regulated kinase. *Molecular biotechnology*. [Online] 29 (1), 57–74.
- Chuderland, D. et al. (2008) Identification and characterization of a general nuclear translocation signal in signaling proteins. *Molecular cell*. [Online] 31 (6), 850–861.

- Cingolani, G. et al. (2002) Molecular Basis for the Recognition of a Nonclassical Nuclear Localization Signal by Importin β . *Molecular cell*. [Online] 10 (6), 1345–1353.
- Clark-Lewis, I. et al. (1991) Definition of a consensus sequence for peptide substrate recognition by p44mpk, the meiosis-activated myelin basic protein kinase. *Journal of Biological Chemistry*.
- Cochran, B. et al. (1984) Expression of the c-fos gene and of an fos-related gene is stimulated by platelet-derived growth factor. *Science (New York, N.Y.)*. [Online] 226 (4678), 1080–1082.
- Conti, E. & Kuriyan, J. (2000) Crystallographic analysis of the specific yet versatile recognition of distinct nuclear localization signals by karyopherin alpha. *Structure (London, England : 1993)*. 8 (3), 329–338.
- Conti, E. et al. (2006) Karyopherin flexibility in nucleocytoplasmic transport. *Current opinion in structural biology*. [Online] 16 (2), 237–244.
- Cook, A. et al. (2007) Structural biology of nucleocytoplasmic transport. *Annual review of biochemistry*. [Online] 76647–671.
- Cooper, J A (1987) Effects of cytochalasin and phalloidin on actin. *The Journal of cell biology*. 105 (4), 1473–1478.
- Cooper, Jonathan A et al. (1982) Similar effects of platelet-derived growth factor and epidermal growth factor on the phosphorylation of tyrosine in cellular proteins. *Cell*. [Online] 31 (1), 263–273.
- Copeland, J. W. & Treisman, R. (2002) The diaphanous-related formin mDia1 controls serum response factor activity through its effects on actin polymerization. *Molecular biology of the cell*. [Online] 13 (11), 4088–4099.
- Coué, M. et al. (1987) Inhibition of actin polymerization by latrunculin A. *FEBS letters*. 213 (2), 316–318. [online].
- Coutavas, E. et al. (1993) Characterization of proteins that interact with the cell-cycle regulatory protein Ran/TC4. *Nature*. [Online] 366 (6455), 585–587.
- Crabtree, G. R. (1999) Generic signals and specific outcomes: signaling through Ca²⁺, calcineurin, and NF-AT. *Cell*. 96 (5), 611–614.
- Cruzalegui, F. H. et al. (1999) ERK activation induces phosphorylation of Elk-1 at multiple S/T-P motifs to high stoichiometry. *Oncogene*. [Online] 18 (56), 7948–7957.
- Davies, S. P. et al. (2000) Specificity and mechanism of action of some commonly used protein kinase inhibitors. *The Biochemical journal*. 351 (Pt 1), 95–105.
- Day, R. N. & Davidson, M. W. (2009) The fluorescent protein palette: tools for cellular imaging. *Chemical Society reviews*. [Online] 38 (10), 2887–2921.

- Delphin, C. et al. (1997) RanGTP targets p97 to RanBP2, a filamentous protein localized at the cytoplasmic periphery of the nuclear pore complex. *Molecular biology of the cell*. 8 (12), 2379–2390.
- Denning, D. P. et al. (2002) The *Saccharomyces cerevisiae* nucleoporin Nup2p is a natively unfolded protein. *The Journal of biological chemistry*. [Online] 277 (36), 33447–33455.
- Devos, D. et al. (2004) Components of coated vesicles and nuclear pore complexes share a common molecular architecture. *PLoS biology*. [Online] 2 (12), e380.
- Didsbury, J. et al. (1989) rac, a novel ras-related family of proteins that are botulinum toxin substrates. *The Journal of biological chemistry*. 264 (28), 16378–16382.
- Dingwall, C. & Laskey, R. A. (1998) Nuclear import: a tale of two sites. *Current biology : CB*. 8 (25), R922–R924. [online].
- Dingwall, C. et al. (1982) A polypeptide domain that specifies migration of nucleoplasmin into the nucleus. *Cell*. 30 (2), 449–458.
- Dominguez, R. (2004) Actin-binding proteins – a unifying hypothesis. *Trends in biochemical sciences*. [Online] 29 (11), 572–578.
- Dominguez, R. & Holmes, K. C. (2011) Actin structure and function. *Annual review of biophysics*. [Online] 40169–186.
- Dong, X. et al. (2009) Structural basis for leucine-rich nuclear export signal recognition by CRM1. *Nature*. [Online] 458 (7242), 1136–1141.
- Dopie, J. et al. (2012) Active maintenance of nuclear actin by importin 9 supports transcription. *Proceedings of the National Academy of Sciences*. [Online] 109 (9), E544–E552.
- DOWNWARD, J. (2003) Role of receptor tyrosine kinases in G-protein-coupled receptor regulation of Ras: transactivation or parallel pathways? *The Biochemical journal*. [Online] 376 (3), e9.
- Dumaz, N. et al. (2002) Cyclic AMP blocks cell growth through Raf-1-dependent and Raf-1-independent mechanisms. *Molecular and cellular biology*. 22 (11), 3717–3728.
- Duncia, J. V. et al. (1998) MEK inhibitors: the chemistry and biological activity of U0126, its analogs, and cyclization products. *Bioorganic & medicinal chemistry letters*. 8 (20), 2839–2844.
- Egelman, E. H. et al. (1982) F-actin is a helix with a random variable twist. *Nature*. [Online] 298 (5870), 131–135.
- Eick, D. & Geyer, M. (2013) The RNA polymerase II carboxy-terminal domain (CTD) code. *Chemical reviews*. [Online] 113 (11), 8456–8490.

- Eiseler, T. et al. (2007) PKD is recruited to sites of actin remodelling at the leading edge and negatively regulates cell migration. *FEBS letters*. [Online] 581 (22), 4279–4287.
- Eiseler, T. et al. (2009) Protein kinase D1 regulates cofilin-mediated F-actin reorganization and cell motility through slingshot. *Nature cell biology*. [Online] 11 (5), 545–556.
- Engelsma, D. et al. (2004) Supraphysiological nuclear export signals bind CRM1 independently of RanGTP and arrest at Nup358. *The EMBO journal*. [Online] 23 (18), 3643–3652.
- Esnault, C. et al. (2014) Rho-actin signaling to the MRTF coactivators dominates the immediate transcriptional response to serum in fibroblasts. *Genes & development*. [Online] 28 (9), 943–958.
- Farooq, A. & Zhou, M.-M. (2004) Structure and regulation of MAPK phosphatases. *Cellular signalling*. [Online] 16 (7), 769–779.
- Fenteany, G. & Zhu, S. (2003) Small-molecule inhibitors of actin dynamics and cell motility. *Current topics in medicinal chemistry*. 3 (6), 593–616.
- Flach, J. et al. (1994) A yeast RNA-binding protein shuttles between the nucleus and the cytoplasm. *Molecular and cellular biology*. 14 (12), 8399–8407.
- Fornerod, M. et al. (1997) CRM1 is an export receptor for leucine-rich nuclear export signals. *Cell*. 90 (6), 1051–1060.
- Fox, A. M. et al. (2011) Electrostatic interactions involving the extreme C terminus of nuclear export factor CRM1 modulate its affinity for cargo. *The Journal of biological chemistry*. [Online] 286 (33), 29325–29335.
- Frey, S. & Görlich, D. (2007) A saturated FG-repeat hydrogel can reproduce the permeability properties of nuclear pore complexes. *Cell*. [Online] 130 (3), 512–523.
- Frey, S. & Görlich, D. (2009) FG/FxFG as well as GLFG repeats form a selective permeability barrier with self-healing properties. *The EMBO journal*. [Online] 28 (17), 2554–2567.
- Frey, S. et al. (2006) FG-rich repeats of nuclear pore proteins form a three-dimensional meshwork with hydrogel-like properties. *Science (New York, N.Y.)*. [Online] 314 (5800), 815–817.
- Fu, S.-C. et al. (2013) ValidNESs: a database of validated leucine-rich nuclear export signals. *Nucleic acids research*. [Online] 41 (Database issue), D338–D343.
- Fujioka, A. et al. (2006) Dynamics of the Ras/ERK MAPK cascade as monitored by fluorescent probes. *The Journal of biological chemistry*. [Online] 281 (13), 8917–8926.

- Fukuda, M. et al. (1997) Interaction of MAP kinase with MAP kinase kinase: its possible role in the control of nucleocytoplasmic transport of MAP kinase. *The EMBO journal*. [Online] 16 (8), 1901–1908.
- Galarneau, L. et al. (2000) Multiple links between the NuA4 histone acetyltransferase complex and epigenetic control of transcription. *Molecular cell*. 5 (6), 927–937.
- Galbraith, M. D. et al. (2013) ERK phosphorylation of MED14 in promoter complexes during mitogen-induced gene activation by Elk-1. *Nucleic acids research*. [Online] 41 (22), 10241–10253.
- Galkin, V. E. et al. (2002) A new internal mode in F-actin helps explain the remarkable evolutionary conservation of actin's sequence and structure. *Current biology : CB*. 12 (7), 570–575.
- Galkin, V. E. et al. (2010) Structural polymorphism in F-actin. *Nature structural & molecular biology*. [Online] 17 (11), 1318–1323.
- Garai, Á. et al. (2012) Specificity of linear motifs that bind to a common mitogen-activated protein kinase docking groove. *Science signaling*. [Online] 5 (245), ra74.
- Geneste, O. et al. (2002) LIM kinase and Diaphanous cooperate to regulate serum response factor and actin dynamics. *The Journal of cell biology*. [Online] 157 (5), 831–838.
- Gerber, A. et al. (2013) Blood-borne circadian signal stimulates daily oscillations in actin dynamics and SRF activity. *Cell*. [Online] 152 (3), 492–503.
- Ghosh, S. & Karin, M. (2002) Missing pieces in the NF-kappaB puzzle. *Cell*. 109 SupplS81–S96.
- Ghosh, S. et al. (1998) NF-kappa B and Rel proteins: evolutionarily conserved mediators of immune responses. *Annual review of immunology*. [Online] 16225–260.
- Gilchrist, D. et al. (2002) Accelerating the Rate of Disassembly of Karyopherin·Cargo Complexes. *Journal of Biological Chemistry*.
- Gnad, F. et al. (2011) PHOSIDA 2011: the posttranslational modification database. *Nucleic acids research*. [Online] 39 (Database issue), D253–D260.
- Goldfarb, D. S. et al. (2004) Importin alpha: a multipurpose nuclear-transport receptor. *Trends in cell biology*. [Online] 14 (9), 505–514.
- Goldfarb, D. S. et al. (1986) Synthetic peptides as nuclear localization signals. *Nature*. [Online] 322 (6080), 641–644.
- Gontan, C. et al. (2009) Exportin 4 mediates a novel nuclear import pathway for Sox family transcription factors. *The Journal of cell biology*. [Online] 185 (1), 27–34.

- Gonzalez, F. A. et al. (1991) Identification of substrate recognition determinants for human ERK1 and ERK2 protein kinases. *The Journal of biological chemistry*. 266 (33), 22159–22163.
- Göckler, N. et al. (2009) Harmine specifically inhibits protein kinase DYRK1A and interferes with neurite formation. *The FEBS journal*. [Online] 276 (21), 6324–6337.
- Görlich, D. & Kutay, U. (1999) Transport between the cell nucleus and the cytoplasm. *Annual review of cell and developmental biology*. [Online] 15607–660.
- Görlich, D. et al. (1996) Identification of different roles for RanGDP and RanGTP in nuclear protein import. *The EMBO journal*. 15 (20), 5584–5594.
- Görlich, D. et al. (1995) Two different subunits of importin cooperate to recognize nuclear localization signals and bind them to the nuclear envelope. *Current biology : CB*. 5 (4), 383–392.
- Graceffa, P. & Dominguez, R. (2003) Crystal structure of monomeric actin in the ATP state. Structural basis of nucleotide-dependent actin dynamics. *The Journal of biological chemistry*. [Online] 278 (36), 34172–34180.
- Grammer, T. C. & Blenis, J. (1997) Evidence for MEK-independent pathways regulating the prolonged activation of the ERK-MAP kinases. *Oncogene*. [Online] 14 (14), 1635–1642.
- Greenberg, M. E. & Ziff, E. B. (1984) Stimulation of 3T3 cells induces transcription of the c-fos proto-oncogene. *Nature*. 311 (5985), 433–438.
- Griner, E. M. & Kazanietz, M. G. (2007) Protein kinase C and other diacylglycerol effectors in cancer. *Nature reviews. Cancer*. [Online] 7 (4), 281–294.
- Guettler, S. et al. (2008) RPEL motifs link the serum response factor cofactor MAL but not myocardin to Rho signaling via actin binding. *Molecular and cellular biology*. [Online] 28 (2), 732–742.
- Gupton, S. L. & Gertler, F. B. (2007) Filopodia: the fingers that do the walking. *Science's STKE : signal transduction knowledge environment*. [Online] 2007 (400), re5.
- Güttler, T. et al. (2010) NES consensus redefined by structures of PKI-type and Rev-type nuclear export signals bound to CRM1. *Nature structural & molecular biology*. [Online] 17 (11), 1367–1376.
- Haberland, J. & Gerke, V. (1995) Recombinant expression and domain structure of the Rna1 protein from *Schizosaccharomyces pombe*. *FEBS letters*. 357 (2), 173–177.
- Haché, R. J. et al. (1999) Nucleocytoplasmic trafficking of steroid-free glucocorticoid receptor. *The Journal of biological chemistry*. 274 (3), 1432–1439.

- Hall, F. L. & Vulliet, P. R. (1991) Proline-directed protein phosphorylation and cell cycle regulation. *Current opinion in cell biology*. [Online] 3 (2), 176–184.
- Hanson, J. & Lowy, J. (1963) The structure of F-actin and of actin filaments isolated from muscle. *Journal of molecular biology*. [Online] 6 (1), 46–IN5.
- Harreman, M. T. et al. (2003) Characterization of the auto-inhibitory sequence within the N-terminal domain of importin alpha. *The Journal of biological chemistry*. [Online] 278 (24), 21361–21369.
- Hatano, N. et al. (2003) Essential role for ERK2 mitogen-activated protein kinase in placental development. *Genes to cells : devoted to molecular & cellular mechanisms*. 8 (11), 847–856.
- Hayashi, K. & Morita, T. (2013) Differences in the nuclear export mechanism between myocardin and myocardin-related transcription factor A. *The Journal of biological chemistry*. [Online] 288 (8), 5743–5755.
- Hayden, M. S. & Ghosh, S. (2004) Signaling to NF-kappaB. *Genes & development*. [Online] 18 (18), 2195–2224.
- Heasman, S. J. & Ridley, A. J. (2008) Mammalian Rho GTPases: new insights into their functions from in vivo studies. *Nature reviews. Molecular cell biology*. [Online] 9 (9), 690–701.
- Henderson, B. R. & Eleftheriou, A. (2000) A comparison of the activity, sequence specificity, and CRM1-dependence of different nuclear export signals. *Experimental cell research*. [Online] 256 (1), 213–224.
- Henderson, B. R. & Percipalle, P. (1997) Interactions between HIV Rev and nuclear import and export factors: the Rev nuclear localisation signal mediates specific binding to human importin-beta. *Journal of molecular biology*. [Online] 274 (5), 693–707.
- Henderson, J. N. (2006) The Kindling Fluorescent Protein: A Transient Photoswitchable Marker. *Physiology*. [Online] 21 (3), 162–170.
- Herman, I. M. (1993) Actin isoforms. *Current opinion in cell biology*. 5 (1), 48–55.
- Hetzer, M. W. (2010) The Nuclear Envelope. *Cold Spring Harbor Perspectives in Biology*. [Online] 2 (3), a000539–a000539.
- Heyduk, T. & Lee, J. C. (1990) Application of fluorescence energy transfer and polarization to monitor Escherichia coli cAMP receptor protein and lac promoter interaction. *Proceedings of the National Academy of Sciences of the United States of America*. 87 (5), 1744–1748.
- Heyduk, T. et al. (1996) *Methods in Enzymology*. Vol. 274. [Online]. Elsevier.
- Higuchi, C. et al. (2009) Transient dynamic actin cytoskeletal change stimulates the osteoblastic differentiation. *Journal of bone and mineral metabolism*. [Online] 27 (2), 158–167.

- Hill, C. S. & Treisman, R. (1995) Transcriptional regulation by extracellular signals: mechanisms and specificity. *Cell*. 80 (2), 199–211.
- Hill, C. S. et al. (1994) Serum-regulated transcription by serum response factor (SRF): a novel role for the DNA binding domain. *The EMBO journal*. 13 (22), 5421–5432.
- Hill, C. S. et al. (1995) The Rho family GTPases RhoA, Rac1, and CDC42Hs regulate transcriptional activation by SRF. *Cell*. 81 (7), 1159–1170.
- Himpel, S. et al. (2000) Specificity determinants of substrate recognition by the protein kinase DYRK1A. *The Journal of biological chemistry*. 275 (4), 2431–2438.
- Ho, J. H. et al. (2000) Nmd3p is a Crm1p-dependent adapter protein for nuclear export of the large ribosomal subunit. *The Journal of cell biology*. 151 (5), 1057–1066.
- Holmes, K. C. et al. (1990) Atomic model of the actin filament. *Nature*.
- Huet, G. et al. (2013) Actin-regulated feedback loop based on Phactr4, PP1 and cofilin maintains the actin monomer pool. *Journal of cell science*. [Online] 126 (Pt 2), 497–507.
- Hung, R.-J. et al. (2011) Direct redox regulation of F-actin assembly and disassembly by Mical. *Science (New York, N.Y.)*. [Online] 334 (6063), 1710–1713.
- Hülsmann, B. B. et al. (2012) The Permeability of Reconstituted Nuclear Pores Provides Direct Evidence for the Selective Phase Model. *Cell*. [Online] 150 (4), 738–751.
- Jockusch, B. M. et al. (2006) Tracking down the different forms of nuclear actin. *Trends in cell biology*. [Online] 16 (8), 391–396.
- Johnson, C. et al. (1999) An N-terminal nuclear export signal is required for the nucleocytoplasmic shuttling of I κ B α . *The EMBO journal*. [Online] 18 (23), 6682–6693.
- Johnson, L. N. (2009) The regulation of protein phosphorylation. - Abstract - Europe PubMed Central. *Biochemical Society Transactions*.
- Johnson, L. N. & Lewis, R. J. (2001) Structural basis for control by phosphorylation. *Chemical reviews*.
- Kabsch, W. et al. (1990) Atomic structure of the actin: DNase I complex. *Nature*.
- Kalita, K. et al. (2006) Role of megakaryoblastic acute leukemia-1 in ERK1/2-dependent stimulation of serum response factor-driven transcription by BDNF or increased synaptic activity. *The Journal of neuroscience : the official journal of the Society for Neuroscience*. [Online] 26 (39), 10020–10032.

- Keyse, S. M. (2000) Protein phosphatases and the regulation of mitogen-activated protein kinase signalling. *Current opinion in cell biology*. 12 (2), 186–192.
- Khokhlatchev, A. V. et al. (1998) Phosphorylation of the MAP kinase ERK2 promotes its homodimerization and nuclear translocation. *Cell*. 93 (4), 605–615.
- Kitzing, T. M. et al. (2007) Positive feedback between Dia1, LARG, and RhoA regulates cell morphology and invasion. *Genes & development*. [Online] 21 (12), 1478–1483.
- Klebe, C. et al. (1995) Interaction of the nuclear GTP-binding protein Ran with its regulatory proteins RCC1 and RanGAP1. *Biochemistry*. 34 (2), 639–647.
- Kobe, B. (1999) Autoinhibition by an internal nuclear localization signal revealed by the crystal structure of mammalian importin alpha. *Nature structural biology*. [Online] 6 (4), 388–397.
- Kolch, W. et al. (1993) Protein kinase C alpha activates RAF-1 by direct phosphorylation. *Nature*. [Online] 364 (6434), 249–252.
- Korn, E. D. (1982) Actin polymerization and its regulation by proteins from nonmuscle cells. *Physiological reviews*. 62 (2), 672–737.
- Kose, S. et al. (1999) beta-subunit of nuclear pore-targeting complex (importin-beta) can be exported from the nucleus in a Ran-independent manner. *The Journal of biological chemistry*. 274 (7), 3946–3952.
- Kosugi, S. et al. (2009) Six classes of nuclear localization signals specific to different binding grooves of importin alpha. *The Journal of biological chemistry*. [Online] 284 (1), 478–485.
- Kõivomägi, M. et al. (2013) Multisite phosphorylation networks as signal processors for Cdk1. *Nature structural & molecular biology*. [Online] 20 (12), 1415–1424.
- Köster, M. et al. (2005) Nucleocytoplasmic shuttling revealed by FRAP and FLIP technologies. *Current opinion in biotechnology*. [Online] 16 (1), 28–34.
- Kruse, J. P. & Gu, W. (2008) SnapShot: p53 posttranslational modifications. *Cell*.
- Kudo, N. et al. (1999) Leptomycin B inactivates CRM1/exportin 1 by covalent modification at a cysteine residue in the central conserved region. *Proceedings of the National Academy of Sciences of the United States of America*. 96 (16), 9112–9117.
- Kudryashov, D. S. et al. (2010) A nucleotide state-sensing region on actin. *The Journal of biological chemistry*. [Online] 285 (33), 25591–25601.
- Kutay, U. & Güttlinger, S. (2005) Leucine-rich nuclear-export signals: born to be weak. *Trends in cell biology*. [Online] 15 (3), 121–124.

- Kutay, U. et al. (1997) Export of importin alpha from the nucleus is mediated by a specific nuclear transport factor. *Cell*. 90 (6), 1061–1071.
- Kutay, U. et al. (1998) Identification of a tRNA-specific nuclear export receptor. *Molecular cell*. 1 (3), 359–369.
- Kyriakis, J. M. & Avruch, J. (2012) Mammalian MAPK Signal Transduction Pathways Activated by Stress and Inflammation: A 10-Year Update. *Physiological reviews*. [Online] 92 (2), 689–737.
- la Cour, T. et al. (2004) Analysis and prediction of leucine-rich nuclear export signals. *Protein engineering, design & selection : PEDS*. [Online] 17 (6), 527–536.
- Lane, N. J. (1969) INTRANUCLEAR FIBRILLAR BODIES IN ACTINOMYCIN D-TREATED OOCYTES. *The Journal of cell biology*. 40 (1), 286.
- Lauffenburger, D. A. & Horwitz, A. F. (1996) Cell migration: a physically integrated molecular process. *Cell*. 84 (3), 359–369.
- Lavin, M. F. & Gueven, N. (2006) The complexity of p53 stabilization and activation. *Cell death and differentiation*. [Online] 13 (6), 941–950.
- Le Gallic, L. et al. (2004) ERF nuclear shuttling, a continuous monitor of Erk activity that links it to cell cycle progression. *Molecular and cellular biology*. 24 (3), 1206–1218.
- Leder, S. et al. (1999) Cloning and characterization of DYRK1B, a novel member of the DYRK family of protein kinases. *Biochemical and biophysical research communications*. [Online] 254 (2), 474–479. [online].
- Lee, S. J. et al. (2003) The Structure of Importin- β Bound to SREBP-2: Nuclear Import of a Transcription Factor. *Science (New York, N.Y.)*.
- Lefloch, R. et al. (2008) Single and combined silencing of ERK1 and ERK2 reveals their positive contribution to growth signaling depending on their expression levels. *Molecular and cellular biology*. [Online] 28 (1), 511–527.
- Lemmon, M. A. & Schlessinger, J. (2010) Cell signaling by receptor tyrosine kinases. *Cell*. [Online] 141 (7), 1117–1134.
- Lenormand, P. et al. (1998) Growth factor-induced p42/p44 MAPK nuclear translocation and retention requires both MAPK activation and neosynthesis of nuclear anchoring proteins. *The Journal of cell biology*. 142 (3), 625–633.
- Li, J. et al. (2005) Myocardin-related transcription factor B is required in cardiac neural crest for smooth muscle differentiation and cardiovascular development. *Proceedings of the National Academy of Sciences*. [Online] 102 (25), 8916–8921.

- Li, S. et al. (2006) Requirement of a myocardin-related transcription factor for development of mammary myoepithelial cells. *Molecular and cellular biology*. [Online] 26 (15), 5797–5808.
- Lim, S. & Kaldis, P. (2013) Cdks, cyclins and CKIs: roles beyond cell cycle regulation. *Development (Cambridge, England)*. [Online] 140 (15), 3079–3093.
- Lloyd, A. C. (2006) Distinct functions for ERKs? *Journal of biology*. [Online] 5 (5), 13.
- Lorenz, M. et al. (1993) Refinement of the F-actin model against X-ray fiber diffraction data by the use of a directed mutation algorithm. *Journal of molecular biology*. [Online] 234 (3), 826–836.
- Lundquist, M. R. et al. (2014) Redox modification of nuclear actin by MICAL-2 regulates SRF signaling. *Cell*. [Online] 156 (3), 563–576.
- Luttrell, L. M. et al. (2001) Activation and targeting of extracellular signal-regulated kinases by β -arrestin scaffolds. *Proceedings of the National Academy of Sciences*. [Online] 98 (5), 2449–2454.
- Lynch, K. W. (2006) Cotranscriptional splicing regulation: it's not just about speed. *Nature*.
- Ma, Z. et al. (2001) Fusion of two novel genes, RBM15 and MKL1, in the t(1;22)(p13;q13) of acute megakaryoblastic leukemia. *Nature genetics*. [Online] 28 (3), 220–221.
- Macara, I. G. (2001) Transport into and out of the Nucleus. *Microbiology and Molecular Biology Reviews*.
- Mahajan, R. et al. (1997) A small ubiquitin-related polypeptide involved in targeting RanGAP1 to nuclear pore complex protein RanBP2. *Cell*. 88 (1), 97–107.
- Manning, G. et al. (2002) The protein kinase complement of the human genome. *Science (New York, N.Y.)*. [Online] 298 (5600), 1912–1934.
- Mansour, S. J. et al. (1994) Transformation of mammalian cells by constitutively active MAP kinase kinase. *Science (New York, N.Y.)*. 265 (5174), 966–970.
- Marinissen, M. J. & Gutkind, J. S. (2005) Scaffold proteins dictate Rho GTPase-signaling specificity. *Trends in biochemical sciences*. [Online] 30 (8), 423–426.
- Marquardt, B. et al. (1994) Signalling from TPA to MAP kinase requires protein kinase C, raf and MEK: reconstitution of the signalling pathway in vitro. *Oncogene*. 9 (11), 3213–3218.
- Marshall, C. J. (1995) Specificity of receptor tyrosine kinase signaling: transient versus sustained extracellular signal-regulated kinase activation. *Cell*. 80 (2), 179–185.

- Matsuura, Y. & Stewart, M. (2005) Nup50/Npap60 function in nuclear protein import complex disassembly and importin recycling. *The EMBO journal*. [Online] 24 (21), 3681–3689.
- Matunis, M. J. et al. (1996) A novel ubiquitin-like modification modulates the partitioning of the Ran-GTPase-activating protein RanGAP1 between the cytosol and the nuclear pore complex. *The Journal of cell biology*. 135 (6 Pt 1), 1457–1470.
- McGee, K. M. et al. (2011) Nuclear transport of the serum response factor coactivator MRTF-A is downregulated at tensional homeostasis. *EMBO reports*. [Online] 12 (9), 963–970.
- Medjkane, S. et al. (2009) Myocardin-related transcription factors and SRF are required for cytoskeletal dynamics and experimental metastasis. *Nature cell biology*. [Online] 11 (3), 257–268.
- Mercher, T. et al. (2001) Involvement of a human gene related to the *Drosophila* spen gene in the recurrent t(1;22) translocation of acute megakaryocytic leukemia. *Proceedings of the National Academy of Sciences of the United States of America*. [Online] 98 (10), 5776–5779.
- Meyer, T. et al. (2002) Constitutive and IFN-gamma-induced nuclear import of STAT1 proceed through independent pathways. *The EMBO journal*. [Online] 21 (3), 344–354.
- Milburn, M. V. et al. (1990) Molecular switch for signal transduction: structural differences between active and inactive forms of protooncogenic ras proteins. *Science (New York, N.Y.)*. 247 (4945), 939–945.
- Miralles, F. et al. (2003) Actin dynamics control SRF activity by regulation of its coactivator MAL. *Cell*. 113 (3), 329–342.
- Miyawaki, A. (2005) Innovations in the imaging of brain functions using fluorescent proteins. *Neuron*. [Online] 48 (2), 189–199.
- Miyawaki, A. (2011) Proteins on the move: insights gained from fluorescent protein technologies. *Nature reviews. Molecular cell biology*. [Online] 12 (10), 656–668.
- Mizuguchi, M. et al. (2014) Transient α -helices in the disordered RPEL motifs of the serum response factor coactivator MKL1. *Scientific reports*. [Online] 45224.
- Mohun, T. et al. (1987) *Xenopus* cytoskeletal actin and human c-fos gene promoters share a conserved protein-binding site. *The EMBO journal*. 6 (3), 667–673.
- Molina, D. M. et al. (2005) Characterization of an ERK-binding domain in microphthalmia-associated transcription factor and differential inhibition of ERK2-mediated substrate phosphorylation. *The Journal of biological chemistry*. [Online] 280 (51), 42051–42060.

- Moll, U. M. & Petrenko, O. (2003) The MDM2-p53 interaction. *Molecular cancer research : MCR.* 1 (14), 1001–1008.
- Monecke, T. et al. (2009) Crystal structure of the nuclear export receptor CRM1 in complex with Snurportin1 and RanGTP. *Science (New York, N.Y.).* [Online] 324 (5930), 1087–1091.
- Monecke, T. et al. (2013) Structural basis for cooperativity of CRM1 export complex formation. *Proceedings of the National Academy of Sciences.* [Online] 110 (3), 960–965.
- Moore, M. S. & Blobel, G. (1994) Purification of a Ran-interacting protein that is required for protein import into the nucleus. *Proceedings of the National Academy of Sciences of the United States of America.* 91 (21), 10212–10216.
- Morton, W. M. et al. (2000) Latrunculin alters the actin-monomer subunit interface to prevent polymerization. *Nature cell biology.* [Online] 2 (6), 376–378.
- Mosammamarast, N. & Pemberton, L. F. (2004) Karyopherins: from nuclear-transport mediators to nuclear-function regulators. *Trends in cell biology.* [Online] 14 (10), 547–556.
- Mouilleron, S. et al. (2008) Molecular basis for G-actin binding to RPEL motifs from the serum response factor coactivator MAL. *The EMBO journal.* [Online] 27 (23), 3198–3208.
- Mouilleron, S. et al. (2011) Structure of a pentavalent G-actin*MRTF-A complex reveals how G-actin controls nucleocytoplasmic shuttling of a transcriptional coactivator. *Science signaling.* [Online] 4 (177), ra40.
- Mouilleron, S. et al. (2012) Structures of the Phactr1 RPEL domain and RPEL motif complexes with G-actin reveal the molecular basis for actin binding cooperativity. *Structure (London, England : 1993).* [Online] 20 (11), 1960–1970.
- Muehlich, S. et al. (2008) Serum-induced phosphorylation of the serum response factor coactivator MKL1 by the extracellular signal-regulated kinase 1/2 pathway inhibits its nuclear localization. *Molecular and cellular biology.* [Online] 28 (20), 6302–6313.
- Murphy, L. O. et al. (2002) Molecular interpretation of ERK signal duration by immediate early gene products. *Nature cell biology.* [Online] 4 (8), 556–564.
- Mylonis, I. et al. (2006) Identification of MAPK phosphorylation sites and their role in the localization and activity of hypoxia-inducible factor-1alpha. *The Journal of biological chemistry.* [Online] 281 (44), 33095–33106.
- Nakagawa, K. & Kuzumaki, N. (2005) Transcriptional activity of megakaryoblastic leukemia 1 (MKL1) is repressed by SUMO modification. *Genes to cells : devoted to molecular & cellular mechanisms.* [Online] 10 (8), 835–850.

- Nemergut, M. E. et al. (2001) Chromatin docking and exchange activity enhancement of RCC1 by histones H2A and H2B. *Science (New York, N.Y.)*. [Online] 292 (5521), 1540–1543.
- Nilsson, J. et al. (2002) The C-terminal extension of the small GTPase Ran is essential for defining the GDP-bound form. *Journal of molecular biology*. [Online] 318 (2), 583–593.
- Northwood, I. C. et al. (1991) Isolation and characterization of two growth factor-stimulated protein kinases that phosphorylate the epidermal growth factor receptor at threonine 669. *The Journal of biological chemistry*. 266 (23), 15266–15276.
- Oda, T. et al. (2009) The nature of the globular- to fibrous-actin transition. *Nature*. [Online] 457 (7228), 441–445.
- Oh, J. et al. (2005) Requirement of myocardin-related transcription factor-B for remodeling of branchial arch arteries and smooth muscle differentiation. *Proceedings of the National Academy of Sciences of the United States of America*. [Online] 102 (42), 15122–15127.
- Olsen, J. V. et al. (2006) Global, in vivo, and site-specific phosphorylation dynamics in signaling networks. *Cell*. [Online] 127 (3), 635–648.
- Owens, D. M. & Keyse, S. M. (2007) Differential regulation of MAP kinase signalling by dual-specificity protein phosphatases. *Oncogene*. [Online] 26 (22), 3203–3213.
- P Lang, F. G. M. D.-C. R. S. M. P. J. B. (1996) Protein kinase A phosphorylation of RhoA mediates the morphological and functional effects of cyclic AMP in cytotoxic lymphocytes. *The EMBO journal*. 15 (3), 510.
- Pagès, G. et al. (1999) Defective thymocyte maturation in p44 MAP kinase (Erk 1) knockout mice. *Science (New York, N.Y.)*. 286 (5443), 1374–1377.
- Paine, P. L. et al. (1975) Nuclear envelope permeability. *Nature*. [Online] 254 (5496), 109–114.
- Palacios, I. et al. (1997) Nuclear import of U snRNPs requires importin beta. *The EMBO journal*. [Online] 16 (22), 6783–6792.
- Paradise, A. et al. (2007) Significant proportions of nuclear transport proteins with reduced intracellular mobilities resolved by fluorescence correlation spectroscopy. *Journal of molecular biology*. [Online] 365 (1), 50–65.
- Paraskeva, E. et al. (1999) CRM1-mediated recycling of snurportin 1 to the cytoplasm. *The Journal of cell biology*. 145 (2), 255–264.
- Patel, S. S. et al. (2007) Natively unfolded nucleoporins gate protein diffusion across the nuclear pore complex. *Cell*. [Online] 129 (1), 83–96.

- Patterson, G. H. & Lippincott-Schwartz, J. (2002) A photoactivatable GFP for selective photolabeling of proteins and cells. *Science (New York, N.Y.)*. [Online] 297 (5588), 1873–1877.
- Pawłowski, R. et al. (2010) An actin-regulated importin α/β -dependent extended bipartite NLS directs nuclear import of MRTF-A. *The EMBO journal*. [Online] 29 (20), 3448–3458.
- Percipalle, P. (2013) Co-transcriptional nuclear actin dynamics. *Nucleus (Austin, Tex.)*. [Online] 4 (1), 43–52.
- Perrin, B. J. & Ervasti, J. M. (2010) The actin gene family: function follows isoform. *Cytoskeleton (Hoboken, N.J.)*. [Online] 67 (10), 630–634.
- Peters, R. (2005) Translocation Through the Nuclear Pore Complex: Selectivity and Speed by Reduction-of-Dimensionality - Peters - 2005 - Traffic - Wiley Online Library. *Traffic*.
- Peters, R. (2009) Translocation through the nuclear pore: Kaps pave the way. *BioEssays : news and reviews in molecular, cellular and developmental biology*. [Online] 31 (4), 466–477.
- Peterson, J. R. & Mitchison, T. J. (2002) Small Molecules, Big Impact A History of Chemical Inhibitors and the Cytoskeleton. *Chemistry & biology*. [Online] 9 (12), 1275–1285.
- Petosa, C. et al. (2004) Architecture of CRM1/Exportin1 suggests how cooperativity is achieved during formation of a nuclear export complex. *Molecular cell*. [Online] 16 (5), 761–775.
- Pfaendtner, J. et al. (2009) Nucleotide-dependent conformational states of actin. *Proceedings of the National Academy of Sciences*. [Online] 106 (31), 12723–12728.
- Pinna, L. A. & Ruzzene, M. (1996) How do protein kinases recognize their substrates? *Biochimica et biophysica acta*. 1314 (3), 191–225.
- Plotnikov, A. et al. (2011) Nuclear Extracellular Signal-Regulated Kinase 1 and 2 Translocation Is Mediated by Casein Kinase 2 and Accelerated by Autophosphorylation. ... *and cellular biology*.
- Pollard, T. D. (1986) Rate constants for the reactions of ATP- and ADP-actin with the ends of actin filaments. *The Journal of cell biology*. 103 (6 Pt 2), 2747–2754.
- Pollard, T. D. & Borisy, G. G. (2003) Cellular motility driven by assembly and disassembly of actin filaments. *Cell*. 112 (4), 453–465.
- Pollard, T. D. & Cooper, John A (2009) Actin, a central player in cell shape and movement. *Science (New York, N.Y.)*. [Online] 326 (5957), 1208–1212.

- Posern, G. & Treisman, R. (2006) Actin' together: serum response factor, its cofactors and the link to signal transduction. *Trends in cell biology*. [Online] 16 (11), 588–596.
- Posern, G. et al. (2002) Mutant actins demonstrate a role for unpolymerized actin in control of transcription by serum response factor. *Molecular biology of the cell*. [Online] 13 (12), 4167–4178.
- Posern, G. et al. (2004) Mutant actins that stabilise F-actin use distinct mechanisms to activate the SRF coactivator MAL. *The EMBO journal*. [Online] 23 (20), 3973–3983.
- Prives, C. (1998) Signaling to p53: breaking the MDM2-p53 circuit. *Cell*. 95 (1), 5–8.
- Raghavan, M. et al. (1989) Analytical determination of methylated histidine in proteins: actin methylation. *Analytical biochemistry*. 178 (1), 194–197.
- Raman, M. et al. (2007) Differential regulation and properties of MAPKs. *Oncogene*. [Online] 26 (22), 3100–3112.
- Rao, A. et al. (1997) Transcription factors of the NFAT family: regulation and function. *Annual review of immunology*. [Online] 15707–747.
- Reddy, P. et al. (2013) Actin cytoskeleton regulates Hippo signaling. *PLoS one*. [Online] 8 (9), e73763.
- Remedios, dos, C. G. et al. (2003) Actin binding proteins: regulation of cytoskeletal microfilaments. *Physiological reviews*. [Online] 83 (2), 433–473.
- Reszka, A. A. et al. (1995) Association of mitogen-activated protein kinase with the microtubule cytoskeleton. *Proceedings of the National Academy of Sciences of the United States of America*. 92 (19), 8881–8885.
- Ridley, A. J. (2011) Life at the leading edge. *Cell*. [Online] 145 (7), 1012–1022.
- Riedl, J. et al. (2008) Lifeact: a versatile marker to visualize F-actin. *Nature methods*. [Online] 5 (7), 605–607.
- Rittinger, K. et al. (1999) Structural analysis of 14-3-3 phosphopeptide complexes identifies a dual role for the nuclear export signal of 14-3-3 in ligand binding. *Molecular cell*. 4 (2), 153–166.
- Rohatgi, R. et al. (2000) Mechanism of N-WASP activation by CDC42 and phosphatidylinositol 4, 5-bisphosphate. *The Journal of cell biology*. 150 (6), 1299–1310.
- Roskoski, R. (2012) ERK1/2 MAP kinases: structure, function, and regulation. *Pharmacological research : the official journal of the Italian Pharmacological Society*. [Online] 66 (2), 105–143.

- Rout, M. P. et al. (2003) Virtual gating and nuclear transport: the hole picture. *Trends in cell biology*. 13 (12), 622–628.
- Rubinfeld, H. et al. (1999) Identification of a cytoplasmic-retention sequence in ERK2. *The Journal of biological chemistry*. 274 (43), 30349–30352.
- Sagara, J. et al. (2009) Scapinin, the protein phosphatase 1 binding protein, enhances cell spreading and motility by interacting with the actin cytoskeleton. *PloS one*. [Online] 4 (1), e4247.
- Saito, N. & Matsuura, Y. (2013) A 2.1-Å-resolution crystal structure of unliganded CRM1 reveals the mechanism of autoinhibition. *Journal of molecular biology*. [Online] 425 (2), 350–364.
- Sakamoto, Y. et al. (1997) Inhibition of the DNA-binding and transcriptional repression activity of the Wilms' tumor gene product, WT1, by cAMP-dependent protein kinase-mediated phosphorylation of Ser-365 and Ser-393 in the zinc finger domain. *Oncogene*. [Online] 15 (17), 2001–2012.
- Salvany, L. et al. (2014) The core and conserved role of MAL is homeostatic regulation of actin levels. *Genes & development*. [Online] 28 (10), 1048–1053.
- Samuels, M. L. et al. (1993) Conditional transformation of cells and rapid activation of the mitogen-activated protein kinase cascade by an estradiol-dependent human raf-1 protein kinase. *Molecular and cellular biology*. 13 (10), 6241–6252.
- Schmid, M. F. et al. (2004) Structure of the acrosomal bundle. *Nature cell biology*. [Online] 431 (7004), 104–107.
- Schoenenberger, C.-A. et al. (2005) Conformation-specific antibodies reveal distinct actin structures in the nucleus and the cytoplasm. *Journal of structural biology*. [Online] 152 (3), 157–168.
- Schönwasser, D. C. et al. (1998) Activation of the mitogen-activated protein kinase/extracellular signal-regulated kinase pathway by conventional, novel, and atypical protein kinase C isoforms. *Molecular and cellular biology*. 18 (2), 790–798.
- Seewald, M. J. et al. (2002) RanGAP mediates GTP hydrolysis without an arginine finger. *Nature*. [Online] 415 (6872), 662–666.
- Sharrocks, A. D. et al. (2000) Docking domains and substrate-specificity determination for MAP kinases. *Trends in biochemical sciences*. 25 (9), 448–453.
- Shaw, P. E. et al. (1989) The ability of a ternary complex to form over the serum response element correlates with serum inducibility of the human c-fos promoter. *Cell*. [Online] 56 (4), 563–572.
- Shen, X. et al. (2000) A chromatin remodelling complex involved in transcription and DNA processing. *Nature*. [Online] 406 (6795), 541–544.

- Sheth, P. R. et al. (2011) Fully activated MEK1 exhibits compromised affinity for binding of allosteric inhibitors U0126 and PD0325901. *Biochemistry*. [Online] 50 (37), 7964–7976.
- Snapp, E. L. et al. (2003) Measuring protein mobility by photobleaching GFP chimeras in living cells. *Current protocols in cell biology / editorial board, Juan S. Bonifacino ... [et al.]*. [Online] Chapter 21Unit21.1.
- Solsbacher, J. et al. (1998) Cse1p is involved in export of yeast importin alpha from the nucleus. *Molecular and cellular biology*. 18 (11), 6805–6815.
- Songyang, Z. et al. (1996) A structural basis for substrate specificities of protein Ser/Thr kinases: primary sequence preference of casein kinases I and II, NIMA, phosphorylase kinase, calmodulin-dependent kinase II, CDK5, and Erk1. *Molecular and cellular biology*. 16 (11), 6486–6493.
- Songyang, Z. et al. (1994) Use of an oriented peptide library to determine the optimal substrates of protein kinases. *Current biology : CB*. 4 (11), 973–982.
- Sotiropoulos, A. et al. (1999) Signal-regulated activation of serum response factor is mediated by changes in actin dynamics. *Cell*. 98 (2), 159–169. [online].
- Spector, I. et al. (1983) Latrunculins: novel marine toxins that disrupt microfilament organization in cultured cells. *Science (New York, N.Y.)*. [Online] 219 (4584), 493–495.
- Spudich, J. A. & Watt, S. (1971) The regulation of rabbit skeletal muscle contraction. I. Biochemical studies of the interaction of the tropomyosin-troponin complex with actin and the proteolytic fragments of myosin. *The Journal of biological chemistry*. 246 (15), 4866–4871.
- Storm, S. M. et al. (1990) Expression of raf family proto-oncogenes in normal mouse tissues. *Oncogene*. 5 (3), 345–351.
- Strambio-De-Castillia, C. et al. (2010) The nuclear pore complex: bridging nuclear transport and gene regulation. *Nature reviews. Molecular cell biology*. [Online] 11 (7), 490–501.
- Stüven, T. et al. (2003) Exportin 6: a novel nuclear export receptor that is specific for profilin.actin complexes. *The EMBO journal*. [Online] 22 (21), 5928–5940.
- Sun, Q. et al. (2013) Nuclear export inhibition through covalent conjugation and hydrolysis of Leptomycin B by CRM1. *Proceedings of the National Academy of Sciences*. [Online] 110 (4), 1303–1308.
- Sun, Y. et al. (2006) Acute Myeloid Leukemia-Associated Mkl1 (Mrtf-a) Is a Key Regulator of Mammary Gland Function. *Molecular and cellular biology*. [Online] 26 (15), 5809–5826.
- Suzuki, R. et al. (2009) Solution structures and DNA binding properties of the N-terminal SAP domains of SUMO E3 ligases from *Saccharomyces cerevisiae* and *Oryza sativa*. *Proteins*. [Online] 75 (2), 336–347.

- Tanoue, T. & Nishida, E. (2003) Molecular recognitions in the MAP kinase cascades. *Cellular signalling*. 15 (5), 455–462.
- Teis, D. et al. (2002) Localization of the MP1-MAPK scaffold complex to endosomes is mediated by p14 and required for signal transduction. *Developmental cell*. 3 (6), 803–814.
- Terry, L. J. & Wenthe, S. R. (2009) Flexible gates: dynamic topologies and functions for FG nucleoporins in nucleocytoplasmic transport. *Eukaryotic cell*. [Online] 8 (12), 1814–1827.
- Therrien, M. et al. (1996) KSR modulates signal propagation within the MAPK cascade. *Genes & development*. 10 (21), 2684–2695.
- Tirion, M. M. et al. (1995) Normal modes as refinement parameters for the F-actin model. *Biophysical journal*. [Online] 68 (1), 5–12.
- Torres, E. & Rosen, M. K. (2003) Contingent phosphorylation/dephosphorylation provides a mechanism of molecular memory in WASP. *Molecular cell*. 11 (5), 1215–1227.
- Toska, E. & Roberts, S. G. E. (2014) Mechanisms of transcriptional regulation by WT1 (Wilms' tumour 1). *The Biochemical journal*. [Online] 461 (1), 15–32.
- Treisman, R. (1995) Journey to the surface of the cell: Fos regulation and the SRE. *The EMBO journal*. 14 (20), 4905–4913.
- Treisman, R. (1996) Regulation of transcription by MAP kinase cascades. *Current opinion in cell biology*. 8 (2), 205–215.
- Tsien, R. Y. (1998) THE GREEN FLUORESCENT PROTEIN. *Annual review of biochemistry*. [Online] 67 (1), 509–544.
- van Corven, E. J. et al. (1993) Pertussis toxin-sensitive activation of p21ras by G protein-coupled receptor agonists in fibroblasts. *Proceedings of the National Academy of Sciences of the United States of America*. 90 (4), 1257–1261.
- Vartiainen, M. K. (2008) Nuclear actin dynamics--from form to function. *FEBS letters*. [Online] 582 (14), 2033–2040.
- Vartiainen, M. K. et al. (2007) Nuclear actin regulates dynamic subcellular localization and activity of the SRF cofactor MAL. *Science (New York, N.Y.)*. [Online] 316 (5832), 1749–1752.
- Vetter, I. R. & Wittinghofer, A. (2001) The guanine nucleotide-binding switch in three dimensions. *Science (New York, N.Y.)*. [Online] 294 (5545), 1299–1304.
- Vetter, I. R., Arndt, A., et al. (1999) Structural view of the Ran-Importin beta interaction at 2.3 Å resolution. *Cell*. 97 (5), 635–646.

- Vetter, I. R., Nowak, C., et al. (1999) Structure of a Ran-binding domain complexed with Ran bound to a GTP analogue: implications for nuclear transport. *Nature*. [Online] 398 (6722), 39–46.
- Volmat, V. et al. (2001) The nucleus, a site for signal termination by sequestration and inactivation of p42/p44 MAP kinases. *Journal of cell science*. 114 (Pt 19), 3433–3443.
- Voong, L. N. et al. (2008) Mitogen-activated Protein Kinase ERK1/2 Regulates the Class II Transactivator. *Journal of Biological Chemistry*. [Online] 283 (14), 9031–9039.
- Wagner, P. D. & Vu, N. D. (1995) Phosphorylation of ATP-citrate lyase by nucleoside diphosphate kinase. *The Journal of biological chemistry*. 270 (37), 21758–21764.
- Wallar, B. J. et al. (2006) The Basic Region of the Diaphanous-autoregulatory Domain (DAD) Is Required for Autoregulatory Interactions with the Diaphanous-related Formin Inhibitory Domain. *Journal of Biological ...*
- Wang, D. et al. (2001) Activation of cardiac gene expression by myocardin, a transcriptional cofactor for serum response factor. *Cell*. 105 (7), 851–862.
- Wang, D.-Z. et al. (2002) Potentiation of serum response factor activity by a family of myocardin-related transcription factors. *Proceedings of the National Academy of Sciences of the United States of America*. [Online] 99 (23), 14855–14860.
- Wang, G. et al. (2005) Mediator requirement for both recruitment and postrecruitment steps in transcription initiation. *Molecular cell*. [Online] 17 (5), 683–694.
- Wang, H.-R. et al. (2003) Regulation of cell polarity and protrusion formation by targeting RhoA for degradation. *Science (New York, N.Y.)*. [Online] 302 (5651), 1775–1779.
- Wawro, B. et al. (2005) Role of actin DNase-I-binding loop in myosin subfragment 1-induced polymerization of G-actin: implications for the mechanism of polymerization. *Biophysical journal*. [Online] 88 (4), 2883–2896.
- Wälde, S. & Kehlenbach, R. H. (2010) The Part and the Whole: functions of nucleoporins in nucleocytoplasmic transport. *Trends in cell biology*. [Online] 20 (8), 461–469.
- Weis, K. (2003) Regulating Access to the Genome. *Cell*. [Online] 112 (4), 441–451.
- Wellbrock, C. et al. (2004) The RAF proteins take centre stage. *Nature reviews. Molecular cell biology*. [Online] 5 (11), 875–885.
- Wente, S. R. & Rout, M. P. (2010) The nuclear pore complex and nuclear transport. *Cold Spring Harbor Perspectives in Biology*. [Online] 2 (10), a000562.

- Wheeler, A. P. & Ridley, A. J. (2004) Why three Rho proteins? RhoA, RhoB, RhoC, and cell motility. *Experimental cell research*. [Online] 301 (1), 43–49.
- Whitmarsh, A. J. (2007) Regulation of gene transcription by mitogen-activated protein kinase signaling pathways. *Biochimica et Biophysica Acta (BBA) - Molecular Cell Research*. [Online] 1773 (8), 1285–1298.
- Whitmarsh, A. J. & Davis, R. J. (2000) Regulation of transcription factor function by phosphorylation. *Cellular and molecular life sciences : CMLS*. 57 (8-9), 1172–1183.
- Wiezlak, M. et al. (2012) G-actin regulates the shuttling and PP1 binding of the RPEL protein Phactr1 to control actomyosin assembly. *Journal of cell science*. [Online] 125 (Pt 23), 5860–5872.
- Wilde, C. & Aktories, K. (2001) The Rho-ADP-ribosylating C3 exoenzyme from *Clostridium botulinum* and related C3-like transferases. *Toxicon : official journal of the International Society on Toxinology*. 39 (11), 1647–1660.
- Wittinghofer, A. & Nassar, N. (1996) How Ras-related proteins talk to their effectors. *Trends in biochemical sciences*. 21 (12), 488–491.
- Wittmann, T. & Waterman-Storer, C. M. (2001) Cell motility: can Rho GTPases and microtubules point the way? *Journal of cell science*.
- Wolf, I. et al. (2001) Involvement of the activation loop of ERK in the detachment from cytosolic anchoring. *The Journal of biological chemistry*. [Online] 276 (27), 24490–24497.
- Wu, X. et al. (2006) Regulation of RNA-polymerase-II-dependent transcription by N-WASP and its nuclear-binding partners. *Nature cell biology*. [Online] 8 (7), 756–763.
- Wulf, E. et al. (1979) Fluorescent phallotoxin, a tool for the visualization of cellular actin. *Proceedings of the National Academy of Sciences of the United States of America*. 76 (9), 4498–4502.
- Xu, D. et al. (2012) NESdb: a database of NES-containing CRM1 cargoes. *Molecular biology of the cell*. [Online] 23 (18), 3673–3676.
- Xue, Y. et al. (2008) GPS 2.0, a tool to predict kinase-specific phosphorylation sites in hierarchy. *Molecular & cellular proteomics : MCP*. [Online] 7 (9), 1598–1608.
- Yamada, J. et al. (2010) A bimodal distribution of two distinct categories of intrinsically disordered structures with separate functions in FG nucleoporins. *Molecular & cellular proteomics : MCP*. [Online] 9 (10), 2205–2224.
- Yang, S. H. et al. (1998) The Elk-1 ETS-domain transcription factor contains a mitogen-activated protein kinase targeting motif. *Molecular and cellular biology*. 18 (2), 710–720.

- Yang, S.-H. et al. (2003) Transcriptional regulation by the MAP kinase signaling cascades. *Gene*. 3203–21.
- Yao, Y. et al. (2003) Extracellular signal-regulated kinase 2 is necessary for mesoderm differentiation. *Proceedings of the National Academy of Sciences of the United States of America*. [Online] 100 (22), 12759–12764.
- Yoo, Y. et al. (2007) A novel role of the actin-nucleating Arp2/3 complex in the regulation of RNA polymerase II-dependent transcription. *The Journal of biological chemistry*. [Online] 282 (10), 7616–7623.
- Zaromytidou, A.-I. (2007) *Molecular study of SRF-cofactor interactions*.
- Zaromytidou, A.-I. et al. (2006) MAL and ternary complex factor use different mechanisms to contact a common surface on the serum response factor DNA-binding domain. *Molecular and cellular biology*. [Online] 26 (11), 4134–4148.
- Zehorai, E. et al. (2010) The subcellular localization of MEK and ERK--a novel nuclear translocation signal (NTS) paves a way to the nucleus. *Molecular and cellular endocrinology*. [Online] 314 (2), 213–220.
- Zheng, C. F. & Guan, K. L. (1994) Activation of MEK family kinases requires phosphorylation of two conserved Ser/Thr residues. *The EMBO journal*. 13 (5), 1123–1131.
- Zhu, J. et al. (1998) Intramolecular masking of nuclear import signal on NF-AT4 by casein kinase I and MEKK1. *Cell*. 93 (5), 851–861.
- Ziegler, E. C. & Ghosh, S. (2005) Regulating inducible transcription through controlled localization. *Science's STKE : signal transduction knowledge environment*. [Online] 2005 (284), re6.